Lung Development:

Vascular & epithelial branching morphogenesis

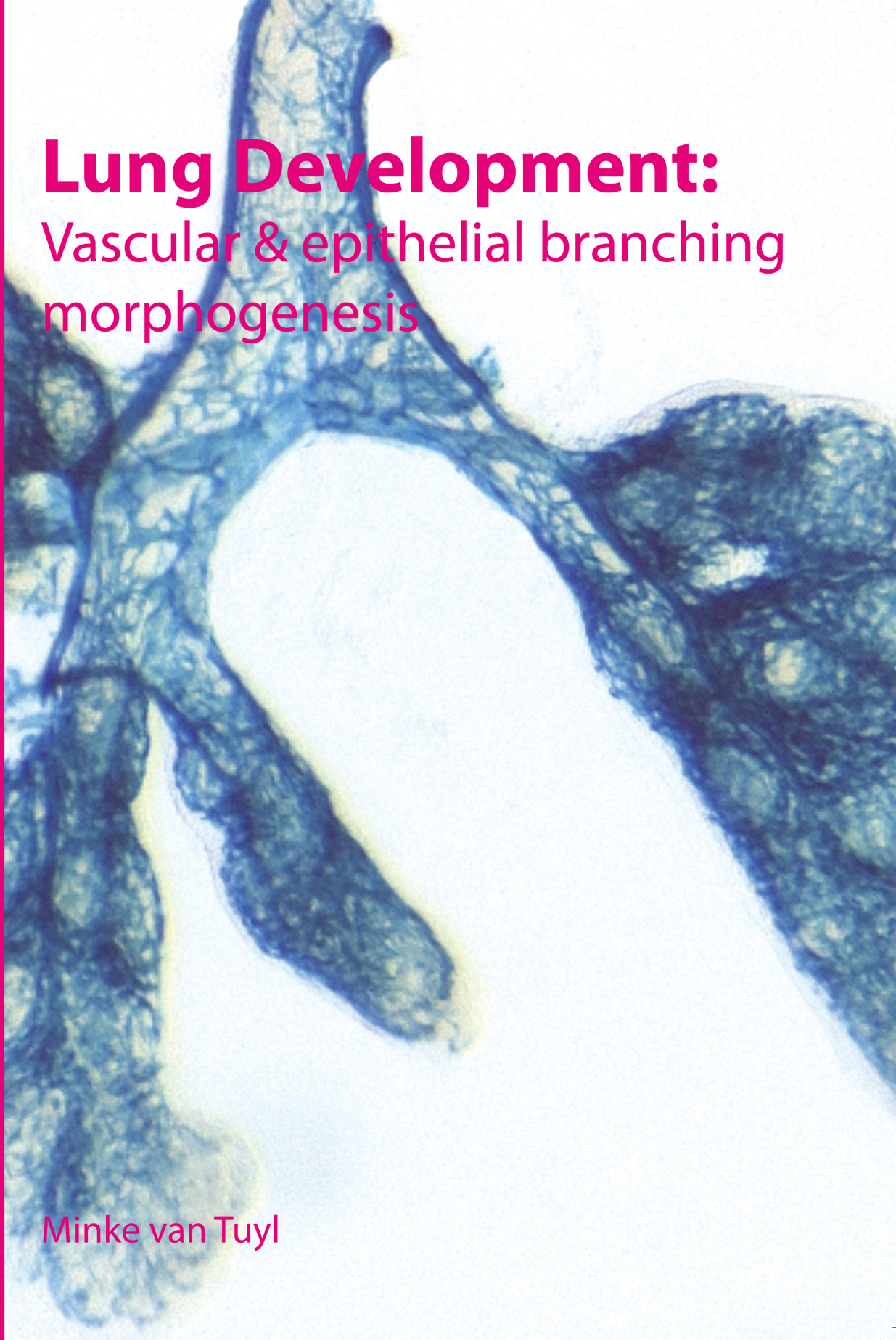

Minke van Tuyl

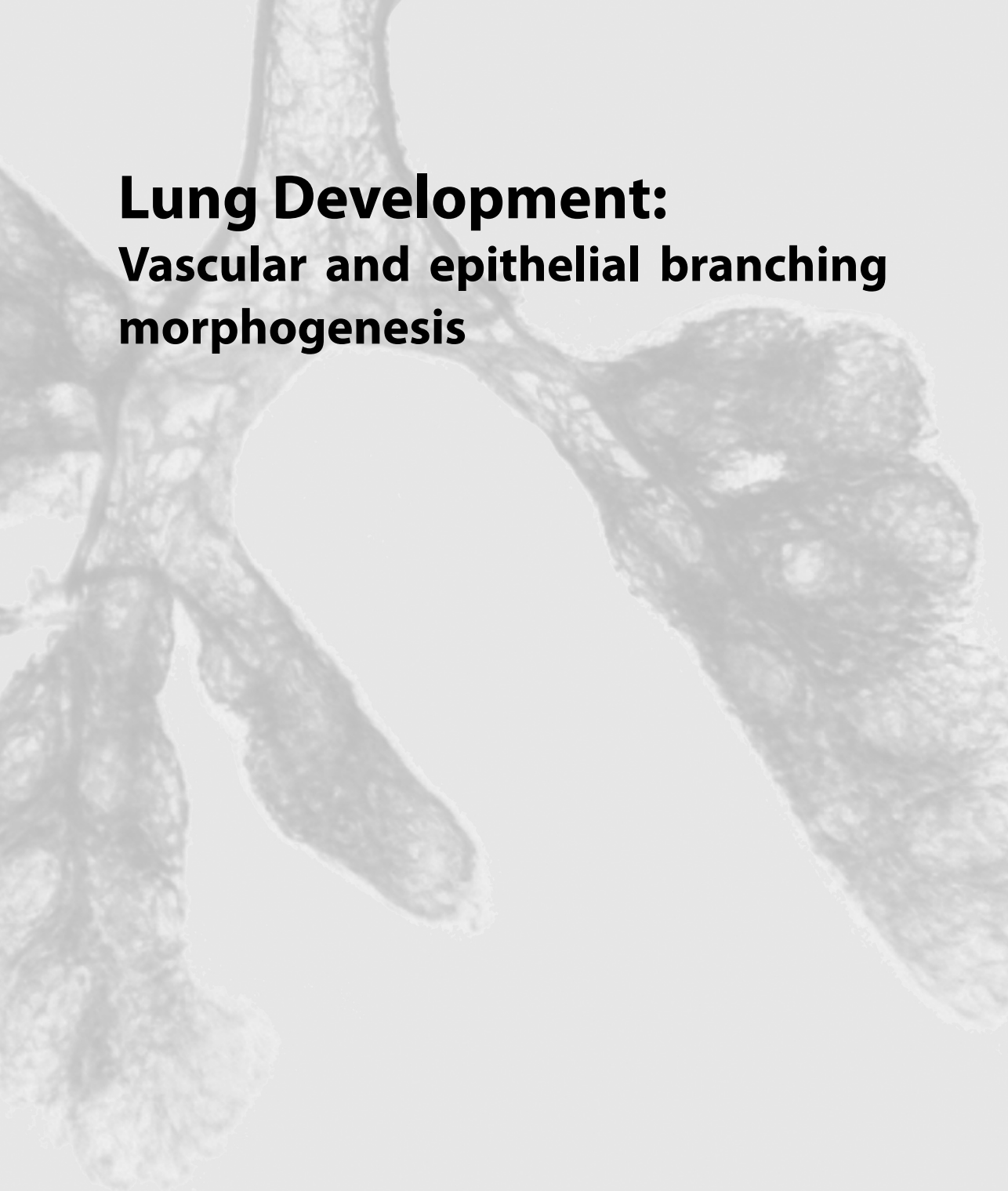

Lung Development:
Vascular and epithelial branching morphogenesis

Lung Development: Vascular and epithelial branching morphogenesis

Thesis, Erasmus University Rotterdam, The Netherlands

ISBN 90-77595-86-4

Cover and layout by: Jarrod Leeds

Printed by: Optima Grafische Communicatie, Rotterdam, The Netherlands

The work presented in this thesis was supported by:

Canadian Institutes of Health Research

Sophia Foundation for Medical Research (SSWO)

David Vervat Foundation

Lung Development:
Vascular and epithelial branching morphogenesis

Long ontwikkeling: vorming van vasculaire en epitheliale vertakkingen

Proefschrift

ter verkrijging van de graad van doctor aan de Erasmus Universiteit Rotterdam op gezag van de Rector Magnificus Prof.dr. S.W.J. Lamberts en volgens besluit van het College voor Promoties

De openbare verdediging zal plaatsvinden op vrijdag 15 oktober 2004 om 13:30 uur door Wilhelmina Goverdina van Tuyl geboren te Heinenoord

Promotiecommissie:

Promotoren:	Prof.dr. D. Tibboel
	Prof.dr. M. Post
Overige leden:	Prof.dr. W.H. Lamers
	Prof.dr. E.A. Dzierzak
	Prof.dr. J.B. van Goudoever

Table of contents

"The organ of respiration is the lung. This derives its motion from the heart; but it is its own large size and spongy texture that affords amplitude of space for entrance of the breath. For when the lung rises up the breath streams in, and is again expelled when the lung collapses. It has been said that the lung exists as a provision to meet the jumping of the heart. But this is out of the question. For man is practically the only animal whose heart presents this phenomenon of jumping, inasmuch as he alone is influenced by hope and anticipation of the future"

Written 350 B.C. by Aristoteles, On the Parts of Animals, Book 3, Chapter 6, translated by William Ogle

Aan Dennis en mijn ouders

Chapter 1

Molecular mechanisms of lung development and lung branching morphogenesis

General introduction

Based on:
Minke van Tuyl and Martin Post*. From fruitflies to mammals: mechanisms of signaling via the Sonic hedgehog pathway in lung development. Respiratory Research 2000, 1:30-35
Minke van Tuyl and Martin Post*. Molecular Mechanisms of Lung Development and Lung Branching Morphogenesis. In: Fetal and Neonatal Physiology 3rd edition. Eds: R.A. Polin, W.W. Fox, and S.H. Abman. Saunders, Philadelphia, Harcourt Health Sciences 2004, 812-821

The Canadian Institutes of Health Research (CIHR) Group in Lung Development, Hospital for Sick Children Research Institute, Departments of Pediatrics and Physiology, University of Toronto, Toronto, ON, Canada

Introduction

Lung development can be subdivided into five distinct stages (Table 1) (1, 2). The early stages of lung development comprise the embryonic and pseudoglandular periods, after which the prospective conductive airways have been formed, and the acinar limits can be recognized. During the pseudoglandular period, the primitive airway epithelium starts to differentiate. Neuroendocrine, ciliated, and goblet cells appear, whereas cartilage and smooth muscle cells emerge from the mesenchyme. In the subsequent canalicular period, the airway branching pattern is completed, and the prospective gas exchange region starts to develop. During this period, respiratory bronchioli appear, interstitial tissue decreases, vascularization of peripheral mesenchyme increases, and distal cuboidal epithelium differentiates into type I and type II cells. In the saccular (terminal sac) period, the growth of the pulmonary parenchyma, thinning of the connective tissue between the air spaces, and maturation of the surfactant system are the most important steps towards *ex utero* life. Although already functional, the lung is structurally still in an immature condition at birth. The airspaces present are smooth-walled transitory ducts and saccules with primitive septa that are thick and contain a double capillary network. During the alveolar period, alveoli are formed through a septation process that greatly increases the gas exchange surface area, and the capillaries fuse to form a single layer. A hallmark throughout lung development is the signaling between the epithelial and mesenchymal tissue layers. The combination and concentration of signals, depending on position and time in gestation, determine lung morphogenesis (branching, growth, and differentiation). Since the 1980s, molecular studies of lung development have started to shed light on the complex series of events that control proper formation of the lung. In this chapter we summarize the current thoughts on the molecular mechanisms that determine lung pattern formation.

Table 1: Stages of lung development

Stage	Gestational age Human (wk)	Mouse (d)	Main events	Epithelial differentiation state
Embryonic	3.5-7	9.5-14.2	Formation of lung bud, trachea, left and right primary bronchus, and major airways	Undifferentiated columnar epithelium
Pseudoglandular	5-17	14.2-16.6	Establishment of the bronchial tree; all preacinar bronchi are formed	Proximal: columnar epithelium; ciliated, nonciliated, basal, neuroendocrine cells Distal: cuboidal epithelium; precursor type II cells
Canalicular	16-26	16.6-17.4	Formation of the prospective pulmonary acinus, increase of capillary bed	Proximal: columnar epithelium; ciliated, nonciliated, basal, neuroendocrine cells Distal: differentiation of cuboid type II to squamous type I cells
Saccular	24-38	17.4-5 postnatal	Formation of saccules, alveolar ducts, and alveolar airsacs	Proximal: columnar epithelium; ciliated, nonciliated, Clara, basal, neuroendocrine cells Distal: type I cells flatten and type II cells mature
Alveolar	36-2 y postnatal	5-30 postnatal	Formation of alveoli by septation of alveolar airsacs, thinning of interalveolar septa, and fusion of the capillary bed to a single layered network	Proximal: columnar epithelium; ciliated, nonciliated, Clara, basal, neuroendocrine cells Distal: mature type I and II cells

EARLY LUNG DEVELOPMENT

Lung development begins as an endodermal outgrowth of the ventral foregut around the fourth week of human development. This foregut mass rapidly elongates into a single tube dividing into a dorsal esophagus and a ventral trachea that, in turn, bifurcates into a right and a left primary lung bud. This process is modified in the mouse, in which the respiratory system develops from paired endodermal buds in the ventral half of the primitive foregut, just anterior to the developing stomach at 9.5 days of gestation (1, 2). The two buds elongate in a posterior-ventral direction. At the same time, starting at the primary branch point, the single gut tube begins to pinch into two tubes, the dorsal esophagus and ventral trachea. In human, the left lung bud will give rise to two main stem bronchi, whereas the right lung bud gives rise to three mainstem bronchi. In the mouse, the right lung characteristically has four stem bronchi, whereas the left lung consists of one stem bronchus. The main bronchi branch and rebranch in a dichotomous manner, a process called *branching morphogenesis*, and they eventually form the airway tree. Endoderm-derived epithelial cells line the airways, whereas the surrounding mesenchyme provides the elastic tissue, smooth muscle, cartilage, vascular system, and other connective tissues. The formation of the bronchial tree is finished at 16 days of gestation in the mouse and at 16 weeks of gestation in humans. At this stage of development, the tracheobronchial tree from the trachea to the terminal bronchioles resembles a system of branching tubules that terminate in exocrine gland-like structures.

MOLECULAR BASIS OF LUNG BUD AND LOBE FORMATION

The outgrowth of the ventral foregut, the formation of the trachea, and the outgrowth of the main pulmonary bronchi take place during the embryonic period of lung development. The crucial event at this stage is the initiation of lung formation at the right place along the anterior-posterior axis of the foregut. What determines the position of the lung, anterior of abdominal organs but posterior to the thyroid (all of which are derived from the foregut)? Genetic studies have implicated several transcription factors and morphogens, including peptide growth factors and their cognate receptors, in specifying the morphogenetic progenitor field of the lung along the foregut axis (Fig. 1) (3-6).

Hepatocyte nuclear factor-3β

One important transcription factor in this process is hepatocyte nuclear factor-3β (Hnf3β) (7). Hnf3β belongs to the winged helix/forkhead family, which has been renamed the Forkhead Box (Fox) family (8). Hnf3β (Foxa2) is expressed in ventral foregut endoderm before and immediately at the start of lung bud formation (9-11). Targeted ablation of Foxa2 in mice leads to embryonic death between E6.5 and E9.5, which is before lung formation (12, 13). However, chimeras rescued for the embryonic-extraembryonic lethality

showed that Foxa2 was essential for foregut and lung formation (14). In the lung, Foxa2 is expressed in epithelial cells from the onset of lung development, and continues to be expressed in bronchiolar-alveolar type II cells after birth (10, 11). Overexpression of Foxa2 in distal pulmonary epithelial cells using the human surfactant protein C (SP-C) promoter arrested lung development in the pseudoglandular stage, and markedly disrupted branching morphogenesis and vasculogenesis (15).

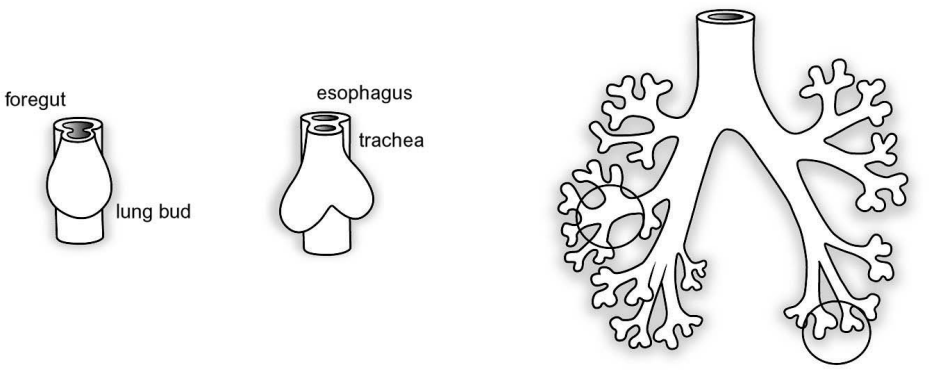

Outgrowth of foregut	Formation of primary bronchi	Branching morphogenesis	Alveolarization
Foxa2	Fgf10	Shh/Gli2	PdgfA
Gli2/Gli3	Fgfr-IIIb	RA/RAR	Pdgfrα
		Hox	RA
		Ttf-1	RAR/RXR
		Gata-6	Fgfr3/4
		N-myc	Ttf-1
		Fgf (1,7,9,10)	
		Tgfβ (1,3)	
		Wnt/β-catenin	

Figure 1. Transcription and growth factors regulating lung development (drawings represent human lungs, which consist of two lobes on the left and three lobes on the right side). See text for details.

Fibroblast growth factors

Fibroblast growth factor-10 (Fgf10) is a member of the large family of Fgfs that are involved in multiple processes during embryonic development (16-18). In the murine lung, Fgf10 mRNA is dynamically expressed in the distal mesenchyme adjacent to the primitive lung buds (19). The importance of Fgf10 for lung development was shown in Fgf10-deficient mice that die at birth as a result of severe respiratory failure (20, 21). The Fgf10-deficient mice exhibit complete lung agenesis (i.e., lung development had stopped after the formation of the trachea) (20, 21). Fgfs bind to and signal via Fgf tyrosine kinase receptors (Fgfr) (16, 17, 22). The Fgf10 receptor (Fgfr2-IIIb), a Fgfr2 splice variant, is expressed in lung bud epithelium (23). The appositional expression of Fgf10 and Fgfr2-IIIb is in line with

the dependence of lung patterning on mesenchymal-epithelial interactions (23). Fgfr2b is capable of binding Fgf1 and Fgf7, which have also been implicated in lung development (16, 19, 24). Because a targeted mutation of Fgfr2 results in an early lethal phenotype owing to placental insufficiency (25, 26), $Fgfr2^{-/-}$ chimeras were created to overcome this early lethality and allow lung development to be analyzed (23). As in Fgf10-deficient mice, only a trachea was formed without any further pulmonary branching (23). Similarly, transgenic mice that overexpress a (soluble) dominant negative Fgfr2-IIIb splice variant in distal lung epithelium using the mouse metallothionein promoter, showed a severe pulmonary defect with only the formation of a rudimentary trachea and two main bronchi, but without any lateral branches (27, 28). Moreover, cre-mediated excision to generate mice lacking the IIIb form of Fgfr2, while retaining expression of the IIIc splice form, resulted in mice that had no lungs and died at birth (29). Taken together, these data indicate that Fgf10 signaling via Fgfr2-IIIb plays a crucial role in the initiation of lung bud formation (Fig. 1). The "no lung" phenotype as a result of inhibited Fgf10 signaling shows a striking similarity to a phenotype resulting from the loss of function of either *Branchless* (*bnl*) or *Breathless* (*btl*) in *Drosophila*. *Bnl* encodes an Fgf homologue that functions as a ligand for *btl*, which encodes a *Drosophila* homologue of Fgfr. Loss of function of either *bnl* or *btl* prevented tracheal branching in the fly (30, 31). *Drosophila Sprouty* (*Spry*) is an antagonist of *Fgfr* signaling during tracheal morphogenesis (32, 33). In murine lung development, Spry-1 and –2 are expressed in distal epithelium, whereas Spry-4 is expressed in both distal epithelium and mesenchyme (34, 35). Indeed, overexpression of Spry-2 or Spry-4 in distal lung epithelium caused lung hypoplasia and decreased branching morphogenesis (35, 36). Epithelial overexpression of Spry-4 increased Fgf10 mRNA in the mesenchyme (36), whereas exogenous Fgf10 increased branching morphogenesis and upregulated Spry-2 mRNA in pulmonary mesenchyme *in vitro* (35). Similarly, antisense oligonucleotide-targeted inhibition of Fgf10 reduced Spry-2 mRNA and decreased branching morphogenesis (35). These results indicate that Spry negatively regulates branching morphogenesis, whereas Fgf and Spry reciprocally increase each other's expression, thereby creating a balanced regulatory loop.

Sonic hedgehog signaling

Sonic hedgehog (Shh) is a secreted signaling molecule and is a mammalian homologue of *Drosophila Hh* involved in many fundamental processes during embryonic development (37). Shh is expressed in early pulmonary epithelium, with highest gene expression at the tips of developing lung branches (38). Shh signals via the mesenchymal-located patched (Ptc) receptor, a finding suggesting a signaling loop between pulmonary epithelium and mesenchyme during lung development (38). The importance of Shh for lung development was shown when the Shh gene was genetically ablated. The Shh null mutant dies at birth with a lung bud consisting of only one lobe on each side of the trachea (39, 40). Thus, in contrast to the Fgf10 null mutant, the initiation of lung formation does occur in Shh null mutants, but they have an incorrect number of lung lobes and a subsequent failure

of branching morphogenesis (39, 40). The mesenchyme was the primary target of Shh deficiency, showing decreased cell proliferation and increased cell death in the absence of Shh (39). Smooth muscle actin, normally surrounding the conducting epithelium in control lungs, was absent in E18.5 Shh null mutant lungs (40). Epithelial specific genes like Foxa2, Ttf-1, and Fgfr2 were expressed normally in the Shh null mutant lung (39, 40). The effect of Shh on pulmonary mesenchyme was also demonstrated when Shh was overexpressed in distal lung epithelium using the surfactant protein (SP)-C promoter (38). Overexpression of Shh resulted in smaller lungs at birth that lacked alveoli but had an increased proportion of mesenchymal mass. Further analysis revealed an increased number of proliferating cells in the mesenchyme of the transgenic lungs (38). An important mechanism in Hh signaling is the regulation by Hedgehog interacting protein-1 (Hip1) (41). Hip1 encodes a membrane-bound protein that directly binds all mammalian Hh proteins and is like Ptc transcriptionally activated in response to Hh signaling (41). In the lung, Hip1 is expressed in the mesenchyme, and Hip1-deficient lungs show defective branching morphogenesis with normal proximal-distal epithelial differentiation (42). In Hip1 mutant lungs, Shh was upregulated, whereas Fgf10 was almost completely absent, which most likely is the cause of the lack of secondary bud formation (42).

All together, these results support a role for Shh/Hip1 in epithelial-mesenchymal signaling during early lung formation. The interaction between Shh and Fgf10 is complicated and not well characterized (43). The lung phenotypes for both null mutants are different is the sense that Fgf10 null mutants do not form anything after the trachea, whereas Shh null mutants do progress towards the formation of two hypoplastic lung buds, indicating that in very early bud formation, the two pathways function independently of each other (20, 21, 39, 40). Also, mesenchymal Fgf10 expression was not different in Shh null mutant lungs (39), although another study did find a change in Fgf10 mRNA expression (40), and moreover, Fgf10 mRNA was upregulated in lungs that overexpress Shh (38). In wild-type lungs, Fgf10 mRNA is highly localized to patches of mesenchyme at a distance from the lung epithelium. However, in Shh-deficient lungs, Fgf10 mRNA was broadly expressed in the mesenchyme immediately adjacent to the epithelium (40). All together, these data provide evidence that Shh negatively regulates Fgf10 expression, which creates a paradox because both factors are essential for lung development. A model was proposed by Lebeche and co-workers and Bellusci and co-workers (19, 38, 44, 45) in which epithelial Shh reduces Fgf10 levels in its immediate surrounding mesenchyme, thereby creating spatially restricted expression of Fgf10 mRNA, and suppressing further chemo attraction of epithelial cells by Fgf10, resulting in cleft formation and hence outgrowth of new lung buds towards newly formed Fgf10 chemo attractant centers at a distance. Alternatively, actual Shh protein activity is restricted by Hip1 and Ptc1, which are themselves upregulated by Shh. Areas with high Hip1 or Ptc1 activity hence sequester Shh protein, creating molecular space for high Fgf10 expression despite high Shh mRNA levels (43).

Gli genes

Shh binds to Ptc and this releases the basal repression that Ptc exerts on Smoothen (Smo), a transmembrane spanning protein that has homology to G-protein-coupled receptors. Inside the cell, Smo activation modifies the activity of *Cubitus interruptus* (*Ci*) or Gli family of transcriptional regulators (37, 46). *Ci* has been identified as a downstream target in *Hh* signaling in *Drosophila* (37). Mammalian Gli genes are the putative homologues of *Drosophila Ci* and have also been implicated in mammalian Shh signaling (37). Three Gli genes have been described in mice: Gli1, Gli2, and Gli3, all of which are expressed in early pulmonary mesenchyme (47). In comparison with the Shh null mutant, an even more dramatic phenotype was observed in mice lacking both Gli2 and Gli3. These $Gli2^{-/-}$,$Gli3^{-/-}$ mutant mice have no lung, trachea, or esophagus and die early in gestation (48). Interestingly other foregut derivatives such as thymus, stomach, and pancreas do develop in $Gli2^{-/-}$,$Gli3^{-/-}$ mutant mice, although these structures are hypoplastic (48). These data suggest that combined Gli2 and Gli3 signaling is crucial for the initiation of lung bud formation (see Fig. 1). The complete absence of trachea and lung formation was already ameliorated by the presence of one Gli3 gene. $Gli2^{-/-}$,$Gli3^{+/-}$ mutants had a lung consisting of one hypoplastic lobe (48). The finding that ablation of both Gli2 and Gli3 resulted in a far worse lung phenotype than the deficiency of Shh alone may indicate that Shh is not the only regulator of Gli genes during lung development. The complete absence of a lung in $Gli2^{-/-}$,$Gli3^{-/-}$ mutant mice is similar to the "no lung" phenotype as seen in Fgf10-deficient mice. However, the trachea and esophagus are present in Fgf10-deficient mice but are absent in Gli2;Gli3-deficient mice, a finding implicating different signaling pathways. Other single or compound mutants for the three Gli genes show a variable degree of lung hypoplasia with an aberrant number of lung lobes and decreased branching morphogenesis (48-50). Haploinsufficiency for Foxf1 caused similar malformations of the lung, trachea, and esophagus as were seen in mutants from the Shh/Gli pathway, and like in Shh-deficient lungs, proximal-distal epithelial differentiation proceeded normally (51). Foxf1 is absent from the trachea and lung area from Shh-deficient mice, whereas exogenous Shh activated Foxf1 expression in lung mesenchyme, a finding indicating that Foxf1 is a possible downstream target in the Shh/Gli signaling cascade (51).

Retinoic acid

All-*trans*-retinoic acid (RA) is the active form of vitamin A (retinal) that plays a crucial role during development and is involved in the developmental process of almost every organ (52-54). Both a deficiency and an excess of RA cause congenital defects during human development in a variety of organs (52, 53). RA exerts its effects via the RAR and RXR retinoic acid receptors, which function as transcriptional regulators of target genes. The RAR family is composed of three genes, which produce several isoforms: $RAR\alpha_{1,2}$, $RAR\beta_{1-4}$, and $RAR\gamma_{1,2}$, all activated by both all-*trans*-RA and 9-*cis*-RA, whereas the three isoforms from the RXR family (RXRα, RXRβ, and RXRγ) are activated only by 9-*cis*-RA (52). Mice deficient for only one of the isoforms showed a less severe phenotype than expected on

the basis of their expression patterns, a finding indicating a high degree of redundancy among the RA receptors (52). In contrast, compound mutant mice had similar congenital defects as seen with fetal vitamin A deficiency (52, 53). RAR$\alpha^{-/-}$,$\beta2^{-/-}$ double-mutant mice die soon after birth with agenesis of the left lung and hypoplasia of the right lung (55). Lung hypoplasia was also reported in RAR$\alpha1^{-/-}$,$\beta^{-/-}$ and RXR$\alpha^{-/-}$,RAR$\alpha^{-/-}$ double-mutant mice (56, 57). In addition, RA has profound influences on lung development during branching morphogenesis and alveolarization (see later).

Hox genes

Furthermore, RA may regulate Hox genes (58-61). Hox genes form a large family of homeobox-containing transcription factors that are implicated in the specification of cells that form morphologic structures along an anterior-posterior axis. Hox genes are arranged in four chromosomal clusters (a, b, c, and d), and the 3' to 5' position of each gene within a cluster corresponds with their expression along the anterior-posterior axis of the developing body (62). Specifically, genes of the 3' regions of the Hox clusters a and b have been shown to be expressed in the developing lung. The Hoxb cluster is predominantly expressed in the early pulmonary mesenchyme (58-61, 63-68). Within the mesenchyme, Hoxb genes express a proximal-distal expression gradient, suggesting a role for Hoxb genes in specifying proximal from distal pulmonary mesenchyme (67). Several mutant mice models confirm the role of Hox genes during lung development. Single-mutant mice for Hox genes are generally normal, most likely because of redundancy. However, compound Hoxa1$^{-/-}$,Hoxb1$^{-/-}$ mutants have severe lung hypoplasia ranging from five hypoplastic lung lobes to only two lung lobes (69). Hoxa5$^{-/-}$ mice die perinatally and have laryngotracheal malformations, a reduced tracheal lumen, and lung hypoplasia (70).

Thyroid transcription factor-1

Another homeodomain transcription factor expressed at the onset of lung morphogenesis is thyroid transcription factor-1 (Ttf-1), also known as Nkx2.1 (71-73). Expression of Ttf-1 mRNA is localized to epithelial cells of the developing pulmonary tubules and decreases in more proximal conducting airways with advancing gestation (11, 74, 75). The Ttf-1 gene continues to be expressed in adult bronchiolar and alveolar epithelial type II cells, in which it plays an important role in the regulation of Clara cell secreted protein (CCSP) and surfactant protein (SP) synthesis (see later). Targeted disruption of Ttf-1 resulted in severe hypoplasia of the thyroid and lung, with a developmental arrest at the pseudoglandular stage of lung development (76, 77). In contrast to the different null mutants in the Shh-Gli pathway, Ttf-1 null mutants lack distal epithelial cell differentiation (73, 77). Shh mRNA was normally expressed in Ttf-1-deficient lungs (73), whereas Ttf-1 mRNA expression was unchanged in Shh null mutant lungs (39, 40). These results indicate that Ttf-1 and Shh probably regulate branching morphogenesis via separate pathways during lung development.

Separating esophagus and trachea

The formation of a septum divides the single tracheoesophageal tube into a trachea on the ventral side and the esophagus on the dorsal side. A failure to form a septum results in a tracheoesophageal fistula, a not uncommon congenital defect in humans (78). Deficiency of all aforementioned growth and transcription factors that are implicated in the etiology of lung agenesis or hypoplasia also results in a tracheoesophageal fistula with different gradations of severity (Table 2). $Gli2^{-/-}$,$Gli3^{-/-}$ mutant mice have no trachea, nor do they form an esophagus (48), whereas $Gli2^{-/-}$,$Gli3^{+/-}$ mutant mice have a single tracheoesophageal tube connected to the stomach (48). In $Shh^{-/-}$ mutant mice, the trachea and esophagus failed to separate, resulting in a tracheoesophageal fistula (39, 40). Mice haploinsufficient for the transcription factor Foxf1 (Hfh8) exhibit foregut abnormalities including narrowing and, sometimes, atresia of the esophagus as well as frequent fusion of trachea and esophagus (51). Foxf1 expression was absent in foregut derivates (trachea, esophagus, oral cavity, lungs) of $Shh^{-/-}$ mutants, a finding indicating that Shh signaling is required for activation of Foxf1 in these tissues (51). Surprisingly, the separation of the trachea and esophagus occurs normally in Fgf10-deficient mice (20, 21), whereas Ttf-1-deficient mice have a complete tracheoesophageal defect (73). $RAR\alpha^{-/-}$,$\beta2^{-/-}$, $RAR\alpha1^{-/-}$,$\beta^{-/-}$, and $RXR\alpha^{-/-}$,$RAR\alpha^{-/-}$ mutant mice all exhibit a tracheoesophageal septum defect and other tracheal malformations such as disorganized cartilage rings and shortening of the trachea (55-57).

Table 2. ***Separating trachea and esophagus****

	Trachea	Esophagus	Remarks
$Fgf10^{-/-}$	+	+	T-E separation, trachea ends blind
$Shh^{-/-}$	+	+	T-E septum defect
$Gli2^{-/-}$	+	+	T-E separation with stenosis
$Gli2^{-/-}$;$Gli3^{+/-}$	+	-	Single (tracheal) tube connecting to the stomach, esophageal atresia
$Gli2^{-/-}$;$Gli3^{-/-}$	-	-	No esophagus, trachea, or lung
$RAR\alpha^{-/-}$; $\beta2^{-/-}$ $RAR\alpha1^{-/-}$;$\beta^{-/-}$	+	+	T-E septum defect, tracheal cartilage malformations
$Ttf\text{-}1^{-/-}$	+	+	T-E septum defect

**Transcription and growth factors involved in the separation of esophagus and trachea around gestational week 4 in humans and day 12 in mice. A failure of separation results in a complete or incomplete tracheoesophageal (T-E) septum defect, a not uncommon congenital anomaly in humans.*

Left-right asymmetry

At around 5 weeks' gestation, five separate lobes can be identified in the human lung: two on the left and three on the right. In the mouse, the right lung characteristically has four major lobes, whereas the left lung consists of only one small lobe. Such left-right asymmetries during development are an integral part of the establishment of a body plan, and until recently, the molecular basis of left-right asymmetry was not well known. Several distinct yet highly conserved mechanisms have since been proposed to initiate the vertebrate left-right axis including the Shh signaling pathway (79). Molecules such as Shh (80, 81), Fgf8 (80, 82), N-cadherin (83), activin β, the activin receptor IIB (84), and Foxj1 (Hfh4) (85) also influence left-right asymmetry during development (Fig. 2). However, it appears that all these pathways converge to influence the expression patterns of genes in the transforming growth factor-β (Tgf-β) family of cell-cell signaling factors, called Nodal and Lefty-1 and 2 (86-89). Shh and Lefty-1 mutants have left pulmonary isomerism with only one lobe on each side of the lung (39, 40, 81, 87). Both Shh and Foxa2 are thought to act upstream of Lefty-1 and were normally expressed in Lefty-$1^{-/-}$ mice (87). Although no data are available on the expression of Lefty in the $Shh^{-/-}$ mutant lung, Lefty-1 is absent in $Shh^{-/-}$ mutant lateral plate mesoderm (LPM) (81). Lefty-$1^{-/-}$ mice show bilateral expression of Nodal and Lefty-2 in LPM, which results in ectopic expression of the homeobox transcription regulator Pitx2 in the right side of the foregut region (87). Pitx2 is clearly a powerful determinant of left-right asymmetry because ectopic expression of Pitx2 in the right LPM alters looping of the heart and gut and reverses body rotation in *Xenopus* embryos (90), whereas the phenotype of $Pitx2^{-/-}$ mice demonstrates right pulmonary isomerism and altered cardiac position (91-93). Growth/differentiation factor-1 (Gdf-1) encodes another member of the Tgf-β superfamily and it is proposed to acts upstream of Nodal, Lefty1 and Lefty2, and Pitx2 (94). Mice deficient for this factor as well as hypomorphic mutants for Nodal exhibit right pulmonary isomerism (89, 94).

Branching morphogenesis

The early branching of the primary bronchi tends to be monopodal. Starting at the level of the secondary bronchus, each bronchus subsequently undergoes dichotomous branching (i.e., each branch bifurcates repeatedly into two branches). The enlarging bronchial tree branches into the surrounding mesenchyme, which will eventually furrow into the characteristic lobes of the lung.

Epithelial-mesenchymal tissue interactions

Branching of the lung buds is controlled by epithelial-mesenchymal tissue interactions (95, 96). The mesenchymal component, most likely a soluble factor, dictates the branching pattern of the epithelium (97). The strong inductive capacity of pulmonary mesenchyme

was shown when pulmonary mesenchyme induced a lung epithelial phenotype in epithelial ureteric buds (98). Branching appears also to be regulated by positional information along the anterior-posterior axis of the lung because proximal mesenchyme (trachea and main bronchi) and distal mesenchyme (lung bud) differ in their ability to support epithelial branching morphogenesis (99-101). On the other hand, pulmonary epithelium is just as important for the survival of the mesenchyme, because it was shown that lung mesenchyme that was cultured in the absence of endoderm degenerated quickly (102, 103). Several lines of evidence point towards Shh as key player from the epithelium in mesenchyme survival and proliferation (38-40). Some progress has been made in elucidating the complex mixture of transcription factors and morphogens, which guide proper lung branching (Fig. 1). Although alterations in cell adhesion and matrix remodeling at the epithelial-mesenchymal interface also contribute to lung branching morphogenesis (104), they are not discussed in this chapter and the reader is referred to a published review (104).

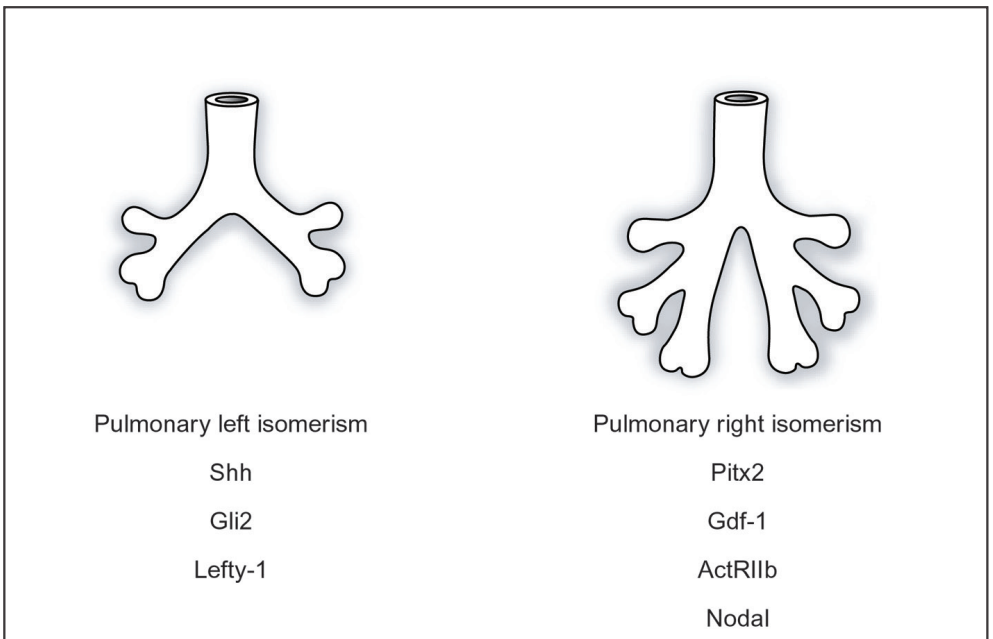

Figure 2. Transcription and growth factors involved in left-right determination of the developing lung (drawings represent human lungs, which in the normal situation consist of two lobes on the left and three lobes on the right side). See text for details.

Gata-6 and N-myc

It is evident from the previous discussion that transcription factors belonging to the Hox, Fox, and Nkx families are likely involved in the process of lung branching morphogenesis. Other transcription factors implicated in this process are Gata-6 and N-myc. Gata-6 belongs to the Gata family of zinc finger-containing transcription factors and is expressed in

epithelial and mesenchymal cells of the developing lung bud (105, 106). Gata-6 is essential for endoderm formation because targeted deletion of Gata-6 resulted in embryonic death long before lung formation owing to failure of visceral endoderm formation (107, 108). In the lung, Gata-6 appears to be important for branching morphogenesis, because inhibition of Gata-6 expression causes decreased branching morphogenesis (106, 107). More recently, expressing a Gata-6 engrailed dominant negative fusion protein in distal lung epithelium resulted in a lack of alveolar type I and a perturbation in alveolar type II cells together with a reduction in the number of proximal airway tubules (109). Conversely, overexpression of Gata-6, using the SP-C promoter, also disrupted branching morphogenesis and caused a lack of distal epithelial cell differentiation (110). In another study, overexpression of Gata-6 did not result in abnormal lung morphology until the early neonatal period (111). In that study, increased expression of Gata-6 impaired alveolarization, limited septation, and resulted in permanently altered lung function. The different outcomes from both Gata-6-overexpression studies is possibly based on the difference in Gata-6 isoform that was used to generate transgenic mice that overexpress Gata-6 (111). Altogether, these results indicate that a balanced Gata-6 expression level is important for branching morphogenesis during the pseudoglandular period of lung development but also during later stages of lung development when alveolar type I and II cells differentiate and the gas exchange area matures.

N-myc is a member of the myc family of proto-oncogenes, which includes N-myc, c-myc, and L-myc. Myc proteins belong to the basic helix-loop-helix (bHLH) class of transcription factors. In the lung, N-myc is expressed in pulmonary epithelium (112, 113). Mice homozygous for the N-myc null mutation die at midgestation (112, 114). Leaky null mutants for N-myc survive to the point when lung development starts; however, pulmonary branching morphogenesis is dramatically reduced, resulting in severe lung hypoplasia (113, 115).

Fibroblast growth factors

Several growth factors, including Fgfs and Tgf-βs have been shown to regulate lung branching morphogenesis (104, 116). Fgfs are generally produced by the pulmonary mesenchyme, whereas Fgfr1 and Fgf2 have been localized to both fetal pulmonary epithelium and mesenchyme (117-119). Also, the splice variant bek (IIIc) from the Fgfr2 is expressed in pulmonary mesenchyme, whereas the Kgfr (IIIb), which is another splice variant from Fgfr2, is localized in the epithelium (23, 120, 121). Transcripts for Fgf7 (also known as keratinocyte growth factor (Kgf)) are detected in lung mesenchyme at sites of active branching morphogenesis (122, 123). Exogenous Fgf7 inhibits rat lung branching morphogenesis *in vitro* (124) but stimulated proliferation of rat pulmonary type II cells *in vitro* (125) and *in vivo* (126, 127). Surprisingly, mice bearing a null mutation of the Fgf7 gene had no obvious lung abnormalities (128), a finding suggesting that Fgf7 can be replaced by other factors, such as Fgf1 and Fgf10. Fgf1, which binds to Fgfr1 and both Fgfr2 splice

variants, Fgfr2-IIIb and Fgfr2-IIIc, is crucial for branching of embryonic mouse epithelium in mesenchyme-free culture (16, 129). Fgf2, which binds to Fgfr1 and Fgfr2-IIIc, but hardly to Fgfr2-IIIb, did not affect epithelial branching in these cultures, a finding suggesting that the effect of Fgf1 on epithelial branching is mediated via Fgfr2-IIIb, which is the only receptor that binds Fgf7 (16, 121, 129). Fgf10 also binds to Fgfr2-IIIb, and both null mutants for Fgfr2-IIIb and Fgf10 have complete lung agenesis (20, 21, 29). Fgf1, Fgf7, and Fgf10 all induced epithelial expansion in E11.5 mouse lung explants and in mesenchyme-free distal lung buds in Matrigel culture, whereas Fgf1 and Fgf10, but never Fgf7, also induced epithelial branching (19, 45, 130). In contrast, epithelial proliferation was induced with Fgf7, but not with Fgf10 (45). Interestingly, embryonic lung mesenchymal cells that were cultured without epithelium showed a decreased expression of Fgf7 mRNA, whereas the expression of Fgf10 mRNA was dramatically increased (44). Taken together, these results indicate different functions for Fgf1, Fgf7, and Fgf10 during lung development. Fgf7 seems to be involved in lung bud expansion and pulmonary type II cell proliferation, but not branching, and it depends on the presence of lung epithelium for its expression in the mesenchyme. Conversely, Fgf1 and Fgf10 are able to induce branching morphogenesis, whereas mesenchymal Fgf10 expression appears to be inhibited by pulmonary epithelium. The finding that Fgf1, Fgf7, and Fgf10 elicit such different physiological responses may explain for example why Fgf7 cannot compensate for loss of Fgf10 *in vivo* (20, 21).

Another member of the Fgf family, Fgf9, is expressed in pulmonary epithelium in early development and at later gestation only in pulmonary mesothelium (23, 131). This expression pattern is different from that of Fgf1, Fgf7, and Fgf10, which are expressed only in the lung mesenchyme. Targeted deletion of Fgf9 resulted in severe lung hypoplasia and immediate postnatal death (131). Analysis of the lungs revealed decreased branching morphogenesis and a lack of alveoli; however, the numbers of lung lobes and primary bronchi were normal (131). Fgf9 deficiency affected lung size by decreased mesenchymal proliferation and reduced Fgf10 mRNA expression, whereas proximal-distal epithelial cell differentiation was normal (131). *In vitro*, Fgf9 inhibited at least some of the effects of recombinant N-Shh on the differentiation of smooth muscle cells in pulmonary mesenchyme (132).

Thyroid transcription factor-1

Severe branching morphogenesis defects were also seen in Ttf-1 null mutant mice (71, 73, 77). Besides the structural abnormalities in trachea and esophagus as a result of Ttf-1 deficiency, a lack of Ttf-1 also abrogates distal branching morphogenesis, which results in a lung comprised of cystic structures, lined with proximal epithelial cell types, and a structurally proximal vascular network (77).

Transforming growth factor-β

Tgf-β belongs to a superfamily that includes activin, bone morphogenetic protein (Bmp), and Tgf-β1, -2, and -3 (133). These peptides can exert a variety of biologic effects including regulation of cell growth and differentiation and expression of various proteins. Tgf-β1 plays an inhibitory role during lung development (134-138). In the lung, Tgf-β1 mRNA and protein were found in the mesenchyme (mRNA and protein) and epithelium (protein) (139-141). Both addition of exogenous Tgf-β1 to cultured embryonic mouse lung explants and *in vivo* overexpression of Tgf-β1 in distal lung epithelial cells resulted in decreased branching morphogenesis (134, 137). Overexpression of Tgf-β1 in distal pulmonary mouse epithelium *in vivo* arrested fetal lung development in the pseudoglandular stage of development, with inhibited epithelial and vascular development and differentiation, resulting in postnatal death (138). Most, if not all, biologic activities of Tgf-β are transmitted via transmembrane Ser/Thr kinase receptors, known as Tgf-β receptors (Tgf-βr) type I and type II (142). Signal transduction requires the formation of a heteromeric complex of Tgf-βrI and Tgf-βrII (142). In line with the negative influence of Tgf-β1 on lung branching, inhibition of Tgf-βrII signaling stimulated lung morphogenesis in whole lung explants *in vitro* (143). *In vivo* studies showed that Tgf-β1 null mutants themselves have no gross developmental abnormalities; however, 50% of the null mutants die before E11.5 because of defects in yolk sac vascularization (144, 145). Tgf-β3 null mutants die postnatally with cleft palate and delayed pulmonary development (146), whereas Tgf-β2-deficient mice die postnatally and display a lung phenotype characterized by postnatal collapse of alveoli and terminal airways (147). Smad proteins are downstream effector proteins in Tgf-β signaling (148). Smad-1 to Smad-3 proteins are expressed in distal lung epithelium, whereas Smad-4 is expressed in both distal lung epithelium and mesenchyme (149, 150). Downregulation of Smad-2/3 and Smad-4 expression increased branching morphogenesis in cultured lung explants (143). Exogenous Tgf-β1 did not reverse this inhibitory effect, a finding consistent with Tgf-βs being upstream of Smad proteins (150).

Wnt signaling

The vertebrate Wnt growth family of secreted glycoproteins comprises a well-known signaling pathway that is involved in cell-cell and epithelial-mesenchymal tissue interactions in many embryonic tissues (151, 152). The β-catenin/LEF-TCF pathway is the most well characterized pathway through which Wnt signals. In this pathway, secreted Wnt proteins bind to the cell membrane receptors of the frizzled family, thereby inhibiting phosphorylation of β-catenin. In this state, β-catenin is translocated to the nucleus where it heterodimerizes with members of the LEF-TCF transcription factor family to activate downstream target genes (151, 152). Several Wnt genes as well as a number of Wnt ligands and receptors are expressed in the developing lung (153, 154). Wnt7b is expressed throughout the airway and tracheal epithelium (40, 153). Mice deficient for Wnt7b die with respiratory failure around birth because of lung hypoplasia and lung hemorrhaging. Their lungs showed an early defect in mesenchymal proliferation and vascular smooth muscle

development (155). Differentiation of Clara cells and alveolar type II cells were normal in these animals, whereas type I cell differentiation was impaired (155). Conditional deletion of β-catenin from distal pulmonary epithelial cells revealed a role for β-catenin in the specification of proximal-distal cell fate and distal branching morphogenesis (156). The lungs in these transgenic mice consisted of primarily proximal airways, suggesting that β-catenin may be involved in the specification of the distal epithelial cell fate (156). Wnt5a was shown to be expressed in both developing pulmonary epithelial and mesenchyme, with highest expression in distal and branching tips (157). The absence of Wnt5a during lung development appeared to cause abnormal overexpansion of the distal airways with thick intersaccular walls, indicative of delayed maturation (157). Epithelial differentiation was somewhat delayed, but normal. In the same study (157) it was furthermore suggested that Wnt5a interacts with signaling pathways like Shh and Fgf10 during lung development. Taken together these data suggest a role for the Wnt signaling pathway in pulmonary branching morphogenesis.

Epithelial Differentiation

As branching proceeds, numerous different cell phenotypes are formed along the anterior-posterior axis of the developing epithelial tubules and associated mesenchymal components, each with different morphologies and patterns of gene expression. This patterning of differentiated lung cells may also be controlled by epithelial-mesenchymal interactions (6, 158, 159). For example, distal lung mesenchyme induced bud formation in the embryonic trachea that had been denuded of its own mesenchyme and normally does not branch (95, 99). Moreover, this induced tracheal epithelium exhibited specific markers of type II cell differentiation, including SP-C which is normally only present in distal pulmonary epithelium (100). Since the early 1990s, important regulatory molecules involved in epithelial morphogenetic patterning in the lung have been identified (Fig. 3).

Notch signaling

The Notch signaling pathway, is a signaling pathway that is involved in cell-cell interactions and cell-fate determination, thereby creating differences between neighboring cells (160, 161). Factors of the Notch signaling pathway such as Mash-1 and Hes1 have recently been localized in the developing lung; however, the functional role of the Notch signaling pathway in lung development remains to be elucidated (162, 163). Pulmonary neuroendocrine cells (PNECs) are the first cells to differentiate in the lungs of humans and animals (164, 165). The development of PNECs seems to be dependent on the expression of Mash-1, because Mash-1-deficient mice failed to develop PNECs (166). Mash-1 is a bHLH gene, expressed in neural precursor cells, directing terminal neural differentiation (167). Conversely, Hes1 represses neural differentiation through suppression of proneural

bHLH factors like Mash-1, and indeed, Hes1-deficient embryos have increased Mash-1 mRNA expression and increased numbers of PNECs in their lungs (162, 167-169). In the lung, Mash-1 is expressed in clusters or single progenitor PNECs (162, 166), whereas Hes1 is expressed in pulmonary epithelial cells other than PNECs (162). These results suggest an essential role for both transcription factors in the differentiation of PNECs, but not in pulmonary development *per se*, because gross lung morphology and differentiation in both mice appears to be unaffected (162, 166).

bHLH regulatory protein

Pod1 is another bHLH protein that acts as a transcriptional regulatory protein that governs cell fate determination and differentiation in a variety of tissues. The pod1 null mutant dies at birth with severely hypoplastic lungs that have a reduced number of tertiary branches and a lack of acinar tubules, terminal airsacs, and alveoli (170). Marker analysis revealed a disturbance in proximal-distal patterning of the lung epithelium with increased CCSP and decreased SP-C expression (170).

Transcription factors

Epithelial transcription factors such as Foxa2, Gata-6, and Ttf-1 have also been shown to influence lung epithelial specification. In both fetal mouse and human lung, the temporal-spatial distribution of Ttf-1 follows the pattern of expression of surfactant proteins (11, 75). It has been shown that Ttf-1 regulates the transcription of SP-A, -B, and -C (171-175) and CCSP (171, 176). Consequently, Ttf-1 null mutants lack distal epithelial cell differentiation (73), whereas the proximal epithelial cell marker Foxj1 (Hfh4) is unaffected (177). Taken together, these data underline the importance of Ttf-1 for the establishment of the distal epithelial cell phenotype. Moreover, Gata-6 transactivates SP-A and Ttf-1 (178, 179), and it has been shown that Gata-6 acts synergistically with Ttf-1 to influence the activity of the SP-C promoter (180). A role for Gata-6 in bronchial epithelial specification has been suggested by the observation that Gata-6$^{-/-}$ embryonic stem cells fail to contribute to bronchial epithelial cells (107). In some respiratory epithelial cells, Ttf-1 is co-expressed with members of the Fox family of transcription factors. Transcripts for Foxa1 and Foxa2 are detected in foregut cells forming the embryonic lung bud and later in the distal epithelium of the developing and mature lung (11, 181). Like Ttf-1, Foxa1 and Foxa2 appear to modulate the expression of SP-B and CCSP (171, 181, 182). Foxa1 and Foxa2 are likely upstream regulators of Ttf-1 (183), and it is possible that both members of the Fox family confer lung-specific gene expression in the primitive foregut through Ttf-1 as the intermediate.

Fibroblast growth factors

Mouse transgenics that overexpressed a (soluble) dominant negative Fgfr2-IIIb splice variant in distal lung epithelium, showed a severe pulmonary defect with only rudimentary formation of the trachea and main bronchi, but without any lateral branches (27, 28).

In these lungs, Ttf-1 was normally expressed in the remaining lung tissue, whereas SP-C expression was absent and virtually replaced by CCSP (27, 28). These results indicate that Fgf signaling is involved in the proximal-distal differentiation of lung epithelium, and that Fgf signaling functions downstream of Ttf-1 or in a parallel, but different, pathway altogether.

Winged helix/forkhead family

Hnf3/forkhead homologue 4 (Hfh4: Foxj1) is a transcription factor of the winged helix/forkhead family, expressed in various tissues during development. In the developing and adult lung, Foxj1 expression is restricted to ciliated cells of the bronchial and bronchiolar epithelium (177, 184). The role of Foxj1 in ciliated cell differentiation was clearly demonstrated when Foxj1 was overexpressed in distal pulmonary epithelial cells. High levels of Foxj1 expression inhibited branching morphogenesis and enhanced the development of ciliated cells, whereas the development of distal epithelial cells was inhibited (185). In contrast, Foxj1 null mutant mice completely lack respiratory ciliated cells (85, 186). These data indicate that Foxj1 is essential for the development of pulmonary ciliated cells.

Bone morphogenetic protein

Secreted morphogens such as Shh appear not to be involved in regulating proximal-distal epithelial specification because SP-C and CCSP are expressed in Shh-deficient mice (40). In *Drosophila*, *Hh* may regulate the expression of *Decapentaplegic* (*Dpp*), the *Drosophila* counterpart of Bmp (37). In the murine lung, Bmp4 is implicated in lung epithelial specification. Bmp4 is expressed in early distal lung tips and at lower levels in the mesenchyme adjacent to the distal lung buds (187, 188). Overexpression of Bmp4 in the distal epithelium *in vivo* resulted in hypoplastic lungs with grossly dilated terminal lung buds separated by abundant mesenchyme (187). Distal epithelial differentiation was abnormal with decreased SP-C expression, whereas proximal differentiation (CCSP expression) was unaffected (187). Conversely, exogenous Bmp4 clearly enhanced peripheral lung epithelial branching morphogenesis and SP-C expression *in vitro* (189), whereas inhibition of Bmp4 signaling also resulted in a severe reduction in distal epithelial cell types, and an increase in proximal cell types (188, 189). Also, *in vitro*, Bmp4 antagonizes the mitogenic effects of Fgf10 on epithelial bud extension and proliferation, whereas Fgf10 itself induces the expression of its own antagonist Bmp4 (190). In a model by Weaver and co-workers (190) it was proposed that Fgf10 is needed for branching, whereas Bmp4 is associated with bud extension, but not with branching. If Bmp4 expression is higher locally than Fgf10 expression, Fgf10 fails to induce further budding, and extension occurs until Bmp4 levels are low enough to permit further branching. A dynamic expression pattern of these two genes is required for the coordinated branching and elongation of airway tubules during lung development. The secreted Bmp antagonist Noggin is expressed in distal mouse lung mesenchyme at early development (188). Overexpression of Xnoggin

or the dominant negative Bmp receptor dnAlk6 in distal pulmonary epithelium resulted in a proximal epithelial phenotype of the fetal lung (188). Similar results were obtained when Gremlin, another Bmp antagonist, was overexpressed in the distal lung epithelium (191). These studies clearly indicate a role for Bmp4 in proximal-distal epithelial differentiation during lung development and as a result probably argue against Shh as a regulator of Bmp4 expression.

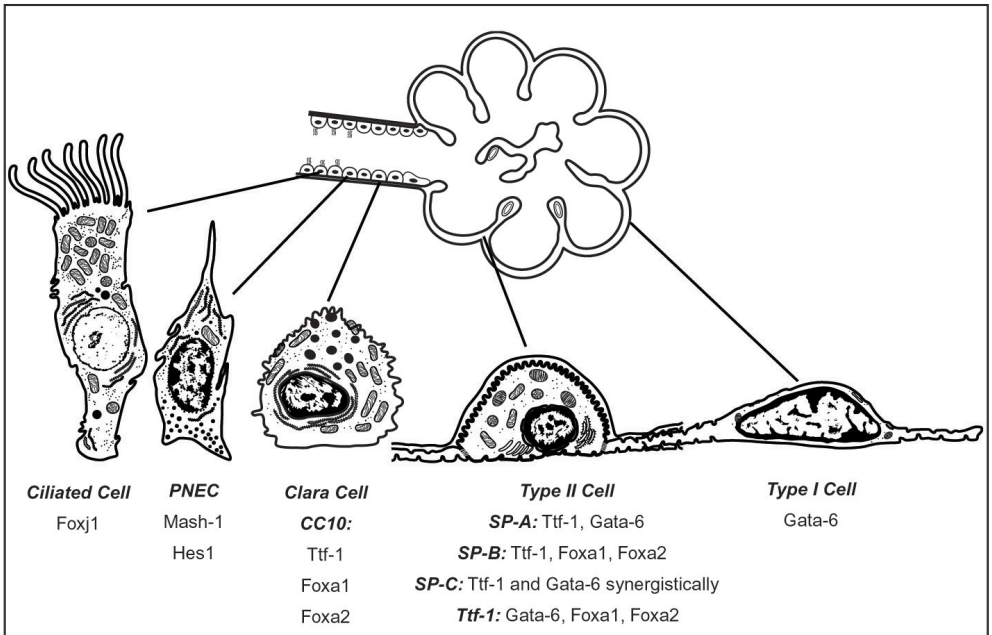

Figure 3. Molecular control of epithelial cell differentiation during lung development. See text for details

ALVEOLAR DEVELOPMENT

Alveolarization is the last step of lung development. Alveoli are formed by septation of the pulmonary saccules that form the immature lung. In both human and rodents, alveolarization occurs predominately after birth. In the first two weeks after birth, alveolar formation, measured as proliferation, occurs in both central and peripheral areas of the murine lung, whereas afterwards, alveolar formation occurs mainly in peripheral areas of the lung (192). Proliferation in alveolar septae is greatly diminished in adult lungs (192).

Platelet-derived growth factors

One of the key elements in the alveolarization process (Fig. 1) appears to be the one of the three isoforms of the platelet-derived growth factors (Pdgf), namely, PdgfA (193). PdgfA mRNA and protein are expressed in early pulmonary epithelium (194-196). The receptor for PdgfA, Pdgfrα, is expressed in the mesenchyme adjacent to the epithelium that expresses PdgfA, a finding suggesting a paracrine signaling loop between epithelium and mesenchyme (194, 196-198). The *in vitro* inhibition of PdgfA or Pdgfrα in embryonic rat

lung explants, decreased both lung size and number of terminal buds, findings indicating a role for PdgfA-Pdgfrα signaling in early lung development (194, 196-199). Conversely, the *in vivo* overexpression of PdgfA in distal airway epithelium, doubled lung size and increased distal branching morphogenesis (200). However, the morphology of these lungs was arrested at the canalicular stage of lung development, with abundant mesenchyme and a lack of airspaces, resulting in postnatal death (200). These results indicate that PdgfA is a potent growth factor for mesenchymal cells in the developing lung. In mice, absence of PdgfA results in prenatal and postnatal death (197, 198). Postnatal deaths were characterized by emphysematous lungs with areas of atelectasis, without any formation of septa and alveoli. Instead, dilated prealveolar saccules were found (197, 198). In normal mice, alveolar septa contain α-smooth muscle actin (α-sma)-positive myofibroblasts. The postnatal PdgfA null mutant lungs lack alveolar staining for α-sma, a finding indicating a lack of alveolar myofibroblasts. In addition, they were almost completely devoid of parenchymal elastin fibers, and this most likely contributed to the failure of alveolar formation (197, 198). Interestingly, myofibroblasts surrounding vessels and bronchioles appeared normal and were tropoelastin positive, a finding suggesting a different developmental lineage (198). Moreover, Pdgfrα positive cells were specifically missing from lungs of PdgfA null mutants, and it has been proposed that these cells are progenitor cells for alveolar myofibroblasts (197, 198). Pdgfrα-deficient mice die *in utero* with severe skeletal malformations and incomplete cephalic closure (201). Pdgfrα-deficient lungs were hypoplastic; however, primary branching and histology were not affected (202, 203). Postnatal alveolar formation could not be examined in these mice. Taken together, these data suggest that PdgfA is needed for the development of alveolar myofibroblasts that produce elastin, which, in turn, is crucial for alveolar septation and formation.

Tropoelastin

The critical value of elastin in the development of proper alveolar structures was demonstrated in mice lacking tropoelastin, the soluble component of the elastic fiber. Tropoelastin null mice exhibited a severe reduction in alveolar formation and decreased terminal airway branching leading to almost immediate postnatal death (204). The tropoelastin-deficient mouse; however, shows alveolar destruction much earlier and more severe than the PdgfA-deficient mouse, suggesting that PdgfA is not the only regulator of elastin (197, 198, 204).

Retinoic acid

At late gestation and early postnatal life, rodent pulmonary fibroblasts contain a considerable amount of vitamin A (205-207). Before birth, pulmonary fibroblasts contain retinyl esters, which around birth are converted into retinol and RA, the active components of vitamin A (206). Both endogenous (208) and exogenous RA (209) increased the level of tropoelastin mRNA almost threefold in neonatal rat lung fibroblasts, whereas inhibition of the production of RA decreased tropoelastin gene expression in

postnatal rat lung fibroblast (208). Two enzymes, Aldh-1 (aldehyde dehydrogenase) and Raldh-2 (retinal dehydrogenase), are rate limiting in the conversion of retinal to RA (54). Both are expressed at high levels in the immediate postnatal mouse lung, the time of maximal alveolarization, and at lower, more adult-like levels, two weeks after birth (192). Aldh-1 is expressed in central regions and alveolar septa, whereas Raldh-2 is expressed in central and subpleural regions (192). Further evidence that RA plays a role in lung elastin maintenance and alveolarization was provided by the genetic manipulation of RAR and RXR in mice. Compound mice homozygous for an RXRγ and heterozygous for an RXRα deletion had a reduced number of alveoli and less elastic fibers in their alveolar walls (210). Conversely, RARβ appears to be an endogenous inhibitor of septation, and indeed, the RARβ null mutant shows early onset septation resulting in twice as many alveoli in the null mutant lungs when compared with wild-type lungs (211).

Fibroblast growth factors

Other factors implicated in postnatal alveolarization include Fgfs, Ttf-1, and Tgf-α. Both Fgfr3 and Fgfr4 are expressed in postnatal pulmonary mesenchyme, whereas their ligands are expressed in pulmonary epithelial cells (212). Although a null mutation of either Fgfr3 or Fgfr4 caused no obvious lung defects, silencing of both receptors resulted in severe overall body growth retardation and a failure of postnatal alveolar formation (212). Despite the large dilated saccules without any proper alveolar septation, differentiation (including α-sma-positive myofibroblasts) and proliferation proceeded normally (212).

Transforming growth factors

Tgf-α is a member of the epidermal growth factor (Egf) family that signals via the Egf receptor (Egfr), and both have been shown to be expressed and involved in pre- and postnatal lung development (213). The Egfr null mutant dies soon after birth with immature lung morphology, impaired alveologenesis, and surfactant protein deficiency (214, 215). Conversely, the Tgf-α null mutant survived into adulthood without reported lung abnormalities, results indicating that factors, other than Tgf-α, signal via the Egfr and are important for lung development (216). However, overexpression of Tgf-α in distal pulmonary epithelial cells using the human SP-C promoter resulted in disruption of postnatal alveolarization causing lung emphysema and fibrosis (217). It increased proliferation of alveolar epithelial cells including SP-C expressing type II cells, without causing inflammation (218). Elastin fibers were shorter and blunter in the bronchiolar regions and deficient in alveolar septae, most likely contributing to the emphysematic lesion (217).

Thyroid transcription factor-1

Besides its role in prenatal lung development, Ttf-1 also regulates postnatal lung development and homeostasis. Postnatally, Ttf-1 expression decreases dramatically, but remains detectable in adult alveolar type II cells (11, 75, 219). Overexpression of

Ttf-1 in distal lung epithelial cells, using the SP-C promoter, did not affect prenatal lung development, but it perturbed postnatal alveolarization and led to emphysema, severe inflammation, and fibrosis (220).

Vascular Development

The lung is composed of a complex network of airways and vessels, and although much has been learned regarding the mechanisms controlling lung bud formation and airway branching, the mechanisms involved in vascular formation during lung development remain obscure. Three processes are believed to control pulmonary vascular development: angiogenesis, which is defined as sprouting of new vessels from pre-existing ones and gives rise to the central vessels; vasculogenesis, which is *de novo* synthesis of blood vessels from blood islands in the periphery of the lung; and the fusion of proximal and peripheral vessels to form the pulmonary circulation (221, 222). Investigators have shown that, even in the early stages of lung development, vascular connections are well established, and that vascular development takes place during all stages of lung development, with completion of a single capillary network during the alveolar period (223, 224).

Vascular endothelial growth factor

The molecular mechanisms involved in pulmonary vascular formation are relatively unknown. Members of the vascular endothelial growth factor (Vegf) family (225-227), the Angiopoietin family (228, 229), and members of the Ephrin family (230) have all been implicated in controlling vascularization of the pulmonary system. Vegf, a potent mitogen for endothelial cells, influences angiogenesis and vasculogenesis (231). It is essential for embryonic development, and even haploinsufficiency of Vegf causes embryonic lethality (232, 233). In the embryonic lung, Vegf mRNA is mainly detected in lung epithelium, and its expression increases only prior to birth, and remains high in the adult lung (234-238). Vegf signals via two high-affinity tyrosine kinase receptors, Vegfr1 (Flt-1) and Vegfr2 (Kdr/Flk-1), which in the embryonic lung are localized in the mesenchyme (235, 236). The complementary expression patterns of Vegf in lung epithelium and the two Vegf receptors in the mesenchyme suggest a paracrine mode of action on the formation of the pulmonary vascular system, which may influence lung branching morphogenesis (102). Alternative splicing of the Vegf gene produces multiple species of mRNA. These encode different Vegf protein isoforms varying from 120 to 205 amino acids. Overexpression of the Vegf 164 isoform in distal airway epithelium of mice resulted in perinatal death (239). The lungs appeared abnormal with dilated respiratory tubules and saccules and a decreased number of terminal buds, as well as a lack of alveolar type I cell differentiation (239). Conversely, mice that lacked the Vegf 164 and 188 isoforms and only expressed the Vegf 120 isoform had a decrease in peripheral vascular development with fewer air-blood

barriers and a general delay in lung development, but normal type I cell differentiation (240). Similarly, neonatal mice that were treated with a soluble decoy receptor for Vegfr1 to block endogenous Vegf signaling, exhibited an overall dramatic decrease in body and organ growth and died within 4-6 days after birth (241). The lungs of these mice were immature with simplification of the alveolar region and a decrease in Vegfr2 expression (241). Inhibition of Vegfr signaling using the Vegfr blocker Su-5416 either before or after birth, also resulted in reduced pulmonary vascularization and alveolarization and increased apoptosis in alveolar septae, which leads to an emphysema-like phenotype (242, 243). An interesting finding in this study was that early inhibition of vascular development caused long-term effects on alveolarization and as pulmonary hypertension (243), and that the development of emphysema was inhibited when a caspase inhibitor was injected simultaneously, findings indicating that alveolar septal cell apoptosis contributes to the pathogenesis of emphysema (242). Taken together, these results again suggest a role for Vegf itself, or vascular development, in alveolar formation.

Forkhead transcription factor-Foxf1

Another factor implicated in pulmonary vascular development is Foxf1 (also known as Hfh8 or Fraec1). Foxf1 null mutant mice die *in utero* because of defects in mesodermal differentiation and cell adhesion (244). In the embryonic lung, Foxf1 expression is restricted to the pulmonary mesenchyme, whereas in the adult lung, Foxf1 is expressed in smooth muscle cells surrounding bronchioles and in the endothelium and fibroblasts of the alveolar sacs (245, 246). Heterozygous mutant mice carrying a disruption of the Foxf1 gene, in which Foxf1 levels are reduced by 80% ($Foxf1^{+/-low}$), displayed a 55% postnatal mortality with lung hemorrhaging. Analysis of these $Foxf1^{+/-low}$ lungs revealed abnormalities in alveolar formation and pulmonary vasculature (246). From these studies, it can be concluded that a disruption in pulmonary vascular development goes hand in hand with impaired branching morphogenesis and lung hypoplasia. The question remains whether impaired airway branching is the indirect result of disrupted vessel formation or whether the factors involved in vascular development directly affect pulmonary branching as well.

Synopsis

Molecular studies of lung development have started to unravel the complex series of events that control proper formation of the lung. Observations such as no lung formation are interesting for understanding organogenesis of the lung itself, but the clinical relevance is minimal, because having no lung is incompatible with life. However, the finding that factors implicated in foregut specification are also regulating lung branching morphogenesis is tremendously intriguing for clinical practice. One of the major complications of preterm

birth is immaturity of the lung. Despite modern management, many infants exhibit lung dysfunction characterized by arrested lung development and interrupted alveolarization. A better understanding of the molecular basis of pulmonary development may guide clinicians in the design of strategies to support normal lung maturation in a premature infant.

References

1. Wert SE: Normal and abnormal structural development of the lung. In Polin RA, Fox WW,Abman SH (eds): Fetal and Neonatal Physiology, 3rd 3rd, vol 1, p 783-794. Philadelphia, Saunders, Harcourt Health Sciences, 2004.

2. Ten Have-Opbroek AA, 1991. Lung development in the mouse embryo. Exp Lung Res. 17:111-130.

3. Perl AK, Whitsett JA, 1999. Molecular mechanisms controlling lung morphogenesis. Clin Genet. 56:14-27.

4. Warburton D, Schwarz M, Tefft D, Flores-Delgado G, Anderson KD, Cardoso WV, 2000. The molecular basis of lung morphogenesis. Mech Dev. 92:55-81.

5. Cardoso WV, 2000. Lung morphogenesis revisited: old facts, current ideas. Dev Dyn. 219:121-130.

6. Hogan BL, Grindley J, Bellusci S, Dunn NR, Emoto H, Itoh N, 1997. Branching morphogenesis of the lung: new models for a classical problem. Cold Spring Harb Symp Quant Biol. 62:249-256.

7. Ang SL, Wierda A, Wong D, Stevens KA, Cascio S, Rossant J, Zaret KS, 1993. The formation and maintenance of the definitive endoderm lineage in the mouse: involvement of HNF3/forkhead proteins. Development. 119:1301-1315.

8. Kaestner KH, Knochel W, Martinez DE, 2000. Unified nomenclature for the winged helix/forkhead transcription factors. Genes Dev. 14:142-146.

9. Monaghan AP, Kaestner KH, Grau E, Schutz G, 1993. Postimplantation expression patterns indicate a role for the mouse forkhead/HNF-3 alpha, beta and gamma genes in determination of the definitive endoderm, chordamesoderm and neuroectoderm. Development. 119:567-578.

10. Stahlman MT, Gray ME, Whitsett JA, 1998. Temporal-spatial distribution of hepatocyte nuclear factor-3beta in developing human lung and other foregut derivatives. J Histochem Cytochem. 46:955-962.

11. Zhou L, Lim L, Costa RH, Whitsett JA, 1996. Thyroid transcription factor-1, hepatocyte nuclear factor-3beta, surfactant protein B, C, and Clara cell secretory protein in developing mouse lung. J Histochem Cytochem. 44:1183-1193.

12. Weinstein DC, Ruiz i Altaba A, Chen WS, Hoodless P, Prezioso VR, Jessell TM, Darnell JE, Jr., 1994. The winged-helix transcription factor HNF-3 beta is required for notochord development in the mouse embryo. Cell. 78:575-588.

13. Ang SL, Rossant J, 1994. HNF-3 beta is essential for node and notochord formation in mouse development. Cell. 78:561-574.

14. Dufort D, Schwartz L, Harpal K, Rossant J, 1998. The transcription factor HNF3beta is required in visceral endoderm for normal primitive streak morphogenesis. Development. 125:3015-3025.

15. Zhou L, Dey CR, Wert SE, Yan C, Costa RH, Whitsett JA, 1997. Hepatocyte nuclear factor-3beta limits cellular diversity in the developing respiratory epithelium and alters lung morphogenesis in vivo. Dev Dyn. 210:305-314.

16. Goldfarb M, 1996. Functions of fibroblast growth factors in vertebrate development. Cytokine Growth Factor Rev. 7:311-325.

17. Kato S, Sekine K, 1999. FGF-FGFR signaling in vertebrate organogenesis. Cell Mol Biol (Noisy-le-grand). 45:631-638.

18. Ornitz DM, Itoh N, 2001. Fibroblast growth factors. Genome Biol. 2.

19. Bellusci S, Grindley J, Emoto H, Itoh N, Hogan BL, 1997. Fibroblast growth factor 10 (FGF10) and branching morphogenesis in the embryonic mouse lung. Development. 124:4867-4878.

20. Sekine K, Ohuchi H, Fujiwara M, Yamasaki M, Yoshizawa T, Sato T, Yagishita N, Matsui D, Koga Y, Itoh N, Kato S, 1999. Fgf10 is essential for limb and lung formation. Nat Genet. 21:138-141.

21. Min H, Danilenko DM, Scully SA, Bolon B, Ring BD, Tarpley JE, DeRose M, Simonet WS, 1998. Fgf-10 is required for both limb and lung development and exhibits striking functional similarity to Drosophila branchless. Genes Dev. 12:3156-3161.

22. Ornitz DM, Xu J, Colvin JS, McEwen DG, MacArthur CA, Coulier F, Gao G, Goldfarb M, 1996. Receptor specificity of the fibroblast growth factor family. J Biol Chem. 271:15292-15297.

23. Arman E, Haffner-Krausz R, Gorivodsky M, Lonai P, 1999. Fgfr2 is required for limb outgrowth and lung-branching morphogenesis. Proc Natl Acad Sci U S A. 96:11895-11899.

24. Igarashi M, Finch PW, Aaronson SA, 1998. Characterization of recombinant human fibroblast growth factor (FGF)-10 reveals functional similarities with keratinocyte growth factor (FGF-7). J Biol Chem. 273:13230-13235.

25. Arman E, Haffner-Krausz R, Chen Y, Heath JK, Lonai P, 1998. Targeted disruption of fibroblast growth factor (FGF) receptor 2 suggests a role for FGF signaling in pregastrulation mammalian development. Proc Natl Acad Sci U S A. 95:5082-5087.

26. Xu X, Weinstein M, Li C, Naski M, Cohen RI, Ornitz DM, Leder P, Deng C, 1998. Fibroblast growth factor receptor 2 (FGFR2)-mediated reciprocal regulation loop between FGF8 and FGF10 is essential for limb induction. Development. 125:753-765.

27. Peters K, Werner S, Liao X, Wert S, Whitsett J, Williams L, 1994. Targeted expression of a dominant negative FGF receptor blocks branching morphogenesis and epithelial differentiation of the mouse lung. Embo J. 13:3296-3301.

28. Celli G, LaRochelle WJ, Mackem S, Sharp R, Merlino G, 1998. Soluble dominant-negative receptor uncovers essential roles for fibroblast growth factors in multi-organ induction and patterning. Embo J. 17:1642-1655.

29. De Moerlooze L, Spencer-Dene B, Revest J, Hajihosseini M, Rosewell I, Dickson C, 2000. An important role for the IIIb isoform of fibroblast growth factor receptor 2 (FGFR2) in mesenchymal-epithelial signalling during mouse organogenesis. Development. 127:483-492.

30. Sutherland D, Samakovlis C, Krasnow MA, 1996. branchless encodes a Drosophila FGF homolog that controls tracheal cell migration and the pattern of branching. Cell. 87:1091-1101.

31. Klambt C, Glazer L, Shilo BZ, 1992. breathless, a Drosophila FGF receptor homolog, is essential for migration of tracheal and specific midline glial cells. Genes Dev. 6:1668-1678.

32. Hacohen N, Kramer S, Sutherland D, Hiromi Y, Krasnow MA, 1998. sprouty encodes a novel antagonist of FGF signaling that patterns apical branching of the Drosophila airways. Cell. 92:253-263.

33. Placzek M, Skaer H, 1999. Airway patterning: A paradigm for restricted signalling. Curr Biol. 9:R506-510.

34. Zhang S, Lin Y, Itaranta P, Yagi A, Vainio S, 2001. Expression of Sprouty genes 1, 2 and 4 during mouse organogenesis. Mech Dev. 109:367-370.

35. Mailleux AA, Tefft D, Ndiaye D, Itoh N, Thiery JP, Warburton D, Bellusci S, 2001. Evidence that SPROUTY2 functions as an inhibitor of mouse embryonic lung growth and morphogenesis. Mech Dev. 102:81-94.

36. Perl AK, Hokuto I, Impagnatiello MA, Christofori G, Whitsett JA, 2003. Temporal effects of Sprouty on lung morphogenesis. Dev Biol. 258:154-168.

37. Ingham PW, McMahon AP, 2001. Hedgehog signaling in animal development: paradigms and principles. Genes Dev. 15:3059-3087.

38. Bellusci S, Furuta Y, Rush MG, Henderson R, Winnier G, Hogan BL, 1997. Involvement of Sonic hedgehog (Shh) in mouse embryonic lung growth and morphogenesis. Development. 124:53-63.

39. Litingtung Y, Lei L, Westphal H, Chiang C, 1998. Sonic hedgehog is essential to foregut development. Nat Genet. 20:58-61.

40. Pepicelli CV, Lewis PM, McMahon AP, 1998. Sonic hedgehog regulates branching morphogenesis in the mammalian lung. Curr Biol. 8:1083-1086.

41. Chuang PT, McMahon AP, 1999. Vertebrate Hedgehog signalling modulated by induction of a Hedgehog-binding protein. Nature. 397:617-621.

42. Chuang PT, Kawcak T, McMahon AP, 2003. Feedback control of mammalian Hedgehog signaling by the Hedgehog-binding protein, Hip1, modulates Fgf signaling during branching morphogenesis of the lung. Genes Dev. 17:342-347.

43. Chuang PT, McMahon AP, 2003. Branching morphogenesis of the lung: new molecular insights into an old problem. Trends Cell Biol. 13:86-91.

44. Lebeche D, Malpel S, Cardoso WV, 1999. Fibroblast growth factor interactions in the developing lung. Mech Dev. 86:125-136.

45. Park WY, Miranda B, Lebeche D, Hashimoto G, Cardoso WV, 1998. FGF-10 is a chemotactic factor for distal epithelial buds during lung development. Dev Biol. 201:125-134.

46. Nybakken K, Perrimon N, 2002. Hedgehog signal transduction: recent findings. Curr Opin Genet Dev. 12:503-511.

47. Grindley JC, Bellusci S, Perkins D, Hogan BL, 1997. Evidence for the involvement of the Gli gene family in embryonic mouse lung development. Dev Biol. 188:337-348.

48. Motoyama J, Liu J, Mo R, Ding Q, Post M, Hui CC, 1998. Essential function of Gli2 and Gli3 in the formation of lung, trachea and oesophagus. Nat Genet. 20:54-57.

49. Bai CB, Joyner AL, 2001. Gli1 can rescue the in vivo function of Gli2. Development. 128:5161-5172.

50. Park HL, Bai C, Platt KA, Matise MP, Beeghly A, Hui CC, Nakashima M, Joyner AL, 2000. Mouse Gli1 mutants are viable but have defects in SHH signaling in combination with a Gli2 mutation. Development. 127:1593-1605.

51. Mahlapuu M, Enerback S, Carlsson P, 2001. Haploinsufficiency of the forkhead gene Foxf1, a target for sonic hedgehog signaling, causes lung and foregut malformations. Development. 128:2397-2406.

52. Ross SA, McCaffery PJ, Drager UC, De Luca LM, 2000. Retinoids in embryonal development. Physiol Rev. 80:1021-1054.

53. Zile MH, 2001. Function of vitamin A in vertebrate embryonic development. J Nutr. 131:705-708.

54. Duester G, 2001. Genetic dissection of retinoid dehydrogenases. Chem Biol Interact. 130-132:469-480.

55. Mendelsohn C, Lohnes D, Decimo D, Lufkin T, LeMeur M, Chambon P, Mark M, 1994. Function of the retinoic

acid receptors (RARs) during development (II). Multiple abnormalities at various stages of organogenesis in RAR double mutants. Development. 120:2749-2771.

56. Luo J, Sucov HM, Bader JA, Evans RM, Giguere V, 1996. Compound mutants for retinoic acid receptor (RAR) beta and RAR alpha 1 reveal developmental functions for multiple RAR beta isoforms. Mech Dev. 55:33-44.

57. Kastner P, Mark M, Ghyselinck N, Krezel W, Dupe V, Grondona JM, Chambon P, 1997. Genetic evidence that the retinoid signal is transduced by heterodimeric RXR/RAR functional units during mouse development. Development. 124:313-326.

58. Packer AI, Mailutha KG, Ambrozewicz LA, Wolgemuth DJ, 2000. Regulation of the Hoxa4 and Hoxa5 genes in the embryonic mouse lung by retinoic acid and TGFbeta1: implications for lung development and patterning. Dev Dyn. 217:62-74.

59. Cardoso WV, Mitsialis SA, Brody JS, Williams MC, 1996. Retinoic acid alters the expression of pattern-related genes in the developing rat lung. Dev Dyn. 207:47-59.

60. Cardoso WV, 1995. Transcription factors and pattern formation in the developing lung. Am J Physiol. 269: L429-L442.

61. Volpe MV, Vosatka RJ, Nielsen HC, 2000. Hoxb-5 control of early airway formation during branching morphogenesis in the developing mouse lung. Biochim Biophys Acta. 1475:337-345.

62. Krumlauf R, 1994. Hox genes in vertebrate development. Cell. 78:191-201.

63. Kappen C, 1996. Hox genes in the lung. Am J Respir Cell Mol Biol. 15:156-162.

64. Krumlauf R, Holland PW, McVey JH, Hogan BL, 1987. Developmental and spatial patterns of expression of the mouse homeobox gene, Hox 2.1. Development. 99:603-617.

65. Wall NA, Jones CM, Hogan BL, Wright CV, 1992. Expression and modification of Hox 2.1 protein in mouse embryos. Mech Dev. 37:111-120.

66. Bogue CW, Gross I, Vasavada H, Dynia DW, Wilson CM, Jacobs HC, 1994. Identification of Hox genes in newborn lung and effects of gestational age and retinoic acid on their expression. Am J Physiol. 266: L448-454.

67. Bogue CW, Lou LJ, Vasavada H, Wilson CM, Jacobs HC, 1996. Expression of Hoxb genes in the developing mouse foregut and lung. Am J Respir Cell Mol Biol. 15:163-171.

68. Volpe MV, Martin A, Vosatka RJ, Mazzoni CL, Nielsen HC, 1997. Hoxb-5 expression in the developing mouse lung suggests a role in branching morphogenesis and epithelial cell fate. Histochem Cell Biol. 108:495-504.

69. Rossel M, Capecchi MR, 1999. Mice mutant for both Hoxa1 and Hoxb1 show extensive remodeling of the hindbrain and defects in craniofacial development. Development. 126:5027-5040.

70. Aubin J, Lemieux M, Tremblay M, Berard J, Jeannotte L, 1997. Early postnatal lethality in Hoxa-5 mutant mice is attributable to respiratory tract defects. Dev Biol. 192:432-445.

71. Kimura S, Hara Y, Pineau T, Fernandez-Salguero P, Fox CH, Ward JM, Gonzalez FJ, 1996. The T/ebp null mouse: thyroid-specific enhancer-binding protein is essential for the organogenesis of the thyroid, lung, ventral forebrain, and pituitary. Genes Dev. 10:60-69.

72. Lazzaro D, Price M, de Felice M, Di Lauro R, 1991. The transcription factor TTF-1 is expressed at the onset

of thyroid and lung morphogenesis and in restricted regions of the foetal brain. Development. 113:1093-1104.

73. Minoo P, Su G, Drum H, Bringas P, Kimura S, 1999. Defects in tracheoesophageal and lung morphogenesis in Nkx2.1(-/-) mouse embryos. Dev Biol. 209:60-71.

74. Zhou H, Morotti RA, Profitt SA, Langston C, Wert SE, Whitsett JA, Greco MA, 2001. Expression of thyroid transcription factor-1, surfactant proteins, type I cell-associated antigen, and Clara cell secretory protein in pulmonary hypoplasia. Pediatr Dev Pathol. 4:364-371.

75. Stahlman MT, Gray ME, Whitsett JA, 1996. Expression of thyroid transcription factor-1(TTF-1) in fetal and neonatal human lung. J Histochem Cytochem. 44:673-678.

76. Kimura S, Ward JM, Minoo P, 1999. Thyroid-specific enhancer-binding protein/thyroid transcription factor 1 is not required for the initial specification of the thyroid and lung primordia. Biochimie. 81:321-327.

77. Yuan B, Li C, Kimura S, Engelhardt RT, Smith BR, Minoo P, 2000. Inhibition of distal lung morphogenesis in Nkx2.1(-/-) embryos. Dev Dyn. 217:180-190.

78. Albers GM, Wood RE: The Lower Respiratory Organs: Tracheoesophageal Fistula. In Stevenson RE, Hall JG,Goodman RM (eds): Oxford Monographs on Medical Genetics no 27; Human Malformations and Related Anomalies, vol II, p 350-351. Oxford, New York, Oxford University Press, 1993.

79. Hamada H, Meno C, Watanabe D, Saijoh Y, 2002. Establishment of vertebrate left-right asymmetry. Nat Rev Genet. 3:103-113.

80. Meyers EN, Martin GR, 1999. Differences in left-right axis pathways in mouse and chick: functions of FGF8 and SHH. Science. 285:403-406.

81. Tsukui T, Capdevila J, Tamura K, Ruiz-Lozano P, Rodriguez-Esteban C, Yonei-Tamura S, Magallon J, Chandraratna RA, Chien K, Blumberg B, Evans RM, Belmonte JC, 1999. Multiple left-right asymmetry defects in Shh(-/-) mutant mice unveil a convergence of the shh and retinoic acid pathways in the control of Lefty-1. Proc Natl Acad Sci U S A. 96:11376-11381.

82. Boettger T, Wittler L, Kessel M, 1999. FGF8 functions in the specification of the right body side of the chick. Curr Biol. 9:277-280.

83. Garcia-Castro MI, Vielmetter E, Bronner-Fraser M, 2000. N-Cadherin, a cell adhesion molecule involved in establishment of embryonic left-right asymmetry. Science. 288:1047-1051.

84. Oh SP, Li E, 1997. The signaling pathway mediated by the type IIB activin receptor controls axial patterning and lateral asymmetry in the mouse. Genes Dev. 11:1812-1826.

85. Chen J, Knowles HJ, Hebert JL, Hackett BP, 1998. Mutation of the mouse hepatocyte nuclear factor/forkhead homologue 4 gene results in an absence of cilia and random left-right asymmetry. J Clin Invest. 102:1077-1082.

86. Meno C, Saijoh Y, Fujii H, Ikeda M, Yokoyama T, Yokoyama M, Toyoda Y, Hamada H, 1996. Left-right asymmetric expression of the TGF beta-family member lefty in mouse embryos. Nature. 381:151-155.

87. Meno C, Shimono A, Saijoh Y, Yashiro K, Mochida K, Ohishi S, Noji S, Kondoh H, Hamada H, 1998. lefty-1 is required for left-right determination as a regulator of lefty-2 and nodal. Cell. 94:287-297.

88. Meno C, Takeuchi J, Sakuma R, Koshiba-Takeuchi K, Ohishi S, Saijoh Y, Miyazaki J, ten Dijke P, Ogura T, Hamada H, 2001. Diffusion of nodal signaling activity in the absence of the feedback inhibitor Lefty2. Dev Cell. 1:127-138.

89. Lowe LA, Yamada S, Kuehn MR, 2001. Genetic dissection of nodal function in patterning the mouse embryo. Development. 128:1831-1843.

90. Campione M, Steinbeisser H, Schweickert A, Deissler K, van Bebber F, Lowe LA, Nowotschin S, Viebahn C, Haffter P, Kuehn MR, Blum M, 1999. The homeobox gene Pitx2: mediator of asymmetric left-right signaling in vertebrate heart and gut looping. Development. 126:1225-1234.

91. Lin CR, Kioussi C, O'Connell S, Briata P, Szeto D, Liu F, Izpisua-Belmonte JC, Rosenfeld MG, 1999. Pitx2 regulates lung asymmetry, cardiac positioning and pituitary and tooth morphogenesis. Nature. 401:279-282.

92. Lu MF, Pressman C, Dyer R, Johnson RL, Martin JF, 1999. Function of Rieger syndrome gene in left-right asymmetry and craniofacial development. Nature. 401:276-278.

93. Gage PJ, Suh H, Camper SA, 1999. Dosage requirement of Pitx2 for development of multiple organs. Development. 126:4643-4651.

94. Rankin CT, Bunton T, Lawler AM, Lee SJ, 2000. Regulation of left-right patterning in mice by growth/differentiation factor-1. Nat Genet. 24:262-265.

95. Alescio TC, A, 1962. Induction in vitro of tracheal buds by pulmonary mesenchyme grafted on tracheal epithelium. J Exp Zool. 150:83-94.

96. Spooner BS, Wessells NK, 1970. Mammalian lung development: interactions in primordium formation and bronchial morphogenesis. J Exp Zool. 175:445-454.

97. Masters JR, 1976. Epithelial-mesenchymal interaction during lung development: the effect of mesenchymal mass. Dev Biol. 51:98-108.

98. Lin Y, Zhang S, Rehn M, Itaranta P, Tuukkanen J, Heljasvaara R, Peltoketo H, Pihlajaniemi T, Vainio S, 2001. Induced repatterning of type XVIII collagen expression in ureter bud from kidney to lung type: association with sonic hedgehog and ectopic surfactant protein C. Development. 128:1573-1585.

99. Wessells NK, 1970. Mammalian lung development: interactions in formation and morphogenesis of tracheal buds. J Exp Zool. 175:455-466.

100. Shannon JM, 1994. Induction of alveolar type II cell differentiation in fetal tracheal epithelium by grafted distal lung mesenchyme. Dev Biol. 166:600-614.

101. Shannon JM, Nielsen LD, Gebb SA, Randell SH, 1998. Mesenchyme specifies epithelial differentiation in reciprocal recombinants of embryonic lung and trachea. Dev Dyn. 212:482-494.

102. Gebb SA, Shannon JM, 2000. Tissue interactions mediate early events in pulmonary vasculogenesis. Dev Dyn. 217:159-169.

103. Taderera JV, 1967. Control of lung differentiation in vitro. Dev Biol. 16:489-512.

104. Keijzer R, Post M: Lung branching morphogenesis: Role of growth factors and extracellular matrix. In Gaultier C, Bourbon JR,Post M (eds): Lung Development, p 1-27. New York, Oxford University Press Inc., 1999.

105. Morrisey EE, Ip HS, Lu MM, Parmacek MS, 1996. GATA-6: a zinc finger transcription factor that is expressed in multiple cell lineages derived from lateral mesoderm. Dev Biol. 177:309-322.

106. Keijzer R, van Tuyl M, Meijers C, Post M, Tibboel D, Grosveld F, Koutsourakis M, 2001. The transcription factor GATA6 is essential for branching morphogenesis and epithelial cell differentiation during fetal pulmonary

development. Development. 128:503-511.

107. Morrisey EE, Tang Z, Sigrist K, Lu MM, Jiang F, Ip HS, Parmacek MS, 1998. GATA6 regulates HNF4 and is required for differentiation of visceral endoderm in the mouse embryo. Genes Dev. 12:3579-3590.

108. Koutsourakis M, Langeveld A, Patient R, Beddington R, Grosveld F, 1999. The transcription factor GATA6 is essential for early extraembryonic development. Development. 126:723-732.

109. Yang H, Lu MM, Zhang L, Whitsett JA, Morrisey EE, 2002. GATA6 regulates differentiation of distal lung epithelium. Development. 129:2233-2246.

110. Koutsourakis M, Keijzer R, Visser P, Post M, Tibboel D, Grosveld F, 2001. Branching and differentiation defects in pulmonary epithelium with elevated Gata6 expression. Mech Dev. 105:105-114.

111. Liu C, Ikegami M, Stahlman MT, Dey CR, Whitsett JA, 2003. Inhibition of alveolarization and altered pulmonary mechanics in mice expressing GATA-6. Am J Physiol Lung Cell Mol Physiol. 285:L1246-1254.

112. Stanton BR, Perkins AS, Tessarollo L, Sassoon DA, Parada LF, 1992. Loss of N-myc function results in embryonic lethality and failure of the epithelial component of the embryo to develop. Genes Dev. 6:2235-2247.

113. Moens CB, Auerbach AB, Conlon RA, Joyner AL, Rossant J, 1992. A targeted mutation reveals a role for N-myc in branching morphogenesis in the embryonic mouse lung. Genes Dev. 6:691-704.

114. Charron J, Malynn BA, Fisher P, Stewart V, Jeannotte L, Goff SP, Robertson EJ, Alt FW, 1992. Embryonic lethality in mice homozygous for a targeted disruption of the N-myc gene. Genes Dev. 6:2248-2257.

115. Moens CB, Stanton BR, Parada LF, Rossant J, 1993. Defects in heart and lung development in compound heterozygotes for two different targeted mutations at the N-myc locus. Development. 119:485-499.

116. Desai TJ, Cardoso WV, 2002. Growth factors in lung development and disease: friends or foe? Respir Res. 3:2.

117. Han RN, Liu J, Tanswell AK, Post M, 1992. Expression of basic fibroblast growth factor and receptor: immunolocalization studies in developing rat fetal lung. Pediatr Res. 31:435-440.

118. Gonzalez AM, Hill DJ, Logan A, Maher PA, Baird A, 1996. Distribution of fibroblast growth factor (FGF)-2 and FGF receptor-1 messenger RNA expression and protein presence in the mid-trimester human fetus. Pediatr Res. 39:375-385.

119. Powell PP, Wang CC, Horinouchi H, Shepherd K, Jacobson M, Lipson M, Jones R, 1998. Differential expression of fibroblast growth factor receptors 1 to 4 and ligand genes in late fetal and early postnatal rat lung. Am J Respir Cell Mol Biol. 19:563-572.

120. Peters KG, Werner S, Chen G, Williams LT, 1992. Two FGF receptor genes are differentially expressed in epithelial and mesenchymal tissues during limb formation and organogenesis in the mouse. Development. 114:233-243.

121. Orr-Urtreger A, Bedford MT, Burakova T, Arman E, Zimmer Y, Yayon A, Givol D, Lonai P, 1993. Developmental localization of the splicing alternatives of fibroblast growth factor receptor-2 (FGFR2). Dev Biol. 158:475-486.

122. Post M, Souza P, Liu J, Tseu I, Wang J, Kuliszewski M, Tanswell AK, 1996. Keratinocyte growth factor and its receptor are involved in regulating early lung branching. Development. 122:3107-3115.

123. Mason IJ, Fuller-Pace F, Smith R, Dickson C, 1994. FGF-7 (keratinocyte growth factor) expression during

mouse development suggests roles in myogenesis, forebrain regionalisation and epithelial- mesenchymal interactions. Mech Dev. 45:15-30.

124. Shiratori M, Oshika E, Ung LP, Singh G, Shinozuka H, Warburton D, Michalopoulos G, Katyal SL, 1996. Keratinocyte growth factor and embryonic rat lung morphogenesis. Am J Respir Cell Mol Biol. 15:328-338.

125. Panos RJ, Rubin JS, Csaky KG, Aaronson SA, Mason RJ, 1993. Keratinocyte growth factor and hepatocyte growth factor/scatter factor are heparin-binding growth factors for alveolar type II cells in fibroblast-conditioned medium. J Clin Invest. 92:969-977.

126. Panos RJ, Bak PM, Simonet WS, Rubin JS, Smith LJ, 1995. Intratracheal instillation of keratinocyte growth factor decreases hyperoxia-induced mortality in rats. J Clin Invest. 96:2026-2033.

127. Ulich TR, Yi ES, Longmuir K, Yin S, Biltz R, Morris CF, Housley RM, Pierce GF, 1994. Keratinocyte growth factor is a growth factor for type II pneumocytes in vivo. J Clin Invest. 93:1298-1306.

128. Guo L, Degenstein L, Fuchs E, 1996. Keratinocyte growth factor is required for hair development but not for wound healing. Genes Dev. 10:165-175.

129. Nogawa H, Ito T, 1995. Branching morphogenesis of embryonic mouse lung epithelium in mesenchyme-free culture. Development. 121:1015-1022.

130. Cardoso WV, Itoh A, Nogawa H, Mason I, Brody JS, 1997. FGF-1 and FGF-7 induce distinct patterns of growth and differentiation in embryonic lung epithelium. Dev Dyn. 208:398-405.

131. Colvin JS, White AC, Pratt SJ, Ornitz DM, 2001. Lung hypoplasia and neonatal death in Fgf9-null mice identify this gene as an essential regulator of lung mesenchyme. Development. 128:2095-2106.

132. Weaver M, Batts L, Hogan BL, 2003. Tissue interactions pattern the mesenchyme of the embryonic mouse lung. Dev Biol. 258:169-184.

133. Balemans W, Van Hul W, 2002. Extracellular regulation of BMP signaling in vertebrates: a cocktail of modulators. Dev Biol. 250:231-250.

134. Zhou L, Dey CR, Wert SE, Whitsett JA, 1996. Arrested lung morphogenesis in transgenic mice bearing an SP-C-TGF-beta 1 chimeric gene. Dev Biol. 175:227-238.

135. Bragg AD, Moses HL, Serra R, 2001. Signaling to the epithelium is not sufficient to mediate all of the effects of transforming growth factor beta and bone morphogenetic protein 4 on murine embryonic lung development. Mech Dev. 109:13-26.

136. Serra R, Moses HL, 1995. pRb is necessary for inhibition of N-myc expression by TGF-beta 1 in embryonic lung organ cultures. Development. 121:3057-3066.

137. Serra R, Pelton RW, Moses HL, 1994. TGF beta 1 inhibits branching morphogenesis and N-myc expression in lung bud organ cultures. Development. 120:2153-2161.

138. Zeng X, Gray M, Stahlman MT, Whitsett JA, 2001. TGF-beta1 perturbs vascular development and inhibits epithelial differentiation in fetal lung in vivo. Dev Dyn. 221:289-301.

139. Pelton RW, Johnson MD, Perkett EA, Gold LI, Moses HL, 1991. Expression of transforming growth factor-beta 1, -beta 2, and -beta 3 mRNA and protein in the murine lung. Am J Respir Cell Mol Biol. 5:522-530.

140. Pelton RW, Saxena B, Jones M, Moses HL, Gold LI, 1991. Immunohistochemical localization of TGF beta 1, TGF beta 2, and TGF beta 3 in the mouse embryo: expression patterns suggest multiple roles during

embryonic development. J Cell Biol. 115:1091-1105.

141. Heine UI, Munoz EF, Flanders KC, Roberts AB, Sporn MB, 1990. Colocalization of TGF-beta 1 and collagen I and III, fibronectin and glycosaminoglycans during lung branching morphogenesis. Development. 109:29-36.

142. Wrana JL, Attisano L, Wieser R, Ventura F, Massague J, 1994. Mechanism of activation of the TGF-beta receptor. Nature. 370:341-347.

143. Zhao J, Bu D, Lee M, Slavkin HC, Hall FL, Warburton D, 1996. Abrogation of transforming growth factor-beta type II receptor stimulates embryonic mouse lung branching morphogenesis in culture. Dev Biol. 180:242-257.

144. Dickson MC, Martin JS, Cousins FM, Kulkarni AB, Karlsson S, Akhurst RJ, 1995. Defective haematopoiesis and vasculogenesis in transforming growth factor-beta 1 knock out mice. Development. 121:1845-1854.

145. Shull MM, Ormsby I, Kier AB, Pawlowski S, Diebold RJ, Yin M, Allen R, Sidman C, Proetzel G, Calvin D, et al., 1992. Targeted disruption of the mouse transforming growth factor-beta 1 gene results in multifocal inflammatory disease. Nature. 359:693-699.

146. Kaartinen V, Voncken JW, Shuler C, Warburton D, Bu D, Heisterkamp N, Groffen J, 1995. Abnormal lung development and cleft palate in mice lacking TGF-beta 3 indicates defects of epithelial-mesenchymal interaction. Nat Genet. 11:415-421.

147. Sanford LP, Ormsby I, Gittenberger-de Groot AC, Sariola H, Friedman R, Boivin GP, Cardell EL, Doetschman T, 1997. TGFbeta2 knockout mice have multiple developmental defects that are non- overlapping with other TGFbeta knockout phenotypes. Development. 124:2659-2670.

148. Attisano L, Tuen Lee-Hoeflich S, 2001. The Smads. Genome Biol. 2.

149. Dick A, Risau W, Drexler H, 1998. Expression of Smad1 and Smad2 during embryogenesis suggests a role in organ development. Dev Dyn. 211:293-305.

150. Zhao J, Lee M, Smith S, Warburton D, 1998. Abrogation of Smad3 and Smad2 or of Smad4 gene expression positively regulates murine embryonic lung branching morphogenesis in culture. Dev Biol. 194:182-195.

151. Huelsken J, Birchmeier W, 2001. New aspects of Wnt signaling pathways in higher vertebrates. Curr Opin Genet Dev. 11:547-553.

152. Wodarz A, Nusse R, 1998. Mechanisms of Wnt signaling in development. Annu Rev Cell Dev Biol. 14:59-88.

153. Weidenfeld J, Shu W, Zhang L, Millar SE, Morrisey EE, 2002. The WNT7b promoter is regulated by TTF-1, GATA6, and Foxa2 in lung epithelium. J Biol Chem. 277:21061-21070.

154. Tebar M, Destree O, de Vree WJ, Ten Have-Opbroek AA, 2001. Expression of Tcf/Lef and sFrp and localization of beta-catenin in the developing mouse lung. Mech Dev. 109:437-440.

155. Shu W, Jiang YQ, Lu MM, Morrisey EE, 2002. Wnt7b regulates mesenchymal proliferation and vascular development in the lung. Development. 129:4831-4842.

156. Mucenski ML, Wert SE, Nation JM, Loudy DE, Huelsken J, Birchmeier W, Morrisey EE, Whitsett JA, 2003. beta-Catenin is required for specification of proximal/distal cell fate during lung morphogenesis. J Biol Chem. 278:40231-40238.

157. Li C, Xiao J, Hormi K, Borok Z, Minoo P, 2002. Wnt5a participates in distal lung morphogenesis. Dev Biol. 248:68-81.

158. Cardoso WV, 2001. Molecular regulation of lung development. Annu Rev Physiol. 63:471-494.

159. Shannon JM, Hyatt BA, 2004. Epithelial-mesenchymal interactions in the developing lung. Annu Rev Physiol. 66:625-645.

160. Artavanis-Tsakonas S, Rand MD, Lake RJ, 1999. Notch signaling: cell fate control and signal integration in development. Science. 284:770-776.

161. Irvine KD, 1999. Fringe, Notch, and making developmental boundaries. Curr Opin Genet Dev. 9:434-441.

162. Ito T, Udaka N, Yazawa T, Okudela K, Hayashi H, Sudo T, Guillemot F, Kageyama R, Kitamura H, 2000. Basic helix-loop-helix transcription factors regulate the neuroendocrine differentiation of fetal mouse pulmonary epithelium. Development. 127:3913-3921.

163. Post LC, Ternet M, Hogan BL, 2000. Notch/Delta expression in the developing mouse lung. Mech Dev. 98:95-98.

164. Sunday ME, 1996. Pulmonary Neuroendocrine Cells and Lung Development. Endocr Pathol. 7:173-201.

165. Cutz E, 1982. Neuroendocrine cells of the lung. An overview of morphologic characteristics and development. Exp Lung Res. 3:185-208.

166. Borges M, Linnoila RI, van de Velde HJ, Chen H, Nelkin BD, Mabry M, Baylin SB, Ball DW, 1997. An achaete-scute homologue essential for neuroendocrine differentiation in the lung. Nature. 386:852-855.

167. Kageyama R, Ishibashi M, Takebayashi K, Tomita K, 1997. bHLH transcription factors and mammalian neuronal differentiation. Int J Biochem Cell Biol. 29:1389-1399.

168. Kageyama R, Ohtsuka T, 1999. The Notch-Hes pathway in mammalian neural development. Cell Res. 9:179-188.

169. Ito T, Udaka N, Ikeda M, Yazawa T, Kageyama R, Kitamura H, 2001. Significance of proneural basic helix-loop-helix transcription factors in neuroendocrine differentiation of fetal lung epithelial cells and lung carcinoma cells. Histol Histopathol. 16:335-343.

170. Quaggin SE, Schwartz L, Cui S, Igarashi P, Deimling J, Post M, Rossant J, 1999. The basic-helix-loop-helix protein pod1 is critically important for kidney and lung organogenesis. Development. 126:5771-5783.

171. Bohinski RJ, Di Lauro R, Whitsett JA, 1994. The lung-specific surfactant protein B gene promoter is a target for thyroid transcription factor 1 and hepatocyte nuclear factor 3, indicating common factors for organ-specific gene expression along the foregut axis. Mol Cell Biol. 14:5671-5681.

172. Bruno MD, Bohinski RJ, Huelsman KM, Whitsett JA, Korfhagen TR, 1995. Lung cell-specific expression of the murine surfactant protein A (SP-A) gene is mediated by interactions between the SP-A promoter and thyroid transcription factor-1. J Biol Chem. 270:6531-6536.

173. Margana RK, Boggaram V, 1997. Functional analysis of surfactant protein B (SP-B) promoter. Sp1, Sp3, TTF-1, and HNF-3alpha transcription factors are necessary for lung cell- specific activation of SP-B gene transcription. J Biol Chem. 272:3083-3090.

174. Kelly SE, Bachurski CJ, Burhans MS, Glasser SW, 1996. Transcription of the lung-specific surfactant protein C gene is mediated by thyroid transcription factor 1. J Biol Chem. 271:6881-6888.

175. Glasser SW, Burhans MS, Eszterhas SK, Bruno MD, Korfhagen TR, 2000. Human SP-C gene sequences that confer lung epithelium-specific expression in transgenic mice. Am J Physiol Lung Cell Mol Physiol. 278: L933-L945.

176. Toonen RF, Gowan S, Bingle CD, 1996. The lung enriched transcription factor TTF-1 and the ubiquitously expressed proteins Sp1 and Sp3 interact with elements located in the minimal promoter of the rat Clara cell secretory protein gene. Biochem J. 316:467-473.

177. Tichelaar JW, Wert SE, Costa RH, Kimura S, Whitsett JA, 1999. HNF-3/forkhead homologue-4 (HFH-4) is expressed in ciliated epithelial cells in the developing mouse lung. J Histochem Cytochem. 47:823-832.

178. Bruno MD, Korfhagen TR, Liu C, Morrisey EE, Whitsett JA, 2000. GATA-6 activates transcription of surfactant protein A. J Biol Chem. 275:1043-1049.

179. Shaw-White JR, Bruno MD, Whitsett JA, 1999. GATA-6 activates transcription of thyroid transcription factor-1. J Biol Chem. 274:2658-2664.

180. Liu C, Glasser SW, Wan H, Whitsett JA, 2002. GATA-6 and thyroid transcription factor-1 directly interact and regulate surfactant protein-C gene expression. J Biol Chem. 277:4519-4525.

181. Bingle CD, Hackett BP, Moxley M, Longmore W, Gitlin JD, 1995. Role of hepatocyte nuclear factor-3 alpha and hepatocyte nuclear factor- 3 beta in Clara cell secretory protein gene expression in the bronchiolar epithelium. Biochem J. 308:197-202.

182. Bingle CD, Gitlin JD, 1993. Identification of hepatocyte nuclear factor-3 binding sites in the Clara cell secretory protein gene. Biochem J. 295:227-232.

183. Ikeda K, Shaw-White JR, Wert SE, Whitsett JA, 1996. Hepatocyte nuclear factor 3 activates transcription of thyroid transcription factor 1 in respiratory epithelial cells. Mol Cell Biol. 16:3626-3636.

184. Blatt EN, Yan XH, Wuerffel MK, Hamilos DL, Brody SL, 1999. Forkhead transcription factor HFH-4 expression is temporally related to ciliogenesis. Am J Respir Cell Mol Biol. 21:168-176.

185. Tichelaar JW, Lim L, Costa RH, Whitsett JA, 1999. HNF-3/forkhead homologue-4 influences lung morphogenesis and respiratory epithelial cell differentiation in vivo. Dev Biol. 213:405-417.

186. Brody SL, Yan XH, Wuerffel MK, Song SK, Shapiro SD, 2000. Ciliogenesis and left-right axis defects in forkhead factor HFH-4-null mice. Am J Respir Cell Mol Biol. 23:45-51.

187. Bellusci S, Henderson R, Winnier G, Oikawa T, Hogan BL, 1996. Evidence from normal expression and targeted misexpression that bone morphogenetic protein (Bmp-4) plays a role in mouse embryonic lung morphogenesis. Development. 122:1693-1702.

188. Weaver M, Yingling JM, Dunn NR, Bellusci S, Hogan BL, 1999. Bmp signaling regulates proximal-distal differentiation of endoderm in mouse lung development. Development. 126:4005-4015.

189. Shi W, Zhao J, Anderson KD, Warburton D, 2001. Gremlin negatively modulates BMP-4 induction of embryonic mouse lung branching morphogenesis. Am J Physiol Lung Cell Mol Physiol. 280:L1030-L1039.

190. Weaver M, Dunn NR, Hogan BL, 2000. Bmp4 and Fgf10 play opposing roles during lung bud morphogenesis. Development. 127:2695-2704.

191. Lu MM, Yang H, Zhang L, Shu W, Blair DG, Morrisey EE, 2001. The bone morphogenic protein antagonist gremlin regulates proximal- distal patterning of the lung. Dev Dyn. 222:667-680.

192. Hind M, Corcoran J, Maden M, 2002. Alveolar proliferation, retinoid synthesizing enzymes, and endogenous retinoids in the postnatal mouse lung. Different roles for Aldh-1 and Raldh-2. Am J Respir Cell Mol Biol. 26:67-73.

193. Betsholtz C, Karlsson L, Lindahl P, 2001. Developmental roles of platelet-derived growth factors. Bioessays.

23:494-507.

194. Orr-Urtreger A, Lonai P, 1992. Platelet-derived growth factor-A and its receptor are expressed in separate, but adjacent cell layers of the mouse embryo. Development. 115:1045-1058.

195. Han RN, Mawdsley C, Souza P, Tanswell AK, Post M, 1992. Platelet-derived growth factors and growth-related genes in rat lung. III. Immunolocalization during fetal development. Pediatr Res. 31:323-329.

196. Souza P, Kuliszewski M, Wang J, Tseu I, Tanswell AK, Post M, 1995. PDGF-AA and its receptor influence early lung branching via an epithelial-mesenchymal interaction. Development. 121:2559-2567.

197. Boström H, Willetts K, Pekny M, Leveen P, Lindahl P, Hedstrand H, Pekna M, Hellstrom M, Gebre-Medhin S, Schalling M, Nilsson M, Kurland S, Tornell J, Heath JK, Betsholtz C, 1996. PDGF-A signaling is a critical event in lung alveolar myofibroblast development and alveogenesis. Cell. 85:863-873.

198. Lindahl P, Karlsson L, Hellstrom M, Gebre-Medhin S, Willetts K, Heath JK, Betsholtz C, 1997. Alveogenesis failure in PDGF-A-deficient mice is coupled to lack of distal spreading of alveolar smooth muscle cell progenitors during lung development. Development. 124:3943-3953.

199. Souza P, Tanswell AK, Post M, 1996. Different roles for PDGF-alpha and -beta receptors in embryonic lung development. Am J Respir Cell Mol Biol. 15:551-562.

200. Li J, Hoyle GW, 2001. Overexpression of PDGF-A in the lung epithelium of transgenic mice produces a lethal phenotype associated with hyperplasia of mesenchymal cells. Dev Biol. 239:338-349.

201. Soriano P, 1997. The PDGF alpha receptor is required for neural crest cell development and for normal patterning of the somites. Development. 124:2691-2700.

202. Boström H, Gritli-Linde A, Betsholtz C, 2002. PDGF-A/PDGF alpha-receptor signaling is required for lung growth and the formation of alveoli but not for early lung branching morphogenesis. Dev Dyn. 223:155-162.

203. Sun T, Jayatilake D, Afink GB, Ataliotis P, Nister M, Richardson WD, Smith HK, 2000. A human YAC transgene rescues craniofacial and neural tube development in PDGFRalpha knockout mice and uncovers a role for PDGFRalpha in prenatal lung growth. Development. 127:4519-4529.

204. Wendel DP, Taylor DG, Albertine KH, Keating MT, Li DY, 2000. Impaired distal airway development in mice lacking elastin. Am J Respir Cell Mol Biol. 23:320-326.

205. Okabe T, Yorifuji H, Yamada E, Takaku F, 1984. Isolation and characterization of vitamin-A-storing lung cells. Exp Cell Res. 154:125-135.

206. Shenai JP, Chytil F, 1990. Vitamin A storage in lungs during perinatal development in the rat. Biol Neonate. 57:126-132.

207. Chytil F, 1996. Retinoids in lung development. Faseb J. 10:986-992.

208. McGowan SE, Doro MM, Jackson SK, 1997. Endogenous retinoids increase perinatal elastin gene expression in rat lung fibroblasts and fetal explants. Am J Physiol. 273:L410-L416.

209. Liu B, Harvey CS, McGowan SE, 1993. Retinoic acid increases elastin in neonatal rat lung fibroblast cultures. Am J Physiol. 265:L430-437.

210. McGowan S, Jackson SK, Jenkins-Moore M, Dai HH, Chambon P, Snyder JM, 2000. Mice bearing deletions of retinoic acid receptors demonstrate reduced lung elastin and alveolar numbers. Am J Respir Cell Mol Biol. 23:162-167.

211. Massaro GD, Massaro D, Chan WY, Clerch LB, Ghyselinck N, Chambon P, Chandraratna RA, 2000. Retinoic acid receptor-beta: an endogenous inhibitor of the perinatal formation of pulmonary alveoli. Physiol Genomics. 4:51-57.

212. Weinstein M, Xu X, Ohyama K, Deng CX, 1998. FGFR-3 and FGFR-4 function cooperatively to direct alveogenesis in the murine lung. Development. 125:3615-3623.

213. Strandjord TP, Clark JG, Guralnick DE, Madtes DK, 1995. Immunolocalization of transforming growth factor-alpha, epidermal growth factor (EGF), and EGF-receptor in normal and injured developing human lung. Pediatr Res. 38:851-856.

214. Miettinen PJ, Berger JE, Meneses J, Phung Y, Pedersen RA, Werb Z, Derynck R, 1995. Epithelial immaturity and multiorgan failure in mice lacking epidermal growth factor receptor. Nature. 376:337-341.

215. Miettinen PJ, Warburton D, Bu D, Zhao JS, Berger JE, Minoo P, Koivisto T, Allen L, Dobbs L, Werb Z, Derynck R, 1997. Impaired lung branching morphogenesis in the absence of functional EGF receptor. Dev Biol. 186:224-236.

216. Mann GB, Fowler KJ, Gabriel A, Nice EC, Williams RL, Dunn AR, 1993. Mice with a null mutation of the TGF alpha gene have abnormal skin architecture, wavy hair, and curly whiskers and often develop corneal inflammation. Cell. 73:249-261.

217. Korfhagen TR, Swantz RJ, Wert SE, McCarty JM, Kerlakian CB, Glasser SW, Whitsett JA, 1994. Respiratory epithelial cell expression of human transforming growth factor-alpha induces lung fibrosis in transgenic mice. J Clin Invest. 93:1691-1699.

218. Hardie WD, Piljan-Gentle A, Dunlavy MR, Ikegami M, Korfhagen TR, 2001. Dose-dependent lung remodeling in transgenic mice expressing transforming growth factor-alpha. Am J Physiol Lung Cell Mol Physiol. 281: L1088-L1094.

219. Ikeda K, Clark JC, Shaw-White JR, Stahlman MT, Boutell CJ, Whitsett JA, 1995. Gene structure and expression of human thyroid transcription factor-1 in respiratory epithelial cells. J Biol Chem. 270:8108-8114.

220. Wert SE, Dey CR, Blair PA, Kimura S, Whitsett JA, 2002. Increased expression of thyroid transcription factor-1 (TTF-1) in respiratory epithelial cells inhibits alveolarization and causes pulmonary inflammation. Dev Biol. 242:75-87.

221. Hislop AA, 2002. Airway and blood vessel interaction during lung development. J Anat. 201:325-334.

222. deMello DE, Sawyer D, Galvin N, Reid LM, 1997. Early fetal development of lung vasculature. Am J Respir Cell Mol Biol. 16:568-581.

223. Burri PH: Lung development and pulmonary angiogenesis. In Gaultier C, Bourbon JR,Post M (eds): Lung Development, p 122-151. New York, Oxford University Press Inc, 1999.

224. Schachtner SK, Wang Y, Scott Baldwin H, 2000. Qualitative and quantitative analysis of embryonic pulmonary vessel formation. Am J Respir Cell Mol Biol. 22:157-165.

225. Bhatt AJ, Amin SB, Chess PR, Watkins RH, Maniscalco WM, 2000. Expression of vascular endothelial growth factor and Flk-1 in developing and glucocorticoid-treated mouse lung. Pediatr Res. 47:606-613.

226. Healy AM, Morgenthau L, Zhu X, Farber HW, Cardoso WV, 2000. VEGF is deposited in the subepithelial matrix at the leading edge of branching airways and stimulates neovascularization in the murine embryonic lung. Dev Dyn. 219:341-352.

227. D'Angio CT, Maniscalco WM, 2002. The role of vascular growth factors in hyperoxia-induced injury to the

developing lung. Front Biosci. 7:d1609-d1623.

228. Maisonpierre PC, Suri C, Jones PF, Bartunkova S, Wiegand SJ, Radziejewski C, Compton D, McClain J, Aldrich TH, Papadopoulos N, Daly TJ, Davis S, Sato TN, Yancopoulos GD, 1997. Angiopoietin-2, a natural antagonist for Tie2 that disrupts in vivo angiogenesis. Science. 277:55-60.

229. Colen KL, Crisera CA, Rose MI, Connelly PR, Longaker MT, Gittes GK, 1999. Vascular development in the mouse embryonic pancreas and lung. J Pediatr Surg. 34:781-785.

230. Hall SM, Hislop AA, Haworth SG, 2002. Origin, differentiation, and maturation of human pulmonary veins. Am J Respir Cell Mol Biol. 26:333-340.

231. Neufeld G, Cohen T, Gengrinovitch S, Poltorak Z, 1999. Vascular endothelial growth factor (VEGF) and its receptors. Faseb J. 13:9-22.

232. Carmeliet P, Ferreira V, Breier G, Pollefeyt S, Kieckens L, Gertsenstein M, Fahrig M, Vandenhoeck A, Harpal K, Eberhardt C, Declercq C, Pawling J, Moons L, Collen D, Risau W, Nagy A, 1996. Abnormal blood vessel development and lethality in embryos lacking a single VEGF allele. Nature. 380:435-439.

233. Ferrara N, Carver-Moore K, Chen H, Dowd M, Lu L, O'Shea KS, Powell-Braxton L, Hillan KJ, Moore MW, 1996. Heterozygous embryonic lethality induced by targeted inactivation of the VEGF gene. Nature. 380:439-442.

234. Monacci WT, Merrill MJ, Oldfield EH, 1993. Expression of vascular permeability factor/vascular endothelial growth factor in normal rat tissues. Am J Physiol. 264:C995-C1002.

235. Breier G, Albrecht U, Sterrer S, Risau W, 1992. Expression of vascular endothelial growth factor during embryonic angiogenesis and endothelial cell differentiation. Development. 114:521-532.

236. Millauer B, Wizigmann-Voos S, Schnurch H, Martinez R, Moller NP, Risau W, Ullrich A, 1993. High affinity VEGF binding and developmental expression suggest Flk-1 as a major regulator of vasculogenesis and angiogenesis. Cell. 72:835-846.

237. Berse B, Brown LF, Van de Water L, Dvorak HF, Senger DR, 1992. Vascular permeability factor (vascular endothelial growth factor) gene is expressed differentially in normal tissues, macrophages, and tumors. Mol Biol Cell. 3:211-220.

238. Greenberg JM, Thompson FY, Brooks SK, Shannon JM, McCormick-Shannon K, Cameron JE, Mallory BP, Akeson AL, 2002. Mesenchymal expression of vascular endothelial growth factors D and A defines vascular patterning in developing lung. Dev Dyn. 224:144-153.

239. Zeng X, Wert SE, Federici R, Peters KG, Whitsett JA, 1998. VEGF enhances pulmonary vasculogenesis and disrupts lung morphogenesis in vivo. Dev Dyn. 211:215-227.

240. Galambos C, Ng YS, Ali A, Noguchi A, Lovejoy S, D'Amore PA, DeMello DE, 2002. Defective pulmonary development in the absence of heparin-binding vascular endothelial growth factor isoforms. Am J Respir Cell Mol Biol. 27:194-203.

241. Gerber HP, Hillan KJ, Ryan AM, Kowalski J, Keller GA, Rangell L, Wright BD, Radtke F, Aguet M, Ferrara N, 1999. VEGF is required for growth and survival in neonatal mice. Development. 126:1149-1159.

242. Kasahara Y, Tuder RM, Taraseviciene-Stewart L, Le Cras TD, Abman S, Hirth PK, Waltenberger J, Voelkel NF, 2000. Inhibition of VEGF receptors causes lung cell apoptosis and emphysema. J Clin Invest. 106:1311-1319.

243. Le Cras TD, Markham NE, Tuder RM, Voelkel NF, Abman SH, 2002. Treatment of newborn rats with a VEGF

receptor inhibitor causes pulmonary hypertension and abnormal lung structure. Am J Physiol Lung Cell Mol Physiol. 283:L555-L562.

244. Mahlapuu M, Ormestad M, Enerback S, Carlsson P, 2001. The forkhead transcription factor Foxf1 is required for differentiation of extra-embryonic and lateral plate mesoderm. Development. 128:155-166.

245. Peterson RS, Lim L, Ye H, Zhou H, Overdier DG, Costa RH, 1997. The winged helix transcriptional activator HFH-8 is expressed in the mesoderm of the primitive streak stage of mouse embryos and its cellular derivatives. Mech Dev. 69:53-69.

246. Kalinichenko VV, Lim L, Stolz DB, Shin B, Rausa FM, Clark J, Whitsett JA, Watkins SC, Costa RH, 2001. Defects in pulmonary vasculature and perinatal lung hemorrhage in mice heterozygous null for the Forkhead Box f1 transcription factor. Dev Biol. 235:489-506.

Chapter 2

Why study lung development?

Outline of the thesis

Why study lung development?

Clinical

In the surgical and neonatal intensive care units, pediatricians are daily confronted with prematurely born infants that have poor lung function as a result of immaturity, whereas full term infants present with respiratory distress as a result of pulmonary hypoplasia in the case of congenital hernia diaphragmatica, of persistent pulmonary hypertension or as a result of rare cases of abnormal pulmonary vascular and/or airway development. Mechanical ventilation and oxygen therapy are life saving in infants dealing with severe respiratory distress, but both therapies cause extensive lung injury resulting in bronchopulmonary dysplasia (BPD) characterized by airway epithelial lesions and fibroproliferation. The use of exogenous surfactant therapy and gentle ventilation strategies have greatly reduced the severity of neonatal respiratory distress syndrome (RDS) and BPD. Nonetheless, in the premature neonates, the disease of "old" BPD with extensive epithelial lesions has however been replaced by "new" BPD characterized by less severe epithelial lesions but an apparent arrest in alveolar development leading to alveolar hypoplasia with dysmorphic capillaries.

Basic

Studying lung development is central to our understanding of "pulmonary health". Moreover, developmental regulators are deployed repeatedly, not only during development but also in the replacement of tissues in the adult, in response to injury, infection and in cancer. Hence the fields of lung biology and pathology overlap significantly, pressuring the need to understand normal lung development. Well-established controlled programs like cell adhesion, migration, differentiation, proliferation, and programmed cell death define organogenesis and their morphogenetic boundaries, repetitively using the same signaling pathways of morphogens, transcription and growth factors and hormones with their receptors. The concept that there are key fetal adaptive responses to a suboptimal intrauterine environment leading to adult disease is demanding attention and further underlines the need to understand normal fetal development.

This thesis

Lung development is a highly orchestrated process leading to a functioning organ for respiration consisting of at least 40 different cell types. In order to obtain a surface for gas exchange that reaches the size of 70 m^2, the pulmonary epithelial branches have to branch and rebranch, a process called branching morphogenesis. To establish undisturbed gas exchange, the pulmonary blood vessels have to be in close contact to the airways to form the so-called air-blood barrier. These developmental processes are regulated by epithelial-mesenchymal tissue interactions (**Chapter 1**).

Chapter 3 describes the development of blood vessels in the embryonic lung. It is important to realize that lung development takes place in the relative hypoxic environment of the uterus. Also, pulmonary vascular development has for a long time been regarded as a passive process. An increasing amount of evidence is however surfacing that proposes a more active and guiding role for vessels in organ development. We therefore investigated the reciprocal interaction of pulmonary vasculature and airway development. **Chapter 4** takes the hypothesis from the previous chapter a step further. We hypothesize that severe lung hypoplasia as seen in mice deficient for the morphogen Sonic hedgehog, is caused by abnormal vascular development.

Transcription factors have a highly regulating role in organogenesis. In the lung, epithelial-mesenchymal tissue interactions orchestrate differences in proximal and distal structures. Proximal structures are predominantly conducting airway with some secretory function, whereas distal structures are responsible for gas exchange and surfactant production. Numerous pathways have been identified that regulate proximal-distal development during lung maturation. **Chapter 5** describes the role of the Iroquois (Irx) family of transcription factors during lung development. The early and epithelial-specific expression pattern of Irx genes suggests a developmental role in processes involved in epithelial-mesenchymal tissue interactions and proximal-distal differentiation in the lung.

The specification and differentiation of the large number of different cell types in the lung necessitates exquisite control mechanisms and signal transduction between adjacent cells in this tissue during development. The Notch signaling pathway is an evolutionary conserved pathway involved in creating differences and borders between (groups of) neighboring cells. In the lung, downstream factors in the Notch signaling pathway are involved in neuroendocrine development. Although pulmonary endocrine cells are the first to differentiate during lung development, their role is not entirely clear. In **Chapter 6**, the role of Lunatic fringe in the development of pulmonary (endocrine) cells is investigated. Lunatic fringe intervenes with the Notch signaling pathway at the receptor-ligand level.

Congenital diaphragmatica hernia (CDH) is a severe congenital anomaly characterized

by a diaphragmatic defect and lung hypoplasia. Respiration and ventilation support in these infants is severely hampered by lung hypoplasia and pulmonary hypertension. Surfactant is produced by alveolar type II cells and functions to lower surface tension, thereby preventing alveolar collapse at end-expiration. Exogenous surfactant therapy has greatly enhanced pulmonary function and support in premature babies that are surfactant-deficient because of immaturity of the surfactant producing system. In **Chapter 7** the option of surfactant protein deficiency in CDH is investigated for this could be an explanation for therapy-resistant respiratory distress in CDH.

Thyroid hormone has a profound role in (in)vertebrate development of many organs including the lung. In **Chapter 8** we sought to determine the effect of hypothyroidism on lung development based on recent reports that (subclinical) hypothyroidism of the mother during pregnancy has adverse effects on neonatal development.

Taken together, the general theme of this thesis is embryonic lung development. Both vascular development and epithelial differentiation have a key position throughout the chapters. A summary of the results with respect to the advancement of the field is presented and the relevance for postnatal lung health and disease is discussed.

Chapter 3

Role of oxygen and vascular development in epithelial branching morphogenesis of the developing mouse lung

Minke van Tuyl[1,2], Jason Liu[1], Jinxia Wang[1], Maciek Kuliszewski[1], Robin Han[1], Dick Tibboel[2], and Martin Post[1]

[1]Canadian Institutes of Health Research (CIHR) Group in Lung Development, Hospital for Sick Children Research Institute, Departments of Pediatrics and Physiology, University of Toronto, Toronto, ON, Canada
[2]Department of Pediatric Surgery, Sophia Children's Hospital, Erasmus University Medical Center Rotterdam, Rotterdam, The Netherlands

Submitted for revision, American Journal of Physiology-Lung Cellular and Molecular Physiology

Abstract

Recent investigations have suggested an active role for endothelial cells in organ development, including the lung. Herein, we investigated some of the molecular mechanisms underlying normal pulmonary vascular development and their influence on epithelial branching morphogenesis. Because the lung *in utero* develops in a relative hypoxic environment, we first investigated the influence of low oxygen on epithelial and vascular branching morphogenesis. Two transgenic mouse models, namely the C101-LacZ (epithelial-LacZ marker) and the Tie2-LacZ (endothelial-LacZ marker) mouse were used. At embryonic day (E)11.5, primitive lung buds were dissected and cultured at either 20% or 3% oxygen. At 24-hour intervals, epithelial and endothelial LacZ gene expression was visualized by X-gal staining. The rate of branching of both tissue elements was increased in explants cultured at 3% oxygen compared to 20% oxygen. Low oxygen increased the expression of vascular endothelial growth factor (Vegf), but not that of the Vegf receptor (Flk-1). Expression of two crucial epithelial branching factors, fibroblast growth factor-10 (Fgf10) and bone morphogenetic protein-4 (Bmp4) were not affected by low oxygen. Epithelial differentiation was maintained at low oxygen as shown by SP-C *in situ* hybridization. To explore epithelial-vascular interactions, we inhibited vascular development with antisense oligonucleotides (ODNs) targeted against either hypoxia inducible factor (Hif)-1α or vascular endothelial growth factor (Vegf). Epithelial branching morphogenesis *in vitro* was dramatically abrogated when pulmonary vascular development was inhibited. Collectively, the *in vitro* data show that a low oxygen environment enhances branching of both distal lung epithelium and vascular tissue and that pulmonary vascular development appears to be rate limiting for epithelial branching morphogenesis.

Introduction

The molecular base of pulmonary development has been subject of extensive research over the past decades. Many growth- and transcription factors and morphogens have been shown to play key roles in pulmonary development, regulating trachea and lobe formation, branching morphogenesis, proximal-distal epithelial differentiation, and mesenchymal development (1, 2). Pulmonary vascular development has gained substantial interest over the past years because of the putative vascular involvement in neonatal diseases such as respiratory distress syndrome (RDS) and bronchopulmonary dysplasia (BPD) (3-5). Furthermore, it has been postulated that lung abnormalities in congenital diaphragmatic hernia (CDH) have a vascular origin (6, 7). Two processes have been implicated in vascular development: angiogenesis, which is the sprouting of new vessels from pre-existing ones and vasculogenesis, which is the development of blood islands *de novo* leading to the establishment of vessels (8). Both processes are believed to occur during pulmonary vascular development (9). Recently, it has been shown that vascular development takes place during all stages of lung development (10).

It is important to realize that normal pulmonary development takes place in the relative hypoxic environment of the uterus (11). Several studies have shown that the low fetal oxygen environment is beneficial for embryo development (12, 13) and for cardiovascular (14) and kidney (15) organogenesis, but relatively little is known about the influence of oxygen on fetal lung development. Preliminary studies in rats have shown that a fetal oxygen tension (hypoxia) maintains lung morphogenesis *in vitro* (16). Midtrimester human fetal lung explants that were cultured at fetal oxygen tension had increased expression of vascular endothelial growth factor A (Vegf) compared with explants cultured at ambient oxygen cultures (17). Vegf is a potent mitogen for endothelial cells, influencing angiogenesis and vasculogenesis (18). Vegf expression is regulated by hypoxia inducible factor (Hif)-1α, which encodes a transcription factor that is expressed in most, if not all, cells in response to hypoxia (19, 20). Moreover Hif-1α is essential for embryonic vascularization and survival, hypoxia-induced pulmonary vascular remodeling, and tumor vascularization (21). In *Drosophila*, oxygen is delivered to the cells via an extensive network of tubules that deliver oxygen directly to the cells without interference of a vascular system (22). The master gene in regulating tracheal cell specification in *Drosophila* is the bHLH-PAS domain containing gene *Trachealess,* which displays high homology to mammalian bHLH-PAS proteins, including Hif-1α (23, 24). Interestingly, a basic amino acid sequence immediately near the N terminus of the HLH domain, which is known to be the site for DNA recognition, is completely conserved between Hif-1α and *Trachealess* (23, 24). Thus, the protein that is involved in the hypoxic response and vascular development in mammalians seems to regulate tracheal development in *Drosophila*. Recent studies have demonstrated that a fetal oxygen tension indeed stimulates the branching of the *Drosophila* tracheal system (25).

Because a hypoxic environment is critical for vascularization, it is feasible that lung airway branching morphogenesis *in utero* is controlled by oxygen-regulated pulmonary vascular development. Recent reports have indeed suggested an active role for vascularization in lung development. Schwarz *et al*. (26) showed that the inhibition of neovascularization with endothelial monocyte activating polypeptide II (EMAPII) resulted in an arrest of lung airway epithelial morphogenesis. Furthermore, overexpression of the Vegf isoform 164 in distal airway epithelium of the developing lung resulted in increased (27) or decreased (28) peritubular vascularity, depending on the time of Vegf-164 overexpression. In both studies gross abnormalities in lung branching morphogenesis were noted, with a concomitant decrease in epithelial acinar tubules and mesenchyme (27, 28).

The objectives of the present study were to investigate the influence of fetal physiological oxygen tension on the developing lung and to determine the interaction between the developing vascular bed and the pulmonary epithelium.

Materials and Methods

Transgenic mice

Tie2-LacZ mice were obtained from Jackson Laboratory, Bar Harbor, MN, U.S.A. (29). In Tie2-Lac transgenic mice, the 2.1 kb 5′ flanking region of the murine Tie2 promoter drives the expression of the bacterial LacZ reporter gene exclusively to endothelial cells (29). In C101-LacZ or *cordon-bleu*-LacZ transgenic mice, the C101 promoter drives the LacZ gene expression specifically to epithelial cells (30). Cells transcribing the LacZ gene can be viewed by staining for β-galactosidase activity. Both transgenic lines were maintained on a CD1 background. All mouse protocols were in accordance with CACC guidelines and were approved by the Animal Care and Use Committee of the Hospital for Sick Children, Toronto, ON, Canada.

Whole lung organ culture

Lung buds were dissected from embryonic day (E)11.5 CD1, C101-LacZ, or Tie2-LacZ mouse embryos (day of vaginal plug is E0.5) and placed on a floating (8 µm Whatman Nuclepore polycarbonate) membrane (Integra Environmental Inc. Burlington, ON, Canada). Explants were grown in DMEM supplemented with 10% FCS (Gibco, Grand Islands, NY, U.S.A.) and maintained in an atmosphere of either 3% O_2, 92% N_2, and 5% CO_2 or 20% O_2, 75% N_2, and 5% CO_2 at 37˚C. Antisense oligonucleotides (ODNs) targeted against the translation initiation site of murine Hif-1α (antisense: 5′-TGCCGTCGCCGCCATC-3′, sense: 5′-GATGGCGGCGACGGCA-3′) and Vegf (31) were added to the medium in a final concentration of 20 µM. The medium and ODN were changed every other day. In control lung explants, lung growth and branching morphogenesis proceeded as described previously (32).

X-gal staining

Cultured LacZ-lung explants were fixed (in 1% formaldehyde, 0.1% glutaraldehyde, 2 mM $MgCl_2$, and 5 mM EGTA in 0.1 M sodium phosphate buffer pH 7.8-8.0 for 45 minutes at 4°C), washed (in 2 mM $MgCl_2$, 0.01% deoxycholate, and 0.02% NP-40 in 0.1 M sodium phosphate buffer pH 7.8-8.0) 4 times for 30 minutes at 4°C, and stained overnight at 37°C in X-gal staining solution (5 mM $K_4Fe(CN)_6$:$3H_2O$, 5 mM $K_3Fe(CN)_6$ in wash buffer, mixed 40:1 with X-gal stock solution (40 mg/ml in dimethyl formamide), Invitrogen, Burlington, ON, Canada). Explants were washed in 70% ethanol, fixed in 4% paraformaldehyde (PFA) in phosphate buffered saline (PBS) overnight at 4°C, and stored in 70% ethanol. For imaging, explants were dehydrated 2x 30 minutes in methanol and cleared in methyl salicylate. For sectioning, explants were dehydrated in a graded series of ethanol, kept overnight in 1-butanol, embedded in paraplast, and mounted onto Superfrost slides (Fisher Scientific, Unionville, ON, Canada). Digital images were taken with a Leica digital imaging system.

Immunostaining for Pecam

Cultured CD1 lung explants were fixed overnight in 4% PFA in PBS at 4°C. Explants were washed twice in PBS, dehydrated through a graded series of ethanol, kept overnight in 1-butanol, and embedded in paraplast. Seven µm-thick sections were cut and endogenous peroxidase activity was quenched with 0.15% hydrogen peroxide in methanol. Sections were incubated with trypsin (0.6 mg/ml) for 5 minutes at room temperature (RT). Non-specific binding sites were blocked using 5% normal goat serum and 1% bovine serum albumin followed by overnight incubation at 4°C with rat anti-mouse CD31 antibody (1:60; Pecam-1, BD Biosciences Pharmingen, Mississauga, ON, Canada) and incubation with biotinylated secondary sheep anti-rat antibody (1:300) at RT. Color detection was performed according to instructions in the Vectastain ABC and DAB kit (Vector Laboratories, Burlingame, CA, U.S.A.). Slides were lightly counterstained with Carazzi haematoxylin. Digital images were taken using a Leica digital imaging system.

Whole mount *in situ* hybridization

Whole mount *in situ* hybridization was performed essentially as described by Riddle *et al*. (33). Briefly, cultured CD1 lung explants were fixed overnight in 4% PFA in PBS at 4°C. Explants were washed in PBS-T (PBS containing 0.1% Tween-20), dehydrated in graded series of methanol in PBS-T, and stored in 100% methanol. After rehydration, explants were bleached in hydrogen peroxide, treated with proteinase K (20 µg/ml), postfixed in 4% PFA and 0.2% glutaraldehyde, and pre-hybridized for 1 hour at 70°C. Explants were then hybridized with the appropriate digoxigenin (DIG)-labeled riboprobe (1 µg/ml) overnight at 70°C. After washes in 50% formamide, 5x SSC, pH 4.5, and 1% SDS at 70°C followed by washes in 50% formamide, 2x SSC, pH 4.5 at 65°C, and Tris-buffered saline (TBS)-T (TBS containing 1% Tween-20) at RT, explants were pre-blocked with sheep serum in TBS-T, and subsequently incubated with anti-DIG alkaline phosphatase 1:5000 in blocking solution (Roche, Montreal, QC, Canada) at 4°C. The next day, explants were washed in PBS-T followed

by washes in NTM-T (100 mM NaCl, 100 mM Tris, pH 9.5, 50 mM $MgCl_2$, and 0.1% Tween) and then incubated with 5-bromo-4-chloro-3-indolyl phosphate/nitro blue tetrazolium chromogen (NBT/BCIP; Roche, Montreal, QC, Canada) at RT until purple color appeared. After color development, explants were washed in NTM-T and PBS-T, dehydrated in a graded series of methanol in PBS-T, and stored in PBS-T at 4°C. Digital images were taken using a Leica digital imaging system.

Tissue section *in situ* hybridization

Cultured CD1 lung explants were fixed overnight in 4% PFA in PBS, dehydrated in ethanol, and embedded in paraplast. Sections of 12 µm were cut and mounted on Superfrost slides (Fisher Scientific, Unionville, ON, Canada). Explants were then assayed for non-radioactive RNA *in situ* hybridization according to Moorman *et al*. (34). Briefly, after dewaxing and rehydrating, tissue sections were permeabilized with proteinase K (20 µg/ml), postfixed in 4% PFA and 0.2% glutaraldehyde, and pre-hybridized for 1 hour at 70°C. The sections were hybridized overnight at 70°C with a DIG-labeled riboprobe for surfactant protein (SP)-C (1 µg/ml). The next day, sections were washed in 50% formamide in 2x SSC, pH 4.5 at 65 C followed by PBS-T washes. Subsequently, the sections were incubated with anti-DIG alkaline phosphatase 1:1000 in blocking solution (Roche, Montreal, QC, Canada) at 4°C. The next day, sections were washed in PBS-T followed by washes in NTM (100 mM NaCl, 100 mM Tris, pH 9.5, and 50 mM $MgCl_2$) and then incubated with NBT/BCIP (Roche, Montreal, QC, Canada) at RT until the purple color appeared (4-5 hours). All slides were stopped at the same time to make comparison over different stages of development possible. After color development, sections were washed in distilled water, dehydrated in a graded series of ethanol and xylene, and mounted with coverslips using permount (Fisher Scientific, Unionville, ON, Canada). Digital images were taken using a Leica digital imaging system.

RNA isolation and real-time RT-PCR

CD1 lung explants, cultured at 3% or 20% oxygen, were rinsed in ice-cold PBS after 2, 4, and 6 days in culture (12 lungs from 3 litters at 2 and 4 days and 9 lungs from 2 litters at 6 days), immediately frozen in liquid nitrogen and stored at -70°C. Explants from each time group were divided into three groups and RNA was extracted using the RNeasy kit (Qiagen, Mississauga, ON, Canada). One µg of RNA was reverse transcribed (37°C) using random-hexamers (Applied Biosystems, Foster City, CA, USA). The resulting templates (50 ng of cDNA for our target genes and 5 ng for 18S) were quantified by real-time PCR (ABI Prism 7700). Primers and TaqMan probes for total Vegf, Vegf receptor Flk-1 (kinase insert domain-containing receptor/fetal liver kinase-1; KDR/Flk-1 or Vegfr2), angiopoietin (Ang)-1, and Ang-2 were similar to previously published sequences (35), whereas primers and TaqMan probes for Pecam-1, Tie2, fibroblast growth factor-10 (Fgf10) and the Fgf receptor-2 (Fgfr2) (for both Fgfr2-IIIb and -IIIc isoforms) were purchased from ABI as Assays-on-Demand™ for murine genes. For each probe a dilution series determined the efficiency of amplification of each primer-probe set and the relative quantification method was employed (36). For

the relative quantitation, PCR signals were compared between groups after normalization using 18S as an internal reference. Briefly, relative expression was calculated as $2^{-(Ct_{gene\ of\ interest} - Ct_{18S})}$ and fold-change was calculated according to Livak et al. (36). A $p<0.05$ was considered statistically significant.

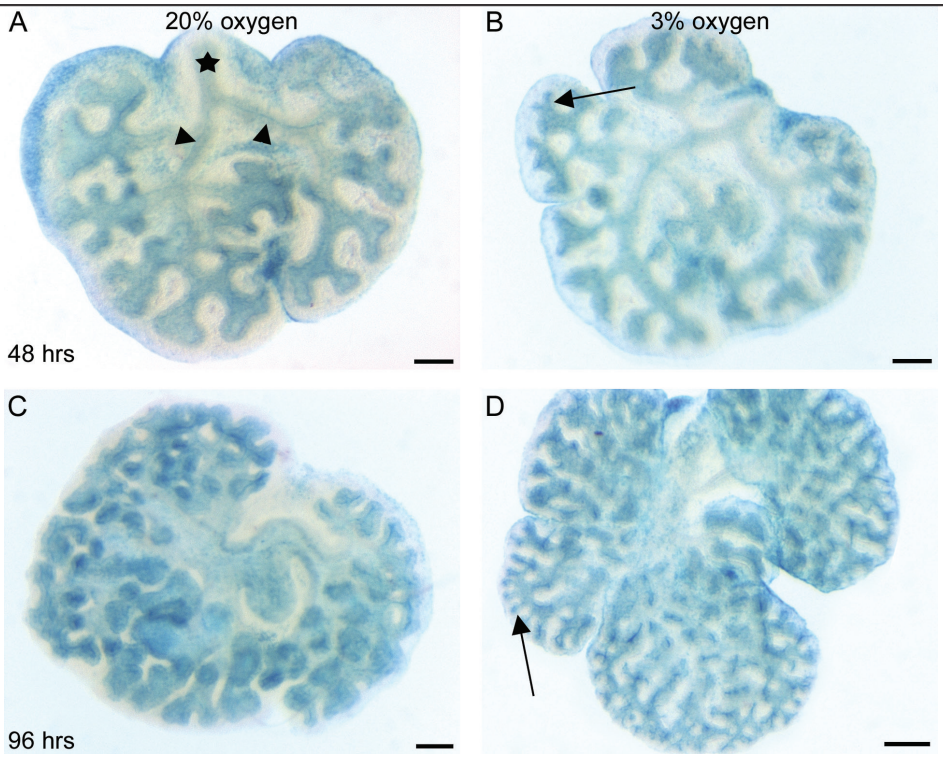

Figure 1. Low oxygen enhances epithelial branching morphogenesis in vitro. C101-LacZ expression in E11.5 lung explants after 48 (A, B) and 96 (C, D) hours in culture. Explants cultured at 3% oxygen (B, D) showed more complex branching compared to explants cultured at 20% oxygen (A, C). Asterisk is located in the trachea, arrowheads point at main bronchi, and arrows at increased distal branch tips. Blue color is X-gal staining in airway epithelial cells. Bar: 100 µm.

Results

Low oxygen enhances epithelial branching morphogenesis

The effect of low oxygen on epithelial branching *in vitro* was investigated using C101-LacZ mice. Lungs were dissected at E11.5 and cultured at either 3% or 20% oxygen. Whole mount LacZ staining revealed a complete image of the developing airways. On E11.5, the lung rudiments consisted of two epithelial buds that over time (48 hours) in culture progressed towards two main airways (arrowheads in Fig. 1A) and four lobes on the right and one lobe on the left side of the trachea (asterisk in Fig. 1A). Additional branching (96 hours) provided the exponential growth and complexity of distal airways (Fig. 1C, D).

LacZ staining in lung explants cultured at 3% oxygen showed that the distal branches had more tips (arrows in Fig. 1B, D) compared with explants cultured at 20% oxygen (Fig. 1B, D *versus* A, C, respectively). Because C101-LacZ is solely expressed in epithelial cells of the airways and not in mesenchymal or endothelial cells, these results suggest that a low oxygen environment benefits epithelial branching morphogenesis.

In *Drosophila* tracheal development, terminal branching is mainly controlled by oxygen. A low oxygen tension stimulates terminal branch formation and high oxygen tension suppresses it (25). Oxygen-starved cells were shown to generate a signal that functions as a chemo attractant for terminal branches. This signal was identified as *Branchless*, the *Drosophila* orthologue for Fgf (25). In mammalian development, Fgf10 and its receptor Fgfr2 play a role in airway branching that is reminiscent of that described for *Branchless* and its receptor *Breathless* in *Drosophila* trachea development (37). Both Fgf10 and Fgfr2 have been shown to be indispensable for murine lung development (38-40). Based on these data, we tested the possibility that increased airway branching morphogenesis in lung explants cultured at 3% oxygen was caused by an increase in Fgf10/Fgfr2 signaling. Whole mount *in situ* hybridization was performed to investigate Fgf10 mRNA expression in lung explants. Fgf10 was mainly expressed in the mesenchyme of distal airways of E11.5 lung explants cultured for 24 hours at 20% oxygen (Fig. 2A). Fgf10 was unevenly expressed, that is, high levels of expression were detected in the mesenchyme between the distal buds (arrows in Fig. 2A, B) and low expression was detected at the distal branch tips (arrowheads, Fig. 2A, B). A similar spatial expression pattern was reported for the developing murine lung *in vivo* (41). Explants cultured at 3% oxygen demonstrated a similar spatial expression pattern as those kept at 20% oxygen (Fig. 2B vs. 2A). To confirm these results, we performed real-time RT-PCR for Fgf10 and Fgfr2 in explants cultured at either 3% or 20% oxygen for 2, 4, and 6 days. No significant changes in gene expression of both signaling molecules were found between explants cultured at 3% or 20% oxygen (Fig. 2C, D).

In addition to Fgf10, also bone morphogenetic protein-4 (Bmp4) was shown to be required for the coordinated branching and elongation of airway tubules during lung development (42). Therefore, we performed whole mount *in situ* hybridization for Bmp4 to investigate whether culturing of lung explants at 3% oxygen influenced Bmp4 expression. In explants cultured for 48 hours at 20% oxygen, Bmp4 was mainly expressed in the pulmonary epithelium with markedly enhanced expression at the distal branch tips (arrow in Fig. 2E). This spatial expression pattern is similar to that of the embryonic murine lung *in vivo* (43). Bmp4 expression in explants cultured at 3% oxygen showed a similar spatial expression pattern (Fig. 2F). The increased number of Bmp4-positive distal branch tips in lung explants cultured at 3% oxygen reflects the enhanced airway branching of the lung in low oxygen (arrow in Fig. 2F). Taken together, the results suggest that the increased epithelial branching morphogenesis of explants cultured at 3% oxygen is likely not due to

changes in Fgf10 and Bmp4 signaling.

Distal airway epithelium is normally lined with SP-C-positive cells. To investigate whether low oxygen maintained epithelial differentiation, we performed section *in situ* hybridization for SP-C on E11.5 explants cultured at either 3% or 20% oxygen. In lung explants cultured at 20% oxygen, SP-C mRNA was detected in the distal epithelium (Fig. 2G, I, for 96 and 144 hours, respectively). Explants cultured at 3% oxygen demonstrated enhanced SP-C expression in distal epithelial branches (Fig. 2H, J, for 96 and 144 hours, respectively). These results are in line with a preliminary report by Gebb and Shannon (44) and indicate that explants cultured at 3% oxygen maintain their appropriate epithelial morphogenesis.

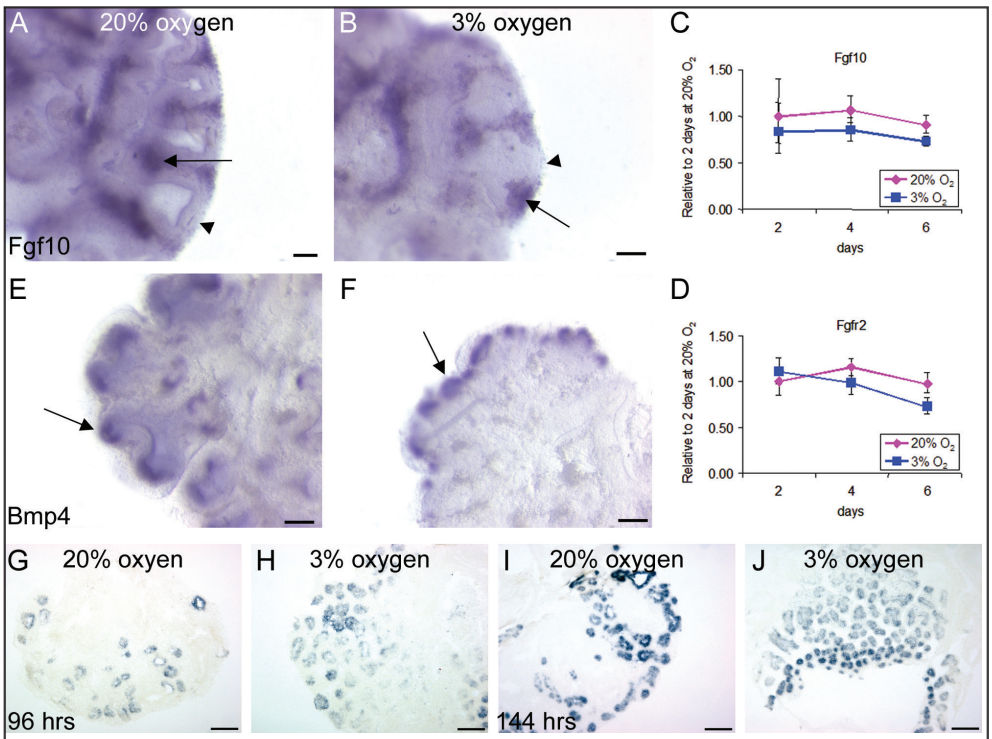

Figure 2. Low oxygen does not affect Fgf10 and Bmp 4 expression. Whole mount in situ hybridization for Fgf10 (A, B) and Bmp4 (E, F) mRNA in lung explants cultured for 24 hours at 20% (A, E) or 3% oxygen (B, F). Fgf10 was highly expressed in the mesenchyme between branches (arrows), but less in distal branch tips (arrowheads). Bmp4 was strongly expressed in the epithelium of distal branch tips (arrows). Low oxygen did not affect the spatial expression of Fgf10 or Bmp4. Real-time RT-PCR (n = 3 from 3 separate experiments and expressed as fold-change ±SD, relative to explants cultured at 20% oxygen for 2 days) revealed no significant differences in the mRNA expression of Fgf10 (C) or its receptor Fgfr2 (D). Section in situ hybridization for SP-C mRNA in explants cultured for 96 (G, H) or 144 hours (I, J) at 20% (G, I) or 3% oxygen (H, J) revealed enhanced SP-C expression in the distal parts of explants cultured at 3% oxygen (H, J). Dark purple color is positive ISH staining. Bar: 125 µm (A, B, E, F); 100 µm (G-J).

Low oxygen enhances vascular development

The effect of hypoxia on the development of the pulmonary vascular system *in vitro* was investigated using Tie2-LacZ mice. Lungs were dissected at E11.5 and cultured at either 3% or 20% oxygen. Whole mount LacZ staining revealed a complete image of the developing vascular bed. Explants cultured for 48 hours at 3% oxygen showed a more complex vascular network in the mesenchyme surrounding the developing lung buds than explants cultured at 20% oxygen (Fig. 3B *versus* 3A). The enhanced vascularization in 3% oxygen explants was even more evident after 72 hours of culture (Fig. 3D *versus* 3C). Noteworthy is the arrangement of the vessels between the explants cultured at different oxygen tensions. In explants cultured at 20% oxygen, X-gal positive vessels were detected along the trachea (arrow), main bronchi and along smaller distal airways. No vascularization; however, was detected along the distal branch tips (edges) of the explants (arrowheads in Fig. 3C). In explants cultured at 3% oxygen; however, a considerable density of X-gal positive vessels was detected along the trachea (arrow), main bronchi and smaller airways up to the distal branch tips (edges) of the explants (arrowheads in Fig. 3D). Sectioning of the explants confirmed the increased extent of the vascular bed in explants cultured at 3% oxygen (Fig. 3F) compared with explants cultured at 20% oxygen (Fig. 3E). These results indicate that low oxygen enhances vascular development in embryonic lung explants and stimulates vascular growth in the periphery of the lung, thereby covering all distal airways.

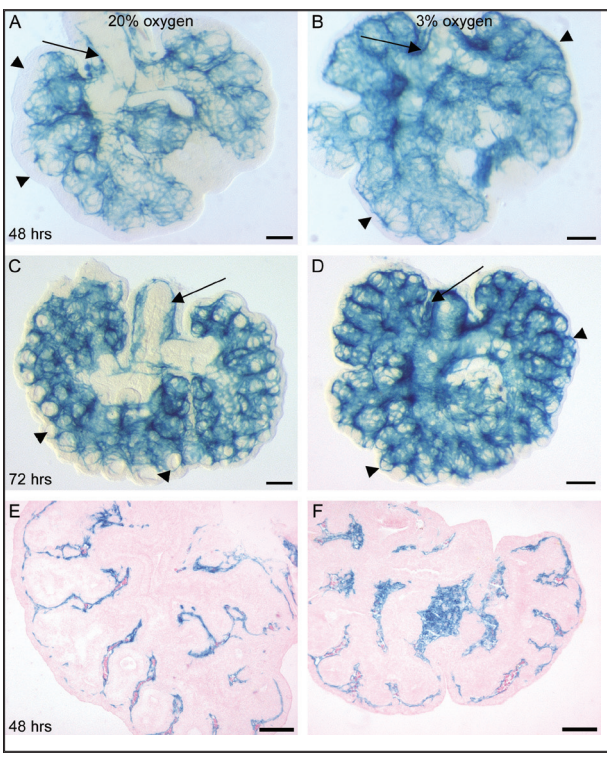

Figure 3. Low oxygen stimulates pulmonary vascular development in vitro. Tie-LacZ expression in E11.5 lung explants after 48 (A, B) and 72 (C-F) hours in culture. Explants cultured at 3% oxygen (B, D) showed more complex vascular branching compared to explants cultured at 20% oxygen (A, C). In explants kept at 3% oxygen, vessels extended to the most distal branch tips (arrowheads), whereas in explants kept at 20% oxygen, the vessels did not reach the distal branch tips (arrowheads). Sectioning of E11.5 Tie-LacZ lung explants after 48 hours in culture confirmed enhanced X-gal staining in explants cultured at 3% oxygen (F) compared to explants cultured at 20% oxygen (E). Sections were counterstained with eosin. Blue color is X-gal staining in endothelial cells. Bar: 100 µm. sion in the distal parts of explants cultured at 3% oxygen (H, J). Dark purple color is positive ISH staining. Bar: 125 µm (A, B, E, F); 100 µm (G-J).

Low oxygen increases Pecam-1 and Vegf expression

To confirm the increase in vascularization in Tie2-LacZ lung explants cultured at 3% oxygen, we performed immunohistochemistry for Pecam-1 (CD31), which is an endothelial marker. After 72 hours in culture, greater Pecam-1 immunopositive reactivity was observed in the mesenchyme from explants cultured at 3% oxygen (Fig. 4B) when compared to explants cultured at 20% oxygen (Fig. 4A). Note the more complex pattern of tubular epithelial branching in explants cultured at 3% oxygen (Fig. 4B), which is consistent with the increased airway branching seen in C101-LacZ explants cultured at 3% oxygen (Fig. 1B, D). We then performed real-time RT-PCR for Pecam-1 in E11.5 lung explants cultured for 2, 4, and 6 days at either 3 or 20% oxygen. Culturing explants at 3% oxygen significantly increased Pecam-1 mRNA expression compared to explants cultured at 20% oxygen (Fig. 4C). These results confirm that low oxygen stimulates vascular development in embryonic lung explants.

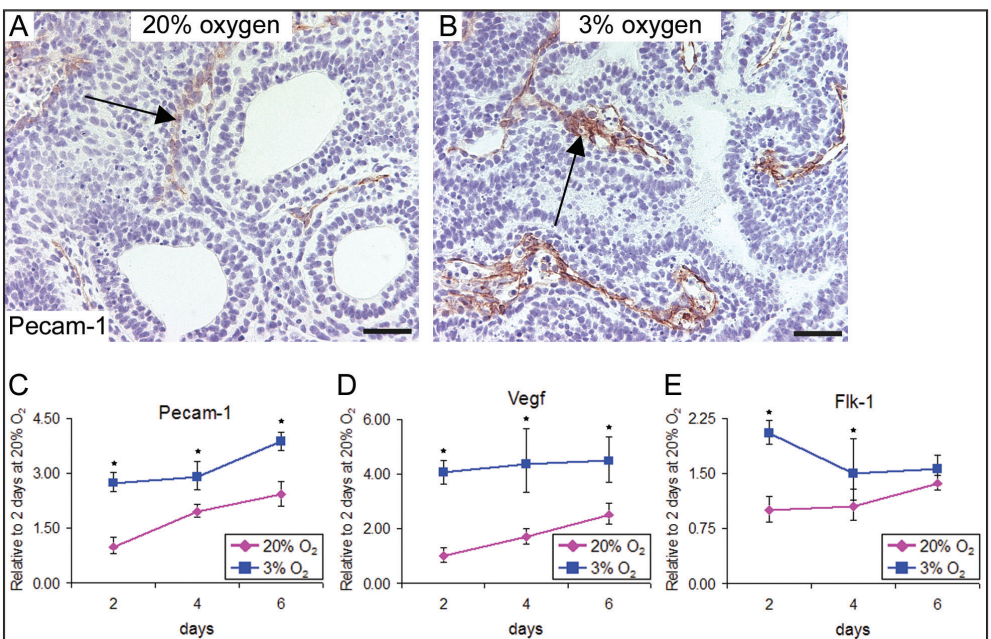

Figure 4. Low oxygen stimulates Pecam-1 and Vegf expression. Pecam-1 (CD31) immunohistochemistry in E11.5 lung explants after 72 hours in 3% (B) or 20% oxygen (A) culture. Sections were counterstained with Carazzi haematoxylin. Explants cultured at 3% oxygen (B) showed increased Pecam-1 staining compared to explants cultured at 20% oxygen (A). Brown color is positive staining. Real-time RT-PCR (n = 3 from 3 different experiments and expressed as fold-change ±SD relative to explants cultured at 20% oxygen for 2 days) showed increased expression of Pecam-1 (C) and Vegf (D) in explants cultured at 3% oxygen. Vegfr2 (Flk-1) expression (E) was initially upregulated in explants at low oxygen, but its expression was not different from 20% oxygen explants when cultured for longer periods. $^{*}P<0.05$*, Bar: 250 µm.*

Many genes that are involved in angiogenesis and vessel growth are upregulated by hypoxia, including Vegf (45). Because a hypoxic environment increased vascular density in cultured lung explants, we performed real-time RT-PCR for total Vegf in E11.5 lung explants. Vegf mRNA was dramatically upregulated in explants exposed to 3% oxygen compared with lung explants cultured at 20% oxygen (Fig. 4D). Expression of Vegfr2/Flk-1 was initially (2 and 4 days culture) upregulated in lung explants kept at 3% oxygen compared with explants cultured at 20% oxygen, but no differences in Vegfr2/Flk-1 transcript levels were noted between lung explants cultured for longer times (6 days) (Fig. 4E). The expression levels of other angiogenic cytokines, such as Ang-1 and Ang-2, were not affected by low oxygen levels (not shown).

Vascular development influences epithelial branching morphogenesis

To investigate whether vascularization affects epithelial branching morphogenesis, we inhibited vascularization using antisense ODNs targeting either Vegf or Hif-1α. E11.5 lung explants from Tie2-LacZ mice were cultured at 3% oxygen in the presence or absence of either antisense ODNs. After 48 hours in culture, intense vascular LacZ staining was detected in control and sense Hif-1α ODN-treated lung explants (Fig. 5A, B, respectively). A fine vascular network wrapped around the trachea, main bronchi, and covered the epithelial tubules as far as the distal branch tips (arrowheads). In contrast, antisense Hif-1α ODN-treated lung explants showed a dramatic decrease in vascular development (Fig. 5C). Although vessels ran from the trachea area down along the main bronchi and some proximal epithelial branches, most of the peripheral tissue was devoid of vessels (arrow in Fig. 5C). Antisense ODNs targeted against Vegf exhibited a similar effect. After 72 hours in culture, an extensive vascular network was visible in control (arrowhead, Fig. 5D) and sense Vegf ODN-treated lung explants (arrowhead, Fig. 5E). Similar to antisense Hif-1α ODN-treated lung explants, large areas of antisense Vegf ODN-treated lung explants were devoid of vessels (arrows in Fig. 5F, I). The inhibitory effect of antisense Vegf ODN on vascularization was clearly observed after 96 hours in culture (Fig. 5G, H, I, for control, sense, and antisense Vegf ODN-treated lung explants, respectively). These results show that antisense knockdown of either Hif-1α or Vegf reduces vascular development in lung explants cultured at 3% oxygen. Vascularization was more affected by antisense Hif-1α ODN than antisense Vegf ODN treatment; findings that may be explained by the position of both factors in the hypoxic signaling cascade leading to vascular development. Hif-1α is the key player and functions upstream in this cascade, regulating Vegf and numerous other genes (45).

To investigate the effect of reduced vascular development on epithelial branching morphogenesis, C101-LacZ lung explants were treated with sense and antisense ODNs targeted against Hif-1α or Vegf. LacZ staining of epithelial airway cells revealed an almost complete abrogation of epithelial branching morphogenesis in antisense Hif-1α ODN-treated lung explants (Fig. 6C, F). After 72 hours in culture, LacZ staining was observed in

the trachea, two main bronchi, and subsequent branches of control, sense, and antisense Hif-1α ODN-treated lung explants. No obvious differences were observed between control (Fig. 6A) and sense Hif-1α ODN-treated lung explants (Fig. 6B). Conversely, antisense Hif-1α ODN-treated lung explants showed dramatically reduced epithelial branching with abnormal, blunt tips of distal branches (Fig. 6C). LacZ staining of explants cultured for 96 hours showed that epithelial branching morphogenesis in control (Fig. 6D) and sense (Fig. 6E) Hif-1α ODN-treated lung explants had progressed towards a complex network of fine epithelial branches that had extended and rebranched multiple times in culture. In contrast, antisense Hif-1α ODN-treated lung explants demonstrated a complete stop in branching morphogenesis (Fig. 6F). The treatment of explants with antisense ODNs targeted against Vegf resulted in similar results, although branching in these explants, after 72 hours culture at 3% oxygen, was less affected compared to treatment with antisense Hif-1α ODNs (Fig. 6G, H for control and antisense Vegf ODN-treated lung explants, respectively).

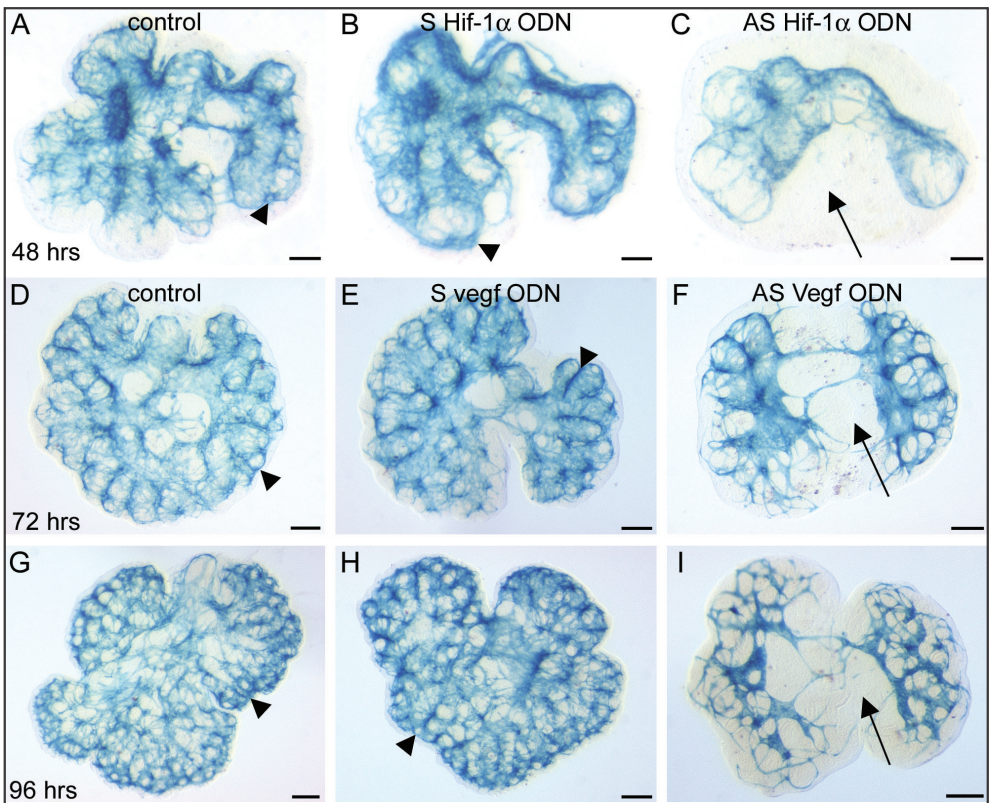

Figure 5. Antisense inhibition of Hif-1α and Vegf reduces pulmonary vascularization in vitro. Tie-LacZ expression in E11.5 lung explants after 48 (A-C), 72 (D-F), and 96 (G-I) hours at 3% oxygen. Explants treated with antisense ODNs targeted against Hif-1α (C) or Vegf (F, I) demonstrated abnormal vessel formation compared to sense-treated (Hif-1α: B; Vegf: E, H) or control (A, D, G) explants. Large areas without vessels were seen in antisense ODN-treated explants (arrows in C, F, I), whereas in control and sense ODN-treated explants, the whole explant was covered with vessels (arrowheads in A-B, D-E, G-H). Blue color is X-gal staining in endothelial cells. Bar: 100 µm.

These results suggest that the inhibition of pulmonary vascular development results in a dramatic reduction in epithelial branching morphogenesis, indicating that in the context of epithelial-mesenchymal tissue interactions, the vascular network within the mesenchyme is a key factor for epithelial branching morphogenesis.

Discussion

In this study we demonstrate that a low oxygen environment (3% oxygen) stimulates pulmonary vascular and epithelial branching morphogenesis *in vitro*. Increased epithelial branching was accompanied by increased SP-C expression, implying that low oxygen maintains an appropriate epithelial differentiation pattern. However, the expression of Fgf10 and Bmp4, two critical signaling components for normal distal epithelial branching (38), were not affected by a low oxygen environment. Low oxygen levels stimulated vascularization and this was accompanied by a significant increase in Pecam-1 expression. Also, Vegf expression was significantly increased by low oxygen. Similar observations have been reported for another branching organ; the kidney (46). Low oxygen stimulated tubule formation and ureteric bud growth from E14.5 metanephroi *in vitro*. Moreover, low oxygen exposure of metanephroi increased the number of Vegfr (Flt-1 and Flk-1) positive endothelial cells and induced a 10-fold increase in Vegf mRNA (46). These data highlight the importance of a low oxygen environment for proper development of branched organs. Moreover, we show that the inhibition of vascularization *in vitro*, results in a dramatic decrease in epithelial branching morphogenesis, suggesting that pulmonary vascular development is rate limiting for epithelial branching morphogenesis.

The enhancement of lung epithelial branching morphogenesis by low oxygen has been reported by Gebb and co-workers (16). They showed increased terminal branching and cellular proliferation in fetal rat lung explants that were cultured at 3% oxygen compared with 21% oxygen (16). Additionally, they reported that low oxygen suppressed the activity of metalloproteinases, which are zinc-dependent enzymes that modify the extracellular matrix (ECM) structure and function, what resulted in the accumulation of specific ECM components, including tenascin-C, which has been shown to influence lung branching (16). Wilborn and co-workers (47) reported a loss of morphology in E12.5 mouse lung explants after 48 hours culturing at 10% oxygen. It should be mentioned that Wilborn and co-workers (47) did not use serum in their cultures, whereas in the present study we used 10% fetal calf serum. It is plausible that fetal calf serum contains factors that are needed for the survival of the explants at low oxygen. Human fetal lung tissues have been shown to differentiate spontaneously in an atmosphere of 20% oxygen; however, morphological differentiation and SP-A expression disappeared when the tissues were maintained at 1% oxygen (48). Also, the low oxygen effect on morphological differentiation was rapidly

reversed when tissues were exposed to 20% oxygen after five days at 1% oxygen (48). These findings led the authors to conclude that oxygen plays an important permissive role in the spontaneous differentiation (and SP-A expression) of human fetal lung *in vitro*. We observed that increased airway branching in a low oxygen environment was associated with proper terminal differentiation (SP-C expression). The finding that SP-A mRNA disappeared in the study of Acarregui *et al*. (48), whereas we show SP-C mRNA staining at low oxygen levels might be explained by the difference in oxygen levels that were used. In the present study, 3% oxygen was used, whereas Acarregui and co-workers used 1% oxygen levels. Also in their study, incubation at 5% oxygen already increased SP-A levels. Whether the discrepant findings are due to species differences remains to be established.

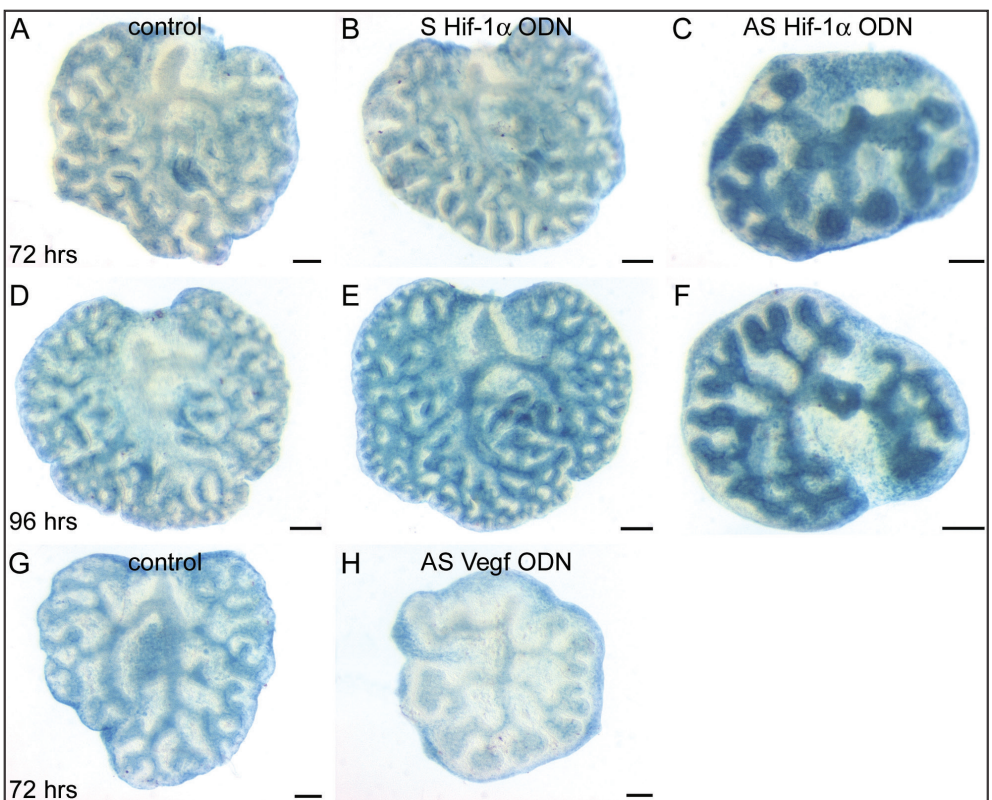

Figure 6. Antisense inhibition of pulmonary vascular development decreases epithelial branching morphogenesis. C101-LacZ expression in E11.5 lung explants after 72 (A-C, G-H) and 96 (D-F) hours at 3% oxygen. Explants treated with antisense ODNs targeted against Hif-1α (C, F) or Vegf (H) demonstrated an almost complete stop of epithelial branching morphogenesis compared to sense Hif-1α ODN-treated (B, E) or control (A, D, G) explants. Blue color is X-gal staining in airway epithelial cells. Bar: 100 µm.

The important role of Fgf10 and Fgfr2-IIIb in lung development was shown when both Fgf10-deficient mice (38, 39) and Fgfr2$^{-/-}$ chimeras (49) formed a trachea without any further pulmonary branching (49). Similarly, transgenic mice that overexpress a (soluble)

dominant negative Fgfr2-IIIb splice variant in distal lung epithelium, had a severe pulmonary defect with only the formation of a rudimentary trachea and two main bronchi, but without any lateral branches (50, 51). Moreover, cre-mediated excision to generate mice lacking the IIIb form of Fgfr2, while retaining expression of the IIIc splice form, resulted in mice that had no lungs and died at birth (40). In *Drosophila*, hypoxia greatly enhances the branching of terminal tubules during tracheal development (25). Although *Bnl*, the fly homologue for Fgf, was identified as the critical signal in this hypoxic response, no oxygen-dependent differences in the expression of Fgf10 and its receptor Fgfr2 were observed in the present study. Nevertheless, the real-time PCR assay used in the current study does not differentiate between the Fgfr2 splice isoforms, Fgfr2-IIIb and Fgfr2-IIIc. Thus, it is possible that different oxygen tensions trigger Fgfr2 isoform specific effects. Another possible mediator of hypoxia-induced branching morphogenesis is insulin-like growth factor (Igf)-I. It has been shown that hypoxia significantly increases both Igf-I and Igf-I type 1 receptor (Igfr-I) mRNA in the neonatal rat lung (52). Furthermore, Han *et al*. (53) showed that immuno-inhibition of Igfr-I in human fetal lung explants resulted in reduced branching as well as a loss of endothelial cells. They concluded that Igfs via Igfr-I affect lung development, most likely by acting as endothelial survival factors (53). Because a low oxygen environment stimulates both components of this signaling pathway, it may account for the increased vascularization and subsequent epithelial branching seen in the present study.

Numerous studies have provided evidence that Vegf acts as a potent inducer of endothelial cell growth and that hypoxia is one of its key stimuli (18, 54). In this study, we show that Vegf and Vegfr2/Flk-1 mRNA levels are significantly upregulated in lung explants cultured at 3% oxygen. Similar findings have been reported for Vegf levels in human (17) and rat (16) fetal lung explants cultured at low oxygen. Vegf is indispensable for embryonic development because it was shown that even haploinsufficiency of Vegf is enough to cause embryonic lethality (55, 56). In the embryonic lung, Vegf transcripts are mainly detected in the lung epithelium and its expression increases with advancing gestation and remains high in the adult lung (57-59). Vegf signals via two endothelial specific, high affinity tyrosine kinase receptors, Vegfr1 (Flt-1) and Vegfr2 (Flk-1) (60). During lung development, both receptors are strongly expressed in the embryonic lung endothelium (57). Although alveolar epithelium expresses Flk-1 (61, 62), exogenous Vegf did not directly induce fetal type II cell proliferation or surfactant protein production (61). The adjacent expression patterns of Vegf in pulmonary epithelium and the two Vegf receptors in pulmonary endothelium, suggest a regulatory signaling loop between the two tissue components during lung development. This suggestion is supported by findings of Gebb *et al.* (63) who showed that the expression of endothelial Flk-1 within the mesenchyme required the presence of pulmonary epithelium. So far as we know, no oxygen-dependent upregulation of Vegfr2/Flk-1 expression in the lung has been reported.

In the present study we observed that inhibition of vascularization with antisense ODNs targeted against either Hif-1α or Vegf, reduced epithelial branching morphogenesis. We chose to target Hif-1α and Vegf because both factors are key factors in the hypoxic response and in vascular development. Hif-1α is upregulated in response to hypoxia and in turn upregulates the expression of oxygen-sensitive target genes such as Vegf (19, 20). Hif-1α is expressed in the fetal lung (64), whereas Hif-1α-deficient mice die *in utero* and exhibit severe vascularization defects (65). We found that both the antisense knockdown of Hif-1α and Vegf reduced pulmonary vascular development, although the vascular reduction was more severe in explants treated with antisense Hif-1α ODN than with antisense Vegf ODN. The latter is not surprising because Hif-1α regulates many more genes than Vegf alone (45). Our key finding that the antisense inhibition of vascularization almost completely abrogated epithelial branching morphogenesis is remarkable and suggests that vascular development is essential for airway branching. Likewise, several studies have recently highlighted the importance of endothelial cells for developing organs (66). Matsumoto and co-workers (67) showed that when livers from Flk-1-deficient mice, that die early in embryogenesis due to a lack of blood vessel formation (68), were cultured, initial epithelial layers formed, but subsequent migration of liver epithelial cells into the surrounding septum transversum failed. Also, Lammert *et al*. (69) showed with *in vitro* and *in vivo* experiments, that endothelial cells induced essential steps in pancreas formation, specifically with respect to endocrine differentiation. Moreover, there is some evidence that distal airway branching and vascular formation are linked during pulmonary development. Inhibition of neovascularization in an embryonic lung allograft model with endothelial monocyte activating polypeptide (Emap II), which is an anti-angiogenic protein, resulted in an arrest of airway epithelial morphogenesis at the canalicular stage of lung development (26). Similarly, lungs of mice that lack the heparin sulfate-bound Vegf isoforms 164 and 188, and only express freely diffusible Vegf 120, showed a decrease in peripheral vascular development with fewer air-blood barriers and delayed airspace formation (70). Likewise, neonatal mice that were treated with a soluble decoy receptor for Vegfr1 to block endogenous Vegf signaling, exhibited a dramatic decrease in body and organ growth and died within 4 to 6 days after birth (71). The lungs of these mice were immature with simplification of the alveolar region and a decrease in Flk-1 expression (71). Inhibition of Vegfr signaling using the Vegfr blocker Su-5416 either before or after birth, also resulted in reduced pulmonary vascularization and alveolarization (72, 73). Based on published results and the data presented in this study, we conclude that pulmonary vascular development has a rate-limiting role in epithelial branching morphogenesis.

The aforementioned conclusion does not exclude the finding that pulmonary vascular development depends on signals from the lung epithelium for its survival (63). One driving force behind endothelial proliferation and guidance is clearly epithelial-derived Vegf. Reciprocal, paracrine Vegf signaling was shown to be important for the formation and vascularization of pancreatic islets (74). In the lung, Raoul and co-workers (5) found

that the stimulatory effect of Vegf upon fetal type II cells was not directly, but was exerted indirectly through reciprocal paracrine interactions, most likely involving mesenchymal and endothelial cells types (61). Hence, a regulatory loop is established, in which epithelial-derived Vegf induces vascular development, upon which the endothelium signals back, either directly, or indirectly via the mesenchymal compartment, to stimulate epithelial branching and differentiation. The key finding in our study that the antisense knockdown of the angiogenic factors Hif-1α and Vegf results in profoundly arrested airway branching, adds to this model that vessels play an active and guiding role in pulmonary branching morphogenesis, and are not merely following the developing airways.

Acknowledgements

This work was supported by the Sophia Foundation for Medical Research (SSWO 342, M.v.T.) and Canadian Institutes of Health Research (CIHR FRN-15273, M.P.). The authors thank Irene Tseu for technical assistance, Pooja Agarwal for advice on whole mount *in situ* hybridization, and Angie Griffin for animal handling and care. Martin Post is holder of a Canadian Research Chair (tier 1) in Fetal, Neonatal, and Maternal Health.

References

1. Shannon JM, Hyatt BA, 2004. Epithelial-mesenchymal interactions in the developing lung. Annu Rev Physiol. 66:625-645.
2. Warburton D, Schwarz M, Tefft D, Flores-Delgado G, Anderson KD, Cardoso WV, 2000. The molecular basis of lung morphogenesis. Mech Dev. 92:55-81.
3. Abman SH, 2001. Bronchopulmonary dysplasia: "a vascular hypothesis". Am J Respir Crit Care Med. 164:1755-1756.
4. Rabinovitch M, Bland R, 2002. Novel notions on newborn lung disease. Nat Med. 8:664-666.
5. Compernolle V, Brusselmans K, Acker T, Hoet P, Tjwa M, Beck H, Plaisance S, Dor Y, Keshet E, Lupu F, Nemery B, Dewerchin M, Van Veldhoven P, Plate K, Moons L, Collen D, Carmeliet P, 2002. Loss of HIF-2alpha and inhibition of VEGF impair fetal lung maturation, whereas treatment with VEGF prevents fatal respiratory distress in premature mice. Nat Med. 8:702-710.
6. Coleman C, Zhao J, Gupta M, Buckley S, Tefft JD, Wuenschell CW, Minoo P, Anderson KD, Warburton D, 1998. Inhibition of vascular and epithelial differentiation in murine nitrofen-induced diaphragmatic hernia. Am J Physiol. 274:L636-646.
7. Shehata SM, Tibboel D, Sharma HS, Mooi WJ, 1999. Impaired structural remodelling of pulmonary arteries in newborns with congenital diaphragmatic hernia: a histological study of 29 cases. J Pathol. 189:112-118.
8. Risau W, 1997. Mechanisms of angiogenesis. Nature. 386:671-674.
9. Hislop AA, 2002. Airway and blood vessel interaction during lung development. J Anat. 201:325-334.
10. Burri PH: Lung development and pulmonary angiogenesis. In Gaultier C, Bourbon JR,Post M (eds): Lung Development, p 122-151. New York, Oxford University Press Inc, 1999.
11. Lee YM, Jeong CH, Koo SY, Son MJ, Song HS, Bae SK, Raleigh JA, Chung HY, Yoo MA, Kim KW, 2001. Determination of hypoxic region by hypoxia marker in developing mouse embryos in vivo: a possible signal for vessel development. Dev Dyn. 220:175-186.
12. Chen EY, Fujinaga M, Giaccia AJ, 1999. Hypoxic microenvironment within an embryo induces apoptosis and is essential for proper morphological development. Teratology. 60:215-225.
13. Maltepe E, Simon MC, 1998. Oxygen, genes, and development: an analysis of the role of hypoxic gene regulation during murine vascular development. J Mol Med. 76:391-401.
14. Yue X, Tomanek RJ, 1999. Stimulation of coronary vasculogenesis/angiogenesis by hypoxia in cultured

embryonic hearts. Dev Dyn. 216:28-36.

15. Loughna S, Yuan HT, Woolf AS, 1998. Effects of oxygen on vascular patterning in Tie1/LacZ metanephric kidneys in vitro. Biochem Biophys Res Commun. 247:361-366.

16. Gebb SA, Jones PL, 2003. Hypoxia and lung branching morphogenesis. Adv Exp Med Biol. 543:117-125.

17. Acarregui MJ, Penisten ST, Goss KL, Ramirez K, Snyder JM, 1999. Vascular endothelial growth factor gene expression in human fetal lung in vitro. Am J Respir Cell Mol Biol. 20:14-23.

18. Neufeld G, Cohen T, Gengrinovitch S, Poltorak Z, 1999. Vascular endothelial growth factor (VEGF) and its receptors. Faseb J. 13:9-22.

19. Maxwell PH, Ratcliffe PJ, 2002. Oxygen sensors and angiogenesis. Semin Cell Dev Biol. 13:29-37.

20. Semenza GL, 2000. Expression of hypoxia-inducible factor 1: mechanisms and consequences. Biochem Pharmacol. 59:47-53.

21. Kotch LE, Iyer NV, Laughner E, Semenza GL, 1999. Defective vascularization of HIF-1alpha-null embryos is not associated with VEGF deficiency but with mesenchymal cell death. Dev Biol. 209:254-267.

22. Ghabrial A, Luschnig S, Metzstein MM, Krasnow MA, 2003. Branching morphogenesis of the Drosophila tracheal system. Annu Rev Cell Dev Biol. 19:623-647.

23. Isaac DD, Andrew DJ, 1996. Tubulogenesis in Drosophila: a requirement for the trachealess gene product. Genes Dev. 10:103-117.

24. Wilk R, Weizman I, Shilo BZ, 1996. trachealess encodes a bHLH-PAS protein that is an inducer of tracheal cell fates in Drosophila. Genes Dev. 10:93-102.

25. Jarecki J, Johnson E, Krasnow MA, 1999. Oxygen regulation of airway branching in Drosophila is mediated by branchless FGF. Cell. 99:211-220.

26. Schwarz MA, Zhang F, Gebb S, Starnes V, Warburton D, 2000. Endothelial monocyte activating polypeptide II inhibits lung neovascularization and airway epithelial morphogenesis. Mech Dev. 95:123-132.

27. Zeng X, Wert SE, Federici R, Peters KG, Whitsett JA, 1998. VEGF enhances pulmonary vasculogenesis and disrupts lung morphogenesis in vivo. Dev Dyn. 211:215-227.

28. Akeson AL, Greenberg JM, Cameron JE, Thompson FY, Brooks SK, Wiginton D, Whitsett JA, 2003. Temporal and spatial regulation of VEGF-A controls vascular patterning in the embryonic lung. Dev Biol. 264:443-455.

29. Schlaeger TM, Bartunkova S, Lawitts JA, Teichmann G, Risau W, Deutsch U, Sato TN, 1997. Uniform vascular-endothelial-cell-specific gene expression in both embryonic and adult transgenic mice. Proc Natl Acad Sci U S A. 94:3058-3063.

30. Gasca S, Hill DP, Klingensmith J, Rossant J, 1995. Characterization of a gene trap insertion into a novel gene, cordon- bleu, expressed in axial structures of the gastrulating mouse embryo. Dev Genet. 17:141-154.

31. Driver SE, Robinson GS, Flanagan J, Shen W, Smith LE, Thomas DW, Roberts PC, 1999. Oligonucleotide-based inhibition of embryonic gene expression. Nat Biotechnol. 17:1184-1187.

32. Souza P, Sedlackova L, Kuliszewski M, Wang J, Liu J, Tseu I, Liu M, Tanswell AK, Post M, 1994. Antisense oligodeoxynucleotides targeting PDGF-B mRNA inhibit cell proliferation during embryonic rat lung development. Development. 120:2163-2173.

33. Riddle RD, Johnson RL, Laufer E, Tabin C, 1993. Sonic hedgehog mediates the polarizing activity of the ZPA. Cell. 75:1401-1416.

34. Moorman AF, Houweling AC, de Boer PA, Christoffels VM, 2001. Sensitive nonradioactive detection of mRNA in tissue sections: novel application of the whole-mount in situ hybridization protocol. J Histochem Cytochem. 49:1-8.

35. Elson DA, Thurston G, Huang LE, Ginzinger DG, McDonald DM, Johnson RS, Arbeit JM, 2001. Induction of hypervascularity without leakage or inflammation in transgenic mice overexpressing hypoxia-inducible factor-1alpha. Genes Dev. 15:2520-2532.

36. Livak KJ, Schmittgen TD, 2001. Analysis of relative gene expression data using real-time quantitative PCR and the 2(-Delta Delta C(T)) Method. Methods. 25:402-408.

37. Sutherland D, Samakovlis C, Krasnow MA, 1996. branchless encodes a Drosophila FGF homolog that controls tracheal cell migration and the pattern of branching. Cell. 87:1091-1101.

38. Min H, Danilenko DM, Scully SA, Bolon B, Ring BD, Tarpley JE, DeRose M, Simonet WS, 1998. Fgf-10 is required for both limb and lung development and exhibits striking functional similarity to Drosophila branchless. Genes Dev. 12:3156-3161.

39. Sekine K, Ohuchi H, Fujiwara M, Yamasaki M, Yoshizawa T, Sato T, Yagishita N, Matsui D, Koga Y, Itoh N, Kato S, 1999. Fgf10 is essential for limb and lung formation. Nat Genet. 21:138-141.

40. De Moerlooze L, Spencer-Dene B, Revest J, Hajihosseini M, Rosewell I, Dickson C, 2000. An important role for the IIIb isoform of fibroblast growth factor receptor 2 (FGFR2) in mesenchymal-epithelial signalling during mouse organogenesis. Development. 127:483-492.

41. Bellusci S, Grindley J, Emoto H, Itoh N, Hogan BL, 1997. Fibroblast growth factor 10 (FGF10) and branching morphogenesis in the embryonic mouse lung. Development. 124:4867-4878.

42. Weaver M, Dunn NR, Hogan BL, 2000. Bmp4 and Fgf10 play opposing roles during lung bud morphogenesis. Development. 127:2695-2704.

43. Bellusci S, Henderson R, Winnier G, Oikawa T, Hogan BL, 1996. Evidence from normal expression and targeted misexpression that bone morphogenetic protein (Bmp-4) plays a role in mouse embryonic lung morphogenesis. Development. 122:1693-1702.

44. Gebb S, Shannon J, 1999. Hypoxia stimulates fetal lung branching in vitro. Am J Respir Crit Care Med. 159: A744.

45. Semenza GL, 1999. Regulation of mammalian O2 homeostasis by hypoxia-inducible factor 1. Annu Rev Cell Dev Biol. 15:551-578.

46. Tufro-McReddie A, Norwood VF, Aylor KW, Botkin SJ, Carey RM, Gomez RA, 1997. Oxygen regulates vascular endothelial growth factor-mediated vasculogenesis and tubulogenesis. Dev Biol. 183:139-149.

47. Wilborn AM, Evers LB, Canada AT, 1996. Oxygen toxicity to the developing lung of the mouse: role of reactive oxygen species. Pediatr Res. 40:225-232.

48. Acarregui MJ, Snyder JM, Mendelson CR, 1993. Oxygen modulates the differentiation of human fetal lung in vitro and its responsiveness to cAMP. Am J Physiol. 264:L465-474.

49. Arman E, Haffner-Krausz R, Gorivodsky M, Lonai P, 1999. Fgfr2 is required for limb outgrowth and lung-branching morphogenesis. Proc Natl Acad Sci U S A. 96:11895-11899.

50. Peters K, Werner S, Liao X, Wert S, Whitsett J, Williams L, 1994. Targeted expression of a dominant negative FGF receptor blocks branching morphogenesis and epithelial differentiation of the mouse lung. Embo J. 13:3296-3301.

51. Celli G, LaRochelle WJ, Mackem S, Sharp R, Merlino G, 1998. Soluble dominant-negative receptor uncovers essential roles for fibroblast growth factors in multi-organ induction and patterning. Embo J. 17:1642-1655.

52. Moromisato DY, Moromisato MY, Zanconato S, Roberts CT, Jr., 1996. Effect of hypoxia on lung, heart, and liver insulin-like growth factor-I gene and receptor expression in the newborn rat. Crit Care Med. 24:919-924.

53. Han X, Amar S, 2003. Role of insulin-like growth factor-1 signaling in dental fibroblast apoptosis. J Periodontol. 74:1176-1182.

54. Ferrara N, 2000. Vascular endothelial growth factor and the regulation of angiogenesis. Recent Prog Horm Res. 55:15-35; discussion 35-16.

55. Carmeliet P, Ferreira V, Breier G, Pollefeyt S, Kieckens L, Gertsenstein M, Fahrig M, Vandenhoeck A, Harpal K, Eberhardt C, Declercq C, Pawling J, Moons L, Collen D, Risau W, Nagy A, 1996. Abnormal blood vessel development and lethality in embryos lacking a single VEGF allele. Nature. 380:435-439.

56. Ferrara N, Carver-Moore K, Chen H, Dowd M, Lu L, O'Shea KS, Powell-Braxton L, Hillan KJ, Moore MW, 1996. Heterozygous embryonic lethality induced by targeted inactivation of the VEGF gene. Nature. 380:439-442.

57. Breier G, Albrecht U, Sterrer S, Risau W, 1992. Expression of vascular endothelial growth factor during embryonic angiogenesis and endothelial cell differentiation. Development. 114:521-532.

58. Greenberg JM, Thompson FY, Brooks SK, Shannon JM, McCormick-Shannon K, Cameron JE, Mallory BP, Akeson AL, 2002. Mesenchymal expression of vascular endothelial growth factors D and A defines vascular patterning in developing lung. Dev Dyn. 224:144-153.

59. Healy AM, Morgenthau L, Zhu X, Farber HW, Cardoso WV, 2000. VEGF is deposited in the subepithelial matrix at the leading edge of branching airways and stimulates neovascularization in the murine embryonic lung. Dev Dyn. 219:341-352.

60. Ferrara N, Davis-Smyth T, 1997. The biology of vascular endothelial growth factor. Endocr Rev. 18:4-25.

61. Raoul W, Chailley-Heu B, Barlier-Mur AM, Delacourt C, Maitre B, Bourbon JR, 2004. Effects of vascular endothelial growth factor (VEGF) on isolated fetal alveolar type II cells. Am J Physiol Lung Cell Mol Physiol. 286:L1293-1301.

62. Lassus P, Turanlahti M, Heikkila P, Andersson LC, Nupponen I, Sarnesto A, Andersson S, 2001. Pulmonary vascular endothelial growth factor and Flt-1 in fetuses, in acute and chronic lung disease, and in persistent pulmonary hypertension of the newborn. Am J Respir Crit Care Med. 164:1981-1987.

63. Gebb SA, Shannon JM, 2000. Tissue interactions mediate early events in pulmonary vasculogenesis. Dev Dyn. 217:159-169.

64. Madan A, Varma S, Cohen HJ, 2002. Developmental stage-specific expression of the alpha and beta subunits of the HIF-1 protein in the mouse and human fetus. Mol Genet Metab. 75:244-249.

65. Iyer NV, Kotch LE, Agani F, Leung SW, Laughner E, Wenger RH, Gassmann M, Gearhart JD, Lawler AM, Yu AY, Semenza GL, 1998. Cellular and developmental control of O2 homeostasis by hypoxia- inducible factor 1

alpha. Genes Dev. 12:149-162.

66. Lammert E, Cleaver O, Melton D, 2003. Role of endothelial cells in early pancreas and liver development. Mech Dev. 120:59-64.

67. Matsumoto K, Yoshitomi H, Rossant J, Zaret KS, 2001. Liver organogenesis promoted by endothelial cells prior to vascular function. Science. 294:559-563.

68. Shalaby F, Rossant J, Yamaguchi TP, Gertsenstein M, Wu XF, Breitman ML, Schuh AC, 1995. Failure of blood-island formation and vasculogenesis in Flk-1-deficient mice. Nature. 376:62-66.

69. Lammert E, Cleaver O, Melton D, 2001. Induction of pancreatic differentiation by signals from blood vessels. Science. 294:564-567.

70. Galambos C, Ng YS, Ali A, Noguchi A, Lovejoy S, D'Amore PA, DeMello DE, 2002. Defective pulmonary development in the absence of heparin-binding vascular endothelial growth factor isoforms. Am J Respir Cell Mol Biol. 27:194-203.

71. Gerber HP, Hillan KJ, Ryan AM, Kowalski J, Keller GA, Rangell L, Wright BD, Radtke F, Aguet M, Ferrara N, 1999. VEGF is required for growth and survival in neonatal mice. Development. 126:1149-1159.

72. Jakkula M, Le Cras TD, Gebb S, Hirth KP, Tuder RM, Voelkel NF, Abman SH, 2000. Inhibition of angiogenesis decreases alveolarization in the developing rat lung. Am J Physiol Lung Cell Mol Physiol. 279:L600-607.

73. Le Cras TD, Markham NE, Tuder RM, Voelkel NF, Abman SH, 2002. Treatment of newborn rats with a VEGF receptor inhibitor causes pulmonary hypertension and abnormal lung structure. Am J Physiol Lung Cell Mol Physiol. 283:L555-L562.

74. Lammert E, Gu G, McLaughlin M, Brown D, Brekken R, Murtaugh LC, Gerber HP, Ferrara N, Melton DA, 2003. Role of VEGF-A in vascularization of pancreatic islets. Curr Biol. 13:1070-1074.

Chapter 4

Pulmonary vascular development in sonic hedgehog-deficient mice

Minke van Tuyl[1,2], Jinxia Wang[1], Maciek Kuliszewski[1], Jason Liu[1], Dick Tibboel[2], and Martin Post[1]

[1]Canadian Institutes of Health Research (CIHR) Group in Lung Development, Hospital for Sick Children Research Institute, Departments of Pediatrics and Physiology, University of Toronto, Toronto, ON, Canada
[2]Department of Pediatric Surgery, Sophia Children's Hospital, Erasmus University Medical Center Rotterdam, Rotterdam, The Netherlands

Submitted

Abstract

Sonic hedgehog (Shh) is a morphogen that plays a major role in many aspects of embryonic development. Mice that are deficient for Shh die before birth with defects in brain and neural tube development, cyclopia, and limb defects. Moreover, Shh-deficient mice have defects in airway development, that is, the trachea and esophagus do not separate, whereas their lungs are hypoplastic and display a severe lung branching defect. Recent studies showed that hedgehog signaling is involved in vascular development. In this study we therefore investigated the possibility that diminished airway branching in Shh-deficient mice is due to abnormal pulmonary vascular development. Pulmonary vascular development in Shh-deficient mice was investigated with the use of Shh/Tie2-LacZ compound transgenic mice. Endothelial cell expression of LacZ and CD31 was studied. In embryonic day (E)11.5-13.5 Shh-deficient mice, the pulmonary vascular bed is decreased to the same degree as airway branching. However, when E12.5 Shh-deficient lungs were cultured for 4 to 6 days, the vascular network deteriorated compared to wild-type lungs. The expression of vascular endothelial growth factor-A (Vegf) or its receptor Vegfr2 (KDR/Flk-1), was not different between E12.5-13.5 Shh-deficient and wild-type lungs. In contrast, mRNA expression for angiopoietin-1 (Ang-1), but not for Ang-2 or the angiopoietin receptor Tie2, was downregulated in lungs of E12.5-E13.5 Shh null mutant mice. Recombinant Ang-1 alone was unable to restore branching morphogenesis in Shh-deficient lungs *in vitro*. Conversely, the angiogenic factor fibroblast growth factor-2 (Fgf2) alone, or in combination with Ang-1, dramatically increased vascularization and branching morphogenesis of cultured Shh-deficient lungs. These data indicate that early-stage vascular development, mediated by Vegf/Vegfr2 signaling, proceeds normal in Shh-deficient mice, whereas later-stage vascular development, mediated by the Ang/Tie2 signaling pathway, is defective. Furthermore, we speculate that airway branching morphogenesis in Shh-deficient lungs is partially restored by Fgf2-induced vascularization.

Introduction

The lung is composed of a complex network of airways and vessels and although much has been learned regarding the mechanisms controlling lung bud formation and airway branching, the mechanisms involved in vascular formation during lung development remain somewhat obscure. Three processes are believed to control pulmonary vascular development: angiogenesis, which is defined as sprouting of new vessels from pre-existing ones and gives rise to the central vessels; vasculogenesis, which is *de novo* synthesis of blood vessels from blood islands in the periphery of the lung; and the fusion of proximal and peripheral vessels to form the pulmonary circulation (1-3). Generally, it has been assumed that pulmonary vessels play a somewhat passive role in pulmonary development, that is, they merely follow the developing airways. However, in recent studies, the importance of endothelial cells for the development and differentiation of foregut-organs like the liver and pancreas, were highlighted (4, 5). Furthermore, more and more studies suggest that pulmonary vascular development and airway branching morphogenesis are linked, specifically during the period of alveolar formation. Mice engineered to express only the vascular endothelial growth factor-120 (Vegf-120) isoform, developed to term, but died shortly after birth (6). Their lungs showed impaired peripheral vascular development, a reduced number of air-blood barriers, and delayed airspace formation, suggesting a role for the heparin-binding Vegf isoforms (-164 and -188) in lung branching morphogenesis. Likewise, neonatal mice that were treated with a soluble decoy receptor for Vegf (mFlt(1-3)-IgG) to block endogenous Vegf signaling, exhibited a dramatic decrease in body and organ growth, and died within 4 to 6 days after birth (7). The lungs of these mice were immature with simplification of the alveolar region and a decrease in pulmonary arterial density. In addition, inhibition of vasculogenesis in rat pups with the Vegf receptor (Vegfr)-inhibitor Su-5416 resulted in reduced alveolarization (8, 9). Similarly, inhibition of neovascularization in an embryonic lung allograft model with endothelial monocyte activating polypeptide (Emap II), which is an anti-angiogenic protein, resulted in lung hypoplasia and an arrest of airway epithelial morphogenesis at the canalicular stage of lung development (10). Although these data indicate a linkage between distal airway and vascular formation during the later stages of pulmonary development, it is unknown whether these processes are linked during early lung branching morphogenesis.

Sonic hedgehog (Shh) is an important morphogen known to regulate epithelial-mesenchymal tissue interactions during embryonic organ development, including the lung (11-13). Shh-deficient mice exhibit a severe lung branching defect (12, 13). To our knowledge, the development of the pulmonary vasculature has not been specifically investigated in these mice. Recently, evidence has emerged that Shh is able to induce robust angiogenesis *in vivo* (14), whereas *in vitro*, Shh induced capillary morphogenesis of endothelial cells (15). Furthermore, Shh induced the expression of two families of angiogenic cytokines, including all three Vegf isoforms and Ang-1 and -2 (16). Thus, it

is possible that reduced airway branching in Shh null mice is secondary to a defect in pulmonary vascular development.

In this study, we investigated vascular development in Shh-deficient lungs and observed that the early pulmonary vasculature develops normal, but that this vascular network deteriorates at later stages of development, which may be the result of decreased Ang-1 levels. Exogenous Fgf2, in combination with Ang-1, stimulated both vascular development and airway branching of cultured Shh-deficient lungs, suggesting a role for proper vascularization in normal branching morphogenesis.

Materials and Methods

Mouse mutants

Shh, Gli2, and Gli3 heterozygous ($Shh^{+/-}$, $Gli2^{+/-}$, $Gli3^{+/-}$) mice were obtained from Dr. C. C. Hui, Hospital for Sick Children, Toronto, ON, Canada. Tie2-LacZ mice (17) were obtained from Jackson Laboratory (Bar Harbor, MN, U.S.A.). $Shh^{+/-}$, $Gli2^{+/-}$, and $Gli3^{+/-}$ mice were crossed with Tie2-LacZ mice and embryos obtained from crossings between $Shh^{+/-}$/Tie2-LacZ and $Shh^{+/-}$/Tie2-LacZ, $Gli2^{+/-}$/Tie-LacZ and $Gli2^{+/-}$/Tie-LacZ, and $Gli3^{+/-}$/Tie2-LacZ and $Gli3^{+/-}$/Tie2-LacZ mice respectively, were used for whole mount LacZ staining of embryonic day (E)11.5-E13.5 lungs and whole organ cultures of E12.5 lungs. The Shh, Gli2, and Gli3 genotypes were determined by PCR analysis of genomic DNA (18). All mouse protocols were in accordance with CACC guidelines and were approved by the Animal Care and Use Committee of the Hospital for Sick Children, Toronto, ON, Canada.

Whole lung organ culture

Lung buds were dissected from E12.5 Shh/Tie2-LacZ embryos (day of vaginal plug is E0.5) and placed on a floating (8 µm Whatman Nuclepore polycarbonate) membrane (Integra Environmental Inc. Burlington, ON, Canada). Explants were grown in DMEM/10% FCS (Gibco, Grand Islands, NY, U.S.A.) and maintained in 20% O_2 and 5% CO_2, at 37 C. rhAng-1 (R&D, Minneapolis, MN, U.S.A.) and rhFgf2 (Promega, Madison, WI, U.S.A.) were added to the medium in a final concentration of 500 ng/ml and 250 ng/ml, respectively. Medium and growth factors were changed every other day.

LacZ staining

Shh/Tie2-LacZ, Gli2/Tie-LacZ, and Gli3/Tie-LacZ *in vivo*-lungs and Shh/Tie2-LacZ lung explants were fixed (4°C), washed, and stained (37°C) with X-gal (Invitrogen, Burlington, ON, Canada). For sectioning, lungs were fixed in 4% (w/v) paraformaldehyde (PFA) in phosphate buffered saline (PBS), dehydrated, and embedded in paraplast. Sections (12 µm) were mounted onto Superfrost slides (Fisher Scientific, Unionville, ON, Canada). Digital images were taken using a Leica digital imaging system.

Immunohistochemistry

Lungs were dissected from E11.5-E14.5 $Shh^{+/+}$, $Shh^{+/-}$, and $Shh^{-/-}$ embryos, fixed overnight in 4% PFA in PBS, dehydrated, and embedded in paraplast. Endogenous peroxidase activity was quenched with 0.15% (v/v) hydrogen peroxide in methanol. Sections were incubated with trypsin (0.6 mg/ml) for 5 minutes at room temperature (RT). Non-specific binding sites were blocked with 5% (v/v) normal goat serum and 1% (w/v) bovine serum albumin, followed by overnight incubation at 4°C with rat anti-mouse Pecam-1 antibody (1:60; anti-CD31, BD Biosciences Pharmingen, Mississauga, ON, Canada) and incubation with biotinylated secondary sheep anti-rat antibody (1:300) at RT. Color detection was performed according to instructions in the Vectastain ABC and DAB kit (Vector Laboratories, Burlingname, CA, U.S.A.). Slides were lightly counterstained with Carazzi haematoxylin.

RNA isolation and real-time RT-PCR

Total RNA (1 µg) was extracted from E12.5 (8 $Shh^{+/+}$, 17 $Shh^{+/-}$, and 17 $Shh^{-/-}$; total of 2 sets) and E13.5 (14 $Shh^{+/+}$, 17 $Shh^{+/-}$, and 19 $Shh^{-/-}$; total of 4 sets) lungs using the RNeasy kit (Qiagen, Mississauga, ON, Canada) and was reverse transcribed (37°C) using random-hexamers (Applied Biosystems, Foster City, CA, U.S.A.). The resulting templates (50 ng of cDNA for our target genes and 5 ng for 18S) were quantified by real-time PCR (ABI Prism 7700). Primers and TaqMan probes for total Vegf, Vegf-120, Vegf-164, Vegf-188, Vegf receptor Flk-1 (kinase insert domain-containing receptor/fetal liver kinase-1; KDR/Flk-1 or Vegfr2), angiopoietin (Ang)-1, and Ang-2 were similar to previously published sequences (19), whereas primers and TaqMan probes for Pecam-1, Tie2, fibroblast growth factor-2 (Fgf2), Fgf10, and Fgf receptor-2 (Fgfr2) were purchased from ABI as Assays-on-Demand™ for murine genes. For each probe a dilution series determined the efficiency of amplification of each primer-probe set and the relative quantification method was employed (20). Briefly, relative expression was calculated as $2^{-(Ctgene\ of\ interest-Ct18S)}$ and experimental and control data were compared, after normalization with 18S as internal reference, using JMP® statistical software, by one-way analysis of variance (ANOVA) followed by Student t-tests. Significance was accepted at $p<0.05$.

Results

LacZ staining of Shh-deficient lungs

Whole mount LacZ staining revealed that the lungs of both wild-type ($Shh^{+/+}$) and heterozygous ($Shh^{+/-}$) mice had a branched network of vessels at E11.5 (Fig. 1A, B), which became more complex at E13.5 (Fig. 1D, E). After sectioning of the E13.5 LacZ-stained lungs, we observed that the vessels ran close and around the developing airways of the $Shh^{+/+}$ and $Shh^{+/-}$ lungs (Fig. 1G, H). In Shh-deficient ($Shh^{-/-}$) mice, lung hypoplasia was noticeable as early as E11.5 (Fig. 1C). Whole mount LacZ staining demonstrated, however, an extensive vascular network surrounding the developing lung buds (Fig. 1C), similar to

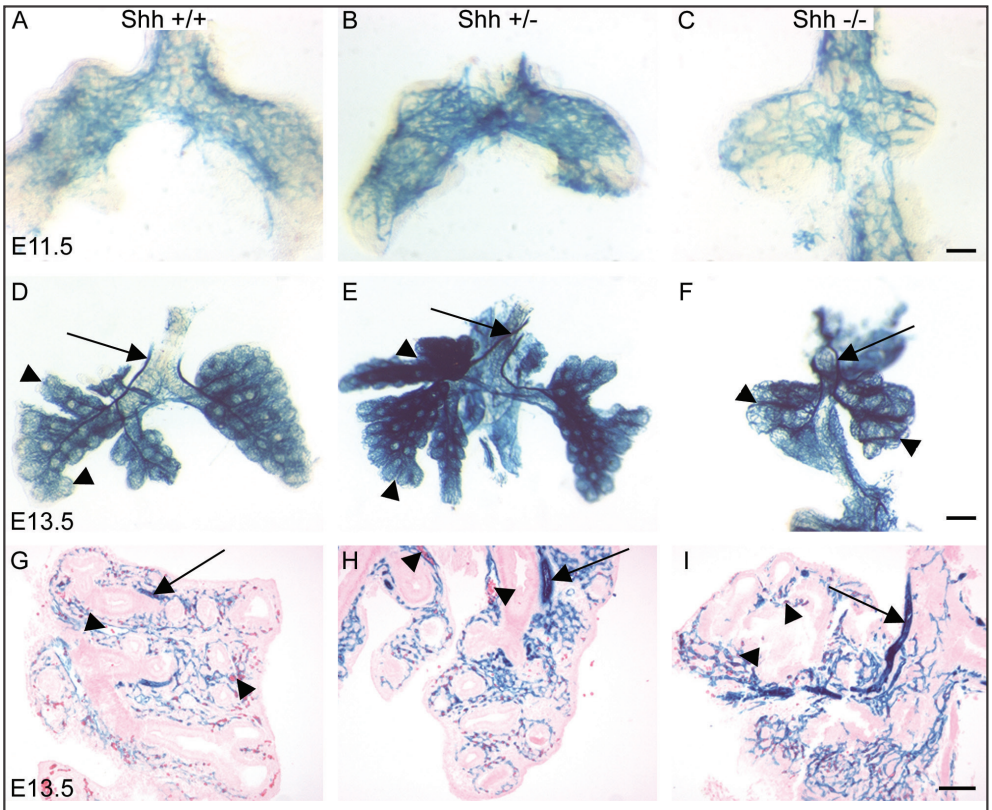

Figure 1. Vascular development in early-stage Shh$^{-/-}$ lungs. (A-C): X-gal-stained lungs of Shh/Tie2-LacZ mice at E11.5. A complex vascular network is present in the lungs of wild-type (Shh$^{+/+}$) embryos (A). Although Shh$^{-/-}$ lungs (C) are much smaller than Shh$^{+/+}$ (A) and Shh$^{+/-}$ (B) lungs, an appropriate vascular network is seen in Shh$^{-/-}$ lungs. (D-F): X-gal-stained lungs of Shh/Tie2-LacZ mice at E13.5. The vascular network has extended significantly in Shh$^{+/+}$ (D) and Shh$^{+/-}$ (E) lungs; large vessels are running along the trachea (arrows), whereas a dense network of microvessels cover the proximal (bronchiolar) and distal (alveolar) areas (arrowheads). In Shh$^{-/-}$ lungs (F), a comparable dense vascular network covers the entire pulmonary area (arrowheads), whereas larger vessels are present on both sides of the tracheoesophageal tube (arrow). Note the small size of Shh$^{-/-}$ lungs (F). (G-I): Sections of X-gal-stained Shh/Tie2-LacZ lungs. Larger vessels are seen in all three lungs (arrows). A comparable microvascular network is found in the mesenchyme surrounding the primitive epithelial tubules of Shh$^{+/+}$ (G), Shh$^{+/-}$ (H), and Shh$^{-/-}$ (I) lungs. Intravascular red blood cells are detected in all three sections (arrowheads). Sections were counterstained with eosin. Blue color is positive X-gal staining in endothelial cells. Bar: 80 µm (A-C); 230 µm (D, F); 320 µm (E); 100 µm (G-I).

the vessels that were seen in Shh$^{+/+}$ and Shh$^{+/-}$ lungs. Lung hypoplasia and reduced airway branching morphogenesis were more evident in E13.5 Shh$^{-/-}$ mice (Fig. 1F). The vascular network, however, was abundant (Fig. 1F) and sections of the E13.5 LacZ-stained lungs showed that vessels ran in close proximity to the airway tubules and wrapped around the tips of the tubules (Fig. 1I). From these results we conclude that early (E11.5-E13.5) Shh-deficient lungs have a vascular network that is appropriate for the extent of epithelial branching. Because Gli2 and Gli3 are thought to be the primary transcriptional mediators

of Shh signaling in the developing lung (21), we analyzed vascular development in lungs of mutants using Gli$^{+/-}$/Tie2-LacZ compound mice. Similar to findings with Shh$^{-/-}$ mice, deletion of either Gli2 or Gli3 had no influence on early pulmonary vascular development (not shown).

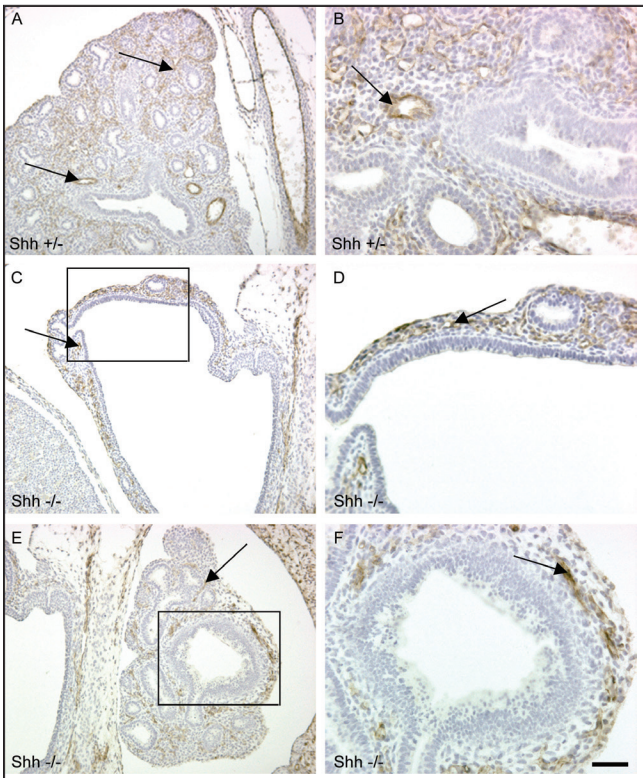

Figure 2. Pecam-1 immunostaining in early-stage Shh$^{-/-}$ lungs. In lungs of E14.5 Shh$^{+/-}$ embryos (A), a vascular network is detected in the mesenchyme surrounding the primitive lung tubules (B). In E14.5 Shh$^{-/-}$ lungs, positive Pecam-1 staining was readily detected in the pulmonary mesenchyme (C; right lung lobe; E; left lung lobe), whereas with higher magnification a vascular network is detected that is appropriate to the size of the primitive lung tubules (D and F, respectively). Note the small size of the Shh$^{-/-}$ lung and the dramatic decrease in branching morphogenesis of the epithelial tubules (C and E). Brown staining is positive Pecam-1 immunostaining. Bar: 100 µm (A, C, E); 40 µm (B, D, F).(arrow). Note the small size of Shh$^{-/-}$ lungs (F). (G-I): Sections of X-gal-stained Shh/Tie2-LacZ lungs. Larger vessels are seen in all three lungs (arrows). A comparable microvascular network is found in the mesenchyme surrounding the primitive epithelial tubules of Shh$^{+/+}$ (G), Shh$^{+/-}$ (H), and Shh$^{-/-}$ (I) lungs. Intravascular red blood cells are detected in all three sections (arrowheads). Sections were counterstained with eosin. Blue color is positive X-gal staining in endothelial cells. Bar: 80 µm (A-C); 230 µm (D, F); 320 µm (E); 100 µm (G-I).

Pecam-1 staining of Shh-deficient lungs

To confirm that Shh-deficient lungs develop a vascular network that is appropriate for the extent of tubular epithelial branching, we performed immunohistochemistry for endothelial specific Pecam-1 (CD31). In E14.5 Shh$^{+/+}$ (not shown) and Shh$^{+/-}$ (Fig. 2A, B) lungs, immunopositive staining for Pecam-1 was observed in the pulmonary mesenchymal mass in which it was detected in the endothelial lining of the vasculature in close proximity to the epithelial tubules. In Shh$^{-/-}$ lungs, a similar pattern of immunopositive Pecam-1 staining was observed (Fig. 2C, D, E, F). Immunopositive vessels ran along the few epithelial tubules that were present in the hypoplastic Shh$^{-/-}$ lungs (Fig. 2D, F). Comparison of the amount of vessels in Shh$^{+/-}$ lungs (Fig. 2A) to the amount of vessels in Shh$^{-/-}$ lungs (Fig. 2C, E)

demonstrated that fewer vessels were present in the $Shh^{-/-}$ lungs. However, looking at the individual lungs, the relative epithelial bud:vessel ratio was fairly similar in both lungs. To confirm this observation we performed real-time RT-PCR for Pecam-1 in E12.5-13.5 $Shh^{+/+}$, $Shh^{+/-}$, and $Shh^{-/-}$ lungs. Comparable levels of Pecam-1 mRNA were found between the three groups of lungs (Fig. 3A). These results support our observation in $Shh^{-/-}$/Tie2-LacZ lungs that early pulmonary vascular development is not affected in Shh-deficient mice.

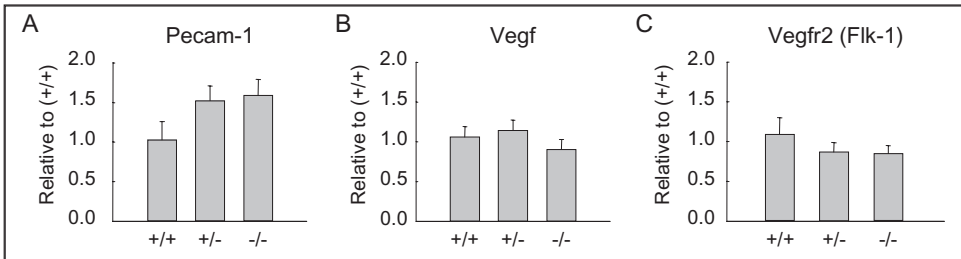

Figure 3. Pecam-1, Vegf, and Flk-1 (Vegfr2) mRNA levels in E12.5-13.5 Shh lungs. Message levels were quantified by real-time(q)RT-PCR. (A): Schematic representation of qRT-PCR results for Pecam-1 expression. No differences were observed in Pecam-1 mRNA expression between $Shh^{+/+}$, $Shh^{+/-}$, and $Shh^{-/-}$ lungs. (B-C): Schematic representation of qRT-PCR results for Vegf and Flk-1 (Vegfr2) expression. Message levels for total Vegf (B) and the Vegf isoforms -120, -164, and -188 (not shown) were similar in E12.5-13.5 $Shh^{+/+}$, $Shh^{+/-}$, and $Shh^{-/-}$ lungs. Flk-1 mRNA levels were similarly unchanged in $Shh^{-/-}$ lungs (C).

Vegf expression in Shh-deficient lungs

Recently, it was reported that Shh influences the expression of Vegf, a potent inducer of vascular development (16). Therefore, we performed real-time RT-PCR for total Vegf in E12.5-13.5 $Shh^{+/+}$, $Shh^{+/-}$, and $Shh^{-/-}$ lungs. No significant differences in total Vegf mRNA expression were found between $Shh^{+/+}$, $Shh^{+/-}$, and $Shh^{-/-}$ lungs (Fig. 3B). Because Vegf exists in three different isoforms as a result of differential splicing, we tested the possibility that the expression of these three isoforms was different between the $Shh^{+/+}$, $Shh^{+/-}$, and $Shh^{-/-}$ lungs. However, no significant differences in mRNA expression of any of the isoforms Vegf-120, -164 or -188 were observed between the three lung groups (not shown). Also, the Vegf receptor Vegfr2 (Flk-1/KDR) was equally expressed between the three groups (Fig. 3C). These results indicate that the Vegf/Vegfr2 signaling loop is unaffected and most likely contributes to the proper vascular network that was seen in early-stage Shh-deficient lungs (Figs 1 and 2).

Ang expression in Shh-deficient lungs

The Angiopoietins Ang-1 and Ang-2 are a relatively new group of angiogenic cytokines that have been shown to contribute to vascular maturation and stability (22-24). Ang-2 is thought to function as the natural antagonist of Ang-1 by binding to, but not activating the Angiopoietin receptor Tie2 (23). Because it was shown that exogenous Shh induced the expression of Ang-1 and Ang-2 from interstitial mesenchymal cells *in vitro* (16), we performed real-time RT-PCR for Ang-1 and Ang-2 in E12.5-13.5 $Shh^{+/+}$, $Shh^{+/-}$, and $Shh^{-/-}$

lungs. Ang-1, but not Ang-2, mRNA expression was significantly ($p<0.05$) decreased in $Shh^{-/-}$ lungs compared to $Shh^{+/+}$ and $Shh^{+/-}$ lungs (Fig. 4A), whereas no difference was observed for the mRNA expression of Tie2 (Fig. 4B). As a control experiment for the validity of the real-time RT-PCR, we compared the mRNA expression levels of Fgf10 and the Fgf receptor, Fgfr2, between $Shh^{+/+}$, $Shh^{+/-}$, and $Shh^{-/-}$ lungs. Fgf10 and Fgfr2 mRNA expression were significantly ($p<0.05$) upregulated in E12.5-13.5 $Shh^{-/-}$ lungs compared to $Shh^{+/+}$ and $Shh^{+/-}$ lungs (Fig. 4C, D), a finding that is in agreement with previous reports (12), Altogether, these data show that early-stage Shh-deficient lungs have an altered balance between Ang-1 and Ang-2, a finding that may explain the vascular abnormalities that are seen at later gestation in Shh-deficient lungs.

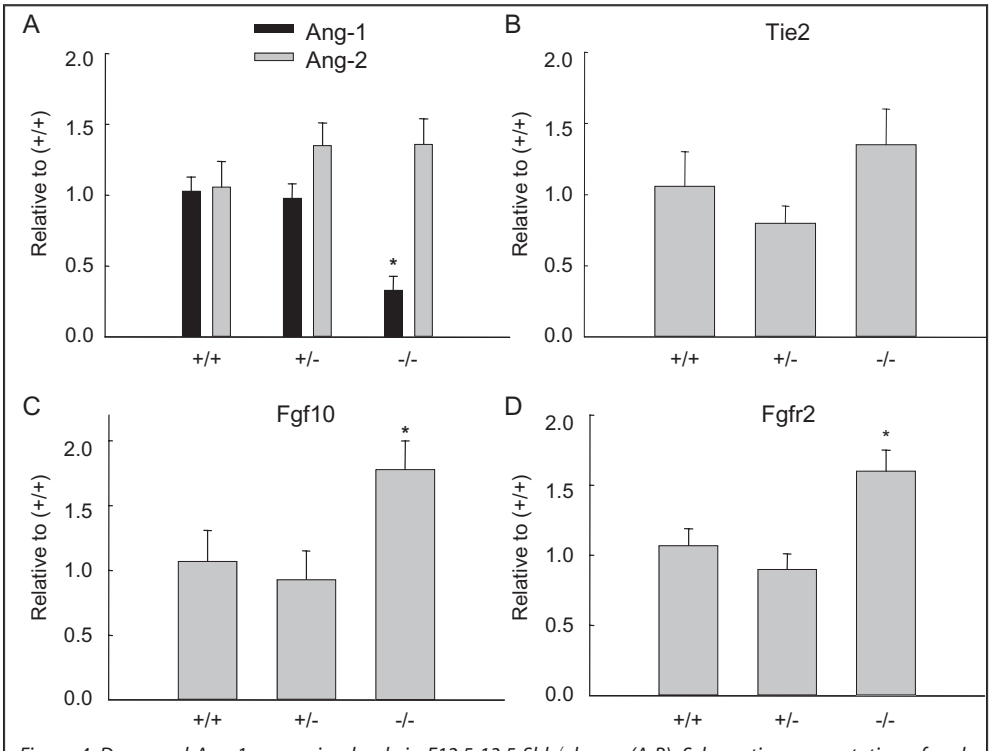

Figure 4. Decreased Ang-1 expression levels in E12.5-13.5 $Shh^{-/-}$ lungs. (A-B): Schematic representation of real-time(q)RT-PCR results for Ang-1, Ang-2, and Tie2 mRNA expression. Ang-1 expression (A) was significantly down-regulated in E12.5-13.5 $Shh^{-/-}$ lungs ($p<0.05$, compared to $Shh^{+/+}$ and $Shh^{+/-}$), whereas Ang-2 (A) and Tie2 (B) mRNA levels were not different from those in $Shh^{+/+}$ and $Shh^{+/-}$ lungs. (C-D): Schematic representation of qRT-PCR results for Fgf10 and Fgfr2 mRNA expression. Fgf10 (C) and Fgfr2 (D) expression levels were upregulated in E12.5-13.5 $Shh^{-/-}$ lungs compared to $Shh^{+/+}$ and $Shh^{+/-}$ lungs (*$p<0.05$).*

Vascular development in cultured Shh-deficient lungs

Most $Shh^{-/-}$ mice die around E14.5 with multiple organ failure (12). To test whether later (>E14.5) vascular development in Shh-deficient lungs was abnormal because of a disturbed balance between Ang-1 and Ang-2, we followed vascular and airway branching

morphogenesis of Shh$^{-/-}$ lungs *in vitro*. No differences were noted in explant growth or vascularization between E12.5 Shh$^{+/+}$ (not shown) and Shh$^{+/-}$ (Fig. 5A-C) lungs after 3 to 5 days in culture. Lung explants from E12.5 Shh$^{+/-}$/Tie2-LacZ compound mice formed an extensive and complex pattern of vessels, as visualized by whole mount LacZ staining, after 3 days in culture (Fig. 5A). Sections of these lung explants revealed a fine capillary network in the mesenchyme surrounding developing epithelial tubules (Fig. 5B). After 5 days in culture, the capillary network was even more extended, whereas the mesenchymal layers separating the airways had become thinner (Fig. 5C). Cultured E12.5 Shh$^{-/-}$ lung explants were severely hypoplastic (Fig. 5D) and lacked airway branching morphogenesis (Fig. 5E). Also, vascular development dramatically deteriorated in E12.5 Shh$^{-/-}$ lung explants after 3 days in culture (Fig. 5D). Sections of these lung explants revealed that only a discontinued, hypoplastic vascular network had remained after 3 to 5 days in culture (Fig. 5E, F). These data show that pulmonary vascular development is profoundly disturbed in later-stage Shh$^{-/-}$ mice.

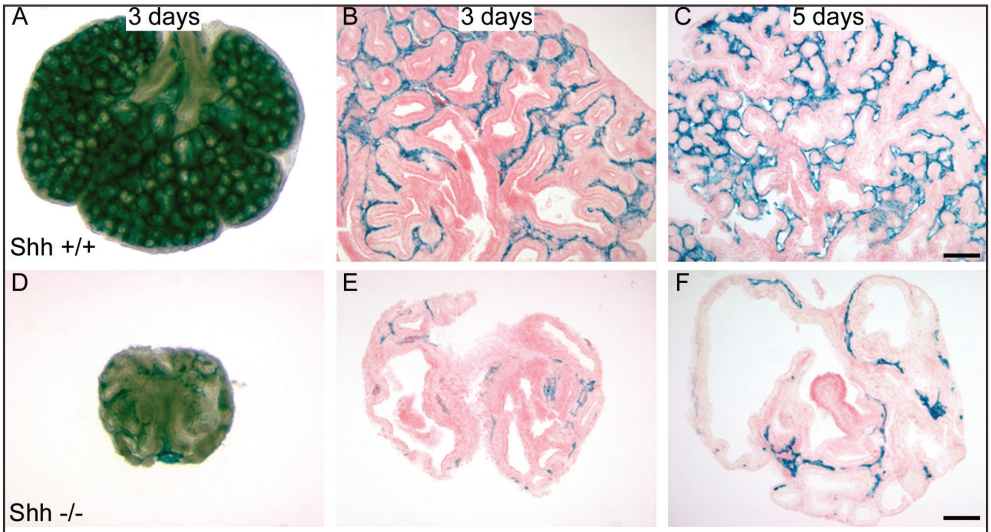

Figure 5. Abnormal in vitro vascular development of Shh$^{-/-}$ lung explants. Because almost no Shh$^{-/-}$ embryos survive till term, further experiments with Shh$^{-/-}$ lungs were carried out in vitro. (A-C): X-gal-stained lungs of E12.5 Shh$^{+/+}$/Tie2-LacZ mice after 3 (A-B) or 5 (C) days in culture. A complex vascular network is present in wild-type (Shh$^{+/+}$) lung explants after 3 days in culture (A). After sectioning, a fine vascular network is observed in the mesenchyme surrounding epithelial tubules (B, C). (D-F): X-gal-stained lungs of E12.5 Shh$^{-/-}$/Tie2-LacZ mice after 3 (D-E) or 5 (F) days in culture. In contrast to wild-type lung explants, the vascular network in Shh$^{-/-}$ lung explants rapidly deteriorates with further culturing in vitro (A versus D). Upon sectioning of the Shh$^{-/-}$ lung explants, the lack of vascular structures (and epithelial branching morphogenesis) after 3 (E) and 5 (F) days in culture is even more evident. Sections were counterstained with eosin. Blue color is positive X-gal staining in endothelial cells. Bar: 160 µm (A, D); 100 µm (B-C, E-F).

Rescue of branching morphogenesis of Shh-deficient lungs

We hypothesized that the epithelial branching defect in $Shh^{-/-}$ lung explants is partially the result of reduced vascular development. Because Ang-1 mRNA was found to be downregulated in E12.5/13.5 $Shh^{-/-}$ lungs, we attempted a rescue experiment in which Shh-deficient lung explants were cultured in the presence or absence of rhAng-1 (Fig. 6). E12.5 $Shh^{-/-}$ lungs, cultured without rhAng-1, showed some branching after 4 days in culture (Fig. 6Aa-d). However, addition of 500 ng/ml of rhAng-1 to the culture medium did not increase branching morphogenesis in $Shh^{-/-}$ lung explants (Fig. 6Ba-d). Given that we previously reported that Fgf2 is a potent mitogen for fetal pulmonary microvascular endothelial cells (25), we then decided to investigate if vascular development in $Shh^{-/-}$ lung explants was stimulated by exogenous Fgf2. Total Fgf2 mRNA expression was not significantly altered in E12.5-13.5 Shh-deficient lungs compared to $Shh^{+/+}$ and $Shh^{+/-}$ lungs (Fig. 7A). Addition of 250 ng/ml rhFgf2 to the culture medium of E12.5 $Shh^{+/-}$/Tie2-LacZ lung explants significantly expanded the vascular bed (Fig. 7C *versus* 7B), indicating that $Shh^{+/-}$ lung explants, which develop indistinguishable from wild-type lung explants, do respond to Fgf2 with increased vascularization. Exposure of $Shh^{-/-}$ lung explants to rhFgf2 resulted in a considerable increase of the mesenchymal mass that surrounded the distal epithelial branches (arrows in Fig. 6Ca-d). From 3 days onwards, the $Shh^{-/-}$ lung explants cultured with rhFgf2 exhibited a dramatic increase in airway branching morphogenesis (Fig. 6Cd) compared to $Shh^{-/-}$ lung explants cultured without exogenous Fgf2 (Fig. 6Ad). Likewise, the pulmonary vascular network as visualized by LacZ staining, was significantly increased in $Shh^{-/-}$ lung explants that were cultured with rhFgf2 (Fig. 8A *versus* 8B). Sections of LacZ-stained $Shh^{-/-}$ lung explants that were cultured for 5 days with exogenous Fgf2 showed that the increase in vascular development was associated with a dramatic increase in epithelial branching morphogenesis (Fig. 8C *versus* 8D). Simultaneous addition of rhFgf2 and rhAng-1 to the culture medium of $Shh^{-/-}$ lung explants improved airway branching morphogenesis even further than with rhFgf2 alone (Fig. 6Da-d). These results show that $Shh^{-/-}$ lungs respond to the combination of angiogenic factors Fgf2 and Ang-1 with increased vascularization and airway branching.

Discussion

In this study, we report that Shh deficiency in mice results in abnormalities in pulmonary vascular development. A loss of Shh does not affect early-stage pulmonary vasculogenesis and angiogenesis, but it reduces the expression of the vascular-stabilizing factor Ang-1 and leads to an abnormal vascular bed at later gestation. Moreover, restoration of the vascular defect in Shh-deficient lungs with the angiogenic factors Fgf2 and Ang-1 partially recovers airway branching morphogenesis. From these and earlier (chapter 3) results, we conclude that proper vascularization is a key factor for normal airway branching morphogenesis.

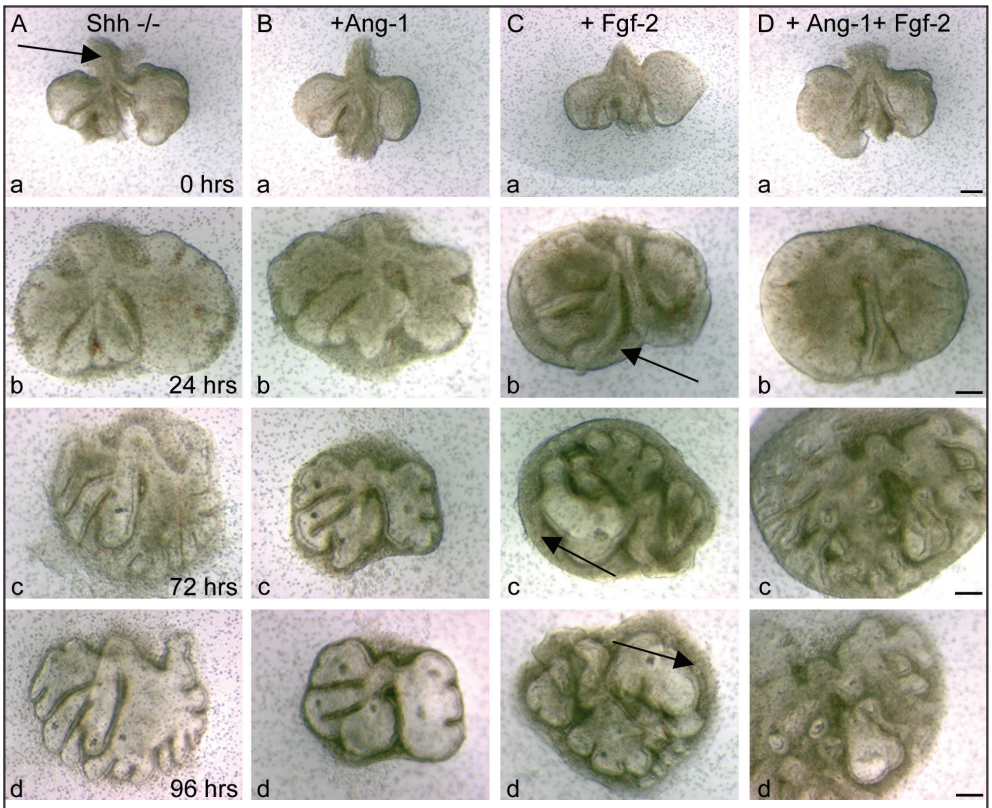

Figure 6. Partial restoration of airway branching morphogenesis in Shh$^{-/-}$ lung explants by Fgf2. (Aa-d): E12.5 Shh$^{-/-}$ explants (Aa) are small in size, exhibit reduced branching morphogenesis, and are connected to a single tracheoesophageal tube (arrow). Untreated Shh$^{-/-}$ lung explants do occasionally show some branching morphogenesis at the distal tips of the explants (Ab-c), but in general, growth and branching morphogenesis remain severely reduced after 4 days is culture (Ad). (Ba-d): Addition of rhAng-1 (500 ng/ml) to E12.5 Shh$^{-/-}$ lung explants did not restore branching morphogenesis (Bb-d, after 1, 3, and 4 days, respectively). (Ca-d): When E12.5 Shh$^{-/-}$ lung explants were cultured with rhFgf2 (250 ng/ml), branching morphogenesis increased dramatically (Cb-d, for 1, 3 and 4 days, respectively), whereas the amount of mesenchyme that surrounded the epithelial tubules increased significantly as a result of exogenous Fgf2 (arrows in Cb-d). (Da-d): Addition of both rhAng-1 (500 ng/ml) and rhFgf2 (250 ng/ml) simultaneously, increased explant size and the degree of branching morphogenesis to a greater extent than when rhFgf2 was added alone (Db-d after 1, 3, and 4 days, respectively). Bar: 200 µm (a); 155 µm (b-d).

Several reports support the idea that Shh is involved in the control of vascularization during development. Ectopic expression of Shh caused hypervascularization of the dorsal neural tube in mice (26), whereas Shh-deficient zebrafish fail to form the dorsal aorta (27). Also, Shh induced robust neovascularization in ischemic hind limbs of aged mice (16). In cultured fibroblasts, Shh upregulated the expression of all three VegfA isoforms and of Ang-1 and Ang-2 (16). Although Kanda and co-workers reported that Shh did not induce proliferation or migration of endothelial cells, they did observe that Shh promoted capillary morphogenesis of cultured endothelial cells (15).

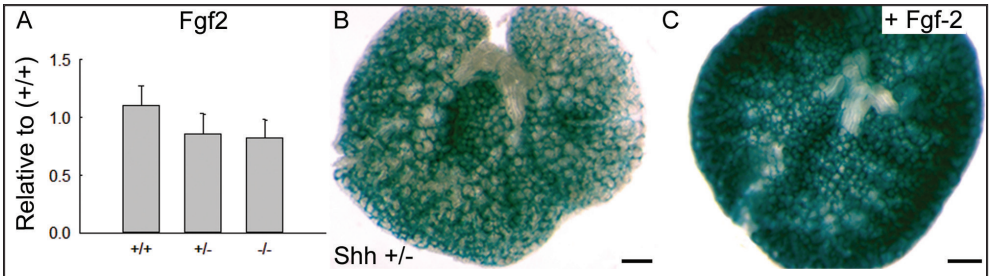

Figure 7. Exogenous Fgf2 increases the vascular network in Shh$^{+/-}$ lungs. (A): Schematic representation of real-time(q)RT-PCR results for Fgf2 mRNA expression in E12.5-13.5 Shh mice. No significant differences were observed between E12.5-13.5 Shh$^{+/+}$, Shh$^{+/-}$, and Shh$^{-/-}$ lungs. (B-C): X-gal-stained lungs of E12.5 Shh$^{+/-}$/Tie2-LacZ mice after 7 days in culture. A complex vascular network is present in Shh$^{+/-}$ lung explants (B). Addition of rhFgf2 (250 ng/ml) to cultured Shh$^{+/-}$ lung explants greatly enhanced the vascular network (C). Blue color is positive X-gal staining in endothelial cells. Bar: 200 µm.

In the present study, we found that early development of the pulmonary vascular network was unaffected in Shh-deficient mice. Early stages of vascular development require Vegf and its endothelial cell-specific receptor Vegfr2 because it was shown that disruption of either gene resulted in early embryonic lethality as a result of vascular defects (28-30). To overcome this limitation, Galambos *et al.* (6) engineered knock-in transgenic mice that expressed only the Vegf-120 isoform, an experiment that led to impaired peripheral vascular development in the lungs, suggesting that Vegf is important for pulmonary vascularization. We found that the expression of total Vegf or any of its three isoforms was unaffected in E12.5-E13.5 Shh-deficient lungs, a finding that may explain the normal development of the early primitive vascular network. In contrast, the angiopoietins do not seem to be important for early vasculogenesis, but instead act at a later stage of vascular development to elicit vascular stabilization via remodeling of the vasculature into a hierarchical network of mature vessels composed of endothelial and adventitial cells (22, 23, 31-36). Ang-1 and Ang-2 exhibit similar binding affinity for the endothelial Tie2 receptor (23). The binding of Ang-1 to Tie2 on endothelial cells results in the phosphorylation of Tie2, whereas Ang-2 binding does not phosphorylates Tie2, a finding that makes Ang-2 the natural antagonist of Ang-1 (23). We found a downregulation of Ang-1, but not of Ang-2, mRNA expression in E12.5-13.5 Shh-deficient lungs and speculate that this alteration in the balance of Ang-1 and Ang-2 caused vascular destabilization that resulted in the deterioration of the vascular network in Shh-deficient lungs at later gestation. In human (37) and murine lungs (38), Shh expression peaks at the late pseudoglandular, early canalicular period of development, a time that exhibits intense pulmonary vascularization. In this period, a loss of Shh likely causes a more pronounced reduction of Ang-1 and, therefore, augments the effect on vascular development, which probably explains why vascular abnormalities were mainly observed after culturing the E12.5-13.5 Shh$^{-/-}$ lungs for several days.

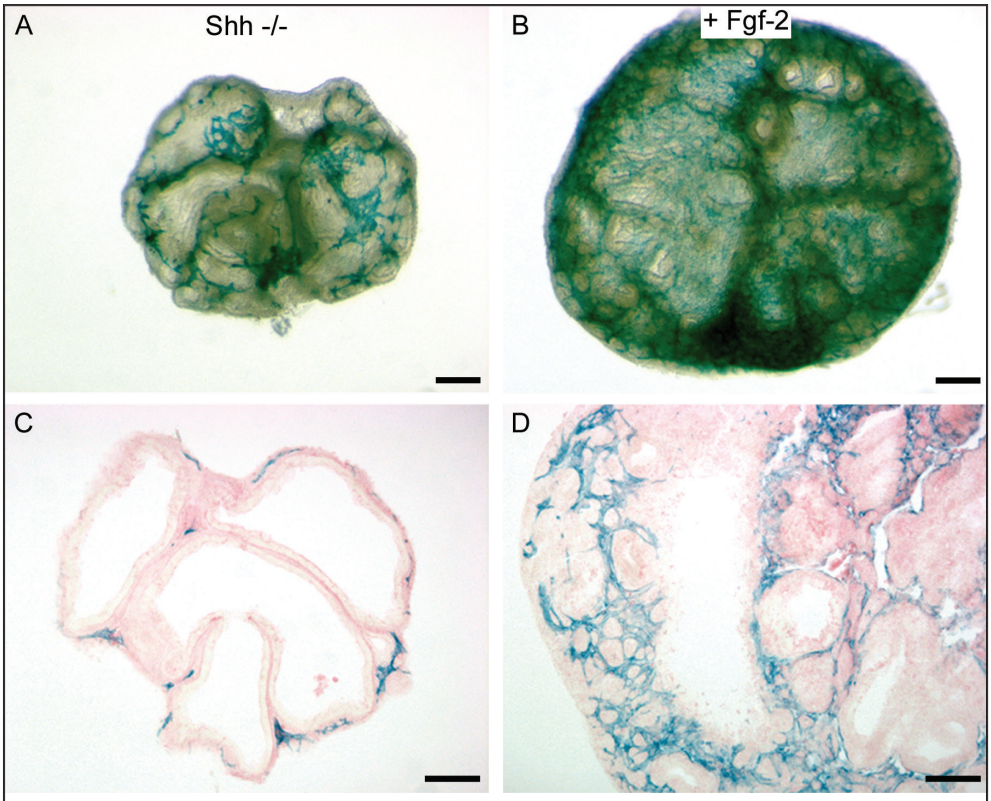

Figure 8. Exogenous Fgf2 restores vascular development in Shh$^{-/-}$ lung explants. (A-B): X-gal-stained lungs of E12.5 Shh$^{-/-}$/Tie2-LacZ mice after 6 days in culture. Few, disorganized vessels are present in untreated Shh$^{-/-}$ lung explants (A). After sectioning, the scarcity of vessels and the lack of branching morphogenesis are obvious (C). The addition of rhFgf2 (250 ng/ml) to the culture significantly enhanced the vascular complex in Shh$^{-/-}$ lungs (B). Sections of the X-gal-stained explants revealed a dramatic increase in vascularization and epithelial branching morphogenesis as a result of exogenous Fgf2 (D). Sections were counterstained with eosin. Blue color is positive X-gal staining in endothelial cells. Bar: 160 µm (A-B); 100 µm (C-D).

In E12.5 mouse lungs, Ang-1 mRNA expression is detected in the mesenchyme and smooth muscle cells surrounding most blood vessels (23). The mesenchymal compartment itself is a direct cellular target of Shh (12, 13) and Shh was shown to be required for the formation of smooth muscle cells (39). Whether Shh mediates its effect on these cells via Ang-1 remains to be investigated, but Ang-1 has been shown to play a role in the interaction of endothelial cells and surrounding support cells such as pericytes and smooth muscle cells (40). Ang-1 acted as a chemotactic, but not as a proliferation factor for endothelial cells and this chemotactic effect was abolished by excess soluble Tie2 receptor (41). A reduction in Ang-1 is a major cause of abnormalities in vascularization, because it was shown that Ang-1 null mutants have an abnormal vasculature characterized by decreased branching and impaired recruitment of periendothelial smooth muscle and pericyte cells (35).

Shh may induce Ang-1 via COUP-TFII activation in mesenchymal cells (42, 43). COUP-TFII is a member of the steroid-thyroid hormone receptor superfamily, which consists of a large group of ligand-activated transcription factors (44). During early-stage lung development COUP-TFII is expressed in the mesenchyme, however, it is undetectable at later stages of lung development (45, 46), at the time that pulmonary Shh expression starts to decline (37). A Shh response element has been identified in the COUP-TFII promoter that binds to a factor distinct from Gli (42). Two-thirds of the heterozygous COUP-TFII mice die before weaning, and a homozygous deletion of COUP-TFII is lethal around 10 days of gestation (43). Ang-1 is downregulated in COUP-TFII mutants, whereas angiogenesis and vascular remodeling are defective in these mice (43). Vasculogenesis appeared normal in COUP-TFII mutants, that is, the development of a primitive vascular plexus with appropriate expression of differentiation marker genes (Vegfr1, Vegfr2, and Pecam-1) was undisturbed (46). However, the formation of a microcapillary network in these mice was impaired (46). Ang-1 was downregulated, whereas Tie2 expression appeared normal. These findings suggest that basal Ang-1 levels are sufficient to maintain Tie2 expression, but not to maintain an effective vascular plexus (46). Conversely, Vegf was upregulated in E9.5 COUP-TFII mutants (46). This combination of normal to elevated levels of Tie2 and Vegf, but decreased levels of Ang-1 expression is very similar to our findings in Shh-deficient lungs. Thus, further research is needed to investigate the possibility that Shh affects Ang-1-mediated pulmonary vascularization via COUP-TFII.

The apparent rescue of the abnormalities in vascular and airway branching in Shh-deficient lungs with rhFgf2 and rhAng-1 is intriguing. Fgf2 and its receptor are expressed in both the epithelial and mesenchymal compartment of the fetal lung (47-49). Lebeche *et al.* (50) showed that Shh did not affect Fgf2 mRNA expression in embryonic lung mesenchymal cells, which is a finding that is in agreement with the results presented in this study. However, we cannot exclude Shh-deficiency-induced changes in the spatial expression of Fgf2. Previous studies have shown that Fgf2 acts primarily as a proliferation factor for fetal lung epithelium (51) but without inducing branching morphogenesis (47, 52). Fgf2 binds to Fgfr1 and Fgfr2-IIIc, but only slightly to Fgfr2-IIIb, which is the Fgfr2 isoform that is expressed in lung epithelium (52-54). Fgfr2 binds Fgf-1, Fgf-7, and Fgf-10, which are, in contrast to Fgf2, implicated in fetal lung epithelial branching (50, 55-58). Thus, the partial recovery of airway branching in Shh-deficient lungs by rhFgf2 is likely not the result of a direct action on the epithelium. We speculate that exogenous Fgf2 increases the amount of mesenchyme that is surrounding the growing buds of $Shh^{-/-}$ lungs and in that way provides a tissue base for vessels to grow, stimulated by exogenous Fgf2, Ang-1, and endogenous Vegf. Indeed, Fgf2 was shown to influence angiogenesis via Vegf and Vegfr2 (59, 60). Alternatively, Fgf2 may stimulate smooth muscle cell proliferation of the vessel wall (61), allowing Ang-1 to stabilize the vascular bed in Shh-deficient lungs. Altogether, the increase in airway branching morphogenesis in Fgf2-treated Shh deficient lungs may be the result of stimulated mesenchymal-vascular growth and stability.

Acknowledgements

This work was supported by the Sophia Foundation for Medical Research (SSWO, #342, M.v.T.) and Canadian Institutes of Health Research (M.P.). Martin Post is holder of a Canadian Research Chair (tier 1) in Fetal, Neonatal, and Maternal Health. The authors thank Angie Griffin for animal handling and care and Irene Tseu for technical assistance.

References

1. Risau W, 1997. Mechanisms of angiogenesis. Nature. 386:671-674.
2. Risau W, Flamme I, 1995. Vasculogenesis. Annu Rev Cell Dev Biol. 11:73-91.
3. deMello DE, Sawyer D, Galvin N, Reid LM, 1997. Early fetal development of lung vasculature. Am J Respir Cell Mol Biol. 16:568-581.
4. Matsumoto K, Yoshitomi H, Rossant J, Zaret KS, 2001. Liver organogenesis promoted by endothelial cells prior to vascular function. Science. 294:559-563.
5. Lammert E, Cleaver O, Melton D, 2003. Role of endothelial cells in early pancreas and liver development. Mech Dev. 120:59-64.
6. Galambos C, Ng YS, Ali A, Noguchi A, Lovejoy S, D'Amore PA, DeMello DE, 2002. Defective pulmonary development in the absence of heparin-binding vascular endothelial growth factor isoforms. Am J Respir Cell Mol Biol. 27:194-203.
7. Gerber HP, Hillan KJ, Ryan AM, Kowalski J, Keller GA, Rangell L, Wright BD, Radtke F, Aguet M, Ferrara N, 1999. VEGF is required for growth and survival in neonatal mice. Development. 126:1149-1159.
8. Jakkula M, Le Cras TD, Gebb S, Hirth KP, Tuder RM, Voelkel NF, Abman SH, 2000. Inhibition of angiogenesis decreases alveolarization in the developing rat lung. Am J Physiol Lung Cell Mol Physiol. 279:L600-607.
9. Le Cras TD, Markham NE, Tuder RM, Voelkel NF, Abman SH, 2002. Treatment of newborn rats with a VEGF receptor inhibitor causes pulmonary hypertension and abnormal lung structure. Am J Physiol Lung Cell Mol Physiol. 283:L555-L562.
10. Schwarz MA, Zhang F, Gebb S, Starnes V, Warburton D, 2000. Endothelial monocyte activating polypeptide II inhibits lung neovascularization and airway epithelial morphogenesis. Mech Dev. 95:123-132.
11. Bellusci S, Furuta Y, Rush MG, Henderson R, Winnier G, Hogan BL, 1997. Involvement of Sonic hedgehog (Shh) in mouse embryonic lung growth and morphogenesis. Development. 124:53-63.
12. Litingtung Y, Lei L, Westphal H, Chiang C, 1998. Sonic hedgehog is essential to foregut development. Nat Genet. 20:58-61.
13. Pepicelli CV, Lewis PM, McMahon AP, 1998. Sonic hedgehog regulates branching morphogenesis in the mammalian lung. Curr Biol. 8:1083-1086.
14. Pola R, Ling LE, Aprahamian TR, Barban E, Bosch-Marce M, Curry C, Corbley M, Kearney M, Isner JM, Losordo DW, 2003. Postnatal recapitulation of embryonic hedgehog pathway in response to skeletal muscle ischemia. Circulation. 108:479-485.

15. Kanda S, Mochizuki Y, Suematsu T, Miyata Y, Nomata K, Kanetake H, 2003. Sonic hedgehog induces capillary morphogenesis by endothelial cells through phosphoinositide 3-kinase. J Biol Chem. 278:8244-8249.

16. Pola R, Ling LE, Silver M, Corbley MJ, Kearney M, Blake Pepinsky R, Shapiro R, Taylor FR, Baker DP, Asahara T, Isner JM, 2001. The morphogen Sonic hedgehog is an indirect angiogenic agent upregulating two families of angiogenic growth factors. Nat Med. 7:706-711.

17. Schlaeger TM, Bartunkova S, Lawitts JA, Teichmann G, Risau W, Deutsch U, Sato TN, 1997. Uniform vascular-endothelial-cell-specific gene expression in both embryonic and adult transgenic mice. Proc Natl Acad Sci U S A. 94:3058-3063.

18. Chiang C, Litingtung Y, Lee E, Young KE, Corden JL, Westphal H, Beachy PA, 1996. Cyclopia and defective axial patterning in mice lacking Sonic hedgehog gene function. Nature. 383:407-413.

19. Elson DA, Thurston G, Huang LE, Ginzinger DG, McDonald DM, Johnson RS, Arbeit JM, 2001. Induction of hypervascularity without leakage or inflammation in transgenic mice overexpressing hypoxia-inducible factor-1alpha. Genes Dev. 15:2520-2532.

20. Livak KJ, Schmittgen TD, 2001. Analysis of relative gene expression data using real-time quantitative PCR and the 2(-Delta Delta C(T)) Method. Methods. 25:402-408.

21. van Tuyl M, Post, M., 2000. From fruitflies to mammals: mechanisms of signalling via the Sonic hedgehog pathway in lung development. Respiratory Research. 1:30-35.

22. Thurston G, Suri C, Smith K, McClain J, Sato TN, Yancopoulos GD, McDonald DM, 1999. Leakage-resistant blood vessels in mice transgenically overexpressing angiopoietin-1. Science. 286:2511-2514.

23. Maisonpierre PC, Suri C, Jones PF, Bartunkova S, Wiegand SJ, Radziejewski C, Compton D, McClain J, Aldrich TH, Papadopoulos N, Daly TJ, Davis S, Sato TN, Yancopoulos GD, 1997. Angiopoietin-2, a natural antagonist for Tie2 that disrupts in vivo angiogenesis. Science. 277:55-60.

24. Suri C, McClain J, Thurston G, McDonald DM, Zhou H, Oldmixon EH, Sato TN, Yancopoulos GD, 1998. Increased vascularization in mice overexpressing angiopoietin-1. Science. 282:468-471.

25. Tanswell AK, Han RN, Jassal D, Fraher LJ, Post M, 1991. The response of small vessel endothelial cells from fetal rat lung to growth factors. J Dev Physiol. 15:199-209.

26. Rowitch DH, B SJ, Lee SM, Flax JD, Snyder EY, McMahon AP, 1999. Sonic hedgehog regulates proliferation and inhibits differentiation of CNS precursor cells. J Neurosci. 19:8954-8965.

27. Brown LA, Rodaway AR, Schilling TF, Jowett T, Ingham PW, Patient RK, Sharrocks AD, 2000. Insights into early vasculogenesis revealed by expression of the ETS-domain transcription factor Fli-1 in wild-type and mutant zebrafish embryos. Mech Dev. 90:237-252.

28. Carmeliet P, Ferreira V, Breier G, Pollefeyt S, Kieckens L, Gertsenstein M, Fahrig M, Vandenhoeck A, Harpal K, Eberhardt C, Declercq C, Pawling J, Moons L, Collen D, Risau W, Nagy A, 1996. Abnormal blood vessel development and lethality in embryos lacking a single VEGF allele. Nature. 380:435-439.

29. Ferrara N, Carver-Moore K, Chen H, Dowd M, Lu L, O'Shea KS, Powell-Braxton L, Hillan KJ, Moore MW, 1996. Heterozygous embryonic lethality induced by targeted inactivation of the VEGF gene. Nature. 380:439-442.

30. Shalaby F, Rossant J, Yamaguchi TP, Gertsenstein M, Wu XF, Breitman ML, Schuh AC, 1995. Failure of blood-island formation and vasculogenesis in Flk-1-deficient mice. Nature. 376:62-66.

31. Yancopoulos GD, Klagsbrun M, Folkman J, 1998. Vasculogenesis, angiogenesis, and growth factors: ephrins

enter the fray at the border. Cell. 93:661-664.

32. Hanahan D, 1997. Signaling vascular morphogenesis and maintenance. Science. 277:48-50.

33. Ferrara N, Davis-Smyth T, 1997. The biology of vascular endothelial growth factor. Endocr Rev. 18:4-25.

34. Gale NW, Yancopoulos GD, 1999. Growth factors acting via endothelial cell-specific receptor tyrosine kinases: VEGFs, angiopoietins, and ephrins in vascular development. Genes Dev. 13:1055-1066.

35. Suri C, Jones PF, Patan S, Bartunkova S, Maisonpierre PC, Davis S, Sato TN, Yancopoulos GD, 1996. Requisite role of angiopoietin-1, a ligand for the TIE2 receptor, during embryonic angiogenesis. Cell. 87:1171-1180.

36. Folkman J, D'Amore PA, 1996. Blood vessel formation: what is its molecular basis? Cell. 87:1153-1155.

37. Unger S, Copland I, Tibboel D, Post M, 2003. Down-regulation of sonic hedgehog expression in pulmonary hypoplasia is associated with congenital diaphragmatic hernia. Am J Pathol. 162:547-555.

38. Miller LA, Wert SE, Whitsett JA, 2001. Immunolocalization of sonic hedgehog (Shh) in developing mouse lung. J Histochem Cytochem. 49:1593-1604.

39. Apelqvist A, Ahlgren U, Edlund H, 1997. Sonic hedgehog directs specialised mesoderm differentiation in the intestine and pancreas. Curr Biol. 7:801-804.

40. Holash J, Wiegand SJ, Yancopoulos GD, 1999. New model of tumor angiogenesis: dynamic balance between vessel regression and growth mediated by angiopoietins and VEGF. Oncogene. 18:5356-5362.

41. Witzenbichler B, Maisonpierre PC, Jones P, Yancopoulos GD, Isner JM, 1998. Chemotactic properties of angiopoietin-1 and -2, ligands for the endothelial-specific receptor tyrosine kinase Tie2. J Biol Chem. 273:18514-18521.

42. Krishnan V, Pereira FA, Qiu Y, Chen CH, Beachy PA, Tsai SY, Tsai MJ, 1997. Mediation of Sonic hedgehog-induced expression of COUP-TFII by a protein phosphatase. Science. 278:1947-1950.

43. Pereira FA, Qiu Y, Zhou G, Tsai MJ, Tsai SY, 1999. The orphan nuclear receptor COUP-TFII is required for angiogenesis and heart development. Genes Dev. 13:1037-1049.

44. Tsai SY, Tsai MJ, 1997. Chick ovalbumin upstream promoter-transcription factors (COUP-TFs): coming of age. Endocr Rev. 18:229-240.

45. Malpel S, Mendelsohn C, Cardoso WV, 2000. Regulation of retinoic acid signaling during lung morphogenesis. Development. 127:3057-3067.

46. Pereira FA, Qiu Y, Tsai MJ, Tsai SY, 1995. Chicken ovalbumin upstream promoter transcription factor (COUP-TF): expression during mouse embryogenesis. J Steroid Biochem Mol Biol. 53:503-508.

47. Han RN, Liu J, Tanswell AK, Post M, 1992. Expression of basic fibroblast growth factor and receptor: immunolocalization studies in developing rat fetal lung. Pediatr Res. 31:435-440.

48. Gonzalez AM, Hill DJ, Logan A, Maher PA, Baird A, 1996. Distribution of fibroblast growth factor (FGF)-2 and FGF receptor-1 messenger RNA expression and protein presence in the mid-trimester human fetus. Pediatr Res. 39:375-385.

49. Powell PP, Wang CC, Horinouchi H, Shepherd K, Jacobson M, Lipson M, Jones R, 1998. Differential expression of fibroblast growth factor receptors 1 to 4 and ligand genes in late fetal and early postnatal rat lung. Am J Respir Cell Mol Biol. 19:563-572.

50. Lebeche D, Malpel S, Cardoso WV, 1999. Fibroblast growth factor interactions in the developing lung. Mech

Dev. 86:125-136.

51. Caniggia I, Tseu I, Han RN, Smith BT, Tanswell K, Post M, 1991. Spatial and temporal differences in fibroblast behavior in fetal rat lung. Am J Physiol. 261:L424-433.

52. Nogawa H, Ito T, 1995. Branching morphogenesis of embryonic mouse lung epithelium in mesenchyme-free culture. Development. 121:1015-1022.

53. Goldfarb M, 1996. Functions of fibroblast growth factors in vertebrate development. Cytokine Growth Factor Rev. 7:311-325.

54. Orr-Urtreger A, Bedford MT, Burakova T, Arman E, Zimmer Y, Yayon A, Givol D, Lonai P, 1993. Developmental localization of the splicing alternatives of fibroblast growth factor receptor-2 (FGFR2). Dev Biol. 158:475-486.

55. Shannon JM, Gebb SA, Nielsen LD, 1999. Induction of alveolar type II cell differentiation in embryonic tracheal epithelium in mesenchyme-free culture. Development. 126:1675-1688.

56. Bellusci S, Grindley J, Emoto H, Itoh N, Hogan BL, 1997. Fibroblast growth factor 10 (FGF10) and branching morphogenesis in the embryonic mouse lung. Development. 124:4867-4878.

57. Park WY, Miranda B, Lebeche D, Hashimoto G, Cardoso WV, 1998. FGF-10 is a chemotactic factor for distal epithelial buds during lung development. Dev Biol. 201:125-134.

58. Post M, Souza P, Liu J, Tseu I, Wang J, Kuliszewski M, Tanswell AK, 1996. Keratinocyte growth factor and its receptor are involved in regulating early lung branching. Development. 122:3107-3115.

59. Seghezzi G, Patel S, Ren CJ, Gualandris A, Pintucci G, Robbins ES, Shapiro RL, Galloway AC, Rifkin DB, Mignatti P, 1998. Fibroblast growth factor-2 (FGF-2) induces vascular endothelial growth factor (VEGF) expression in the endothelial cells of forming capillaries: an autocrine mechanism contributing to angiogenesis. J Cell Biol. 141:1659-1673.

60. Tille JC, Wood J, Mandriota SJ, Schnell C, Ferrari S, Mestan J, Zhu Z, Witte L, Pepper MS, 2001. Vascular endothelial growth factor (VEGF) receptor-2 antagonists inhibit VEGF- and basic fibroblast growth factor-induced angiogenesis in vivo and in vitro. J Pharmacol Exp Ther. 299:1073-1085.

61. Bikfalvi A, Klein S, Pintucci G, Rifkin DB, 1997. Biological roles of fibroblast growth factor-2. Endocr Rev. 18:26-45.

Chapter 5

Rx genes influence proximal-distal morphogenesis during lung development

Minke van Tuyl[1,2], Jason Liu[1], Robin N. Han[1], Vikram Venkatesh[1], Dick Tibboel[2], and Martin Post[1]

[1]Canadian Institutes of Health Research (CIHR) Group in Lung Development, Hospital for Sick Children Research Institute, Departments of Pediatrics and Physiology, University of Toronto, Toronto, ON, Canada
[2]Department of Pediatric Surgery, Sophia Children's Hospital, Erasmus University Medical Center Rotterdam, Rotterdam, The Netherlands

Submitted

Abstract

Lung development is a process that is directed by mesenchymal-epithelial tissue interactions, which coordinate the temporal and spatial expression of multiple regulatory factors. The *Iroquois* homeobox (*Irx*) genes have been implicated in the patterning and specification of several *Drosophila* and vertebrate organs, including the heart. Herein, we investigated whether the Irx genes play a role in lung morphogenesis as well. We found that Irx1-3 and Irx5 expression were confined to the branching pulmonary epithelium, whereas Irx4 was not expressed in the developing lung. Antisense knockdown of pulmonary Irx genes dramatically decreased distal branching morphogenesis *in vitro,* which was accompanied by a downregulation of SP-C-positive epithelial cells and a concomitant increase in CCSP-positive epithelial structures. Furthermore, antisense Irx-inhibition resulted in the loss of lung mesenchyme and in abnormal smooth muscle cell formation. Neither fibroblast growth factors-1 (Fgf1), -7, or -10 nor Fgf receptor-2 (Fgfr2) or bone morphogenetic protein-4 (Bmp4) expression levels were altered in lung explants treated with antisense Irx oligonucleotides (ODNs). Also, all four Irx genes were correctly expressed in Sonic hedgehog (Shh) and Gli2-deficient lungs. Collectively, these results indicate that Irx genes are involved in the regulation of proximal-distal morphogenesis of the developing lung, but are most likely not linked to the Fgf, Bmp, or Shh signaling pathways.

Introduction

During development, the mammalian lung establishes a large diffusible interface with the circulation to facilitate gas exchange beginning at birth. To form such a large surface area, the developing lung undergoes epithelial airway branching and differentiation, whereas the pulmonary mesenchyme provides the vascular, smooth muscle, and cartilage tissue. Although the exact molecular signals that guide lung development are unknown, several morphogenetic factors have been implicated (1, 2). One of them, Sonic hedgehog (Shh), a vertebrate homologue of *Drosophila hedgehog (Hh)* is expressed in the lung epithelium (3). Gli1-3 are the vertebrate counterparts of *Cubitus interruptus (Ci)*, the principal effector of *Hh* signaling in *Drosophila*. In the lung, Gli1-3 are expressed in distinct but overlapping domains in the mesenchyme, with the highest expression in distal tips (3). Null mutant mice for Shh and the Gli genes all exhibit a mild or severe lung phenotype, from minor lobar defects and lung hypoplasia to lung agenesis (4-8). Downstream targets for the Gli proteins however remain to be elucidated. In *Drosophila*, *Ci* may regulate the activity of the *Iroquois*-complex of homeobox genes (9). The *Drosophila Iroquois* complex (*Iro-C*) contains three highly related homeobox genes; *araucan*, *caupolican,* and *mirror*, which are members of an evolutionary conserved family of homeodomain containing transcription factors. The *Iro-C* homeoproteins are essential for dorso-ventral patterning of the *Drosophila* eye, head, and follicle (10-13). Also, in *Drosophila*, *araucan* and *caupolican* are positive controllers of the proneural genes *achaete* and *scute* and vein-forming genes (9). In turn, during wing formation, *araucan* and *caupolican* are positively controlled by *Ci* and *Decapentaplegic* (*Dpp*) (14).

Six vertebrate homologues of the *Iroquois* genes, Irx1-6, have been identified. The six members are organized in two cognate clusters of three genes each, Irx1, Irx2, and Irx4 and Irx3, Irx5, and Irx6, respectively (15). In most tissues, the pattern of expression of the clustered genes, especially of Irx1 and Irx2 and of Irx3 and Irx5, closely resemble each other (16). The Irx genes show temporally and spatially restricted expression patterns during murine neural and cardiac development (17-22).

During chicken development, Irx4 regulates chamber-specific gene expression (23). In *Xenopus*, the amphibian homologues of Iroquois, *Xiro1* and *Xiro2,* control the expression of proneural genes; whereas similarly to *araucan* and *caupolican*, they are positively controlled by *Ci* (24). More recently, Gómez-Skarmeta *et al.* (25) showed that in *Xenopus* neural development, *Xiro1* represses bone morphogenetic protein-4 *(Bmp4)*. Bmp4, a member of the transforming growth factor-β (Tgf-β) superfamily of proteins and the vertebrate counterpart of *Drosophila Dpp*, also plays a major role in lung morphogenesis. Both overexpression and inhibition of Bmp4 signaling resulted in abnormal lung branching (26-28).

Based on the reported findings, we investigated whether the Irx genes are part of the Shh-Gli and/or the Bmp4 signaling pathways that control lung branching morphogenesis. We found that Irx1, Irx2, Irx3, and Irx5, but not Irx4, are specifically expressed in developing lung epithelium during the period of active airway branching. Inhibition of Irx signaling *in vitro* resulted in grossly abnormal lungs with decreased branching and instead proximalization of the lung. Addition of Bmp4 did not recover the observed lung phenotype, a finding that suggests that Bmp4 is not a downstream target of Irx in the developing lung. Furthermore, we observed that the Irx genes were normally expressed in $Shh^{-/-}$ and $Gli2^{-/-}$ mutant lungs, suggesting that Irx genes do not function downstream from the Shh-Gli signaling pathway.

Materials and Methods

Animals

Male and female Wistar rats were obtained from Charles River (St. Constant, QC, Canada) and were bred in our animal facilities. Rats were killed at embryonic days (E) 13.5-20.5 of gestation (term = E22.5). Shh and Gli2 heterozygous ($Shh^{+/-}$ and $Gli2^{+/-}$, respectively) mice were obtained from Dr. C.C. Hui, Hospital for Sick Children, Toronto, ON, Canada. The Shh, Gli2, and Gli3 genotypes were established by PCR analysis of genomic DNA (29). All mouse protocols were in accordance with CACC guidelines and were approved by the Animal Care and Use Committee of the Hospital for Sick Children, Toronto, ON, Canada.

Organ culture

Rat embryos were obtained from timed-pregnant rats at E13.5 (morning of vaginal plug is designated as E0.5). Lungs were dissected under sterile conditions and placed on a floating (8 µm Whatman Nuclepore polycarbonate) membrane (Integra Environmental Inc. Burlington, ON, Canada). Explants were cultured in DMEM (Dulbecco's Modified Eagle Medium; Gibco BRL; Grand Islands, NY, U.S.A.) with 10% (v/v) fetal bovine serum and maintained in 20% O_2 and 5% CO_2, at 37 C. Medium and oligonucleotides (ODNs) were changed every other day. Antisense, sense, and scrambled Irx ODNs were added to a final concentration of 20 µM. Recombinant human Bmp4 (R&D Systems, Minneapolis, MN, U.S.A.) was used in a concentration of 200 ng/ml.

Antisense Irx oligonucleotide inhibition

To inhibit Irx1, -2, -3, and -5 gene expression, we used an antisense phosphorothioate ODN (5'-ATGTCCTTCCCCCAGC-3') that was targeted against the translation initiation site of murine Irx3 and had an overlap of 81% with the translation initiation sites of both murine Irx2 and Irx5 and a 95% overlap with the translation initiation site of murine Irx1. Sense (5'-GCTGGGGGAAGGACAT-3') and scrambled sequence ODNs (5'-CCGATGGCAGTGGAGA-3') were used as controls.

Probes

cDNAs for Irx1, -2, -3, and -5 were a gift from Dr. V. M. Christoffels (Academic Medical Center, University of Amsterdam, Amsterdam, The Netherlands) and described in Christoffels *et al*. (22). Irx4 cDNA was obtained from Dr. B. G. Bruneau (Hospital for Sick Children, University of Toronto, Toronto, ON, Canada). Plasmid containing mouse Mash-1 cDNA was obtained from Dr S. E. Egan (Hospital for Sick Children, Toronto, ON, Canada). Murine SP-C and CCSP cDNA fragments were cloned by RT-PCR. Sense and antisense riboprobes for Irx1 (1050 bp), Irx2 (1800 bp), Irx3 (1000 bp), Irx4 (1050 bp), Irx5 (950 bp), Mash-1 (2.8 kb), SP-C (330 bp), and CCSP (315 bp) were digoxigenin (DIG)-labeled according to a protocol provided by the manufacturer (Roche, Montreal, QC, Canada).

Semiquantitative Reverse Transcription-Polymerase Chain Reaction

Total RNA was isolated by using the RNeasy total RNA kit (Qiagen, Chatham, CA, U.S.A.) and RT-PCR was performed as described previously (30). Primer sequences (from 5' to 3'), size of amplification products, number of cycles, and annealing temperature were described before and as follows: Fgf1 (GCCATAGTGAGTCCGAGGACC and ACCGAGAGGTTCAACCTGCC; 387 bp; 35 cycles; 55°; (31)), Fgf7 (CTTCCCTTTGACAGGAATC CCCTT and ATCCTGCCAACTCTGCTCTACAGA; 509 bp; 35 cycles; 60°C; (32)), Fgf10 (AAGC TCTTGGTCAGGACATGGTGT and TCCATTCAATGCCACATACATTTG; 458 bp; 25 cycles; 55°C; (33)), Fgfr2 (AAGGTTTACAGCGATGCCCA and ACCACCATGCAGGCGATTAA; 345 bp; 35 cycles; 47°C; (34)), Bmp4 (TCCATCACGAAGAACATC and TAGTCGTGTGATGAGGTG; 220 bp, 35 cycles, 56°C (28)).

In situ hybridization

Isolated lungs and cultured lung explants were fixed in 4% (v/v) paraformaldehyde (PFA) in PBS at 4°C for 4-18 hours, dehydrated in ethanol, and embedded in paraplast. Sections of 12 µm were cut and mounted on Superfrost slides (Fisher Scientific, Unionville, ON, Canada). The lungs were then assayed for non-radioactive RNA in situ hybridization according to Moorman et al. (35). Briefly, after dewaxing and rehydrating, tissue sections were permeabilized with proteinase K (20 µg/ml), postfixed in 4% PFA and 0.2% glutaraldehyde, and pre-hybridized for 1 hour at 70°C. The sections were hybridized overnight at 70°C with DIG-labeled riboprobes for Irx1-5, SP-C, or CCSP (1 µg/ml). The next day, sections were washed in 50% formamide in 2x SSC, pH 4.5 at 65°C followed by washes in PBS-T (PBS containing 0.1% Tween-20). Subsequently, the sections were incubated with anti-DIG alkaline phosphatase diluted 1:1000 in blocking solution (Roche, Montreal, QC, Canada) at 4°C. The next day, sections were washed in PBS-T followed by washes in NTM (100 mM NaCl, 100 mM Tris, pH 9.5, 50 mM $MgCl_2$) and then incubated with 5-bromo-4-chloro-3-indolyl phosphate/nitro blue tetrazolium chromogen (NBT/BCIP; Roche, Montreal, QC, Canada) at room temperature (RT) until purple color appeared (4-5 hours). All slides with the same probe were stopped at the same time to make comparison over different stages of development possible. After color development, sections were washed in distilled

water, dehydrated in a graded series of ethanol and xylene, and mounted with coverslips using permount (Fisher Scientific, Unionville, ON, Canada). Digital images were taken using a Leica digital imaging system.

Immunohistochemistry

Lung explants were fixed overnight in 4% PFA in PBS, dehydrated, and embedded in paraplast. Immunohistochemistry was essentially conducted as described by Hsu and coworkers (36). Seven µm sections were deparaffinized and rehydrated in a graded series of ethanol. Antigen retrieval was achieved with heating in sodium citrate, pH 6.0. Endogenous peroxidase activity was quenched with 0.15% (v/v) hydrogen peroxide in methanol. Non-specific binding sites were blocked using 5% (v/v) normal goat serum and 1% (w/v) bovine serum albumin followed by overnight incubation at 4°C with a mouse monoclonal anti-thyroid transcription factor-1 (Ttf-1) (1:50; Neomarkers, Fremont, CA, U.S.A.), a mouse monoclonal anti-hepatocyte nuclear factor family-3β (Hnf3β) (1: 50; Developmental Studies Hybridoma Bank, University of Iowa, U.S.A.), a mouse monoclonal anti-α-smooth muscle actin (α-sma) antibody (1:1000; Neomarkers, Fremont, CA, U.S.A.), or a mouse monoclonal anti-vimentin (1:600; Sigma, St. Louis, MO, U.S.A.) antibody, all diluted in blocking solution (5% NGS and 1% BSA in PBS). Sections were subsequently incubated with biotinylated secondary antibodies and color detection was performed according to instructions in the Vectastain ABC and DAB kit (Vector Laboratories, Burlingname, CA, U.S.A.). Sections were lightly counterstained with Carazzi haematoxylin and mounted in Permount (Fisher Scientific, Unionville, ON, Canada). Digital images were taken using a Leica imaging system.

TUNEL Assay

Lung explants that were cultured for 48 hours with (anti)sense ODNs targeted against Irx1-3, and -5 were fixed in 4% PFA in PBS and then embedded in paraplast. Five µm sections were dewaxed, rehydrated, and treated with proteinase K (20 µg/ml) for 15 minutes at 37°C. After washing in PBS, the terminal transferase dUTP end-labeling (TUNEL) assay was conducted according to the manufacturer's instructions (*in-situ* cell death detection [fluorescein] kit; Roche, Montreal, QC, Canada). Sections were mounted with mounting medium containing DAPI. Digital images were taken using a Leica imaging system.

BrdU labeling of explants

Lung explants that were cultured for 48 hours with (anti)sense ODNs targeted against Irx1-3, and -5 were incubated for 6 hours with 1 µM 5-bromo-2'-deoxyuridine (BrdU). Explants were fixed in Carnoy's fixative, embedded in paraplast, and 5 µm sections were cut and mounted on α-aminopropyltriethoxysilane-coated slides. Tissue sections were then dewaxed in xylene and rehydrated in a graded series of ethanol. The sections were incubated for 20 minutes in 2 M HCl, transferred to PBS, and incubated for 1 hour in 5% (v/v) NGS and 1% (w/v) BSA in PBS. The excess of blocking solution was carefully removed and

tissue sections were incubated overnight at 4°C with 1:20 mouse monoclonal anti-BrdU antibody (Roche, Montreal, QC, Canada). The tissue sections were washed three times in PBS, incubated for 1 hour with a 1:100 dilution of biotinylated secondary sheep anti-mouse IgG, followed by a 1 hour incubation with 1:150 diluted fluorescein isothiocynate (FITC) streptavidin complex. The tissues were washed again in PBS and mounted with antifade mounting solution. No immunofluorescense was observed when primary antibody was omitted. Digital images were taken using a Leica imaging system.

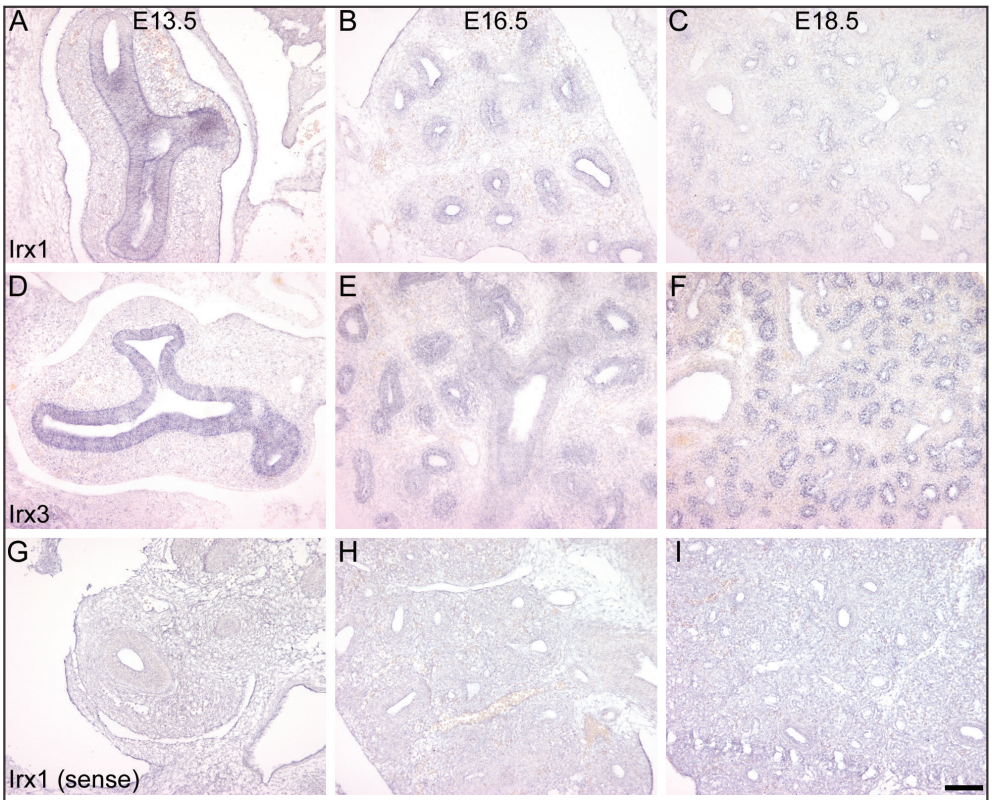

Figure 1. Irx1 (A-C) and Irx3 (D-F) mRNA expression in the developing rat lung. In situ hybridization using antisense DIG-labeled probes showed high Irx1 and Irx3 expression in early-stage (E13.5) rat lung epithelium (A, D). Irx1 mRNA expression had declined at E16.5 (B), but declined significantly further towards E18.5 (C). Irx3 mRNA expression had decreased at E16.5 (E), and stayed at comparable levels towards E18.5 (F). No staining was observed in mesenchymal or endothelial tissue, or when sense probes (G-I for sense Irx1; sense Irx2, -3, and -5 not shown) were used. Dark purple color is positive ISH staining. Bar: 100 µm.

Results

Irx gene expression in the developing rat lung

In situ hybridization analysis revealed that Irx genes -1, -2, -3, and -5 display a temporal and spatial similar expression pattern during rat lung development (Figs 1 and 2). Irx4

was not expressed in the developing lung (results not shown). mRNA for Irx1 (Fig. 1A-C), Irx3 (Fig. 1D-F), Irx2 (Fig. 2A-C), and Irx5 (Fig. 2D-F) was expressed at high levels during the pseudoglandular stage of lung development (E13.5), which is a period of active branching morphogenesis. mRNA expression of Irx1, -2, -3, and -5 was confined to branching lung endoderm, whereas no expression was detected in mesenchymal or endothelial lung tissue. Spatially, Irx mRNA expression was equal throughout the epithelium and appeared not to be restricted to branch points. Irx mRNA expression declined during the late pseudoglandular and the canalicular stage (E16.5-E20.5), and was undetectable in the saccular stage (E20.5-E22.5) of lung development, which is the time that distal gas exchange units develop. For Irx1 and Irx2, the major decline in mRNA expression occurred at E18.5 (Figs 1C and 2C), whereas mRNA expression for Irx3 and Irx5 declined at E16.5 (Figs 1E and 2E), and stayed at comparable levels towards E18.5 (Figs 1F and 2F). These results are in agreement with the finding that in most tissues, the pattern of expression of especially Irx1 and Irx2 and of Irx3 and Irx5, closely resemble each other (16). No positive *in situ* hybridization signal was detected when sense riboprobes were used (Fig. 1G-I). Taken together, the spatial and temporal expression pattern of Irx genes suggests a role for these genes in early lung development, especially during the formation of the bronchial tree.

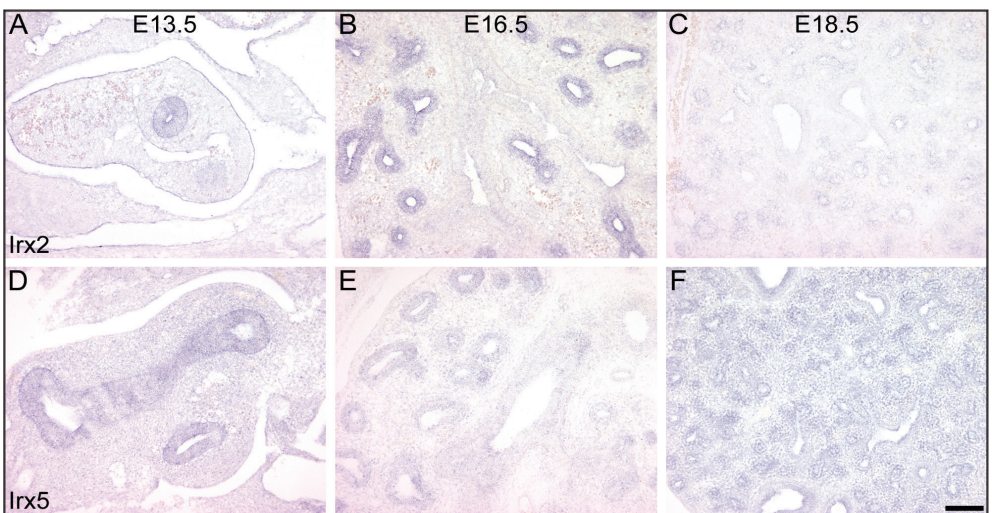

Figure 2. Irx2 (A-C) and Irx5 (D-F) mRNA expression in the developing rat lung. In situ hybridization using antisense DIG-labeled probes showed high Irx2 and Irx5 expression in early-stage (E13.5) rat lung epithelium (A, D). Irx2 mRNA expression had declined substantially at E18.5 (C). Irx3 mRNA expression had decreased at E16.5 (E), and stayed at comparable levels towards E18.5 (F). No staining was observed in mesenchymal or endothelial tissue, or when sense probes were used. Dark purple color is positive ISH staining. Bar: 100 µm.

Antisense inhibition of Irx expression reduces lung branching *in vitro*

To investigate the role of Irx genes during early lung development, E13.5 rat lung explants were cultured in the presence of an antisense oligonucleotide (ODN) targeted against Irx1-3, and -5 (Fig. 3). E13.5 rat lungs consist of two epithelial buds (arrowheads), one

on each side of the trachea (asterisk), which over time in culture undergo progressive branching (Fig. 3A-C). Treatment of explant cultures with missense Irx ODNs (not shown) did not affect lung explant growth or branching morphogenesis compared to control (Fig. 3A-C) or sense Irx ODN-treated lung explants (Fig. 3D-F). However, a dramatic inhibition of lung growth and branching morphogenesis was observed when antisense ODNs targeted against Irx1-3, and -5 was used (Fig. 3G-I). After 2 days in culture, lung explants treated with antisense Irx ODNs displayed a normal number of main bronchi and lobes, but subsequent peripheral branching was reduced (Fig. 3G). With more days in culture, peripheral branching morphogenesis became even more abrogated, whereas proximal airway structures appeared dilated (arrows, Fig. 3H, I).

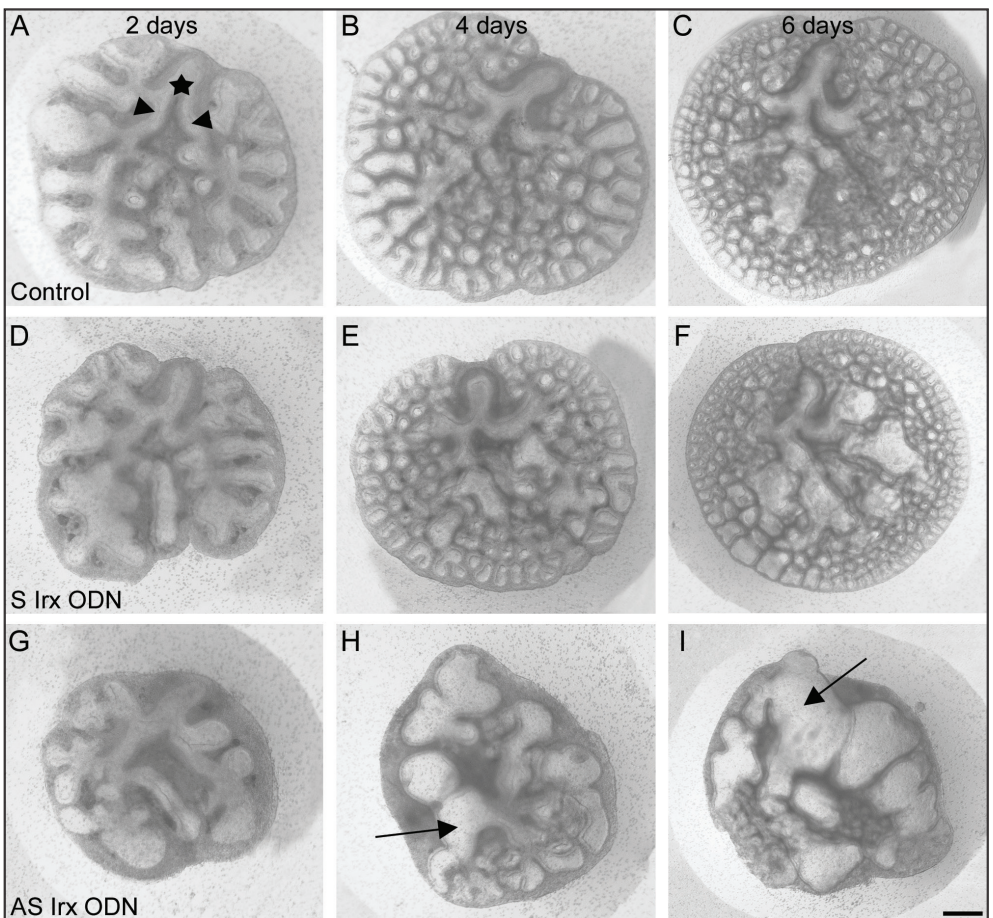

Figure 3. Effect of Irx inhibition on lung branching morphogenesis in vitro. Sense or antisense ODNs targeted against the overlapping translation sequence of Irx1-3, and -5 were added to the cultures in a concentration of 20 µM. Antisense (G-I) Irx ODN-treated lung explants showed a dramatic decrease in distal branching morphogenesis together with a concurrent expansion of proximal airways (arrows) compared to control (A-C) and sense (D-F) Irx ODN-treated explants. Asterisks represents trachea, arrowheads point at main bronchi (A). Bar: 250 µm (A, D, G); 300 µm (B, E, H); 360 µm (C, F, I).

To examine the effectiveness of the antisense ODNs targeted against Irx1-3, and -5, we assessed Irx1, -2, -3, and -5 mRNA expression with non-radioactive *in situ* hybridization in rat lung explants cultured with sense (control) or antisense ODNs. After 3 days in culture, Irx1, -2, -3, and -5 gene expression was detected in the epithelial cells lining the airway tubules of sense-treated explants (arrows in Fig. 4A, E, C, G, respectively). After 6 days in culture, the expression of all four Irx genes declined (not shown) similar to what was observed in *in vivo* lungs (Figs 1 and 2). When lung explants were treated with antisense Irx ODNs targeted against Irx1-3, and -5, epithelial mRNA expression for the subsequent genes was completely abolished after 3 (arrowheads in Fig. 4B, F, D, H, respectively) and 6 days (not shown) in culture. Even prolonged detection times with *in situ* hybridization did not reveal any significant levels of Irx1, -2, -3, or -5 transcripts in the antisense Irx ODN-treated explants. These results indicate that Irx mRNA levels were adequately inhibited with antisense ODNs and that Irx is involved in proximal-distal airway branching during

Proliferation and apoptosis in antisense Irx-treated lung explants

BrdU incorporation into DNA was used to investigate the proliferation in sense (control) and antisense Irx ODN-treated lung explants. Proliferation in epithelial and mesenchymal cells was similar between sense and antisense Irx ODN-treated lung explants after 3 days in culture (Fig. 5Ab and 5Af, respectively). After 6 days in culture, a dramatic decrease in the number of proliferating cells was noted in the antisense Irx ODN-treated lung explants (Fig. 5Ah) compared to sense ODN-treated explants (Fig. 5Ad).

TUNEL assay was performed to assess apoptosis in lung explants. Apoptosis was dramatically increased in antisense Irx ODN-treated lung explants after 3 days in culture (Fig. 5Bd) compared to sense (control) ODN-treated explants (Fig. 5Bb). From figures 5Ah and 5Bd it appears that proliferation and apoptosis are most affected in the mesenchymal compartment of the lungs, a finding suggesting that the mesenchyme is a target for Irx signaling.

Mesenchymal cell markers in antisense Irx-treated lung explants

Because we suggested that the mesenchyme was a target for Irx signaling, we looked at the protein expression of α-smooth muscle actin (α-sma) and vimentin, which are normally expressed in the mesenchymal compartment of the lung. In sense (control) Irx ODN-treated lung explants, α-sma immunopositive staining was detected in a thin layer around the proximal bronchioles and larger blood vessels after 6 days in culture (Fig. 6A, B). In the antisense Irx ODN-treated lung explants, the layer of α-sma-positive cells was severely disorganized after 6 days in culture (Fig. 6D). A higher magnification showed that the α-sma-positive cell layer was repeatedly interrupted and failed to form a smooth layer supporting proximal bronchioles and larger blood vessels (arrows in Fig. 6E). Additionally, it appeared that antisense Irx ODN treatment resulted in a loss of mesenchymal mass (compare Fig. 6A to 6D for sense and antisense Irx ODN-treated, respectively).

Because vimentin is normally expressed throughout the proximal and distal mesenchymal compartments of the lung, we carried out vimentin immunoanalysis. In sense (control) Irx ODN-treated lung explants; abundant positive staining for vimentin was observed throughout the mesenchyme after 6 days in culture (Fig. 6C). In the antisense Irx ODN-treated lung explants, the mesenchyme had indeed decreased in volume, but exhibited positive staining for vimentin (Fig. 6F). These immunohistochemical results suggest that Irx signaling might be involved in the development of the pulmonary smooth muscle cell layer.

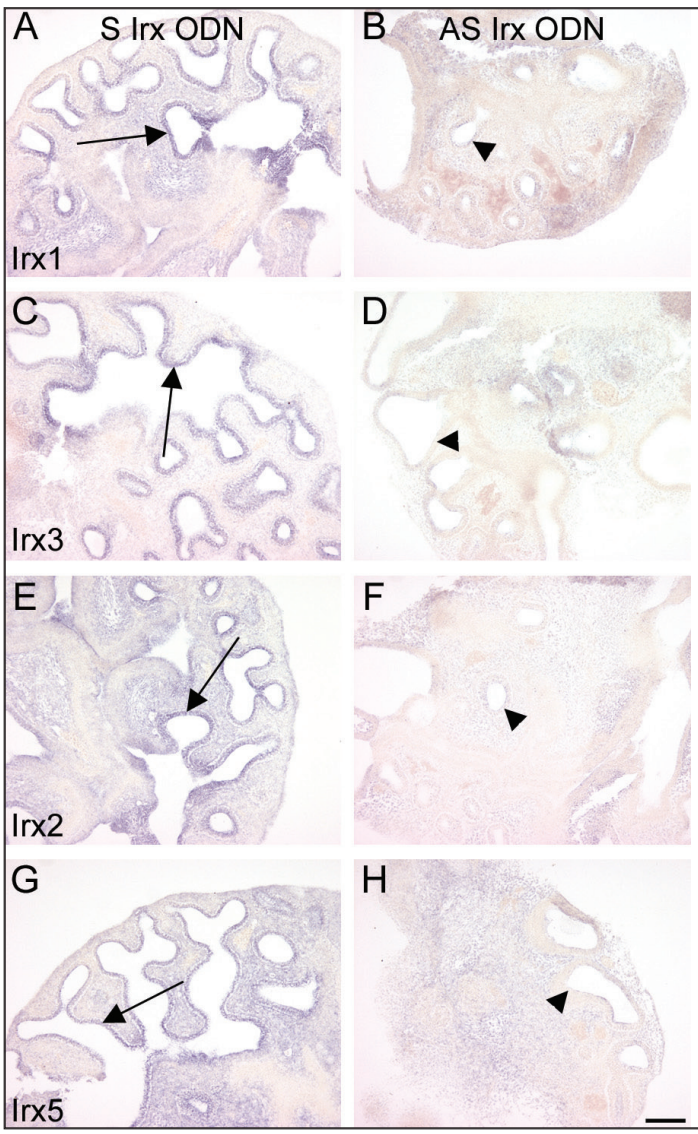

Figure 4. Effect of antisense Irx ODN treatment on the expression of Irx1, -2, -3, and -5. In situ hybridization with DIG-labeled antisense probes for Irx1 (A, B), Irx3 (C, D), Irx2 (E, F), and Irx5 (G, H) genes in lung explants after 3 days in culture. All four Irx genes were expressed in the epithelium of sense Irx ODN-treated explants (arrows in A, C, E, G), whereas no substantial expression was detected in the epithelium of antisense Irx ODN-treated lung explants (arrowheads in B, D, F, H). Dark purple color is positive ISH staining. Bar: 100 µm.

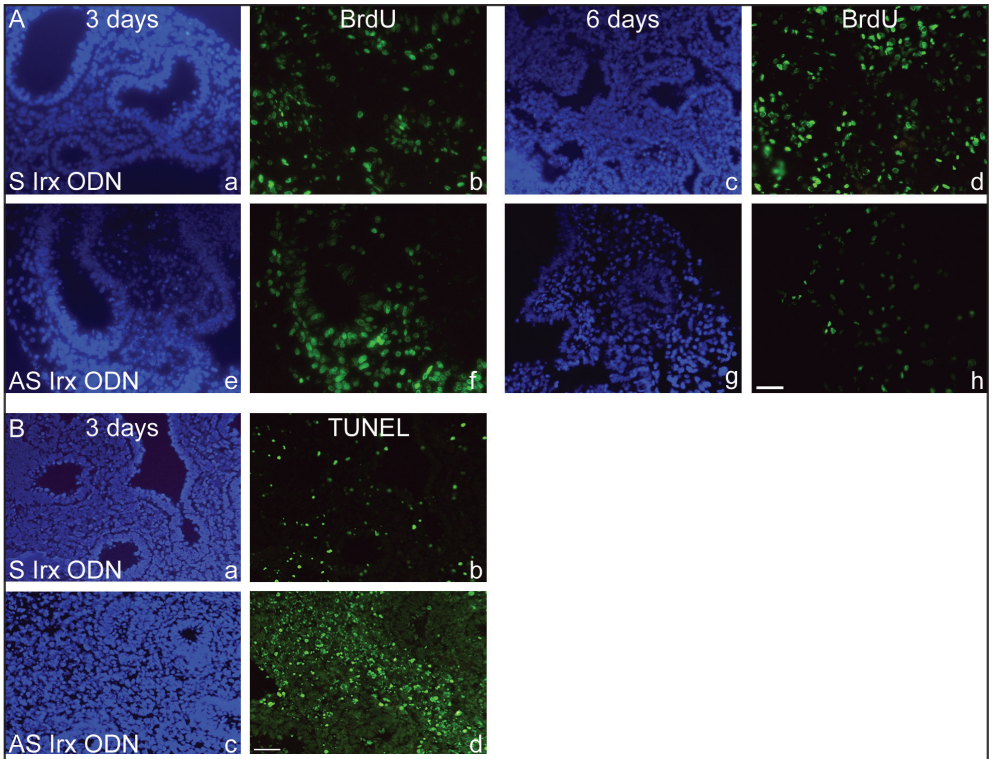

Figure 5. Effect of Irx inhibition on proliferation and apoptosis. A: Explants treated with sense or antisense Irx ODNs for 3 (Aa-b, e-f) or 6 (Ac-d, g-h) days were pulsed with BrdU for 6 hrs and subsequent BrdU incorporation was visualized by anti-BrdU immunofluorescense (Ab, d, f, h). Cell nuclei were visualized with DAPI (Aa, c, e, g). Many BrdU-positive cells were present after 3 days in sense and antisense Irx ODN-treated lung explants (Ab and Af, respectively). BrdU immunopositive staining decreased dramatically in antisense Irx ODN-treated lung explants after 6 days (Ah) compared to sense-treated explants (Ad). B: TUNEL analysis of sense and antisense Irx ODN-treated lung explants after 3 days in culture (Bb, d). Cell nuclei were visualized with DAPI (Ba, c). Few TUNEL-positive cells were seen throughout the epithelium of sense Irx ODN-treated explants (Bb). Many TUNEL-positive cells were found in the mesenchyme of antisense Irx ODN-treated lung explants (Bd). Bar: 100 µm (Aa, b, e, f); 40 µm (Ac, d, g, h); 100 µm (Ba-d).

Endodermal cell markers in antisense Irx-treated lung explants

Because peripheral epithelial branching morphogenesis was severely inhibited in antisense Irx ODN-treated lung explants, whereas proximal airway structures appeared dilated, we investigated epithelial cell differentiation using non-radioactive *in situ* hybridization. Surfactant protein-C (SP-C), which is a marker for distal respiratory epithelium (37), was expressed in distal epithelial cells of lung explants treated for 3 to 6 days with sense (control) Irx ODNs (Fig. 7A). In the antisense Irx ODN-treated lung explants however, SP-C mRNA was barely detectable after 3 days in culture (not shown) and only a few mRNA-positive epithelial clusters were found after 6 days in culture (Fig. 7B). Clara cell-specific protein (CCSP), which is a marker for proximal non-ciliated cells of the trachea, bronchi and bronchioles (38, 39), was seen after 6 days in culture in sense (control) Irx ODN-treated explants and its expression was indeed restricted to the proximal airways (Fig. 7C). In the

antisense Irx ODN-treated lung explants however, almost all epithelial tubules were CCSP-positive (Fig. 7D). Because the expression of SP-C (40) and CCSP (41, 42) are regulated by Ttf-1 and Hnf3β, we then analyzed the protein expression of both transcription factors using immunohistochemistry. Hnf3β and Ttf-1 are expressed in proximal and distal epithelial cells during early lung development, whereas at later stages of normal lung development, the expression of both transcription factors is more pronounced in distal epithelium (39, 43-45). Positive Ttf-1 immunoreactivity was detected in epithelial cells of both the sense (control) and antisense Irx ODN-treated lung explants and no obvious differences were observed in the intensity or pattern of Ttf-1 staining (Fig. 7E, F). Similar results were obtained for Hnf3β protein expression (Fig. 7G, H). Taken together, these results suggest that deficient Irx signa1ling inhibits distal epithelial cell differentiation, whereas the remaining epithelium exhibits a proximal differentiation phenotype. Moreover, the altered expression patterns for SP-C and CCSP are not the result of changes in the expression of Ttf-1 or Hnf3β.

Fgf expression in antisense Irx-treated lung explants

The extended family of fibroblast growth factors (Fgfs) plays a critical role in the development of many organs, including the lung. Fgf1, -2, -7, -9, -10, and -18 are all expressed in the developing lung and they play distinct, partly overlapping, roles in airway expansion (Fgf7) and branching morphogenesis (Fgf1 and Fgf10) (46, 47). Only Fgf10 was shown to be critically necessary for the initiation of lung development, because Fgf10-deficient mice formed a trachea without any further branching (48, 49). Fgf1, Fgf7, and Fgf10 are secreted by pulmonary mesenchyme and bind and activate the Fgf receptor-2 (Fgfr2), which is located on pulmonary epithelial cells (50). Because antisense Irx ODN-treated lung explants exhibit a severe airway branching defect, we investigated whether the Fgf-Fgfr2 signaling pathway was affected. Using semi-quantitative RT-PCR, we found no obvious differences in gene expression of Fgf1, -7, -10, or Fgfr2 between control, sense, and antisense Irx ODN-treated lung explants after 3 or 6 days in culture (Fig. 8A). Although changes in the expression patterns of the Fgf and Fgfr2 genes cannot be excluded, this finding makes it unlikely that reduced branching morphogenesis in the antisense Irx ODN-treated lung explants is the result of deficient Fgf-Fgfr2 signaling.

Bmp4 expression in antisense Irx-treated lung explants

The phenotype of antisense Irx ODN-treated lung explants, which demonstrates a reduction in distal SP-C and enhanced proximal CCSP expression, is very similar to the lung phenotype described for mice that overexpress either Xnoggin, a Bmp4 antagonist, or a dominant-negative Bmp4 receptor in distal pulmonary epithelial cells (27). Both mice displayed a severe reduction in distal epithelial cells and a concurrent increase in proximal cells. Because reduced Bmp4 signaling results in a lung phenotype consisting of mainly proximal cell types, we added recombinant Bmp4 to the medium of sense (control) and antisense Irx ODN-treated lung explant cultures. However, Bmp4 (200 ng/ml) did not

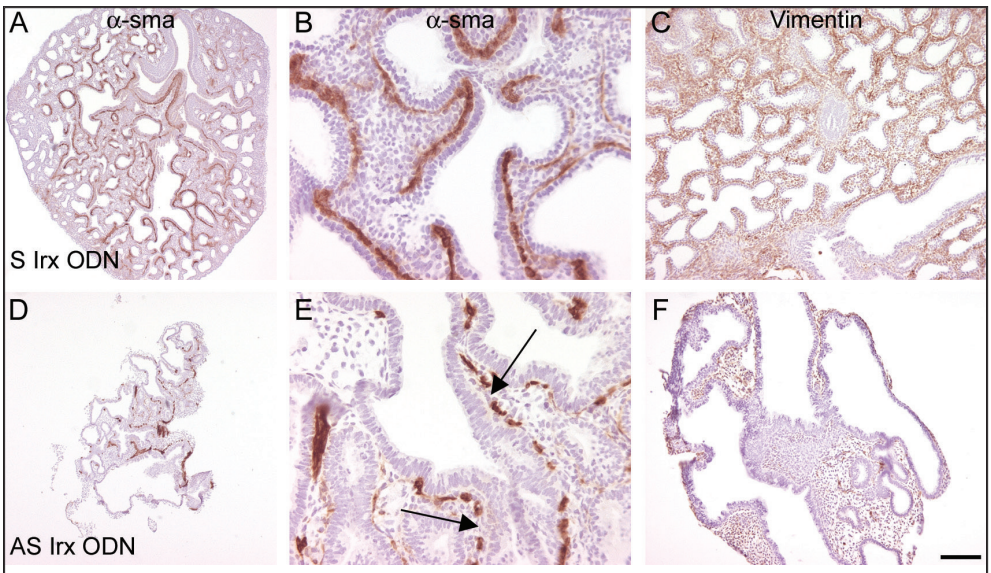

Figure 6. Effect of Irx inhibition on mesenchymal differentiation. Immunostaining was performed for α-smooth muscle actin (α-sma; A-B, D-E) and vimentin (C, F) in sense (A-C) and antisense (D-F) Irx ODN-treated rat lung explants after 6 days in culture. B and E are higher magnifications of A and D, respectively. In sense Irx ODN-treated explants, vimentin immunoreactivity was present in mesenchymal cells surrounding epithelial tubules (C), whereas anti-α-sma stained the smooth muscle cell layer at the base of developing airways (A, B). In antisense Irx ODN-treated lung explants, vimentin (F) and α-sma (D, E) staining was decreased, whereas the smooth muscle cell layer was frequently interrupted (arrows in E). Brown color is positive immunostaining. Bar: 250 μm (A, D); 40 μm (B, E); 100 μm (C, F).

restore distal branching morphogenesis in antisense Irx ODN-treated lung explants after 3 (Fig. 8Ba-d) or 6 (Fig. 8Be-h) days in culture. The *Drosophila Iroquois* genes *araucan* and *caupolican,* which are the counterparts of the vertebrate Irx genes, are positively controlled by *Dpp*, which is in turn the *Drosophila* counterpart of vertebrate Bmp4 (14). Similarly, the Bmp4 antagonist *Noggin* controls the *Xenopus* Irx counterparts *Xiro1* and *Xiro2* and it has been reported that *Xiro1* and *Bmp4* repress each other (24, 25). To analyze whether Bmp4 expression was affected by Irx inhibition in the lung explants, we performed semi-quantitative RT-PCR. However, no obvious differences in the relative expression of Bmp4 mRNA were detected between control, sense, and antisense Irx ODN-treated lung explants after 3 or 6 days in culture (Fig. 8C). Together, these results suggest that almost absent distal epithelial differentiation together with relatively increased proximal epithelial cell differentiation in antisense Irx ODN-treated lung explants is not related to Bmp4.

Irx gene expression in Shh and Gli mutant lungs

The Shh-Gli pathway plays an important role during lung development (4-7, 51). Because *Ci*, which is the *Drosophila* homologue of the vertebrate Gli genes, has been shown to positively control *araucan* and *caupolican*, which are the *Drosophila* counterparts of the vertebrate Irx genes, we investigated gene expression of Irx1, -2, -3, and -5 in lungs of Shh and Gli2 mutant mice. We assessed the developmental (spatial and temporal) pattern of

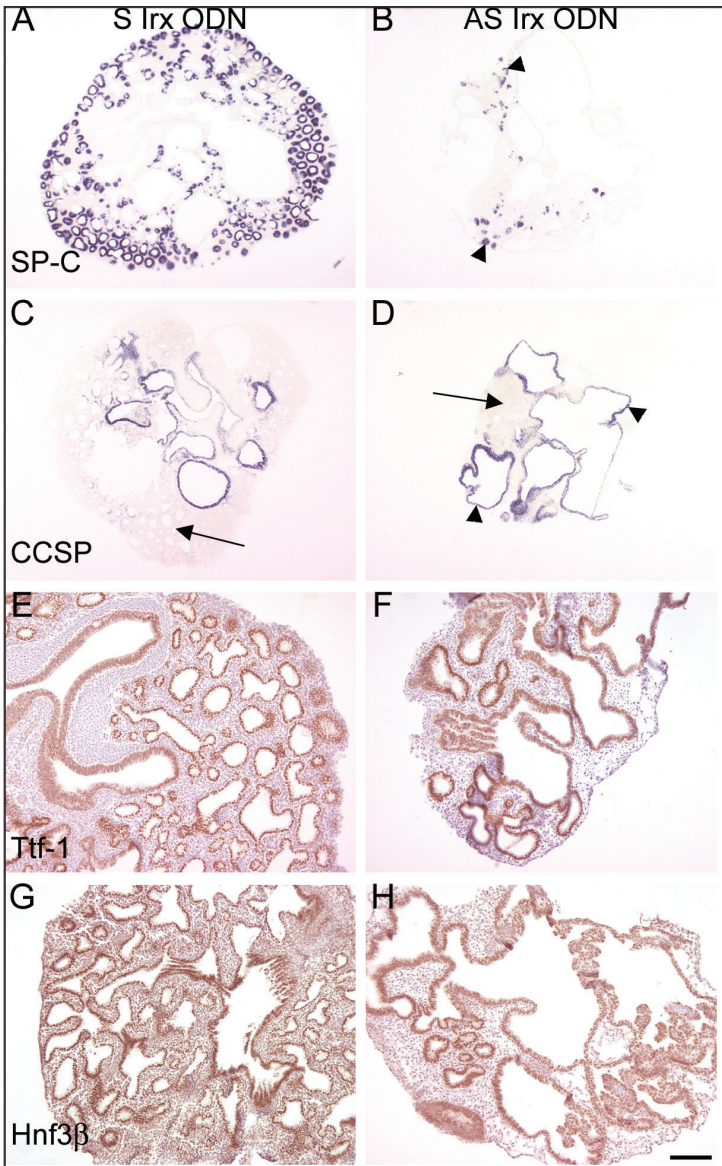

Figure 7. Effect of Irx inhibition on endodermal differentiation. In situ hybridization was performed with DIG-labeled antisense probes for SP-C (A, B) and CCSP (C, D) in sense (A, C, E, G) and antisense (B, D, F, H) Irx ODN-treated rat lung explants after 6 days in culture. In sense-treated explants, SP-C mRNA was expressed in distal pulmonary epithelium (A). In the antisense-treated lung explants, SP-C mRNA expression was dramatically decreased and expression was only observed in some remaining distal epithelial clusters (arrowheads in B). In sense Irx ODN-treated explants, CCSP was expressed in proximal epithelial cells, whereas distal areas were devoid of staining (arrow in C). In antisense-treated explants, CCSP was expressed in virtually all epithelial structures (arrowheads in D), whereas almost no non-staining tissue was detected (arrow in D). Dark purple color is positive ISH staining. Immunohistochemistry for Ttf-1 (E, F) and Hnf3β (G, H) revealed epithelial-specific staining in sense (E, G) and antisense Irx ODN-treated (F, H) lung explants. No difference was observed between sense and antisense-treated lung explants for Ttf-1 or Hnf3β protein expression. Brown staining is positive staining. Bar: 250 µm (A-D); 100 µm (E-H).

Irx1, -2, -3 and -5 gene expression *in vivo*, in wild-type (CD1) mice using *in situ* hybridization and found expression patterns (not shown) that were identical to the expression patterns in rat lungs (Figs 1 and 2). *In situ* hybridization analysis showed that Irx1 (Fig. 9B) and -2 (Fig. 9E) and Irx3 and -5 (not shown) were normally expressed in distal bronchioles of E13.5 and E14.5 $Gli2^{-/-}$ lungs (Fig. 9B, E) compared to wild-type lungs (Fig. 9A, D). $Shh^{-/-}$ lungs were severely hypoplastic, but Irx1 and -2 mRNA (Fig. 9C, F) and Irx3 and -5 mRNA (not shown) expression in these lungs was comparable to the expression of these genes in lungs of

wild-type littermates (Fig. 9A, D). These results indicate that Irx genes -1, -2, -3, and -5 are not downstream in the Shh-Gli signaling cascade.

Discussion

Herein, we demonstrate for the first time that Iroquois (Irx) homeobox genes play a role in branching morphogenesis and in proximal-distal epithelial cell differentiation of the developing lung. Evidence is provided that the Irx genes are not components of well-known signaling pathways that are critical for lung development such as the Shh, Bmp4, or Fgf signaling pathways. We speculate that Irx genes are additional transcriptional components of the complex genetic network directing lung morphogenesis.

We first determined the spatial-temporal expression patterns of the Irx genes in the developing rat lung and found that Irx1, -2, -3, and -5 are specifically expressed in developing epithelium during the period of active airway branching. Houweling *et al.* (16) showed similar expression patterns for these genes in the developing murine lung. In the E10.5 mouse lung, Irx1 and Irx2 were expressed at high levels in the mesoderm adjacent to the endoderm of the laryngotracheal groove, whereas Irx3 and Irx5 expression were restricted to the endoderm of the groove and foregut (16). From E10.5 onwards (until E13.5) however, Irx1, -2, -3, and -5 expression was confined to the epithelial layer of murine lung buds and bronchi (16). Similar expression patterns for Irx1, -2, and -5 during murine lung development have been reported by others (19, 52, 53). In the E11.5 murine lung, Irx2 expression was localized to the distal tips of developing bronchi, whereas it was no longer visible at the end of the pseudoglandular phase (E14.5) of lung development (52). A comparable expression pattern was found for Irx1, with the difference that Irx1 was still prominently expressed throughout the lung epithelium at E13.5, but disappeared in the developing murine lung at the beginning of the alveolar phase (52). In the present study, we show that Irx1, -2, -3, and -5 are expressed throughout the pulmonary rat lung epithelium up to E18.5, which is the canalicular phase of lung development and comparable to E16.5 in mice. Similar to the mouse lung, the intensity of expression of the four Irx genes decreased with advancing gestational age in the rat lungs. However, in contrast to the reported findings in the mouse, we did not observe any specific spatial expression pattern for the Irx genes (that is, no enhanced Irx2 expression was seen at the tips of the developing bronchi). This finding may be the result of the different *in situ* hybridization techniques employed. Becker *et al.* (52) used whole mount *in situ* hybridization to investigate Irx gene expression, whereas we used *in situ* hybridization on tissue sections. A possible explanation for relative prominent distal epithelial staining in later-stage lungs with whole mount *in situ* hybridization is diminished penetration of the DIG-labeled probe and/or BCIP/NBT substrate to the center of the lung tissues.

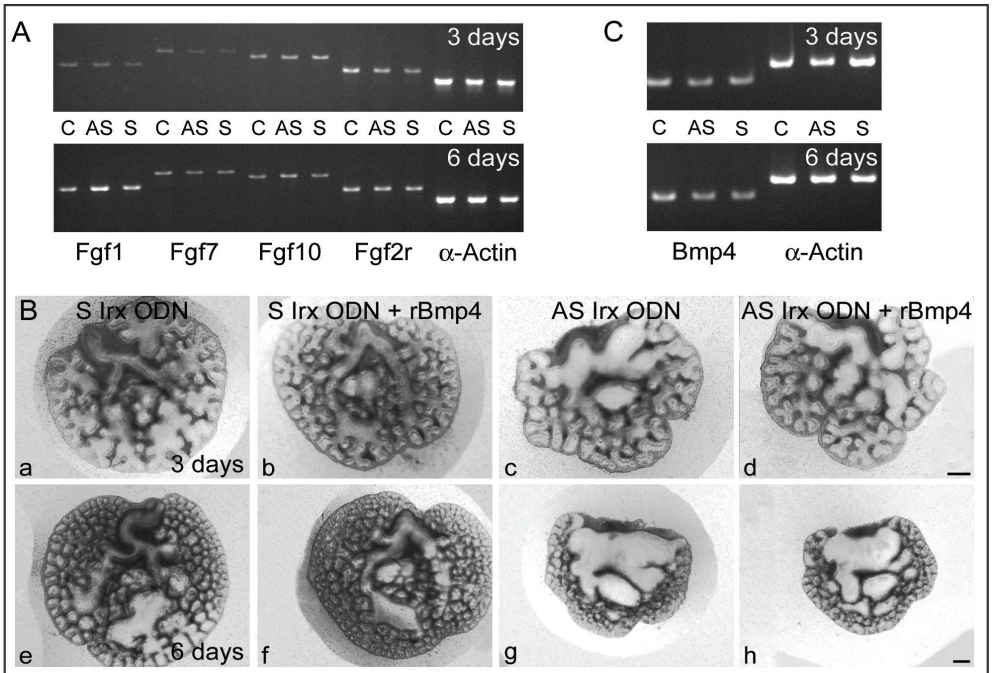

Figure 8. Effect of Irx inhibition on Bmp4, Fgf1, Fgf7, Fgfr2, and Fgf10 expression. A: Semiquantitative RT-PCR showed comparable levels of mRNA expression for Fgf1, Fgf7, Fgf10, and Fgfr2 in control, sense, and antisense Irx ODN-treated lung explants. B: To determine whether Irx genes were upstream of Bmp4, lung explants were incubated for 3 (Ba-d) or 6 (Be-h) days with 200 ng/ml recombinant Bmp4 (rBmp4). Bmp4 treatment of sense-treated lung explants (Bb, f) did not result in obvious differences in epithelial branching compared to untreated control explants (Ba, e). Both antisense (Bc, g) and antisense Irx ODN-treated lung explants cultured with rBmp4 (Bd, h) showed a dramatic decrease in distal airway branching. rBmp4 did not restore distal branching morphogenesis in antisense Irx ODN-treated lung explants after 3 (Bd) or 6 (Bh) days in culture. C: Semiquantitative RT-PCR revealed no differences in Bmp4 mRNA expression between control, sense, and antisense Irx ODN-treated lung explants. RNA integrity and recovery was demonstrated by β-actin RT-PCR. Bar: 250 μm.

Based on their expression patterns, we hypothesized that the Irx genes are involved in early lung branching morphogenesis. Because of their overlapping expression patterns, we decided to inhibit all four pulmonary expressed Irx genes using an *in vitro* antisense ODN approach. *In vivo*-targeting of individual Irx genes has yet not resulted in any major lung phenotype (53), suggesting that the absence of a single Irx gene is compensated by others. The use of antisense ODNs targeted against the translation initiation sequence of Irx1-3, and -5 genes, resulted in a loss of Irx1, -2, -3, and -5 mRNA expression in E13.5 rat lung explants. After 6 days in culture, control E13.5 lung explants displayed a complex branching network with some larger airways in the middle of the explant and more finer and complex branching in the periphery of the explant. In the antisense Irx ODN-treated explants however, only the proximal larger airways seemed to develop, whereas hardly any distal structures were detected. These results indicate that Irx genes do not appear to be required for bronchial branching, but are involved in the formation of smaller, distal airways.

In the present study, mesenchymal and smooth muscle cell markers such as vimentin and α-sma showed a reduced and disorganized pattern of expression in Irx-deficient explants. Furthermore, antisense Irx inhibition increased apoptosis in the mesenchymal compartment of the lung explants, whereas proliferation decreased. Branching of the lung buds is controlled by epithelial-mesenchymal tissue interactions (54, 55). Distal pulmonary mesenchyme induces branching morphogenesis and SP-C expression in epithelial cells, whereas proximal mesenchyme inhibits branching of distal epithelium (56-58). The epithelium, in turn, is needed for the survival of the mesenchyme, because lung mesenchyme that was cultured in the absence of endoderm degenerated quickly (59, 60). In the light of these established data, we speculate that Irx genes play a role in the development of distal mesenchyme, what, in turn, regulates distal epithelial branching morphogenesis. Additionally, the interrupted smooth muscle cell layer along the proximal airways may contribute to the dilated appearance of epithelial tubules in antisense Irx ODN-treated lung explants.

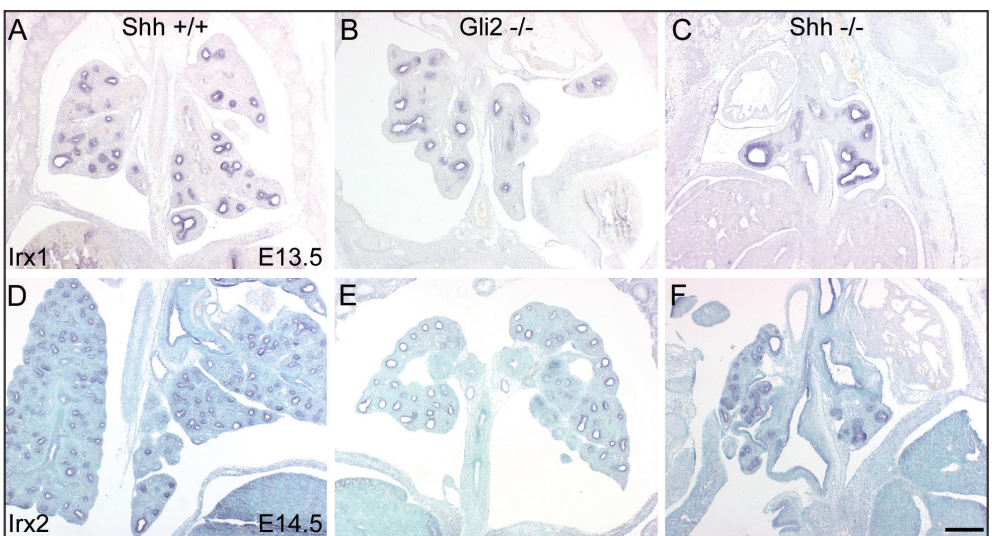

Figure 9. Irx1 and Irx2 expression in murine Gli2$^{-/-}$ and Shh$^{-/-}$ lungs at E13.5 (A-C) and E14.5 (D-F). In situ hybridization using antisense DIG-labeled probes showed Irx1 (A-C) and Irx2 (D-F) expression in the epithelial layer of wild-type lung tubules (A, D). Despite the hypoplastic appearance of Gli2$^{-/-}$ (B, E) and Shh$^{-/-}$ (C, F) lungs, the pattern and level of expression of Irx1 and Irx2 mRNA were similar compared to wild-type lungs (A, D). Dark purple color is positive ISH staining. D-F were counterstained with methyl green. Bar: 250 µm.

SP-C (37) and CCSP (38, 39) are lung specific differentiation markers for distal and proximal epithelial cells, respectively. In this study, *in situ* hybridization analysis revealed that CCSP was abundantly expressed in the epithelial cells lining the large, dilated airways of the antisense Irx ODN-treated lung explants, whereas in control lung explants, CCSP was only expressed in a few larger airways in the center of the explants. In contrast, SP-C was abundantly expressed in the distal airways of control lung explants, whereas it was barely detectable in antisense Irx ODN-treated explants. Expression of both SP-C (40) and CCSP

(41, 42) are transcriptionally regulated by Ttf-1 (or Nkx2.1) and Hnf3β (or Foxa2). Ttf-1 is expressed in pulmonary epithelium from the start of normal lung development (61, 62). Mice deficient for Ttf-1 die at birth with severely hypoplastic lungs, no thyroid gland, and brain abnormalities (62). Additional analysis of the rudimentary Ttf-$1^{-/-}$ lungs revealed cyst-like structures lined with columnar epithelial cells and an overall proximalized phenotype (63, 64), a finding which resembles the phenotype of the Irx-deficient lung explants in the present study. However, immunohistochemical analysis revealed a normal expression pattern for Ttf-1 in antisense Irx ODN-treated lung explants. Also, Hnf3β was normally expressed in these lung explants. Thus, Irx proteins appear not to signal via these transcription factors and we speculate that the observed decrease in SP-C expression is the result of an absolute reduction in distal epithelial cell types because of Irx-deficiency.

Proximalization of the lung has been described as a consequence of inhibited Bmp4 signaling by Weaver *et al.* (27). Interestingly, the *Drosophila* Irx orthologues, *araucan* and *caupolican*, are positively controlled by *Dpp*, the fly homologue of vertebrate Bmp4. In X*enopus* it was shown that *Xiro1*, one of the *Xenopus* Irx orthologues, and Bmp4 control each other (25). Furthermore, *Xiro1* and *Xiro2* are controlled by Noggin, a Bmp4 antagonist (24). Given the finding that inhibition of Bmp4 signaling results in proximalization of the lung (27) and the observed interaction between *Irx* and *Bmp4* orthologues in invertebrates (24), we performed semi-quantitative RT-PCR for Bmp4, but did not find a difference in Bmp4 mRNA expression between sense and antisense Irx ODN-treated lung explants. Also, addition of recombinant Bmp4 to antisense Irx ODN-treated lung cultures did not restore distal branching morphogenesis. These data suggest that the Irx genes are likely not upstream of Bmp4.

In general, Fgfs are very important for lung development. Without Fgf10, no lung will develop below the trachea (48, 49) and *in vitro*, Fgf10 induces outgrowth of two primary lung buds by chemoattraction (65). Fgf7-deficient mice have no lung abnormalities (66) however, *in vitro* studies reveal a role for Fgf7 in widespread epithelial proliferation and SP-C expression (32, 67). The importance of the IIIb splice variant of the Fgf2 receptor was shown when a soluble dominant-negative Fgfr2-IIIb was expressed throughout the entire developing embryo and resulted in lung bud initiation, but no branching morphogenesis (68). Similarly, when soluble dominant-negative Fgfr2-IIIb was overexpressed in distal pulmonary epithelial cells, a trachea and two unbranched bronchi developed, without any further lung formation (69). Marker analysis of the latter lung rudiments revealed CCSP expression in remaining air sacs and no SP-C expression, similar to what we found in antisense Irx ODN-treated lung explants. Shannon *et al*. (70) showed that uncommitted E13.5 rat tracheal epithelium expressed SP-C mRNA when cultured in specified medium with Fgf1 and Fgf7. However, when cultured without Fgf1 and Fgf7, the tracheal epithelium was negative for SP-C, but positive for CCSP, suggesting that Fgf signaling is important for distal epithelial cell differentiation and maintenance. In the present study, loss of Irx

signaling in the explants did not affect the expression of Fgf1, -7, -10, or Fgfr2, indicating that the Irx genes are not upstream components of the Fgf signaling pathway in lung development.

The Shh signaling pathway plays an important role in the development of multiple organs (71). In the lung, Shh is required for proper branching morphogenesis and endoderm patterning (4, 5). The three Gli genes code for zinc finger transcription factors that are the vertebrate counterparts of the gene *Ci*, which is the principal transducer of *Hh* signaling in *Drosophila*. $Gli2^{-/-}$ mice die at birth with severely hypoplastic lungs, consisting of only one lobe on each side of the trachea (6). $Gli3^{-/-}$ mice are viable, but exhibit reductions in size and shape of certain lung lobes (7). $Gli2^{-/-}Gli3^{-/-}$ mice have no lung whatsoever; neither do they form a trachea or esophagus, whereas the presence of one single Gli3 gene restores the phenotype to a lung consisting of only one hypoplastic lobe (6). In *Drosophila*, the *Iro-C* genes *araucan* and *caupolican,* are positively controlled by *Ci* (14). Furthermore, Becker *et al.* (52) showed that Gli1, -2, and -3 and Irx1 and Irx2 genes are co-expressed in the developing lung in adjacent tissues. These authors suggested that Shh and Gli are upstream factors in the Irx signaling cascade (52). The hypoplastic phenotype as seen in both Irx depleted lungs and in Shh and Gli2-deficient lungs, supports an interaction between both signaling cascades. However, the observation that all four Irx genes (Irx1, -2, -3, and -5) were normally expressed in both Shh and Gli2 mutant lungs makes it unlikely that the Irx genes are downstream in the Shh-Gli signaling cascade during lung development.

Bosse and Beckers and co-workers (21,52) suggested a role for Irx signaling in the regulation of Mash-1 based on their overlapping expression patterns during lung development. Mash-1 is a bHLH gene, expressed in neural precursor cells, directing terminal neural differentiation (72). In the lung, Mash-1 is involved in pulmonary neuroendocrine cell (PNEC) differentiation, because Mash-1-deficient mice failed to develop PNECs (73). Also, in *Drosophila*, *araucan* was shown to regulate the gene activity of the *achaete scute-complex* (*AS-C*), which is the homologue of vertebrate Mash-1 (9). However, in this study we found that Irx-ablation did not affect the expression of Mash-1 in the lung (not shown). Altogether, these results indicate that the Irx genes are not upstream or downstream from Mash-1 or Shh-Gli, respectively, and, although it is still possible that the Irx genes function upstream in the Shh-Gli signaling cascade, we speculate that they function in an unrelated, parallel signaling pathway.

A phenotype that resembles the antisense Irx-deficient lungs, was seen in retinoic acid (RA) treated mouse lung explants (74). In *Xenopus*, RA increases *Xiro* expression in the neural plate, but it decreases *Xiro* expression outside this plate (24). If we extrapolate these findings to the present study, it would mean that RA downregulates the Irx genes, which in turn leads to outgrowth of proximal and inhibition of distal lung structures. Further investigations are required to explore a putative RA-Irx interaction in lung development.

In summary, we have demonstrated that Irx1, -2, -3, and -5 are expressed in developing rat lungs in an epithelial and temporal specific fashion. Antisense inhibition experiments *in vitro* revealed that the Irx genes together play an important role in proximal-distal epithelial differentiation and branching morphogenesis of the lung. The importance of each individual Irx gene remains to be investigated, but overall Irx signaling appeared not to be linked to known signaling cascades that are critical for lung development.

Acknowledgments

We thank A. Griffin for animal handling and care and I. Tseu and M. Kuliszewski for technical assistance. This work was supported by the Canadian Institutes of Health Research (M.P.) and the Sophia Foundation for Medical Research (SSWO, #342, M.v.T.). Martin Post is holder of a Canadian Research Chair (tier 1) in Fetal, Neonatal, and Maternal Health.

References

1. Warburton D, Schwarz M, Tefft D, Flores-Delgado G, Anderson KD, Cardoso WV, 2000. The molecular basis of lung morphogenesis. Mech Dev. 92:55-81.

2. van Tuyl M, Post M: Molecular mechanisms of lung development and lung branching morphogenesis. In Polin RA, Fox WW,Abman SH (eds): Fetal and Neonatal Physiology, 3rd edition 3rd edition, vol 1, p 812-821. Philadelphia, Saunders, Harcourt Health Sciences, 2003.

3. van Tuyl M, Post, M., 2000. From fruitflies to mammals: mechanisms of signalling via the Sonic hedgehog pathway in lung development. Respiratory Research. 1:30-35.

4. Litingtung Y, Lei L, Westphal H, Chiang C, 1998. Sonic hedgehog is essential to foregut development. Nat Genet. 20:58-61.

5. Pepicelli CV, Lewis PM, McMahon AP, 1998. Sonic hedgehog regulates branching morphogenesis in the mammalian lung. Curr Biol. 8:1083-1086.

6. Motoyama J, Liu J, Mo R, Ding Q, Post M, Hui CC, 1998. Essential function of Gli2 and Gli3 in the formation of lung, trachea and oesophagus. Nat Genet. 20:54-57.

7. Grindley JC, Bellusci S, Perkins D, Hogan BL, 1997. Evidence for the involvement of the Gli gene family in embryonic mouse lung development. Dev Biol. 188:337-348.

8. Park HL, Bai C, Platt KA, Matise MP, Beeghly A, Hui CC, Nakashima M, Joyner AL, 2000. Mouse Gli1 mutants are viable but have defects in SHH signaling in combination with a Gli2 mutation. Development. 127:1593-1605.

9. Gómez-Skarmeta JL, del Corral RD, de la Calle-Mustienes E, Ferre-Marco D, Modolell J, 1996. Araucan and caupolican, two members of the novel iroquois complex, encode homeoproteins that control proneural and vein-forming genes. Cell. 85:95-105.

10. Cavodeassi F, Diez Del Corral R, Campuzano S, Dominguez M, 1999. Compartments and organising boundaries in the Drosophila eye: the role of the homeodomain Iroquois proteins. Development. 126:4933-4942.

11. Cavodeassi F, Modolell J, Campuzano S, 2000. The Iroquois homeobox genes function as dorsal selectors in the Drosophila head. Development. 127:1921-1929.

12. Jordan KC, Clegg NJ, Blasi JA, Morimoto AM, Sen J, Stein D, McNeill H, Deng WM, Tworoger M, Ruohola-Baker H, 2000. The homeobox gene mirror links EGF signalling to embryonic dorso- ventral axis formation through notch activation. Nat Genet. 24:429-433.

13. McNeill H, Yang CH, Brodsky M, Ungos J, Simon MA, 1997. mirror encodes a novel PBX-class homeoprotein

that functions in the definition of the dorsal-ventral border in the Drosophila eye. Genes Dev. 11:1073-1082.

14. Gómez-Skarmeta JL, Modolell J, 1996. araucan and caupolican provide a link between compartment subdivisions and patterning of sensory organs and veins in the Drosophila wing. Genes Dev. 10:2935-2945.

15. Peters T, Dildrop R, Ausmeier K, Ruther U, 2000. Organization of mouse Iroquois homeobox genes in two clusters suggests a conserved regulation and function in vertebrate development. Genome Res. 10:1453-1462.

16. Houweling AC, Dildrop R, Peters T, Mummenhoff J, Moorman AF, Ruther U, Christoffels VM, 2001. Gene and cluster-specific expression of the Iroquois family members during mouse development. Mech Dev. 107:169-174.

17. Cohen DR, Cheng CW, Cheng SH, Hui CC, 2000. Expression of two novel mouse Iroquois homeobox genes during neurogenesis. Mech Dev. 91:317-321.

18. Mummenhoff J, Houweling AC, Peters T, Christoffels VM, Ruther U, 2001. Expression of Irx6 during mouse morphogenesis. Mech Dev. 103:193-195.

19. Bosse A, Stoykova A, Nieselt-Struwe K, Chowdhury K, Copeland NG, Jenkins NA, Gruss P, 2000. Identification of a novel mouse Iroquois homeobox gene, Irx5, and chromosomal localisation of all members of the mouse Iroquois gene family. Dev Dyn. 218:160-174.

20. Bruneau BG, Bao ZZ, Tanaka M, Schott JJ, Izumo S, Cepko CL, Seidman JG, Seidman CE, 2000. Cardiac expression of the ventricle-specific homeobox gene Irx4 is modulated by Nkx2-5 and dHand. Dev Biol. 217:266-277.

21. Bosse A, Zulch A, Becker MB, Torres M, Gomez-Skarmeta JL, Modolell J, Gruss P, 1997. Identification of the vertebrate Iroquois homeobox gene family with overlapping expression during early development of the nervous system. Mech Dev. 69:169-181.

22. Christoffels VM, Keijser AG, Houweling AC, Clout DE, Moorman AF, 2000. Patterning the embryonic heart: identification of five mouse Iroquois homeobox genes in the developing heart. Dev Biol. 224:263-274.

23. Bao ZZ, Bruneau BG, Seidman JG, Seidman CE, Cepko CL, 1999. Regulation of chamber-specific gene expression in the developing heart by Irx4. Science. 283:1161-1164.

24. Gómez-Skarmeta JL, Glavic A, de la Calle-Mustienes E, Modolell J, Mayor R, 1998. Xiro, a Xenopus homolog of the Drosophila Iroquois complex genes, controls development at the neural plate. Embo J. 17:181-190.

25. Gómez-Skarmeta J, de La Calle-Mustienes E, Modolell J, 2001. The Wnt-activated Xiro1 gene encodes a repressor that is essential for neural development and downregulates Bmp4. Development. 128:551-560.

26. Bellusci S, Henderson R, Winnier G, Oikawa T, Hogan BL, 1996. Evidence from normal expression and targeted misexpression that bone morphogenetic protein (Bmp-4) plays a role in mouse embryonic lung morphogenesis. Development. 122:1693-1702.

27. Weaver M, Yingling JM, Dunn NR, Bellusci S, Hogan BL, 1999. Bmp signaling regulates proximal-distal differentiation of endoderm in mouse lung development. Development. 126:4005-4015.

28. Shi W, Zhao J, Anderson KD, Warburton D, 2001. Gremlin negatively modulates BMP-4 induction of embryonic mouse lung branching morphogenesis. Am J Physiol Lung Cell Mol Physiol. 280:L1030-L1039.

29. Chiang C, Litingtung Y, Lee E, Young KE, Corden JL, Westphal H, Beachy PA, 1996. Cyclopia and defective

axial patterning in mice lacking Sonic hedgehog gene function. Nature. 383:407-413.

30. Wang J, Souza P, Kuliszewski M, Tanswell AK, Post M, 1994. Expression of surfactant proteins in embryonic rat lung. Am J Respir Cell Mol Biol. 10:222-229.

31. Ozawa K, Uruno T, Miyakawa K, Seo M, Imamura T, 1996. Expression of the fibroblast growth factor family and their receptor family genes during mouse brain development. Brain Res Mol Brain Res. 41:279-288.

32. Post M, Souza P, Liu J, Tseu I, Wang J, Kuliszewski M, Tanswell AK, 1996. Keratinocyte growth factor and its receptor are involved in regulating early lung branching. Development. 122:3107-3115.

33. Lebeche D, Malpel S, Cardoso WV, 1999. Fibroblast growth factor interactions in the developing lung. Mech Dev. 86:125-136.

34. De Moerlooze L, Spencer-Dene B, Revest J, Hajihosseini M, Rosewell I, Dickson C, 2000. An important role for the IIIb isoform of fibroblast growth factor receptor 2 (FGFR2) in mesenchymal-epithelial signalling during mouse organogenesis. Development. 127:483-492.

35. Moorman AF, Houweling AC, de Boer PA, Christoffels VM, 2001. Sensitive nonradioactive detection of mRNA in tissue sections: novel application of the whole-mount in situ hybridization protocol. J Histochem Cytochem. 49:1-8.

36. Hsu SM, Raine L, Fanger H, 1981. Use of avidin-biotin-peroxidase complex (ABC) in immunoperoxidase techniques: a comparison between ABC and unlabeled antibody (PAP) procedures. J Histochem Cytochem. 29:577-580.

37. Wert SE, Glasser SW, Korfhagen TR, Whitsett JA, 1993. Transcriptional elements from the human SP-C gene direct expression in the primordial respiratory epithelium of transgenic mice. Dev Biol. 156:426-443.

38. Khoor A, Gray ME, Singh G, Stahlman MT, 1996. Ontogeny of Clara cell-specific protein and its mRNA: their association with neuroepithelial bodies in human fetal lung and in bronchopulmonary dysplasia. J Histochem Cytochem. 44:1429-1438.

39. Zhou L, Lim L, Costa RH, Whitsett JA, 1996. Thyroid transcription factor-1, hepatocyte nuclear factor-3beta, surfactant protein B, C, and Clara cell secretory protein in developing mouse lung. J Histochem Cytochem. 44:1183-1193.

40. Whitsett JA, Glasser SW, 1998. Regulation of surfactant protein gene transcription. Biochim Biophys Acta. 1408:303-311.

41. Bohinski RJ, Di Lauro R, Whitsett JA, 1994. The lung-specific surfactant protein B gene promoter is a target for thyroid transcription factor 1 and hepatocyte nuclear factor 3, indicating common factors for organ-specific gene expression along the foregut axis. Mol Cell Biol. 14:5671-5681.

42. Bingle CD, Hackett BP, Moxley M, Longmore W, Gitlin JD, 1995. Role of hepatocyte nuclear factor-3 alpha and hepatocyte nuclear factor- 3 beta in Clara cell secretory protein gene expression in the bronchiolar epithelium. Biochem J. 308:197-202.

43. Zhou H, Morotti RA, Profitt SA, Langston C, Wert SE, Whitsett JA, Greco MA, 2001. Expression of thyroid transcription factor-1, surfactant proteins, type I cell-associated antigen, and Clara cell secretory protein in pulmonary hypoplasia. Pediatr Dev Pathol. 4:364-371.

44. Stahlman MT, Gray ME, Whitsett JA, 1996. Expression of thyroid transcription factor-1(TTF-1) in fetal and neonatal human lung. J Histochem Cytochem. 44:673-678.

45. Stahlman MT, Gray ME, Whitsett JA, 1998. Temporal-spatial distribution of hepatocyte nuclear factor-3beta

in developing human lung and other foregut derivatives. J Histochem Cytochem. 46:955-962.

46. Bellusci S, Grindley J, Emoto H, Itoh N, Hogan BL, 1997. Fibroblast growth factor 10 (FGF10) and branching morphogenesis in the embryonic mouse lung. Development. 124:4867-4878.

47. Cardoso WV, Itoh A, Nogawa H, Mason I, Brody JS, 1997. FGF-1 and FGF-7 induce distinct patterns of growth and differentiation in embryonic lung epithelium. Dev Dyn. 208:398-405.

48. Min H, Danilenko DM, Scully SA, Bolon B, Ring BD, Tarpley JE, DeRose M, Simonet WS, 1998. Fgf-10 is required for both limb and lung development and exhibits striking functional similarity to Drosophila branchless. Genes Dev. 12:3156-3161.

49. Sekine K, Ohuchi H, Fujiwara M, Yamasaki M, Yoshizawa T, Sato T, Yagishita N, Matsui D, Koga Y, Itoh N, Kato S, 1999. Fgf10 is essential for limb and lung formation. Nat Genet. 21:138-141.

50. Arman E, Haffner-Krausz R, Gorivodsky M, Lonai P, 1999. Fgfr2 is required for limb outgrowth and lung-branching morphogenesis. Proc Natl Acad Sci U S A. 96:11895-11899.

51. Bellusci S, Furuta Y, Rush MG, Henderson R, Winnier G, Hogan BL, 1997. Involvement of Sonic hedgehog (Shh) in mouse embryonic lung growth and morphogenesis. Development. 124:53-63.

52. Becker M, Zulch A, Bosse A, Gruss P, 2001. Irx1 and Irx2 expression in early lung development. Mech Dev. 106:155-158.

53. Lebel M, Agarwal P, Cheng CW, Kabir MG, Chan TY, Thanabalasingham V, Zhang X, Cohen DR, Husain M, Cheng SH, Bruneau BG, Hui CC, 2003. The Iroquois homeobox gene Irx2 is not essential for normal development of the heart and midbrain-hindbrain boundary in mice. Mol Cell Biol. 23:8216-8225.

54. Alescio TC, A, 1962. Induction in vitro of tracheal buds by pulmonary mesenchyme grafted on tracheal epithelium. J Exp Zool. 150:83-94.

55. Spooner BS, Wessells NK, 1970. Mammalian lung development: interactions in primordium formation and bronchial morphogenesis. J Exp Zool. 175:445-454.

56. Wessells NK, 1970. Mammalian lung development: interactions in formation and morphogenesis of tracheal buds. J Exp Zool. 175:455-466.

57. Shannon JM, 1994. Induction of alveolar type II cell differentiation in fetal tracheal epithelium by grafted distal lung mesenchyme. Dev Biol. 166:600-614.

58. Shannon JM, Nielsen LD, Gebb SA, Randell SH, 1998. Mesenchyme specifies epithelial differentiation in reciprocal recombinants of embryonic lung and trachea. Dev Dyn. 212:482-494.

59. Gebb SA, Shannon JM, 2000. Tissue interactions mediate early events in pulmonary vasculogenesis. Dev Dyn. 217:159-169.

60. Taderera JV, 1967. Control of lung differentiation in vitro. Dev Biol. 16:489-512.

61. Lazzaro D, Price M, de Felice M, Di Lauro R, 1991. The transcription factor TTF-1 is expressed at the onset of thyroid and lung morphogenesis and in restricted regions of the foetal brain. Development. 113:1093-1104.

62. Kimura S, Hara Y, Pineau T, Fernandez-Salguero P, Fox CH, Ward JM, Gonzalez FJ, 1996. The T/ebp null mouse: thyroid-specific enhancer-binding protein is essential for the organogenesis of the thyroid, lung, ventral forebrain, and pituitary. Genes Dev. 10:60-69.

63. Minoo P, Su G, Drum H, Bringas P, Kimura S, 1999. Defects in tracheoesophageal and lung morphogenesis

in Nkx2.1(-/-) mouse embryos. Dev Biol. 209:60-71.

64. Yuan B, Li C, Kimura S, Engelhardt RT, Smith BR, Minoo P, 2000. Inhibition of distal lung morphogenesis in Nkx2.1(-/-) embryos. Dev Dyn. 217:180-190.

65. Park WY, Miranda B, Lebeche D, Hashimoto G, Cardoso WV, 1998. FGF-10 is a chemotactic factor for distal epithelial buds during lung development. Dev Biol. 201:125-134.

66. Guo L, Degenstein L, Fuchs E, 1996. Keratinocyte growth factor is required for hair development but not for wound healing. Genes Dev. 10:165-175.

67. Shiratori M, Oshika E, Ung LP, Singh G, Shinozuka H, Warburton D, Michalopoulos G, Katyal SL, 1996. Keratinocyte growth factor and embryonic rat lung morphogenesis. Am J Respir Cell Mol Biol. 15:328-338.

68. Celli G, LaRochelle WJ, Mackem S, Sharp R, Merlino G, 1998. Soluble dominant-negative receptor uncovers essential roles for fibroblast growth factors in multi-organ induction and patterning. Embo J. 17:1642-1655.

69. Peters K, Werner S, Liao X, Wert S, Whitsett J, Williams L, 1994. Targeted expression of a dominant negative FGF receptor blocks branching morphogenesis and epithelial differentiation of the mouse lung. Embo J. 13:3296-3301.

70. Shannon JM, Gebb SA, Nielsen LD, 1999. Induction of alveolar type II cell differentiation in embryonic tracheal epithelium in mesenchyme-free culture. Development. 126:1675-1688.

71. Ingham PW, McMahon AP, 2001. Hedgehog signaling in animal development: paradigms and principles. Genes Dev. 15:3059-3087.

72. Kageyama R, Ishibashi M, Takebayashi K, Tomita K, 1997. bHLH transcription factors and mammalian neuronal differentiation. Int J Biochem Cell Biol. 29:1389-1399.

73. Borges M, Linnoila RI, van de Velde HJ, Chen H, Nelkin BD, Mabry M, Baylin SB, Ball DW, 1997. An achaete-scute homologue essential for neuroendocrine differentiation in the lung. Nature. 386:852-855.

74. Cardoso WV, Williams MC, Mitsialis SA, Joyce-Brady M, Rishi AK, Brody JS, 1995. Retinoic acid induces changes in the pattern of airway branching and alters epithelial cell differentiation in the developing lung in vitro. Am J Respir Cell Mol Biol. 12:464-476.

Chapter 6

Overexpression of Lunatic Fringe does not affect epithelial cell differentiation in the developing mouse lung

Minke van Tuyl[1, 2], Maciek Kuliszewski[1], Jinxia Wang[1], Julie Deimling[1], Dick Tibboel[2], and Martin Post[1]

[1]Canadian Institutes of Health Research (CIHR) Group in Lung Development, Hospital for Sick Children Research Institute, Departments of Pediatrics and Physiology, University of Toronto, Toronto, ON, Canada
[2]Department of Pediatric Surgery, Sophia Children's Hospital, Erasmus University Medical Center Rotterdam, Rotterdam, The Netherlands

Submitted

Abstract

The Notch-Notch-ligand signaling pathway is a pathway that regulates cell fate decisions and patterning in various tissues. Several components of this pathway are expressed in the developing lung, suggesting that it is important for cellular patterning of the airways. Fringe proteins, which modulate Notch signaling, are crucial for defining morphogenic borders in a variety of organs. Their role in controlling cellular differentiation along the anterior-posterior axis of the airways is unknown. Herein, we report the temporal-spatial mRNA expression patterns of Lunatic fringe (Lfng) and the Notch-regulated basic helix-loop-helix factors, Hes1 and Mash-1, during murine lung development. Lfng mRNA was only expressed during early development in epithelial cells lining the larger airways. Those epithelial cells also expressed Hes1, but at later gestation Hes1 mRNA expression was confined to epithelial cells lining the terminal bronchioles. Mash-1 mRNA displayed a very characteristic expression pattern. It followed neural crest migration into the early lung, whereas at later stages Mash-1 was expressed in the neuroendocrine cells of the lung. To clarify whether Lfng influences airway cell differentiation, Lfng was overexpressed in distal epithelial cells of the developing mouse lung. Overexpression of Lfng did not affect the spatial or temporal mRNA expression of Hes1 or Mash-1. Neuroendocrine-specific cGRP and Pgp9.5 protein expression was not altered by Lfng overexpression. Also, mRNA expression of proximal (CC10) and distal epithelial cell (SP-C, T1α) markers was not influenced by an excess of Lfng. Overexpression of Lfng had no effect on mesenchymal cell marker (α-sma, vWF, Pecam-1) protein expression. Collectively, the data suggest that Lfng does not play a significant role in determining cell fate in fetal airway epithelium.

Introduction

Pattern formation during embryonic development depends largely on specific cell-cell interactions and the regulated expression of key signaling molecules. The exact coordination of pattern formation within the developing lung remains an enigma. During early pulmonary development, the trachea and lung primordia are determined by interactions between the foregut endoderm and surrounding splanchnic mesenchyme (1). At later stages of lung development, epithelial-mesenchymal tissue interactions program branching morphogenesis of the primitive respiratory epithelium as well as cell growth and differentiation (2, 3). Some of the morphogenic signaling pathways in the lung have been identified (4, 5), whereas others remain to be discovered.

The Notch signaling pathway is an evolutionary conserved pathway involved in cell fate control through cell-cell interactions (6). The generally accepted function of Notch signaling is to inhibit differentiation in order to prevent two neighboring cells from taking the same fate, thereby creating heterogeneity between cells (6). Notch is a transmembrane receptor that is activated through direct contact with a cell-surface ligand on a neighboring cell (7). Two vertebrate transmembrane ligands have been described, Delta and Jagged. Vertebrate CBF1/rJBk (Suppressor of Hairless in *Drosophila*) is a downstream transcription factor in the Notch signaling pathway, repressing the genes of the Enhancer of split locus, Hes1 and Hes5 (6, 8). Both Hes1 and Hes5 encode basic helix-loop-helix (bHLH) proteins that are upregulated in response to Notch activation and subsequently affect downstream targets. One of the targets is the *Achaete-Scute* complex (Mash-1 in vertebrates), which is involved in the segregation of neuronal and epidermal lineages (6). In flies, *fringe* has been identified as a secreted signaling protein with a key role in dorsal-ventral aspects of wing formation (9). There is genetic and biochemical evidence that the *fringe* genes in the fly modulate the Notch signaling pathway at the extracellular level (10, 11). At the post-transcriptional level, fringe proteins positively regulate signaling via Delta and negatively regulate signaling via Serrate in the wing imaginal disc of flies (10). In vertebrates, three fringe genes have been identified: Manic, Lunatic and Radical fringe (12-14).

Notch signaling has been implicated in epithelial-mesenchymal tissue interactions guiding tooth and kidney development (15, 16). In *Drosophila*, the Notch signaling pathway is essential for the development of the tracheal system (17). In zygotic *Notch* null mutants, tracheal cells were converted into neuroblasts, leaving only rudimentary branches with abnormalities in fusion and terminal branching, implying that Notch signaling is required for tracheal fusion and terminal branching in the fly (17). Recent studies have demonstrated that several members of the Notch signaling pathway are expressed in the developing mouse lung (18, 19). Together, these data suggest that the Notch signaling pathway may be important for mammalian lung development. However, the exact role of Notch signaling and its regulation during lung morphogenesis are unknown. In this study

we investigated the spatial and temporal mRNA expression of Notch regulated basic helix-loop-helix (bHLH) genes such as Hes1 and Mash-1. Both genes have been implicated in pulmonary neuroendocrine development (20). Because Notch signaling is modulated by fringe (21), we also investigated whether overexpression of Lunatic fringe (Lfng) in the distal epithelium of the developing mouse lung would affect lung development.

Materials and Methods

Transgene construction

The SPC-Lfng vector was constructed using full-length mouse Lfng cDNA (generous gift of Dr. S. Egan, Hospital for Sick Children, Toronto, ON, Canada). The 1.2 kb Lfng cDNA was subcloned 3′ of the 3.7 kb human SP-C promoter (22) and 5′ of the SV40 small T intron and polyadenylation sequences. The expression cassette was excised with NdeI and NotI, purified using Glass Milk (Gene Clean Kit Bio101, BioCan, Canada) and Elutip-D columns (Schleier and Schuell, NY, U.S.A.), and ethanol precipitated.

Transgenic SPC-Lfng mice

Transgenic embryos were generated according to Hogan *et al*. (23). DNA injections into the pronuclei of (C57BL/6 x SJL) F2 embryos were carried out at a concentration of 3 ng/μl. The genotype was established by PCR analysis of genomic DNA that was extracted from the embryonic tail and confirmed by Southern blot analysis. The primers used were 5′-TCACCTCTGTCCCCTCTCCCTAG-3′ and 5′-TGGGCCGAGGAGCAGTTGGTGAGC-3′. The annealing temperature was 62°C and 35 cycles were used for amplification.

Probes

The murine cDNAs used as templates for riboprobe generation were a 0.9 kb Hes1 clone, a 2.8 kb full-length Mash-1 clone (provided by Dr. S. Egan, Hospital for Sick Children, Toronto, ON, Canada), and PCR-cloned fragments for SP-C (330 bp), CC10 (CCSP; 315 bp), and Lfng (756 bp). Riboprobes were digoxigenin-labeled according to a protocol provided by the manufacturer (Roche, Montreal, QC, Canada).

Whole mount *in situ* hybridization

Whole mount *in situ* hybridization was performed essentially as described before (24). Briefly, lungs were dissected from E11.5-E13.5 control (CD1) mouse embryos (morning of plug is designated as E0.5) and fixed in 4% paraformaldehyde (PFA) in phosphate-buffered saline (PBS) at 4°C. Lungs were washed in PBS-T (PBS containing 0.1% Tween-20), dehydrated in graded series of methanol in PBS-T, and stored in 100% methanol. After rehydration, lungs were bleached in 6% hydrogen peroxide, treated with proteinase K (20 μg/ml), postfixed in 4% PFA and 0.2% glutaraldehyde, and pre-hybridized for 1 hr at 70°C. Lungs were then hybridized with the appropriate digoxigenin (DIG)-labeled riboprobe (1

μg/ml), overnight at 70°C. After washes in 50% formamide, 5x SSC, pH 4.5, and 1% SDS at 70°C followed by washes in 50% formamide and 2x SSC, pH 4.5 at 65°C and Tris-buffered saline (TBS)-T (TBS containing 1% Tween-20) at RT, lungs were pre-blocked with sheep serum in TBS-T and subsequently incubated with anti-DIG alkaline phosphatase, 1:5000, in blocking solution (Roche, Montreal, QC, Canada) at 4°C. The next day, lungs were washed in PBS-T followed by washes in NTM-T (100 mM NaCl, 100 mM Tris, pH 9.5, 50 mM $MgCl_2$, 0.1% Tween) and then incubated with 5-bromo-4-chloro-3-indolyl phosphate/nitro blue tetrazolium chromogen (Roche, Montreal, QC, Canada) at room temperature (RT) until purple color appeared. After color development, lungs were washed in NTM-T and PBS-T, dehydrated in a graded series of methanol in PBS-T, and stored at 4 C in PBS-T. Digital images were taken using a Leica digital imaging system.

Tissue section *in situ* hybridization

Mouse embryos were obtained from timed-pregnant SPC-Lfng mice (morning of plug is designated as E0.5). Whole embryos and isolated lungs were fixed in 4% PFA in PBS at 4°C for 4-18 hrs, dehydrated in ethanol, and embedded in paraplast. Sections of 12 μm were cut and mounted on Superfrost slides (Fisher Scientific, Unionville, ON, Canada). The lungs were then assayed for non-radioactive RNA *in situ* hybridization according to Moorman *et al*. (25). Briefly, after dewaxing and rehydrating, tissue sections were permeabilized with proteinase K (20 μg/ml), postfixed in 4% PFA/0.2% glutaraldehyde, and pre-hybridized for 1 hr at 70°C. The sections were hybridized overnight at 70°C with DIG-labeled riboprobes for Lfng, SP-C, CC10, Hes1, or Mash-1 (1 μg/ml). The next day, sections were washed in 50% formamide in 2x SSC, pH 4.5 at 65°C followed by PBS-T washes. Subsequently, the sections were incubated with anti-DIG alkaline phosphatase, 1:1000, in blocking solution (Roche, Montreal, QC, Canada) at 4°C. The next day, sections were washed in PBS-T followed by washes in NTM (100 mM NaCl, 100 mM Tris, pH 9.5, 50 mM $MgCl_2$), and then incubated with NBT/BCIP (Roche, Montreal, QC, Canada) at RT until purple color appeared (4-5 hours). All slides for one probe were stopped at the same time to make comparison over different stages of development possible. After color development, sections were washed in distilled water, dehydrated in a graded series of ethanol and xylene, and mounted with coverslips using permount (Fisher Scientific, Unionville, ON, Canada). Digital images were taken using a Leica digital imaging system.

Immunocytochemistry

At embryonic day (E)11.5 to E18.5, SPC-Lfng transgenic and wild-type embryos were sacrificed and lungs were dissected, fixed overnight in 4% PFA in PBS, dehydrated, and embedded in paraplast. Immunostaining was performed using the avidin-biotin (ABC) immunoperoxidase method as described by Hsu *et al*. (26). Seven μm sections were deparaffinized and rehydrated in a graded series of ethanol. Antigen retrieval was achieved with heating in sodium citrate, pH 6.0. Sections were washed in PBS containing 0.1% Triton and endogenous peroxidase was blocked in 2% H_2O_2 in methanol.

Sections were incubated overnight at 4°C with mouse monoclonal anti-rat Ttf-1, 1:50, (Labvision/Neomarkers, Fremont, CA, U.S.A.), hamster monoclonal anti-mouse T1α, 1:50, (Developmental Studies Hybridoma Bank, University of Iowa, U.S.A., Hybridoma #8.1.1), rat monoclonal anti-mouse CD31, 1:60, (Pecam-1, BD Biosciences Pharmingen, Mississauga, ON, Canada), rabbit polyclonal anti-Factor VIII related antigen, 1:80, (Labvision/Neomarkers, Fremont, CA, U.S.A.), mouse monoclonal anti-mouse α-smooth muscle actin, 1:1000, (α-sma, Labvision/Neomarkers, Fremont, CA, U.S.A.), polyclonal rabbit anti-human Pgp9.5, 1:10000, (UltraClone Limited, Isle of White, U.K.), or polyclonal rabbit anti-rat cGRP, 1:13000, (Sigma, St. Louis, MO, U.S.A.) antibody, all diluted in blocking solution (5% NGS and 1% BSA in PBS). Sections were subsequently incubated with biotinylated secondary antibodies and color detection was performed according to instructions in the Vectastain ABC and DAB kit (Vector Laboratories, Burlingname, CA, U.S.A.). For Ttf-1, nickel was added to the DAB solution to enhance black nuclear staining. Sections were counterstained with haematoxylin, except for Ttf-1, which was counterstained with fast red, and mounted in Permount (Fisher Scientific, Unionville, ON, Canada). Digital images were taken using a Leica digital imaging system.

RNA isolation and real-time RT-PCR

Lungs from E15.5 and E16.5 SPC-Lfng transgenic and wild-type embryos were dissected in ice-cold PBS, snap-frozen in liquid nitrogen, and stored at -70°C. Total RNA was extracted using the RNeasy kit (Qiagen, Mississauga, ON, Canada). One µg of RNA was reverse transcribed (37°C) using random-hexamers (Applied Biosystems, Foster City, CA, USA). The resulting templates (50 ng of cDNA for our target genes and 5 ng for 18S) were quantified by real-time PCR (ABI Prism 7700). Primers and TaqMan probes for Lfng, Hes1, and Mash-1 were purchased from ABI as Assays-on-Demand™ for murine genes. For each probe, a dilution series determined the efficiency of amplification of each primer-probe set and the relative quantification method was employed (27). All measurements were performed in triplicates. For the relative quantitation, PCR signals were compared between groups after normalization using 18S as an internal reference. Briefly, relative expression was calculated as $2^{-(Ct\text{gene of interest} - Ct18S)}$. Fold change was calculated according to Livak *et al*. (27). For comparison between 2 groups we used Student's t-test. P values <0.05 were considered significant.

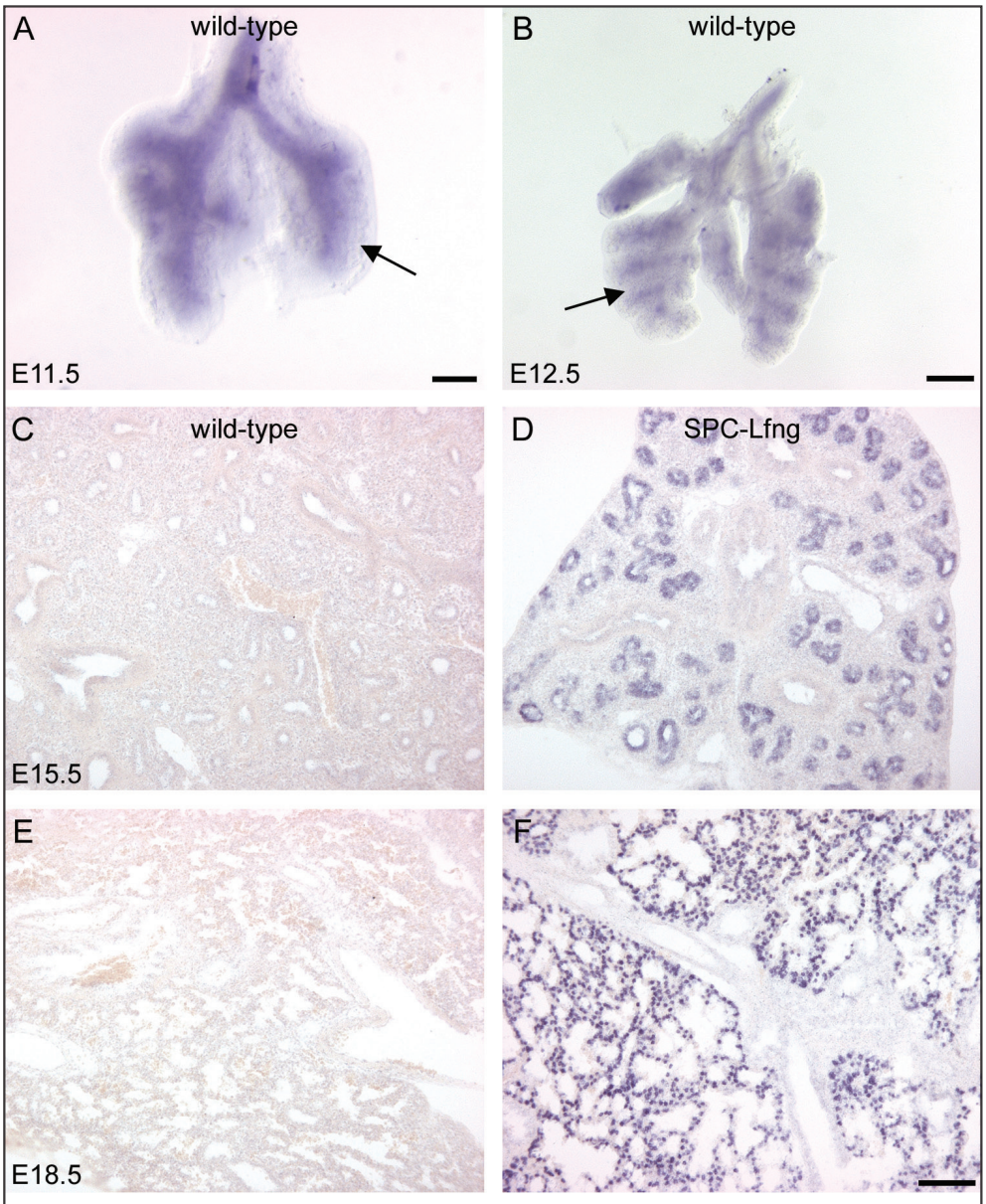

Figure 1. Lfng mRNA expression in wild-type (A-C, E) and SPC-Lfng (D, F) lungs. Whole mount in situ hybridization showed Lfng mRNA expression in the endodermal layer of the trachea and proximal airways of E11.5-E12.5 lungs (A, B). No staining was detected in the mesenchyme surrounding the developing lung buds (arrows in A, B). At later gestation (E15.5 and E18.5), Lfng mRNA expression was undetectable with section in situ hybridization (C, E). In contrast, Lfng mRNA was rapidly detected with section in situ hybridization in the epithelial cells of distal airways of transgenic SPC-Lfng lungs (D, F for E15.5 and E18.5, respectively). Dark purple color is positive ISH staining. Bar: 100 µm (A, C-F); 250 µm (B).

Results

Endogenous Lfng expression in murine lungs

Whole mount *in situ* hybridization demonstrated endogenous Lfng mRNA expression in the E11.5 epithelium of proximal airways (Fig. 1A). The trachea, stem bronchi, and lobar bronchi displayed equal intensity of Lfng expression. At E12.5, Lfng showed a similar expression pattern, that is, expression in the epithelium of trachea and lobar bronchi (Fig. 1B). No expression was noted in the mesenchyme that surrounded the developing airways (arrows in Fig. 1A, B). Similar results have been reported by Post *et al*. (18). Whole mount *in situ* hybridization has limited discrimination value in older tissue, and, therefore, we performed section *in situ* hybridization for lungs older than E13.5. However, we were unable to detect any Lfng mRNA in E15.5 and E18.5 lungs (Fig. 1C, E, respectively), suggesting low or absent Lfng expression at later stages of lung development.

Lfng expression in SPC-Lfng transgenic lungs

To establish a role for Lfng in lung development, we overexpressed full-length mouse Lfng cDNA in distal mouse lung epithelium using the human SP-C enhancer-promoter (SPC-Lfng) (28). With *in situ* hybridization, using an antisense DIG-labeled Lfng probe, we demonstrated strong Lfng mRNA expression in E15.5-E18.5 transgenic lungs in an identical fashion to the expression pattern of endogenous SP-C mRNA (Fig. 1D, F). No endogenous Lfng transcripts were detected in E15.5 and E18.5 wild-type lungs (Fig. 1C, E). Also, no expression was detected in SPC-Lfng lungs when a sense DIG-labeled Lfng probe was used (not shown). These results clearly demonstrate that Lfng is overexpressed in SPC-Lfng transgenic lungs compared to wild-type lungs. Overexpression of Lfng in distal lung epithelial cells caused no embryonic or postnatal lethality, neither were the transgenic mice in obvious respiratory distress. No differences were observed in body or lung weights between wild-type and SPC-Lfng transgenic littermates (not shown). Haematoxylin-eosin-stained sections revealed no obvious differences in gross morphology between SPC-Lfng and wild-type lungs at E15.5 or E18.5 (not shown).

Expression of Hes1 in wild-type and SPC-Lfng transgenic lungs

Hes1 plays a significant role in the Notch signaling pathway and is transcriptionally activated by Notch signaling (8, 29). Hes1 encodes a bHLH transcriptional repressor (30), capable of counteracting the activity of bHLH transcriptional activators (31, 32). Therefore, we first investigated the mRNA expression of Hes1 in the developing murine lung. Whole mount *in situ* hybridization showed that Hes1 was predominantly expressed in airway epithelium during early lung development (Fig. 2A, B, for E11.5 and E13.5 lungs, respectively). Some Hes1 expression was found in the mesenchyme of early embryonic lungs (arrows in Fig. 2A, B). Section *in situ* hybridization confirmed the expression pattern of Hes1 mRNA in early lung development, that is, enhanced expression in larger airways and marginal expression in surrounding mesenchyme (Fig. 2C, D, for E11.5 and E15.5,

respectively). Later in gestation, Hes1 mRNA expression was confined to the epithelial cells of smaller airways (Fig. 2E, E16.5 lungs) and terminal bronchioles (Fig. 2F, E17.5 lungs). A similar expression pattern of Hes1 in pulmonary non-neuroendocrine cells has been reported by Ito *et al.* (20). We then determined whether overexpression of Lf affected Hes1 expression. However, section *in situ* hybridization showed that Hes1 mRNA was expressed in a comparable fashion in the bronchiolar epithelium of E17.5 wild-type (Fig. 2G) and SPC-Lfng transgenic lungs (Fig. 2H).

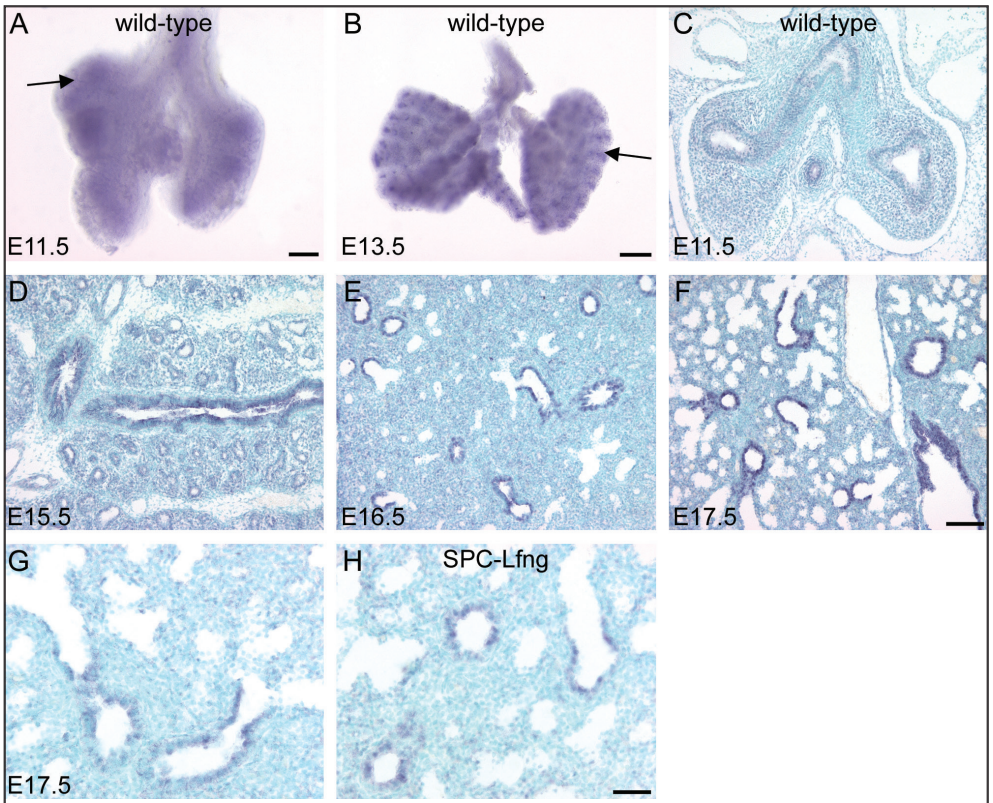

Figure 2. Hes1 mRNA expression in wild-type and SPC-Lfng lungs. Whole mount in situ hybridization showed that Hes1 mRNA was predominantly expressed in early (E11.5-E13.5) airway epithelium, whereas some Hes1 expression was detected in the mesenchymal compartment (arrows in A, B). Section in situ hybridization confirmed the expression pattern of Hes1 mRNA in early (E11.5-E15.5) lung development with enhanced expression in larger airways and weak expression in surrounding mesenchyme (C, D). At later gestation, Hes1 mRNA expression was confined to the epithelium of smaller airways (E) and terminal bronchioles (F). Using section in situ hybridization in E17.5 lungs, no difference in Hes1 mRNA expression between wild-type (G) and SPC-Lfng lungs (H) was found. Dark purple color is positive ISH staining. Sections (C-H) were counterstained with methyl green. Bar: 100 µm (A, C-F); 250 µm (B); 40 µm (G, H).

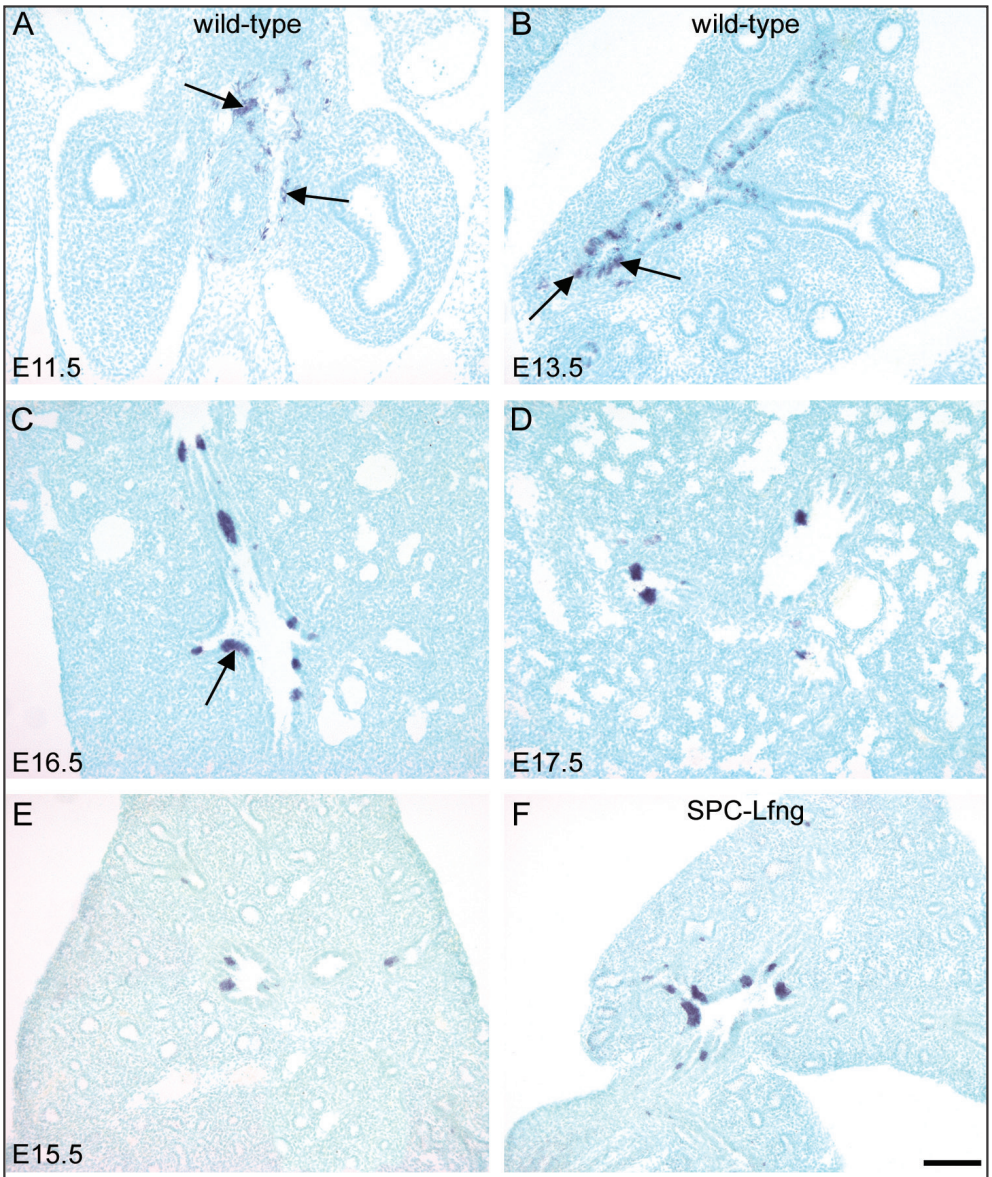

Figure 3. Mash-1 mRNA expression in wild-type and SPC-Lfng lungs using section in situ hybridization. Mash-1-positive cells were detected in the mesenchyme surrounding the trachea and esophagus of E11.5 wild-type lungs (arrows in A). This specific pattern of expression most likely represents the developing neural progenitors invading into the mesenchyme around the esophagus and trachea. Mash-1-positive cells within the lung were first seen at E13.5 (arrows in B). At this stage, Mash-1 was expressed in cell clusters or single cells among epithelial cells lining the larger airways. No Mash-1 expression was detected in the periphery of the lung. At E16.5 (C) and E17.5 (D), Mash-1-positive cell clusters were detected in larger airways, typically at branch-points (arrow in C), suggestive of pulmonary neuroendocrine cells (PNECs). At E15.5, SPC-Lfng transgenic lungs (F) had a comparable amount of Mash-1-positive clusters compared to wild-type lungs (E). Dark purple clusters are positive-staining PNECs. Sections were counterstained with methyl green. Bar: 100 µm (A-F).

Expression of Mash-1 in wild-type and SPC-Lfng transgenic lungs

The proneural gene Mash-1 is a bHLH factor that activates neural differentiation in the ectoderm. In E18.5 Hes1-deficient mice, Mash-1 is significantly upregulated, suggesting that Hes1 represses Mash-1 (20). We investigated Mash-1 mRNA expression in wild-type and SPC-Lfng transgenic lungs using section *in situ* hybridization. Mash-1-positive cells were detected in the mesenchyme surrounding the trachea and esophagus of E11.5 wild-type mice (arrows in Fig. 3A). This specific pattern of expression most likely represents the developing neural progenitors invading into the mesenchyme around the esophagus and trachea (33, 34). The cells are probably neural crest cells that in E11.5 mouse lungs, have been found on the trachea as well as in the vagus, and in processes extending from the vagus into the lung (34). Mash-1-positive staining within the lung was first seen at E13.5 (arrows in Fig. 3B). At this stage, Mash-1 mRNA was expressed in cell clusters or single cells among epithelial cells lining the larger airways. No Mash-1 expression was detected in the periphery of the lung (Fig. 3B). At E16.5 (Fig. 3C) and E17.5 (Fig. 3D), Mash-1-positive cell clusters were detected in larger airways, typically at branch-points (arrow in Fig. 3C), suggesting that they represent pulmonary neuroendocrine cells (PNECs) or pulmonary neuroendocrine bodies (NEBs). This proximal-distal wave of PNEC development is in agreement with previously published immunohistochemical studies (35-37). At E15.5, SPC-Lfng transgenic lungs had a similar number of Mash-1 mRNA-positive clusters compared to wild-type lungs (Fig. 3F *versus* 3E). Additional markers for PNECs were also normally expressed in SPC-Lfng transgenic lungs. Both cGRP (arrows in Fig. 4A, B) and Pgp9.5 protein (arrows in Fig. 4C, D) were expressed in PNECs of larger airways in wild-type (Fig. 4A, C) and SPC-Lfng transgenic lungs (Fig. 4B, D).

Quantitative RT-PCR for Lfng, Hes1, and Mash-1

In order to quantify Lfng overexpression in the SPC-Lfng transgenic lungs, we performed real-time RT-PCR. At E15.5, Lfng mRNA levels were significantly (>9-fold) increased in SPC-Lfng transgenic lungs compared to lungs of wild-type littermates (Fig. 5A). The increase in Lfng mRNA expression in the transgenic lungs was even more pronounced (>44-fold) at E16.5 (Fig. 5B). However, neither Hes1 nor Mash-1 mRNA expression was altered in SPC-Lfng lungs compared to wild-type lungs (Fig. 5C, D), a finding that is in agreement with our qualitative *in situ* hybridization results.

Epithelial differentiation in wild-type and SPC-Lfng transgenic lungs

To investigate whether overexpression of Lfng affected epithelial cell differentiation, we analyzed the expression of Ttf-1, SP-C, CC10, and T1α in wild-type and SPC-Lfng lungs. Ttf-1 is normally expressed in epithelial cells of the trachea and bronchial tubules and is required for lung formation (38, 39). Moreover, Ttf-1 regulates the expression of pulmonary genes like SP- and CC10 (40) and works synergistically with Gata-6 to influence the activity of the SP-C promoter (41). In E17.5 wild-type littermates, Ttf-1 protein was detected in bronchial epithelium and in epithelial cells lining the peripheral acinar tubules (Fig. 6A). In the lungs

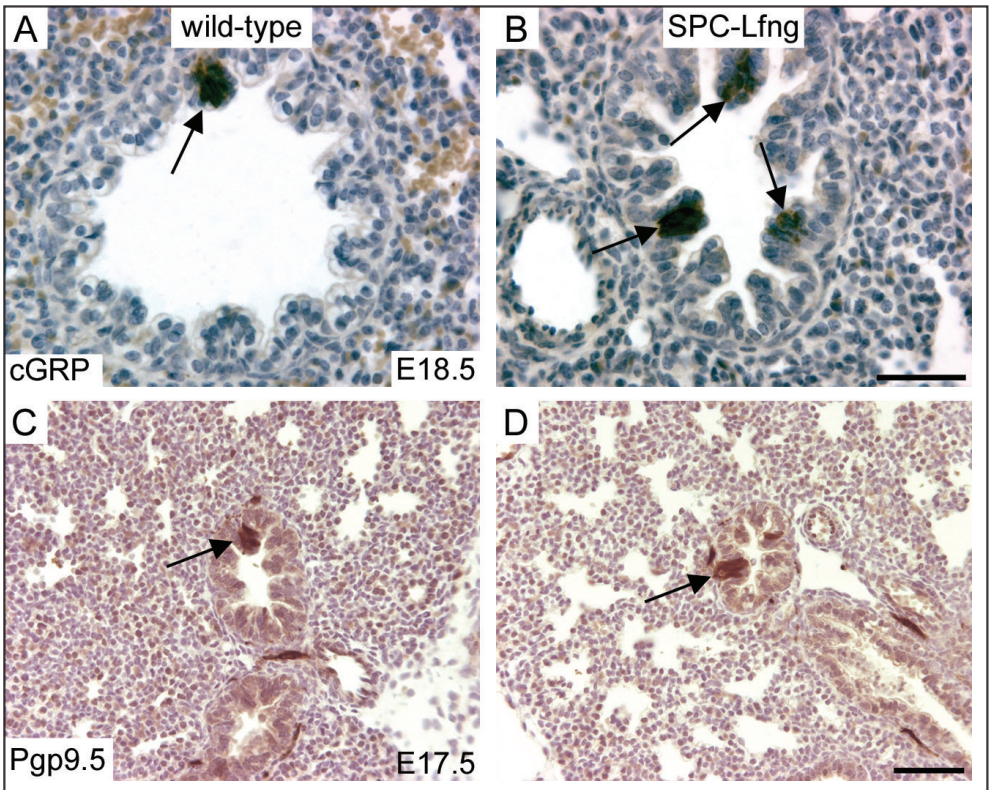

Figure 4. Immunohistochemical staining for cGRP (E18.5) and Pgp9.5 (E17.5) in wild-type (A, C) and SPC-Lfng transgenic (B, D) lungs. Both markers for pulmonary neuroendocrine cells (PNECs) were normally expressed in larger airways of SPC-Lfng transgenic lungs (B, D). Dark brown spots (arrows) are positive staining PNECs. Sections were counterstained with haematoxylin. Bar: 40 µm (A, B); 50 µm (C, D).

of SPC-Lfng transgenic mice, Ttf-1 immunoreactivity was found in a similar pattern (Fig. 6B). Likewise, section *in situ* hybridization for SP-C (Fig. 6C, D) and CC10 mRNA (Fig. 6E, F), respectively markers for distal (type II) and proximal (Clara) pulmonary epithelial cells, revealed an unchanged pattern of expression of both genes in E18.5 SPC-Lfng transgenic lungs. Also T1α protein, a marker for distal type I epithelial cells (42), was equally expressed in lungs of E17.5 wild-type and SPC-Lfng transgenic mice (Fig. 6G, H). Taken together, these results indicate that epithelial differentiation is not affected by an overexpression of Lfng in distal airway epithelial cells.

Expression of vWF and α-sma in wild-type and SPC-Lfng transgenic lungs

To explore whether the overexpression of Lfng would influence endothelial and smooth muscle cell development, we immunohistochemically analyzed the protein expression of Factor VIII related antigen (von Willebrand factor; vWF) and α-smooth muscle actin (α-sma). vWF is normally expressed in the endothelial cells of larger blood vessels within the lung. Immunostaining for vWF was not different between lungs of E17.5 SPC-Lfng transgenic

and wild-type littermates (Fig. 7B *versus* 7A). Another endothelial marker, Pecam-1 (CD-31), which marks the peripheral capillary complex of the lung, was also not changed in SPC-Lfng transgenic lungs (results not shown). Thus, vascular development appears not to be affected by overexpression of Lfng. α-sma, which is expressed in pulmonary smooth muscle cells, was also equally detected in the mesenchyme surrounding the bronchi, bronchiolar tubules, and larger vessels of E15.5 wild-type and SPC-Lfng lungs (Fig. 7C *versus* 7D). Together, these results indicate that endothelial and smooth muscle cell differentiation are not influenced by an excess of Lfng.

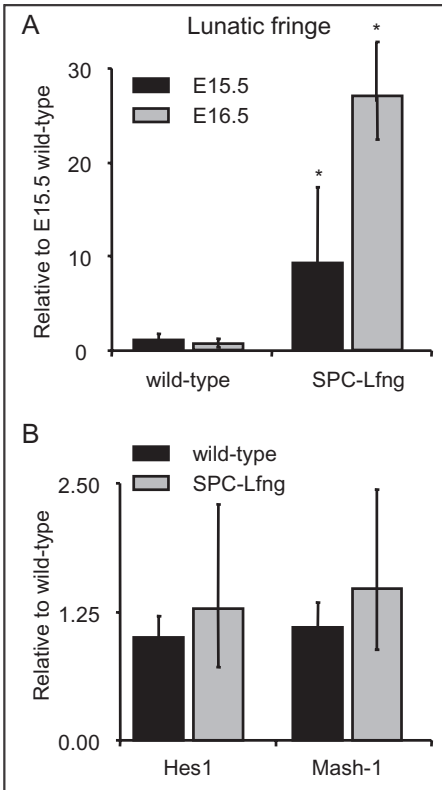

*Figure 5. Quantitative assessment of Lfng, Hes1, and Mash-1 mRNA expression in wild-type and SPC-Lfng transgenic lungs. Real-time RT-PCR showed dramatically increased Lfng expression in E15.5-E16.5 SPC-Lfng lungs (A). Hes1 and Mash-1 expression, both downstream components of the Notch signaling pathway, were unchanged in SPC-Lfng transgenic lungs (B). *P<0.05.*

Discussion

Fringe proteins, which modulate the Notch signaling pathway (11), have been shown to play a crucial role in defining borders in invertebrates and vertebrates. In flies, *fringe* is involved in the determination of the dorsal-ventral border of the *Drosophila* wing disc (43) and eye (44). In vertebrates, fringe genes play roles in the formation of the apical ectodermal ridge at the dorsal-ventral border in the limb bud (45), the boundary of the enamel knot (46), in midline precursor cell fate (47), and in the segmentation of the body plan (48, 49). Herein, we demonstrate that Lunatic fringe does likely not define epithelial morphogenic boundaries along the anterior-posterior axis of the airways in the mouse.

Overexpression of Lfng in distal lung epithelial cells did not influence the expression of downstream bHLH factors, such as Hes1 and Mash-1. Moreover, epithelial differentiation of distal and proximal airways as assessed by cell marker analysis was not altered by overexpression of Lfng.

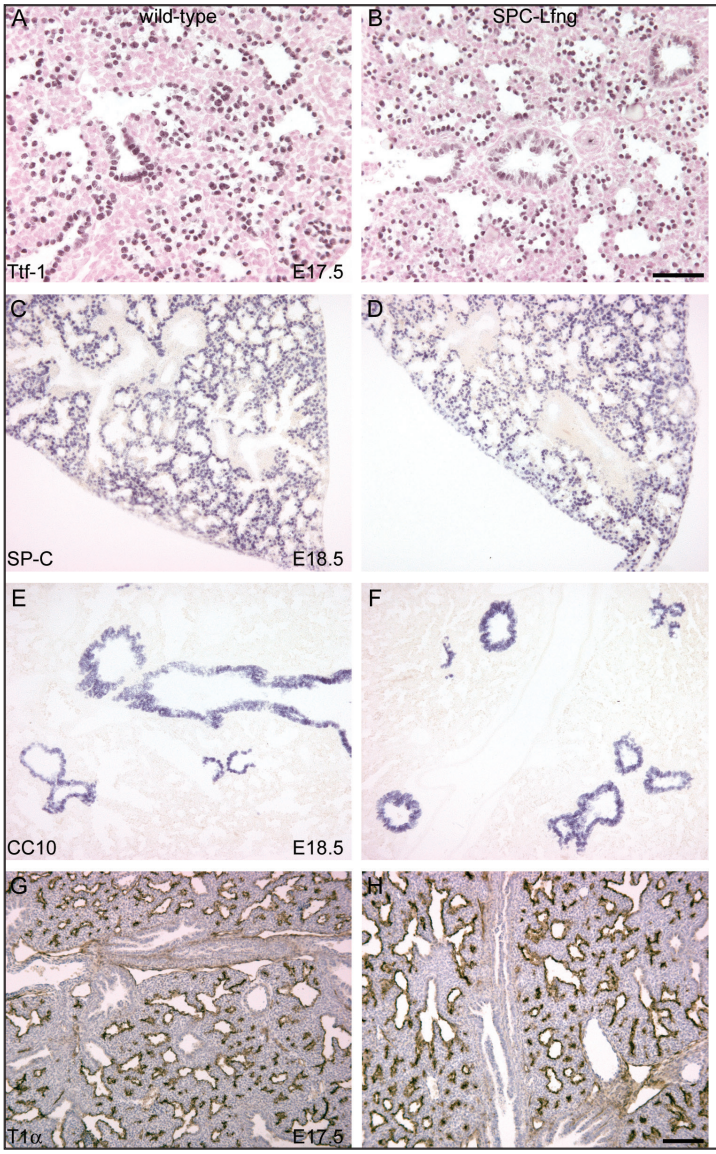

Figure 6. Immunohistochemical staining for Ttf-1 and T1α (E17.5) and in situ hybridization for SP-C and CC10 mRNA (E18.5) in wild-type and transgenic lungs. Expression of the distal type II cell markers Ttf-1 (A, B) and SP-C (C, D) were not different between SPC-Lfng (B, D) and wild-type (A, B) lungs. Similarly, expression of the distal type I cell marker T1α (G, H) and proximal epithelial marker CC10 (E, F) were unaltered in the SPC-Lfng transgenic lungs (H, F) compared to wild-type (G, E) lungs. Black (A, B), dark purple (C-F) and brown (G, H) staining are positive signals. Sections were counterstained with fast red (A, B) and haematoxylin (G, H). Bar: 50 µm (A, B); 100 µm (C-H).

Several Notch signaling components, including the Notch1, Notch2, and Notch3 receptors and their ligands, Jagged-1, Jagged-2, and Delta-1 (Dll1), were reported to be expressed in the developing murine lung (18, 19), suggesting a role for this conserved signaling pathway in lung development. In the early mouse lung, Notch1 and Dll1 are expressed within the distal respiratory epithelium (18), whereas Notch2 and Notch3 are expressed

throughout the mesenchyme (18) and Jagged-1 is found in undifferentiated distal epithelial and mesenchymal cells (19). Jagged-2 is present in epithelial and differentiated mesenchymal cells, but not in airway-associated smooth muscle cells (19). Moreover, Notch1 and Jagged-1 were also found on endothelial cells lining the lung vasculature (50). Antisense gene silencing experiments in murine lung explants have revealed functional diversity of Notch and Jagged family members during development with only partial redundancy (19). Also, overexpression of the activated domain of Notch3 throughout the peripheral lung epithelium caused abnormal tubular formation with diffuse metaplasia and perinatal death (51). Type I alveolar epithelial cells did not develop in these lungs (51). In agreement with previous findings (18) we found that Lfng is solely expressed in the epithelial cells lining the airways. Interestingly, Lfng mRNA expression was absent at the time of pulmonary epithelial cell diversification suggesting a potential role in this process. However, overexpression of Lfng in the developing lung did not influence proximal or distal epithelial cell differentiation.

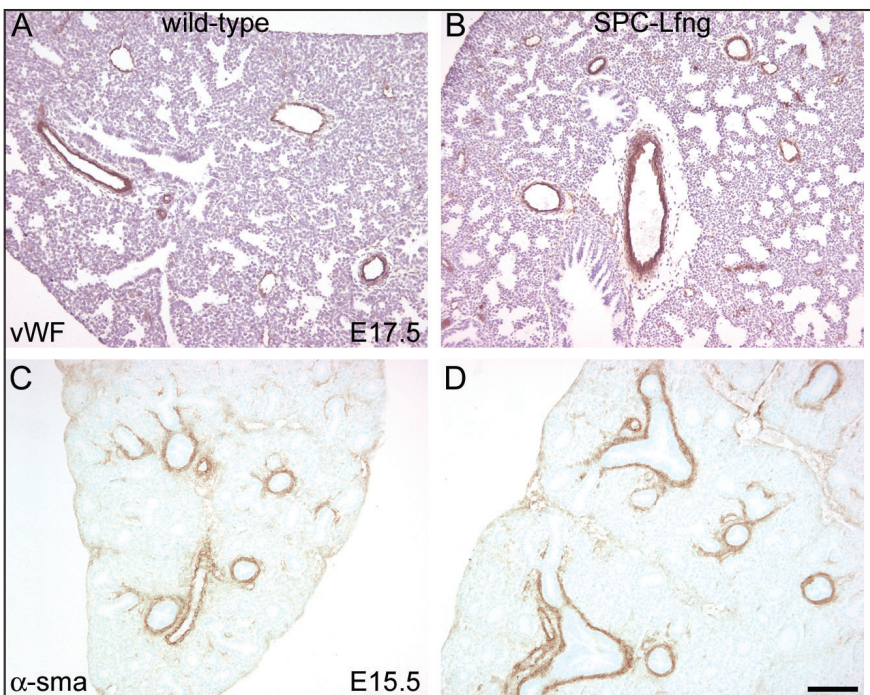

Figure 7. Immunohistochemical staining for Factor VIII related antigen (vWF) and α-sma in wild-type and SPC-Lfng lungs. At E17.5, vWF (A, B) was expressed in the endothelial cell layer of larger pulmonary blood vessels. At 15.5, α-sma (C, D) was detected in the smooth muscle cell layer surrounding larger blood vessels and airways. No differences for vWF or α-sma protein staining were detected between wild-type (A, C) and SPC-Lfng transgenic (B, D) lungs. Brown color is positive staining. Cells were counterstained with haematoxylin (A, B) and fast green (C, D). Bar: 100 µm.

Lfng has high homology to bacterial glycosyltransferases and acts in the Golgi (52). Lfng makes a complex with the Notch receptor before being secreted to the cell-surface, thereby potentiating Dll-induced Notch signaling, whereas inhibiting Jagged-induced Notch signaling (53, 54). Thus, Lfng needs to be present in the same cell as the Notch receptor to have an effect on Notch signaling. In the present study, the SP-C promoter directed Lfng expression towards distal lung endoderm, which is same tissue layer where Notch1 is expressed (18). Antisense inhibition experiments have implicated Notch1 in the regulation of pulmonary neuroendocrine differentiation (19) and, therefore, we speculated that Lfng excess in the same cell as Notch1 would modulate Notch signaling via the bHLH transcription factors Hes1 and Mash-1 (6). We observed that Hes1 mRNA was expressed in the early lung endoderm, but with advancing gestation its expression became restricted to epithelial cells lining terminal branches of bronchioles. This temporal-spatial expression pattern for Hes1 mRNA was not altered by the overexpression of Lfng, suggesting that Notch signaling was not affected. Hes5, another bHLH repressor regulated by Notch (55), is not present in the murine lung (20) and overexpression of Lfng did not trigger its expression (not shown). It was shown that Hes1 binds directly to the promoter of Mash-1, a bHLH transcriptional activator, and represses Mash-1 expression (32). In the lung, Mash-1 is expressed in neuroendocrine cells (20). Neuroendocrine cells are the first cells to differentiate morphologically before any other epithelial cell type within the pulmonary epithelium (36, 56). Mash-1 appeared to be specifically necessary for pulmonary neuroendocrine development, because Mash-1-deficient mice lacked pulmonary neuroendocrine cells, whereas neuroendocrine cells in other organs were unaffected (20, 57). In lungs of Hes1-deficient mice, Mash-1 is upregulated and the number of pulmonary neuroendocrine cells is markedly increased (20). In the present study, we found Mash-1 mRNA-positive cells localized in isolated clusters in larger airways, typically at branch-points, suggestive of pulmonary neuroendocrine cells. Overexpression of Lfng did not affect the temporal-spatial expression of Mash-1 mRNA, a finding which is in agreement with the observation that Hes1 is not altered by Lfng excess. In addition, protein expression of pulmonary neuroendocrine markers such as Pgp9.5 and cGRP, was undisturbed by Lfng overexpression.

In Hes1-deficient mice, the number of proximal epithelial Clara cells appears to be reduced (20). In line with the finding that Hes1 expression was not affected by Lfng overexpression, we observed that the temporal-spatial expression pattern of CC10 mRNA, a Clara cell marker, was not altered by Lfng overexpression. In addition, marker analyses for distal epithelial and mesenchymal cells revealed no change in their phenotypic expression in SPC-Lfng lungs.

The lack of any response to Lfng excess was not due to limited overexpression because we found that Lfng mRNA expression was upregulated 10-40 fold in E15-16 SPC-Lfng lungs. Radical fringe (Rfng) has been shown to be expressed in the lung endoderm (18)

and it is possible that it is Rfng that mediates the interaction with Notch1 during lung development. However, we are not aware of any functional diversity between the fringe proteins.

In conclusion, Notch signaling regulates cell fate in many branched organs (58, 59) including the developing lung (19, 20), but in contrast to fringe in other developmental systems (11), Lfng does not play a crucial role in setting epithelial cell boundaries along the anterior-posterior axis of the murine airways.

Acknowledgments

This work was supported by the David Vervat foundation, The Netherlands (M.v.T.) and the Canadian Institutes of Health Research (CIHR FRN-15273, M.P.). We thank Wahyuni Otmodo for technical assistance with tissue preparation and immunohistochemistry, Pooja Agarwal for assistance with whole mount *in situ* hybridization, and Angie Griffin for animal care and handling. Martin Post is holder of a Canadian Research Chair (tier 1) in Fetal, Neonatal, and Maternal Health.

References

1. Spooner BS, Wessells NK, 1970. Mammalian lung development: interactions in primordium formation and bronchial morphogenesis. J Exp Zool. 175:445-454.

2. Masters JR, 1976. Epithelial-mesenchymal interaction during lung development: the effect of mesenchymal mass. Dev Biol. 51:98-108.

3. Shannon JM, Nielsen LD, Gebb SA, Randell SH, 1998. Mesenchyme specifies epithelial differentiation in reciprocal recombinants of embryonic lung and trachea. Dev Dyn. 212:482-494.

4. van Tuyl M, Post M: Molecular mechanisms of lung development and lung branching morphogenesis. In Polin RA, Fox WW, Abman SH (eds): Fetal and Neonatal Physiology, 3rd edition 3rd edition, vol 1, p 812-821. Philadelphia, Saunders, Harcourt Health Sciences, 2003.

5. Warburton D, Bellusci S, Del Moral PM, Kaartinen V, Lee M, Tefft D, Shi W, 2003. Growth factor signaling in lung morphogenetic centers: automaticity, stereotypy and symmetry. Respir Res. 4:5.

6. Artavanis-Tsakonas S, Rand MD, Lake RJ, 1999. Notch signaling: cell fate control and signal integration in development. Science. 284:770-776.

7. Mumm JS, Kopan R, 2000. Notch signaling: from the outside in. Dev Biol. 228:151-165.

8. Jarriault S, Le Bail O, Hirsinger E, Pourquie O, Logeat F, Strong CF, Brou C, Seidah NG, Isra l A, 1998. Delta-1 activation of notch-1 signaling results in HES-1 transactivation. Mol Cell Biol. 18:7423-7431.

9. Irvine KD, Wieschaus E, 1994. fringe, a Boundary-specific signaling molecule, mediates interactions between dorsal and ventral cells during Drosophila wing development. Cell. 79:595-606.

10. Panin VM, Papayannopoulos V, Wilson R, Irvine KD, 1997. Fringe modulates Notch-ligand interactions. Nature. 387:908-912.

11. Wu JY, Rao Y, 1999. Fringe: defining borders by regulating the notch pathway. Curr Opin Neurobiol. 9:537-543.

12. Cohen B, Bashirullah A, Dagnino L, Campbell C, Fisher WW, Leow CC, Whiting E, Ryan D, Zinyk D, Boulianne G, Hui CC, Gallie B, Phillips RA, Lipshitz HD, Egan SE, 1997. Fringe boundaries coincide with Notch-dependent patterning centres in mammals and alter Notch-dependent development in Drosophila. Nat Genet. 16:283-288.

13. Johnston SH, Rauskolb C, Wilson R, Prabhakaran B, Irvine KD, Vogt TF, 1997. A family of mammalian Fringe

genes implicated in boundary determination and the Notch pathway. Development. 124:2245-2254.

14. Laufer E, Dahn R, Orozco OE, Yeo CY, Pisenti J, Henrique D, Abbott UK, Fallon JF, Tabin C, 1997. Expression of Radical fringe in limb-bud ectoderm regulates apical ectodermal ridge formation. Nature. 386:366-373.

15. Mitsiadis TA, Lardelli M, Lendahl U, Thesleff I, 1995. Expression of Notch 1, 2 and 3 is regulated by epithelial-mesenchymal interactions and retinoic acid in the developing mouse tooth and associated with determination of ameloblast cell fate. J Cell Biol. 130:407-418.

16. McCright B, 2003. Notch signaling in kidney development. Curr Opin Nephrol Hypertens. 12:5-10.

17. Llimargas M, 1999. The Notch pathway helps to pattern the tips of the Drosophila tracheal branches by selecting cell fates. Development. 126:2355-2364.

18. Post LC, Ternet M, Hogan BL, 2000. Notch/Delta expression in the developing mouse lung. Mech Dev. 98:95-98.

19. Kong Y, Glickman J, Subramaniam M, Shahsafaei A, Allamneni KP, Aster JC, Sklar J, Sunday ME, 2004. Functional diversity of notch family genes in fetal lung development. Am J Physiol Lung Cell Mol Physiol. 286:L1075-1083.

20. Ito T, Udaka N, Yazawa T, Okudela K, Hayashi H, Sudo T, Guillemot F, Kageyama R, Kitamura H, 2000. Basic helix-loop-helix transcription factors regulate the neuroendocrine differentiation of fetal mouse pulmonary epithelium. Development. 127:3913-3921.

21. Moloney DJ, Panin VM, Johnston SH, Chen J, Shao L, Wilson R, Wang Y, Stanley P, Irvine KD, Haltiwanger RS, Vogt TF, 2000. Fringe is a glycosyltransferase that modifies Notch. Nature. 406:369-375.

22. Korfhagen TR, Glasser SW, Wert SE, Bruno MD, Daugherty CC, McNeish JD, Stock JL, Potter SS, Whitsett JA, 1990. Cis-acting sequences from a human surfactant protein gene confer pulmonary-specific gene expression in transgenic mice. Proc Natl Acad Sci U S A. 87:6122-6126.

23. Hogan BL, Bedington RCF, Lacy E: Manipulating the mouse embryo: A laboratory manual. Manipulating the mouse embryo: A laboratory manual, 2nd Series. 1994, New York: Cold Spring Harbor Laboratory Press.

24. Riddle RD, Johnson RL, Laufer E, Tabin C, 1993. Sonic hedgehog mediates the polarizing activity of the ZPA. Cell. 75:1401-1416.

25. Moorman AF, Houweling AC, de Boer PA, Christoffels VM, 2001. Sensitive nonradioactive detection of mRNA in tissue sections: novel application of the whole-mount in situ hybridization protocol. J Histochem Cytochem. 49:1-8.

26. Hsu SM, Raine L, Fanger H, 1981. Use of avidin-biotin-peroxidase complex (ABC) in immunoperoxidase techniques: a comparison between ABC and unlabeled antibody (PAP) procedures. J Histochem Cytochem. 29:577-580.

27. Livak KJ, Schmittgen TD, 2001. Analysis of relative gene expression data using real-time quantitative PCR and the 2(-Delta Delta C(T)) Method. Methods. 25:402-408.

28. Wert SE, Glasser SW, Korfhagen TR, Whitsett JA, 1993. Transcriptional elements from the human SP-C gene direct expression in the primordial respiratory epithelium of transgenic mice. Dev Biol. 156:426-443.

29. Jarriault S, Brou C, Logeat F, Schroeter EH, Kopan R, Israel A, 1995. Signalling downstream of activated mammalian Notch. Nature. 377:355-358.

30. Sasai Y, Kageyama R, Tagawa Y, Shigemoto R, Nakanishi S, 1992. Two mammalian helix-loop-helix factors

structurally related to Drosophila hairy and Enhancer of split. Genes Dev. 6:2620-2634.

31. Oellers N, Dehio M, Knust E, 1994. bHLH proteins encoded by the Enhancer of split complex of Drosophila negatively interfere with transcriptional activation mediated by proneural genes. Mol Gen Genet. 244:465-473.

32. Chen H, Thiagalingam A, Chopra H, Borges MW, Feder JN, Nelkin BD, Baylin SB, Ball DW, 1997. Conservation of the Drosophila lateral inhibition pathway in human lung cancer: a hairy-related protein (HES-1) directly represses achaete- scute homolog-1 expression. Proc Natl Acad Sci U S A. 94:5355-5360.

33. Guillemot F, Lo LC, Johnson JE, Auerbach A, Anderson DJ, Joyner AL, 1993. Mammalian achaete-scute homolog 1 is required for the early development of olfactory and autonomic neurons. Cell. 75:463-476.

34. Tollet J, Everett AW, Sparrow MP, 2001. Spatial and temporal distribution of nerves, ganglia, and smooth muscle during the early pseudoglandular stage of fetal mouse lung development. Dev Dyn. 221:48-60.

35. Sorokin SP, Hoyt RF, Jr., Shaffer MJ, 1997. Ontogeny of neuroepithelial bodies: correlations with mitogenesis and innervation. Microsc Res Tech. 37:43-61.

36. Cutz E, 1982. Neuroendocrine cells of the lung. An overview of morphologic characteristics and development. Exp Lung Res. 3:185-208.

37. Ito T, 1999. Differentiation and proliferation of pulmonary neuroendocrine cells. Prog Histochem Cytochem. 34:247-322.

38. Minoo P, Su G, Drum H, Bringas P, Kimura S, 1999. Defects in tracheoesophageal and lung morphogenesis in Nkx2.1(-/-) mouse embryos. Dev Biol. 209:60-71.

39. Yuan B, Li C, Kimura S, Engelhardt RT, Smith BR, Minoo P, 2000. Inhibition of distal lung morphogenesis in Nkx2.1(-/-) embryos. Dev Dyn. 217:180-190.

40. Whitsett JA, Glasser SW, 1998. Regulation of surfactant protein gene transcription. Biochim Biophys Acta. 1408:303-311.

41. Liu C, Morrisey EE, Whitsett JA, 2002. GATA-6 is required for maturation of the lung in late gestation. Am J Physiol Lung Cell Mol Physiol. 283:L468-475.

42. Ramirez MI, Millien G, Hinds A, Cao Y, Seldin DC, Williams MC, 2003. T1alpha, a lung type I cell differentiation gene, is required for normal lung cell proliferation and alveolus formation at birth. Dev Biol. 256:61-72.

43. Kim J, Irvine KD, Carroll SB, 1995. Cell recognition, signal induction, and symmetrical gene activation at the dorsal-ventral boundary of the developing Drosophila wing. Cell. 82:795-802.

44. Papayannopoulos V, Tomlinson A, Panin VM, Rauskolb C, Irvine KD, 1998. Dorsal-ventral signaling in the Drosophila eye. Science. 281:2031-2034.

45. Rodriguez-Esteban C, Schwabe JW, De La Pena J, Foys B, Eshelman B, Belmonte JC, 1997. Radical fringe positions the apical ectodermal ridge at the dorsoventral boundary of the vertebrate limb. Nature. 386:360-366.

46. Mustonen T, Tummers M, Mikami T, Itoh N, Zhang N, Gridley T, Thesleff I, 2002. Lunatic fringe, FGF, and BMP regulate the Notch pathway during epithelial morphogenesis of teeth. Dev Biol. 248:281-293.

47. Appel B, Marasco P, McClung LE, Latimer AJ, 2003. lunatic fringe regulates Delta-Notch induction of hypochord in zebrafish. Dev Dyn. 228:281-286.

48. Evrard YA, Lun Y, Aulehla A, Gan L, Johnson RL, 1998. lunatic fringe is an essential mediator of somite

segmentation and patterning. Nature. 394:377-381.

49. Prince VE, Holley SA, Bally-Cuif L, Prabhakaran B, Oates AC, Ho RK, Vogt TF, 2001. Zebrafish lunatic fringe demarcates segmental boundaries. Mech Dev. 105:175-180.

50. Taichman DB, Loomes KM, Schachtner SK, Guttentag S, Vu C, Williams P, Oakey RJ, Baldwin HS, 2002. Notch1 and Jagged1 expression by the developing pulmonary vasculature. Dev Dyn. 225:166-175.

51. Dang TP, Eichenberger S, Gonzalez A, Olson S, Carbone DP, 2003. Constitutive activation of Notch3 inhibits terminal epithelial differentiation in lungs of transgenic mice. Oncogene. 22:1988-1997.

52. Brückner K, Perez L, Clausen H, Cohen S, 2000. Glycosyltransferase activity of Fringe modulates Notch-Delta interactions. Nature. 406:411-415.

53. Ju BG, Jeong S, Bae E, Hyun S, Carroll SB, Yim J, Kim J, 2000. Fringe forms a complex with Notch. Nature. 405:191-195.

54. Hicks C, Johnston SH, diSibio G, Collazo A, Vogt TF, Weinmaster G, 2000. Fringe differentially modulates Jagged1 and Delta1 signalling through Notch1 and Notch2. Nat Cell Biol. 2:515-520.

55. de la Pompa JL, Wakeham A, Correia KM, Samper E, Brown S, Aguilera RJ, Nakano T, Honjo T, Mak TW, Rossant J, Conlon RA, 1997. Conservation of the Notch signalling pathway in mammalian neurogenesis. Development. 124:1139-1148.

56. Wuenschell CW, Sunday ME, Singh G, Minoo P, Slavkin HC, Warburton D, 1996. Embryonic mouse lung epithelial progenitor cells co-express immunohistochemical markers of diverse mature cell lineages. J Histochem Cytochem. 44:113-123.

57. Borges M, Linnoila RI, van de Velde HJ, Chen H, Nelkin BD, Mabry M, Baylin SB, Ball DW, 1997. An achaete-scute homologue essential for neuroendocrine differentiation in the lung. Nature. 386:852-855.

58. McLaughlin KA, Rones MS, Mercola M, 2000. Notch regulates cell fate in the developing pronephros. Dev Biol. 227:567-580.

59. Apelqvist A, Li H, Sommer L, Beatus P, Anderson DJ, Honjo T, Hrabe de Angelis M, Lendahl U, Edlund H, 1999. Notch signalling controls pancreatic cell differentiation. Nature. 400:877-881.

Chapter 7

Pulmonary surfactant protein-A, -B, and -C mRNA and protein expression in the nitrofen-induced congenital diaphragmatic hernia rat model

Minke van Tuyl[1,2], Pietjan E. Blommaart[1,2], Richard Keijzer[1], Susan E. Wert[3], Jan M. Ruijter[2], Wouter H. Lamers[2], and Dick Tibboel[1]

[1]Department of Pediatric Surgery, Sophia Children's Hospital, Erasmus University Medical Center Rotterdam, Rotterdam, The Netherlands
[2]Department of Anatomy and Embryology, Academic Medical Center, University of Amsterdam, Amsterdam, The Netherlands
[3]Divisions of Pulmonary Biology and Neonatology, Children's Hospital Medical Center, Cincinnati, OH 45229, U.S.A.

Pediatric Research 2003; 54:641-652

Abstract

Neonates with congenital diaphragmatic hernia (CDH) suffer from a diaphragmatic defect, lung hypoplasia, and pulmonary hypertension, with poor lung function forming the major clinical challenge. Despite prenatal diagnosis and advanced postnatal treatment strategies, the mortality rate of CDH is still high. CDH has been subject of extensive research over the past decades, but its etiology remains unknown. A major problem with CDH is the failure to predict the individual response to treatment modalities like high frequency ventilation, inhaled nitric oxide, and extracorporeal membrane oxygenation (ECMO). In this study, we tested the possibility that CDH lungs are surfactant protein deficient, which could explain the respiratory failure and difficulties in treating CDH infants. We investigated this hypothesis in the nitrofen-induced CDH rat model and assessed the cellular concentrations of surfactant protein (SP)-A, -B, and -C mRNA with a quantitative radioactive *in situ* hybridization technique. No differences were observed between control and CDH lungs for SP mRNA expression patterns. The cellular concentration (mean OD) of SP-A and SP-B mRNA was similar at all stages whereas the mean OD of SP-C mRNA and the volume fraction of cells (% Area) expressing SP mRNA was higher in CDH lungs at term. Immunohistochemical analysis revealed no differences between control and CDH lungs for SP protein expression. No differences in the mean OD or % Area for the SP mRNAs were found between the ipsi- and contralateral side of CDH lungs. We conclude that there is no primary deficiency of surfactant proteins in the nitrofen-induced CDH rat model.

Introduction

CDH is an anomaly occurring 1 in 3000 live births (1). It is characterized by a diaphragmatic defect, severe lung hypoplasia, and pulmonary hypertension, and in 40% of the patients other severe birth defects such as cardiac abnormalities are present (2, 3). Despite years of extensive research, the etiology of CDH remains unknown (4). Clinically, pulmonary hypoplasia and pulmonary hypertension form the major problems in CDH (5).

Many CDH studies have focused on treatment modalities such as conventional ventilation with gentle handling of the fragile lung, high frequency ventilation, ECMO, *in utero* tracheal ligation with or without betamethasone injection, inhaled nitric oxide, and prenatal injections of betamethasone, thyrotropin-releasing hormone or a combination of both hormones. Although selected centers have reported improved survival (6, 7), the overall mortality rate, however, is still variably high, so that CDH continues to be a serious problem in the neonatal and pediatric surgical intensive care unit, with optimal treatment for CDH still the subject of ongoing debate (5, 8-10).

It is unknown why CDH infants can be so refractory to treatment, which makes it even more difficult to predict the outcome in the individual patient. Lungs from premature infants suffering from respiratory distress syndrome (RDS) are surfactant-deficient and major breakthroughs in the treatment of these infants were prenatal corticosteroid injections and the postnatal administration of exogenous surfactant (11-14). Surfactant is essential for proper lung function. It decreases the surface tension in the lung, thereby protecting alveoli against collapse at end-expiration (15). We realize that it is not justified to directly compare CDH lungs to RDS lungs, but the possibility that CDH lungs are surfactant-deficient is still not ruled out or proven. In human autopsy material of pulmonary hypoplasia including CDH, normal levels of SP-A, -B, and -C protein were reported (16). Also, normal levels of phospholipids and normal lecithin/sphingomyelin (L/S) ratios (used as indicator of fetal lung maturity) in amniotic and bronchoalveolar lavage (BAL) fluid have been reported (17, 18). Nevertheless, other studies have found decreased amounts of SP-A in human CDH (19, 20). It has to be kept in mind that a secondary surfactant deficiency may develop due to the negative effects of artificial ventilation on surfactant function after birth (21). So far, data from human and different animal CDH models (22) failed to report consistent results concerning the surfactant status in CDH (summarized in Table 1) (17-20, 23-39).

The most common method to determine the amount of RNA in tissue is Northern blot analysis. This method, however, requires tissue homogenization, with the result that all cellular relations are lost. Jonker and co-workers (40) have developed a method to quantify the signal obtained with the *in situ* hybridization procedure. This quantitative *in situ* hybridization technique allows the detection of the concentration of mRNA at the cellular level within the architecture of the tissue.

In this study we have used this technique to accurately assess the cellular concentration of SP-A, -B, and -C mRNA in the nitrofen-induced CDH rat model (41). We observed no differences in the expression patterns or cellular concentration of the SP mRNAs between control and CDH embryonic rat lungs, except for the level of SP-C mRNA, which was higher in CDH than in control lungs near term (gestational day [E]22). No differences between control and CDH lungs were found upon immunohistochemical visualization of the respective surfactant proteins. At term, the volume fraction of SP mRNA-expressing cells was higher in CDH lungs than in controls. Furthermore, no differences in the expression pattern, concentration of SP mRNA per cell or the volume fraction of SP mRNA-expressing cells was found between the ipsilateral (hernia) and contralateral (no hernia) side of a CDH lung. These results demonstrate that the embryonic rat with nitrofen-induced CDH is not deficient for pulmonary SP-A, -B, or -C.

Table 1: Surfactant in congenital diaphragmatic hernia*

		BAL	AF	Biochemicalprotein assay Immunohistochemistry	RNA assay/RT-PCR *In situ* hybridization
L/S	↑				
	=	[18]	[17, 26]		
	↓				
	↑			[37 (E18)]	
%PC	=	[18, 25]		[27 (E19); 38 (E21)]	
	↓	[23, 26, 28, 36]	[19]	[24, 27 (E21); 37 (E20)]	
	↑				
%PG	=	[18, 23, 25, 28]	[17, 26]		
	↓				
	↑				
SP-A	=	[25, 36]		[29 (E19-20); 30, 36]	[29 (E21); 35]
	↓	[28]	[19]	[20, 29 (E21-22); 32, 33 (E21); 37 (E20)]	[29 (E20); 30, 32-34, 38 (E21)]
	↑				
SP-B	=	[36]			[35 (E19); 38 (E21)]
	↓	[28]		[32, 33 (E21); 36]	[31-32, 33-35 (E21)]
	↑				
SP-C	=			[30]	[30, 34 (E21); 35 (E19)]
	↓				[32, 35, 38 (E21)]

**Overview of surfactant protein expression in human or experimental CDH. Numbers between square brackets indicate citations as listed in the references section. In CDH, lecithin/sphingomyelin (L/S) ratios and phosphatidylglycerol as percentage of total phospholipids measured (%PG) were always found to be similar to control values. Phosphatidylcholine as percentage of total phospholipids (%PC) and SP-A and SP-B protein and mRNA levels were mostly normal in CDH during early gestation, whereas both normal and decreased levels were reported for late gestation. SP-C protein and mRNA levels in CDH were reported unchanged in most studies. ↑, increased; ↓, decreased; =, no difference; E, em-*

bryonic day; BAL, bronchoalveolar lavage; AF, amniotic fluid; RT-PCR, reverse-transcriptase polymerase chain reaction; Species: human, references (17-20); lamb (surgical-created CDH), references (23, 26, 28, 32, 36); rat (nitrofen-induced CDH), references (24, 25, 27, 29, 31, 33-35, 37, 38); mouse (nitrofen-induced CDH), reference (30).

Methods

Animals

Adult Wistar rats were purchased from the Broekman Institute B.V. in Someren (The Netherlands). Rats were mated at the end of the morning (E0). To induce CDH and lung hypoplasia, 100 mg of 2,4-dichloro-phenyl-*p*-nitrophenyl ether (nitrofen) dissolved in 1 ml olive oil was administered orally on E10 (term = E23) (38, 41, 42). To determine the surfactant status of lungs from embryonic rats with nitrofen-induced CDH, we examined the expression patterns of SP-A, -B, and -C mRNA and protein in control and CDH fetuses of E15, 18, 20, and 22. In rat, E15 corresponds to the mid-pseudoglandular stage of lung development, E18 to late pseudoglandular, E20 to late canalicular, and E22 to the saccular stage of lung development. Animal experiments were performed in accordance with the guidelines of the animal research committee of the Academic Medical Center of the University of Amsterdam.

Tissue preparation

At E15-E22, pregnant females were sacrificed and the embryos were dissected from the uterus. Embryonic thoraxes were fixed in 4% phosphate-buffered formaldehyde (w/v) (4°C, 16-18 hours), dehydrated in a graded series of ethanol solutions, cleared with 1-butanol, and embedded in Paraplast Plus (Monoject, Kildare, Ireland). Seven micrometer frontal sections were cut and mounted onto RNAse-free 3-aminopropyltriethoxysilane (Sigma Chemical Co., St. Louis, MO, U.S.A.) -coated slides. From each embryo, the entire thorax was embedded and cut, and only embryos that had a visible diaphragmatic hernia and lung hypoplasia were used for the study.

In situ hybridization

Plasmids containing mouse SP-A and SP-C (both in pGEM3Z) and SP-B (in pBS-SKII) cDNA were obtained from Dr. J. A. Whitsett (Division of Pulmonary Biology, Children's Hospital Medical Center, Cincinnati, OH, U.S.A.) (43-45). [α-^{35}S]dCTP-labeled antisense probes for SP-A, -B, and -C were generated with T7 polymerase, after linearization of the plasmids with *Apa*LI, *Eco*RI, and *Hin*dIII, respectively. The hybridization conditions were as described elsewhere (46). Exposure time to nuclear autoradiographic emulsion (Ilford Nuclear Research Emulsion G-5; Ilford, Cheshire, UK) was 14 days for SP-A and 7 days for SP-B and -C. The development time was 4 min. After developing, the sections were dehydrated in a graded series of ethanol and xylol, and mounted in Malinol (Chroma-Gesellshaft, Schmidt Gmbh+Co, Köngen, Germany).

Image acquisition and analysis

For image acquisition, a Photometrics cooled-CCD camera (Tucson, AZ, U.S.A.; 12-bit dynamic range; 1317x1035 pixels), attached to an Axioplan microscope (Carl Zeiss, Oberkochen, Germany) equipped with a 5x objective (N.A.: 0.15), a stabilized power supply and an infrared-blocking filter was used. The low-power objective was used to assure the sampling of several respiratory acini in an image, representing 2.5 mm^2 of the lung section. Digital images from the *in situ* hybridization procedure were recorded using white light (40). The digital transmission images were converted to optical density (OD) images by calculating the negative logarithm of the transmission image divided by an image of the light source ($OD = -^{10}\log(I/I_0)$ for each pixel). This conversion implicitly corrects background shading.

The OD images were analyzed using the public domain image analysis program from the National Institutes of Health-*Image* (available at rsb.info.nih.gov/nih-image; version 1.61). The areas to be measured were marked by an interactive density slice, which identifies structures based on a selected lower and upper density value. Tissue background was defined as non-staining tissue such as esophagus or cartilage tissue. Signal was defined as specific positive staining due to hybridization (signal in the bronchiolar and alveolar epithelium) (40, 46). The definitive signal value, expressed as mean OD, is obtained by subtracting the mean tissue background density from the mean signal density (40, 46). The positive signal is plotted as mean OD (± SEM) per group and age. The volume fraction of SP mRNA-expressing cells (% Area) was calculated from the area of positive staining cells in the section and the total lung area (excluding airspaces). All lung measurements were carried out three times with a randomized series of images. No differences were observed between the three measurements and, therefore, a mean value per lung was calculated.

Immunohistochemistry

All antibodies were obtained from Dr. J.A. Whitsett (Division of Pulmonary Biology, Children's Hospital Medical Center, Cincinnati, OH, U.S.A.). A guinea pig polyclonal antibody against rat SP-A, a rabbit polyclonal antibody against mature bovine SP-B (R28031), and a rabbit polyclonal antibody against human proSP-C (R68514) were applied at a dilution of 1:300, 1:2000, and 1:5000, respectively, to 7 µm deparaffinized sections (47, 48). For SP-A a Vectastain ABC Peroxidase kit and for SP-B and proSP-C a Vector Elite ABC-DAB kit (Vector Laboratories, Burlingame, CA, U.S.A.) were used to detect antigen-antibody complexes (48). The enzymatic reaction product was enhanced with nickel/cobalt to produce a black precipitate. Sections were counterstained with nuclear fast red. For each different protein, slides were handled in similar ways concerning the concentration of the antibody and the times for incubation and detection. Analysis of the pattern and intensity of protein staining was done blindly by two persons.

Statistical analysis

Variation in staining intensity due to the different *in situ* hybridization sessions were removed by subtracting the session effects calculated from the log-transformed data with the general linear model ANOVA without interaction (SPSS version 10.0.7; SPSS Inc., Chicago, IL, U.S.A.). Differences between groups (control *versus* CDH) and age (two animals per group per age for E15, E18, E20, and E22 (control) and three animals per group for E22 (CDH)) and between ipsilateral (hernia) and contralateral (no hernia) lung and age were tested with a two-way ANOVA.

Results

In situ hybridization

SP-A and -B mRNA are normally expressed in both bronchiolar and alveolar epithelial cells, whereas SP-C mRNA is only expressed in alveolar epithelial cells. The patterns of mRNA expression for SP-A, -B, and -C did not differ between control (Figs. 1-3, panels A, C, E) and CDH (Figs. 1-3, panels B, D, F) lungs at the gestational ages analyzed (Figs. 1-3). SP-A and -B mRNA expression started at a very low level at E15 (not shown). SP-A mRNA was expressed in alveolar epithelial cells and from E20 onwards also at low level in bronchiolar epithelial cells (Figs. 1-3, panels A, B). SP-B mRNA was expressed in alveolar epithelial cells and from E20 onwards as well at high level in bronchiolar epithelial cells (Figs. 1-3, panels C, D). At E15, SP-C mRNA was already expressed at a high level in pulmonary epithelial cells (not shown). At later stages, SP-C mRNA was expressed only in alveolar (distal) epithelial cells (Figs. 1-3, panels E, F). No differences in the expression patterns of the respective SP mRNAs were observed between the ipsilateral and the contralateral side of CDH lungs (not shown). Figure 3 also revealed that at E22 the morphology of the CDH lungs differed substantially from the control lungs. Although pictures were taken at the same magnification, CDH lungs (Fig. 3B, D, F) were smaller than control lungs (Fig. 3A, C, E) and contained only a few visible airspaces, in contrast to the control lungs where airspaces were abundant at this gestational age. Note also that the airspaces in CDH lungs (Fig. 3B, D, F) are poorly expanded.

Quantification of the *in situ* hybridization results

The cellular concentration (mean OD) of SP-A, -B, and -C mRNA in control and CDH lungs increased with advancing gestational age (Fig. 4). All SP mRNAs increased in cellular concentration (Fig. 4A, C, E), whereas the volume fraction of cells (% Area) expressing the respective mRNAs also increased (Fig. 4B, D, F). Nevertheless, the behavior of the SP mRNAs differed slightly from each other. SP-C mRNA levels increased early (Fig. 4E) and before SP-A and SP-B mRNA levels (Fig. 4A, C). The mean OD of SP-A and SP-B mRNA was similar between control and CDH lungs at all ages (Fig. 4A, C). The mean OD of SP-C mRNA was similar between control and CDH lungs between E15 and E20, and higher in CDH lungs at

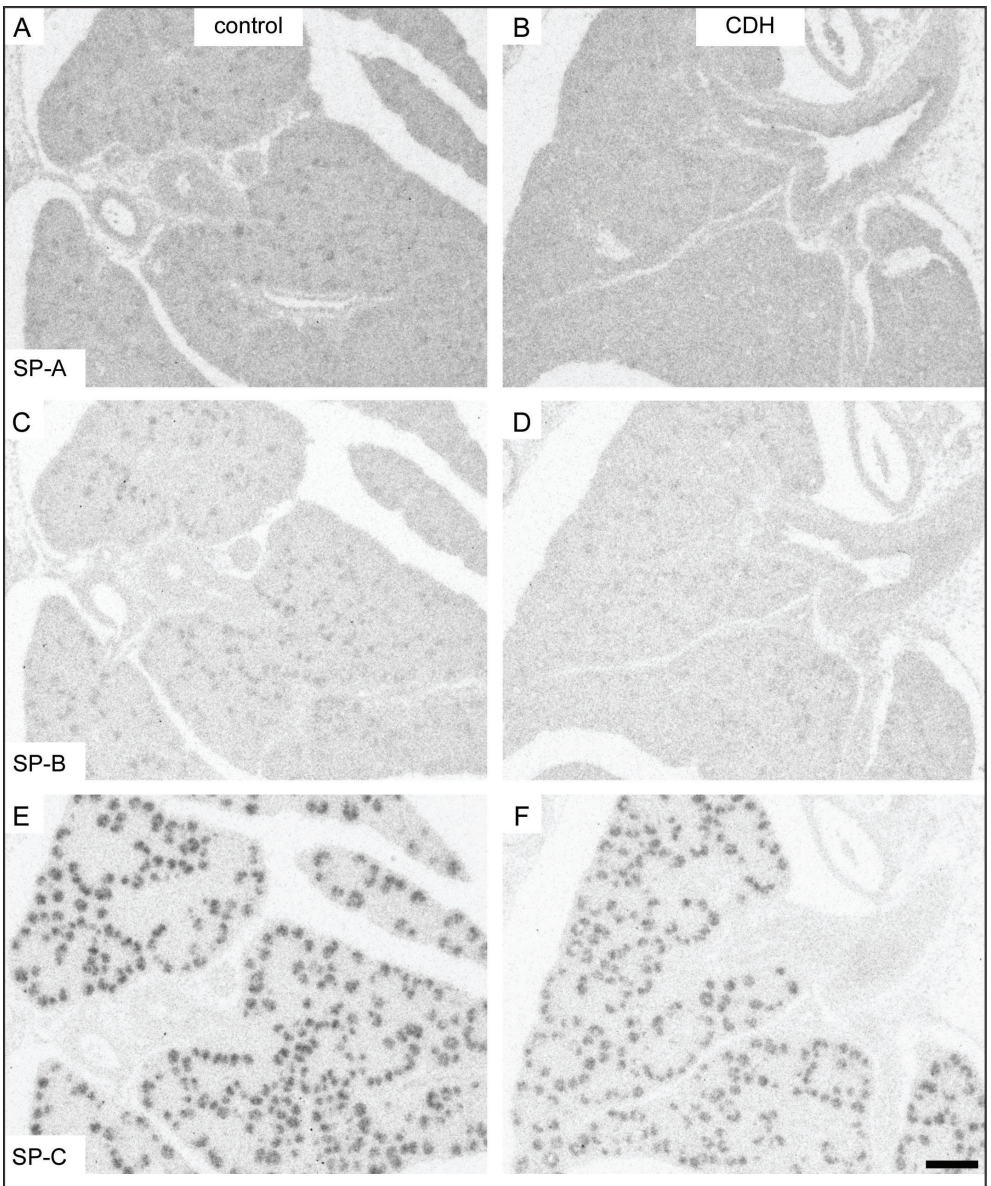

Figure 1. Expression of SP-A (A, B), SP-B (C, D), and SP-C (E, F) mRNA in serial sections of lungs of E18 control (A, C, E) and CDH (B, D, F) rat fetuses. SP-A, -B, and -C mRNA were expressed in the alveolar epithelial cells of both control and CDH lungs. Bar: 200 µm.

E22 (Fig. 4E; group*age effect, p = 0.007). For SP-A, -B, and -C mRNA, the volume fraction of mRNA-expressing cells (% Area) was similar between CDH and control lungs until E20 and was higher in CDH lungs at E22 (Fig. 4B, D, F; group*age effect, p = 0.009, p = 0.014, p = 0.002, respectively). These results show that the cellular concentration (mean OD) of SP mRNA in the CDH lungs is equal to the concentration found in a similar cell in control

lungs for SP-A and -B. For SP-C mRNA there is increased expression in CDH lungs at the end of gestation (E22). Furthermore, the volume fraction of cells (% Area) expressing SP mRNA as a percentage of total lung tissue (excluding airspaces) is higher near term in CDH

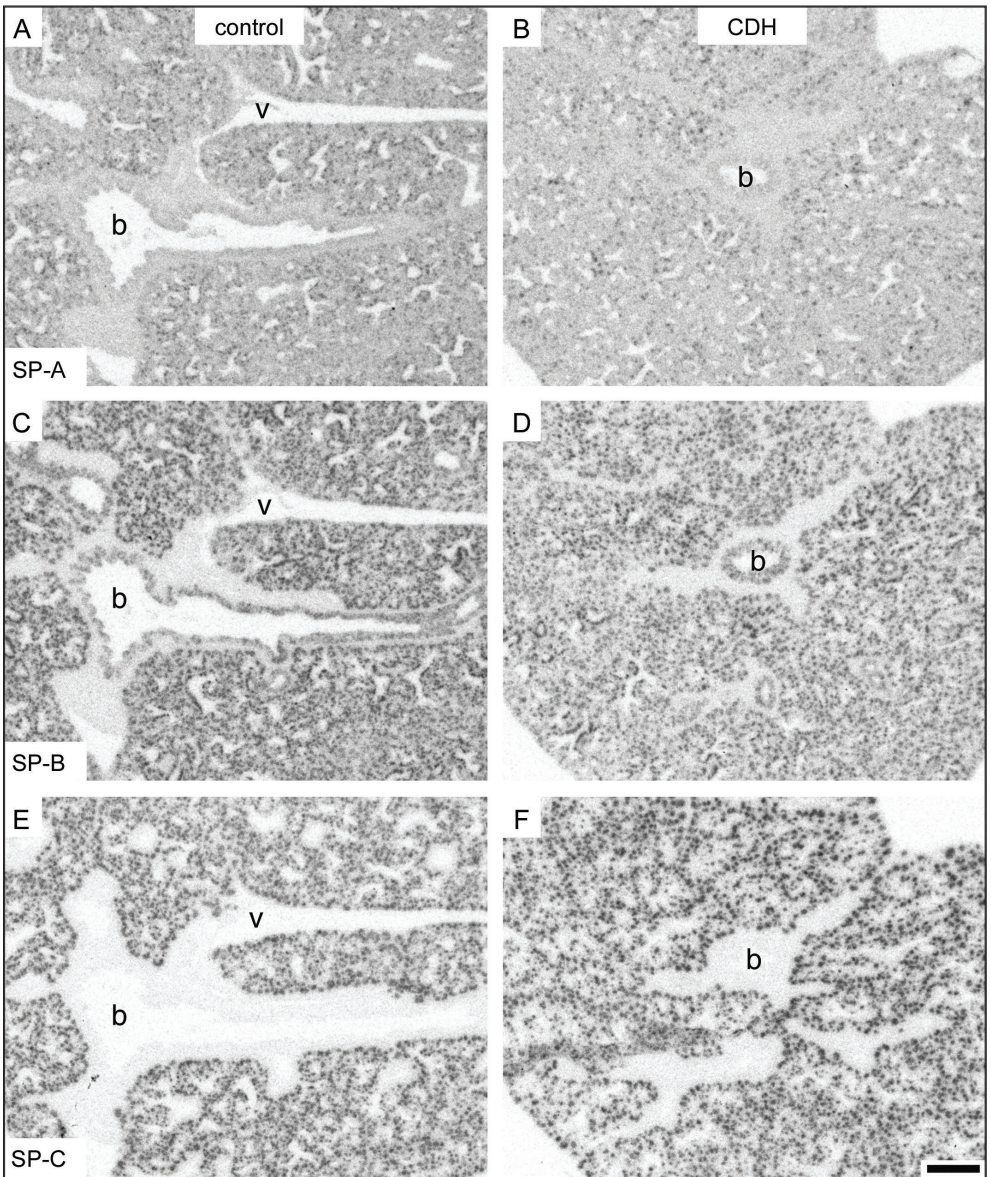

Figure 2. Expression of SP-A (A, B), SP-B (C, D), and SP-C (E, F) mRNA in serial sections of lungs of E20 control (A, C, E) and CDH (B, D, F) rat fetuses. In both control and CDH lungs, the three mRNAs were detected in alveolar epithelial cells. At this stage of development, SP-B mRNA was also detected in bronchiolar epithelial cells of both control and CDH lungs. Weak SP-A and no SP-C mRNA was detected in bronchiolar epithelial cells. v: blood vessel; b: bronchiole. Bar: 200 µm.

lungs. In summary these results indicate that there is no deficiency of SP-A, -B or -C mRNA in CDH lungs.

Because the lung at the side of the diaphragmatic defect (ipsilateral lung) was always more hypoplastic than the contralateral lung, we investigated the cellular concentration

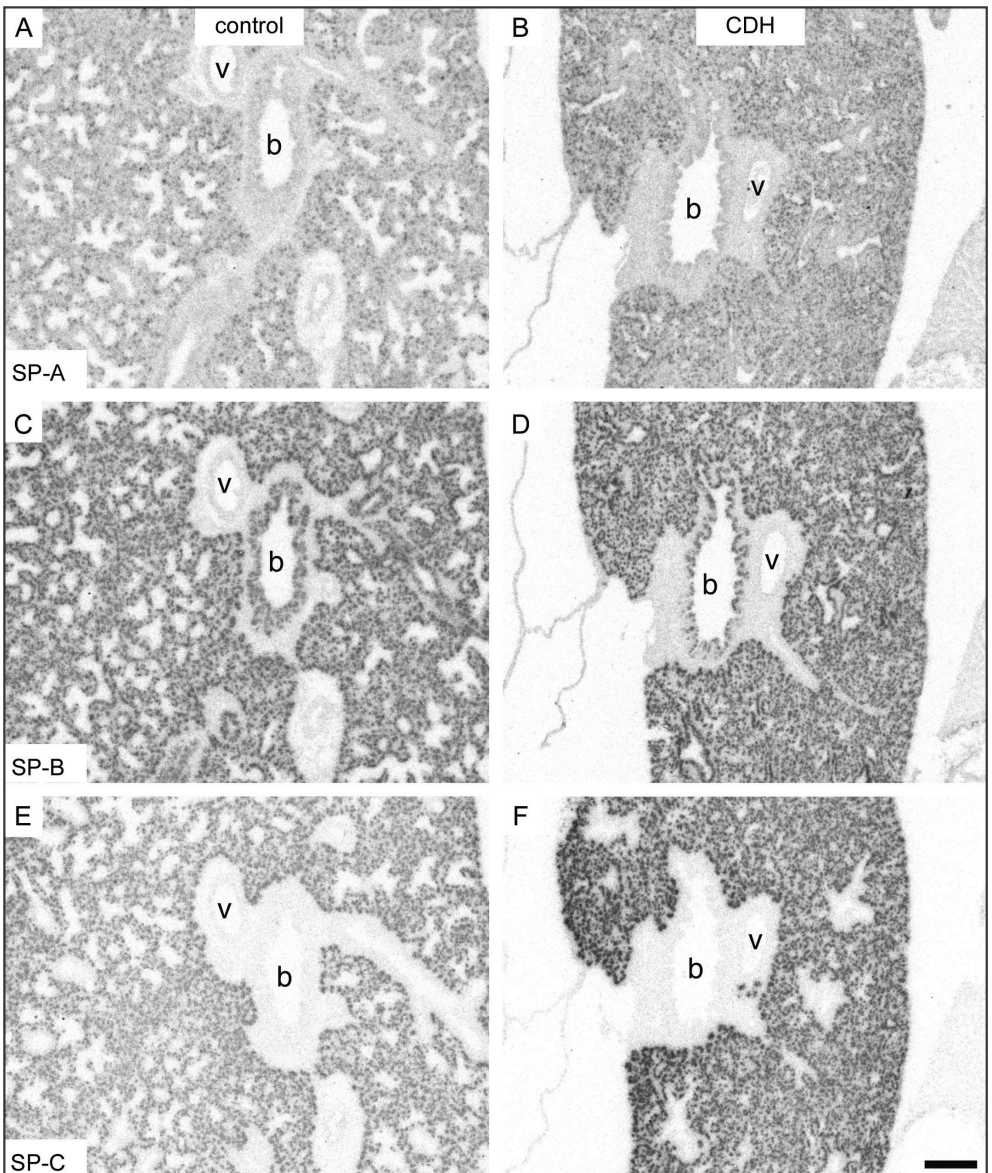

Figure 3. Expression of SP-A (A, B), SP-B (C, D), and SP-C (E, F) mRNA in serial sections of lungs of E22 control (A, C, E) and CDH (B, D, F) rat fetuses. In both control and CDH lungs, SP-A, -B, and -C mRNA were detected in alveolar epithelial cells. SP-A and -B mRNA were also expressed in bronchiolar epithelial cells, whereas SP-C mRNA was never detected in these cells. v: blood vessel; b: bronchiole. Bar: 200 µm.

(mean OD) of SP mRNA (Fig. 5A, C, E) and the volume fraction (% Area) of SP-expressing cells (Fig. 5B, D, F) between the ipsilateral and contralateral side of a CDH lung. In both the ipsilateral and contralateral CDH lung, the mean OD of SP-A, -B, and -C mRNA increased with gestational age and no differences were observed between the two lungs (Fig. 5A, C, E). Similarly, the % Area of SP-expressing cells increased with gestational age and no differences were found between the ipsilateral and contralateral side of a CDH lung (Fig. 5B, D, F).

Immunohistochemistry

SP-A (Fig. 6) and SP-B (Fig. 7) proteins were detected in the bronchiolar and alveolar epithelial cells of both control and CDH lungs. Expression of both proteins increased in control and CDH fetuses with advancing gestational age and no differences in expression pattern or staining intensity were observed between the control (Figs. 6 and 7, A and C) and CDH (Figs. 6 and 7, B and D) lungs at E20 (Figs. 6 and 7, A and B) or E22 (Figs. 6 and 7, C and D). No differences in the pattern or intensity of SP-A or -B staining were observed between the ipsilateral (hernia) and contralateral (no hernia) side of E22 CDH lungs (not shown). Clear proSP-C staining was observed in control (Fig. 8A, C) and CDH (Fig. 8B, D) lungs at E20, where it appeared higher in CDH (Fig. 8B) lungs than in control (Fig. 8A) lungs. However, at E22 (Fig. 8C, D) this difference could no longer be observed. In both control and CDH lungs, proSP-C was only detected in alveolar epithelial cells. At E22, there was no difference in intensity or pattern of proSP-C staining between the ipsilateral and the contralateral side of CDH lungs (not shown). These results show that the respective mRNAs are properly translated into protein and therefore indicate that lungs of nitrofen-induced CDH rat fetuses do not have a primary deficiency of surfactant proteins.

Discussion

CDH is characterized by a diaphragmatic defect, pulmonary hypoplasia and pulmonary hypertension. In the CDH neonate, pulmonary hypoplasia is often complicated by respiratory failure, low lung compliance, increased inspiratory resistance, and hyaline membrane formation (5). Based on inconsistent results from human and experimental animal studies with regard to the use of surfactant (prophylactic or rescue therapy) in CDH, we tested the hypothesis that CDH lungs are surfactant-deficient, which could explain in part the respiratory failure and difficulties in treating CDH infants. In this study, we showed that mRNA and protein expression of SP-A, -B, and -C, in both control and CDH lungs, increased with advancing gestational age and no differences were present in the cellular concentration (mean OD) of SP-A, -B, and -C mRNA between control and CDH lungs except for a higher concentration of SP-C mRNA at term (E22) in CDH lungs. The volume fraction of SP mRNA-expressing cells (% Area) similarly increased with gestational age in

control and CDH lungs and near term more SP mRNA-expressing cells were found in CDH lungs than in controls. This increased volume fraction of SP mRNA-expressing cells is in agreement with the increased number of surfactant-producing type II cells in CDH lungs. Using electron microscopy, it was shown that CDH lungs from fetal lambs (36, 49) and rats (50) had increased numbers of pulmonary type II cells, and more recently it was shown that those cells exhibit normal type II cell maturation (35). Furthermore, no differences were found in the cellular concentration of the SP mRNAs or in the volume fraction of SP mRNA-expressing cells between the ipsilateral (hernia) and contralateral (no hernia) side of CDH lungs. This study therefore demonstrates that there is no primary deficiency of surfactant proteins in the nitrofen-induced CDH rat model. It is, however, possible that the total amount of surfactant protein is less because CDH animals have smaller lungs.

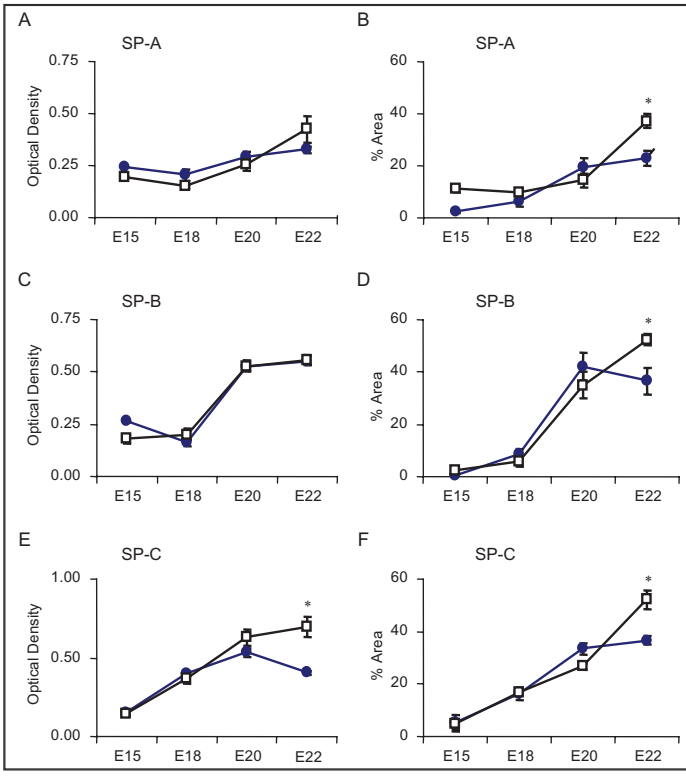

*Figure 4. Quantification of the in situ hybridization signals for SP-A (A, B), SP-B (C, D), and SP-C (E, F) mRNA in control (solid circles) and CDH (open squares) lungs. Mean OD was measured as described in the "Methods" section and indicates the cellular concentration of SP mRNA (A, C, E). The volume fraction of cells expressing SP mRNA is given as a percentage (% Area) of the total lung tissue measured (both staining and nonstaining lung tissue, airspaces excluded) (B, D, F). Both parameters increased with age in control and CDH lungs. At E22, the mean OD of SP-C mRNA and the % Area of cells expressing SP-A, -B, and -C mRNA was higher in CDH than in control lungs (significant group*age effect, p = 0.007, 0.009, 0.014, and 0.002, respectively).*

Data on the surfactant status of CDH humans and experimental animals are not consistent. Both normal and decreased levels for disaturated phosphatidylcholine (DSPC) and SP-A protein and mRNA were reported in CDH lungs. SP-C protein and mRNA levels were more often reported normal than decreased, whereas SP-B protein levels were often decreased, however, normal mRNA levels were also found in CDH compared to control lungs (Table 1). Despite animal data, neither a primary surfactant deficiency nor a beneficial effect of surfactant replacement therapy has been proven in human CDH infants (18, 51-53). These apparent discrepancies and the variably high mortality rate of CDH infants led us

to investigate the surfactant protein status in the nitrofen-induced CDH rat model using a novel *in situ* hybridization technique.

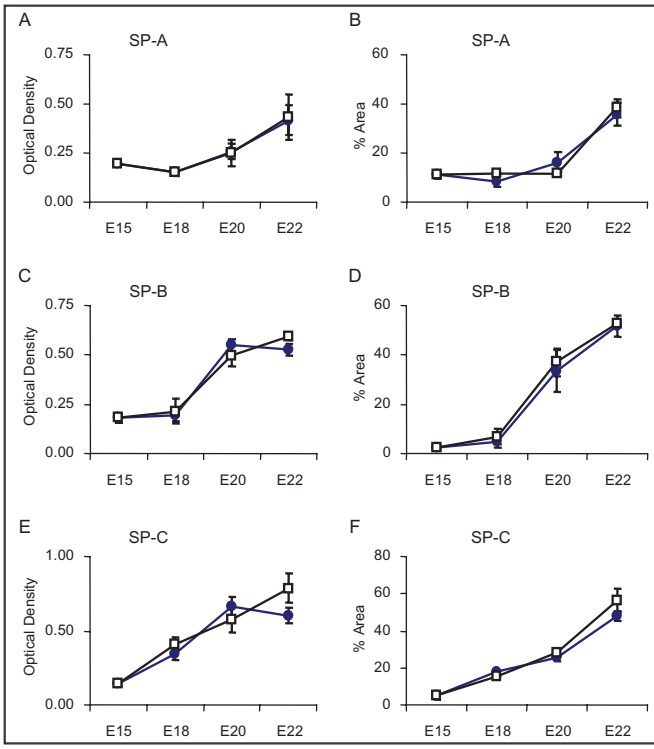

Figure 5. Quantification of the in situ hybridization signals for SP-A (A, B), SP-B (C, D), and SP-C (E, F) mRNA in the contralateral (no hernia, solid circles) and ipsilateral (hernia, open squares) side of CDH lungs. Mean OD was measured as described in the "Methods" section and indicates the cellular concentration of SP mRNA (A, C, E). The volume fraction of cells expressing SP mRNA is given as a percentage (% Area) of the total lung tissue measured (both staining and nonstaining lung tissue, airspaces excluded) (B, D, F). Both parameters increased with advancing gestational age and no differences were found between the ipsilateral and contralateral side of CDH lungs.

The key finding in this study was that with quantitative *in situ* hybridization we showed that in the same sample, the expression pattern and the cellular concentration of SP-A and SP-B mRNA did not differ between CDH and control lungs, whereas the expression pattern of SP-C mRNA was similar, but the level of expression was higher in CDH than in control lungs at the end of gestation (E22). The quantitative *in situ* hybridization technique is an adequate approach to measure differences in mRNA level in the context of changing tissue architecture or a changing expression pattern of a gene (40, 46, 54). These simultaneous observations cannot be made with techniques that require tissue homogenization, such as Northern blot analysis. The advantage of quantitative *in situ* hybridization is that it is possible to locate a positive staining cell in the original tissue and that at the same time it is possible to measure mRNA expression levels per cell. Our study was carried out in the laboratory where the quantitative *in situ* hybridization technique was developed and extensively validated with Northern blot analysis (40, 46). Jonker and co-workers (40) showed that the integrated OD (mean OD) of silver grains produced in liver and intestinal sections by the *in situ* hybridization procedure using ^{35}S-labeled riboprobes (*i.e.* positive signal) is directly proportional to the signal obtained by quantitative Northern blot analysis and, more recently, Moorman *et al*. (55) used the very same technique to distinguish cardiac specific mRNA expression levels in different parts of the developing

heart. In further support, the line of increase of SP mRNA levels with advancing gestational age in control rat lungs in our study is in agreement with published data from Schellhase *et al*. (56). These authors used Northern blot analysis to show that in control fetal rat lungs, SP-A and SP-B mRNA levels are very low before E17 and markedly increase from E18 to E19 and further increase till E21 (term = E22). Similar to our study (term = E23) they also showed that SP-C mRNA levels are already high at E17, increase dramatically towards E19, and further increase towards adult levels by E21 (56).

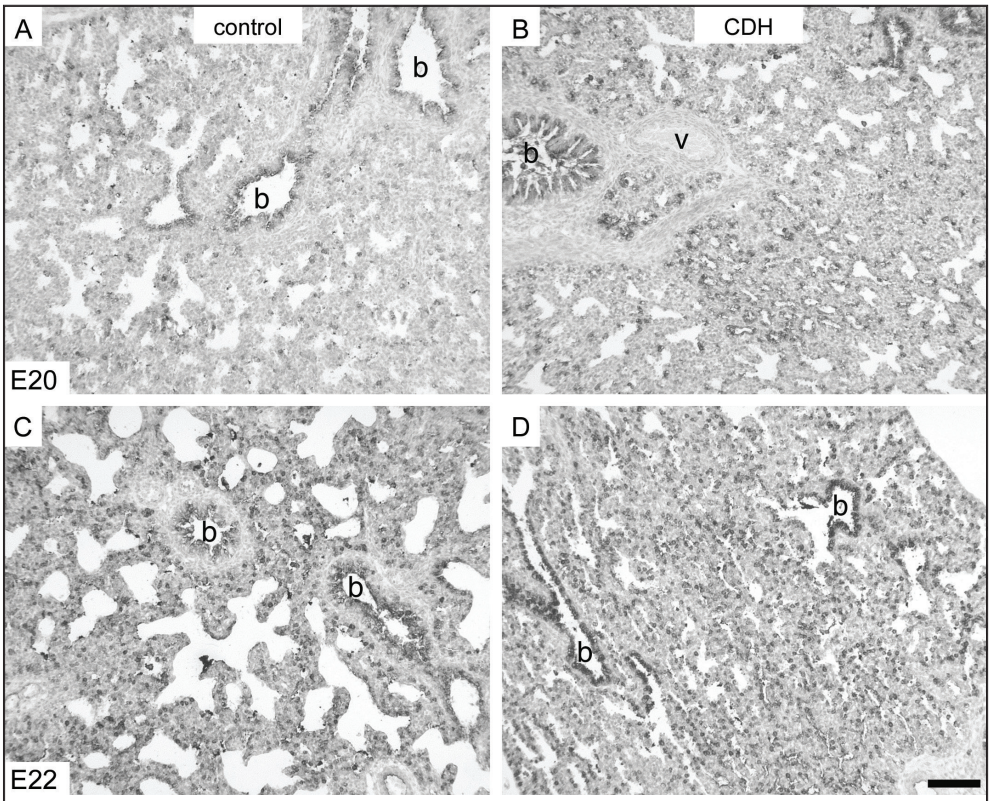

Figure 6. Immunohistochemical staining for SP-A at E20 (A, B) and E22 (C, D) in control (A, C) and CDH (B, D) rat lungs. SP-A was expressed in alveolar and bronchiolar epithelial cells of both control and CDH lungs. Note the difference in morphology between control and CDH lungs at E22. v: blood vessel; b: bronchiole. Bar: 100 µm.

We think that the measurement of mRNA concentration in the cell of interest (*via in situ* hybridization), as opposed to the measurement of mRNA levels per tissue volume (*via* for example Northern blot analysis) can account for the observed differences between our study and that of Thébaud and co-workers (38). Using Northern blot analysis, these latter authors found normal levels of SP-B and decreased levels of SP-A and SP-C mRNA in nitrofen-induced CDH rats at E21 (term = E22). Northern blot analysis includes all cells, including non-SP-producing cells, in the tissue base, whereas the *in situ* hybridization approach only includes SP-producing cells. In view of the altered morphology of CDH lungs, the contribution of non-SP-producing cells (for example fibroblasts) is larger

in hypoplastic CDH lungs than in control lungs, especially near term as was recently shown by Guilbert and co-workers (35). In this case, the key advantage of quantitative *in situ* hybridization is the possibility to avoid the contribution of fibroblast and other nonsurfactant-producing cells and selectively measure SP mRNA levels in pulmonary epithelial cells. From the study by Guilbert and co-workers (35) a similar conclusion can be drawn. These authors used RNA protection assay to measure the different levels of SP mRNA in nitrofen-induced CDH rats and showed normal SP-A, -B, and -C mRNA levels in contralateral CDH lungs compared with control lungs at any time and only decreased levels of SP-B and -C mRNA in ipsilateral CDH lungs at E21 (term = E22), which is the time when morphologic abnormalities (increased ratio of mesenchyme to epithelium) in CDH lungs are most apparent (35, 57). However, they also show with *in situ* hybridization that SP-C mRNA did not differ between control and CDH lungs at E21, which supports the results presented in our study.

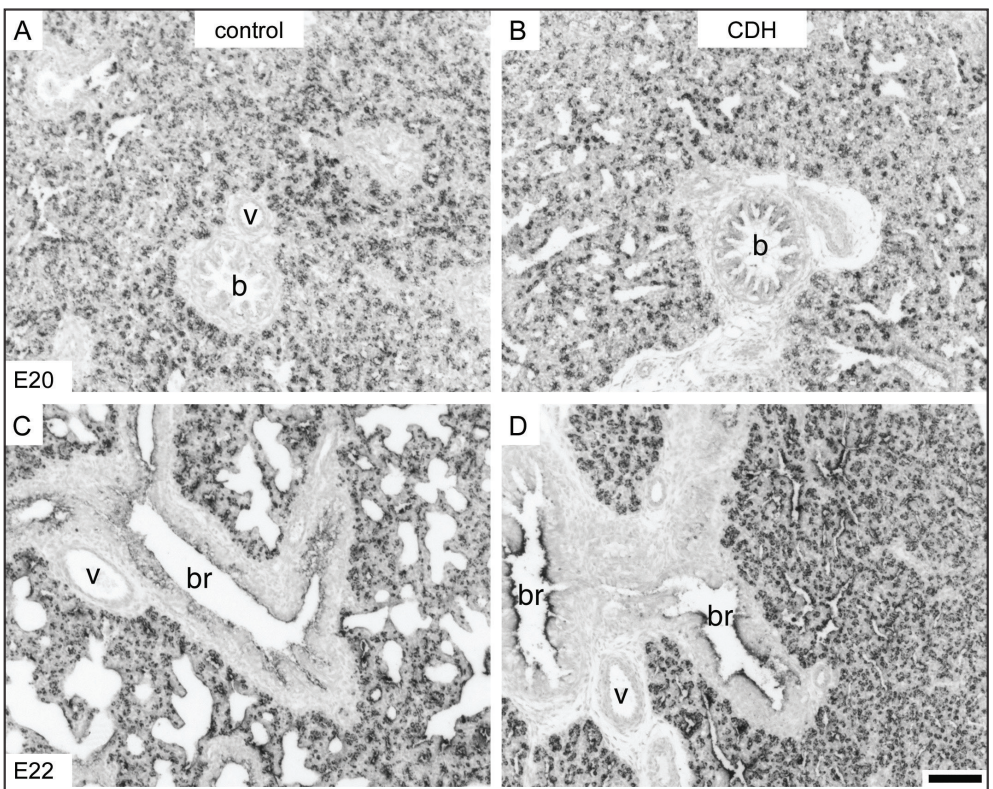

Figure 7. Immunohistochemical staining for SP-B at E20 (A, B) and E22 (C, D) in control (A, C) and CDH (B, D) rat lungs. SP-B was expressed in alveolar epithelial cells of both control and CDH lungs. Some staining is also detected in E20 bronchiolar epithelial cells. At E22, SP-B was expressed at high levels in alveolar and bronchiolar epithelial cells of both control and CDH lungs. v: blood vessel; b: bronchiole; br: bronchus. Bar: 100 µm.

Using immunohistochemistry, we found no differences in the protein staining pattern or intensity of SP-A, -B, and proSP-C, indicating that the respective mRNAs are properly translated into proteins. The surfactant protein antibodies used in this study were previously shown to be highly specific (16, 48). Our immunohistochemistry results are in line with results from Zhou *et al*. (16), who found no differences in the expression of SP-A, -B, and proSP-C proteins in various cases of human lung hypoplasia, including CDH.

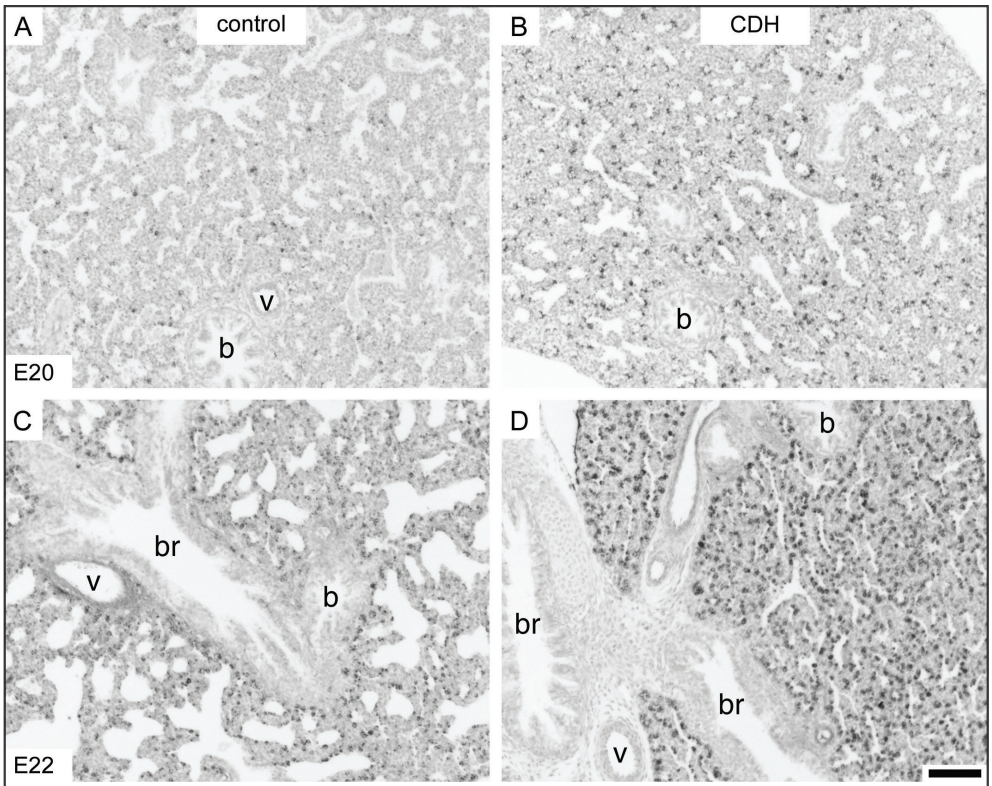

Figure 8. Immunohistochemical staining for proSP-C at E20 (A, B) and E22 (C, D) in control (A, C) and CDH (B, D) rat lungs. ProSP-C was expressed in alveolar epithelial cells of both control and CDH lungs. ProSP-C was never observed in bronchiolar epithelial cells. v: blood vessel; b: bronchiole; br: bronchus. Bar: 100 µm.

DSPC is as important for the function of surfactant as the surfactant proteins. Secreted surfactant is composed of 90% lipids, 9% proteins, and 1% carbohydrate (15). Experimental animal data support both decreased and normal levels of DSPC in CDH (Table 1). Interestingly, a recently published paper showed that DSPC synthesis in human CDH infants on ventilation was not different from control infants (no respiratory disease) on ventilation (52). Similarly, our group showed that CDH infants had a normal percentage DSPC in their BAL fluid (18) and more recently that CDH infants on ECMO are not surfactant-deficient when compared to infants on ECMO who suffer from meconium aspiration or with ventilated CDH infants (51). These results indicate that a primary surfactant deficiency is not likely in CDH infants.

That impaired lung development and subsequent respiratory distress can develop without a primary SP deficiency was also shown in an entirely different experimental model (58). Fetal rats with oligohydramnios suffer from a marked pulmonary hypoplasia; in humans, this often leads to respiratory distress at birth. However, despite the profound pulmonary hypoplasia, normal levels of saturated PC (phosphatidyl choline), SP-A, SP-B, and SP-C mRNA were found (58).

Although we did not find a primary deficiency in surfactant proteins, it is still possible that a secondary deficiency develops postnatally due to the nature of the disease with morphologically immature lungs and/or postnatal ventilation strategies. If (secondary) surfactant deficiency were a major component in the clinical course of CDH, one would expect beneficial results from prenatal corticosteroid injections or surfactant replacement therapy, treatments that have dramatically reduced the mortality rate in surfactant-deficient RDS infants. Although animal CDH models showed an improvement of lung morphology after prenatal corticosteroid treatment (59-62), unfortunately, no human randomized controlled trials for the use of surfactant or prenatal corticosteroids in CDH have been carried out and only anecdotal data are available (63-65), which, as recently reviewed (53), do not support a primary surfactant deficiency in CDH.

In conclusion, this study showed that there is no primary deficiency of surfactant proteins in the nitrofen-induced rat model of CDH. If extrapolation to the human situation is allowed, it is possible that the respiratory failure in CDH infants does not necessarily result from biochemically immature lungs but rather from morphologic immaturity and perhaps vascular abnormalities. Above all, a significant contribution to respiratory insufficiency in CDH is iatrogenic, as suggested in recent papers and a secondary surfactant deficiency cannot be excluded under these circumstances (21).

Acknowledgements

The authors thank Ms. Paula Blair for technical assistance with immunohistochemistry for SP-B and proSP-C. This work was supported by a student's grant (M.v.T.), by the Sophia Foundation and the Ludgardina Bouman Foundation (P.J.E.B.), and, in part, by National Institutes of Health grant HL56387 (S.E.W.).

References

1. Torfs CP, Curry CJ, Bateson TF, Honore LH, 1992. A population-based study of congenital diaphragmatic hernia. Teratology. 46:555-565.
2. Benjamin DR, Juul S, Siebert JR, 1988. Congenital posterolateral diaphragmatic hernia: associated malformations. J Pediatr Surg. 23:899-903.
3. Fauza DO, Wilson JM, 1994. Congenital diaphragmatic hernia and associated anomalies: their incidence, identification, and impact on prognosis. J Pediatr Surg. 29:1113-1117.
4. Tibboel D, Gaag AV, 1996. Etiologic and genetic factors in congenital diaphragmatic hernia. Clin Perinatol. 23:689-699.
5. Thébaud B, Mercier JC, Dinh-Xuan AT, 1998. Congenital diaphragmatic hernia. A cause of persistent pulmonary hypertension of the newborn which lacks an effective therapy. Biol Neonate. 74:323-336.
6. Kays DW, Langham MR, Jr., Ledbetter DJ, Talbert JL, 1999. Detrimental effects of standard medical therapy in congenital diaphragmatic hernia. Ann Surg. 230:340-348.
7. Boloker J, Bateman DA, Wung JT, Stolar CJ, 2002. Congenital diaphragmatic hernia in 120 infants treated consecutively with permissive hypercapnea/spontaneous respiration/elective repair. J Pediatr Surg. 37:357-366.
8. Beresford MW, Shaw NJ, 2000. Outcome of congenital diaphragmatic hernia. Pediatr Pulmonol. 30:249-256.
9. IJsselstijn H, Tibboel D, 1998. The lungs in congenital diaphragmatic hernia: do we understand? Pediatr Pulmonol. 26:204-218.
10. van Tuyl M, Hösgor M, Tibboel D, 2001. Tracheal ligation and corticosteroids in congenital diaphragmatic hernia: for better for worse? Pediatr Res. 50:441-444.
11. 1995. Effect of corticosteroids for fetal maturation on perinatal outcomes. NIH Consensus Development Panel on the Effect of Corticosteroids for Fetal Maturation on Perinatal Outcomes. JAMA. 273:413-418.
12. Bolt RJ, van Weissenbruch MM, Lafeber HN, Delemarre-van de Waal HA, 2001. Glucocorticoids and lung development in the fetus and preterm infant. Pediatr Pulmonol. 32:76-91.
13. Soll RF, Morley CJ, 2001. Prophylactic versus selective use of surfactant in preventing morbidity and mortality in preterm infants (Cochrane Review). Cochrane Database Syst Rev. 2:CD000510.
14. Floros J, Kala P, 1998. Surfactant proteins: molecular genetics of neonatal pulmonary diseases. Annu Rev Physiol. 60:365-384.

15. Haagsman HP, van Golde LM, 1991. Synthesis and assembly of lung surfactant. Annu Rev Physiol. 53:441-464.

16. Zhou H, Morotti RA, Profitt SA, Langston C, Wert SE, Whitsett JA, Greco MA, 2001. Expression of thyroid transcription factor-1, surfactant proteins, type I cell-associated antigen, and Clara cell secretory protein in pulmonary hypoplasia. Pediatr Dev Pathol. 4:364-371.

17. Sullivan KM, Hawgood S, Flake AW, Harrison MR, Adzick NS, 1994. Amniotic fluid phospholipid analysis in the fetus with congenital diaphragmatic hernia. J Pediatr Surg. 29:1020-1023.

18. IJsselstijn H, Zimmermann LJ, Bunt JE, de Jongste JC, Tibboel D, 1998. Prospective evaluation of surfactant composition in bronchoalveolar lavage fluid of infants with congenital diaphragmatic hernia and of age-matched controls. Crit Care Med. 26:573-580.

19. Moya FR, Thomas VL, Romaguera J, Mysore MR, Maberry M, Bernard A, Freund M, 1995. Fetal lung maturation in congenital diaphragmatic hernia. Am J Obstet Gynecol. 173:1401-1405.

20. Asabe K, Tsuji K, Handa N, Kurosaka N, Kajiwara M, 1997. Immunohistochemical distribution of surfactant apoprotein-A in congenital diaphragmatic hernia. J Pediatr Surg. 32:667-672.

21. Sakurai Y, Azarow K, Cutz E, Messineo A, Pearl R, Bohn D, 1999. Pulmonary barotrauma in congenital diaphragmatic hernia: a clinicopathological correlation. J Pediatr Surg. 34:1813-1817.

22. Wilcox DT, Irish MS, Holm BA, Glick PL, 1996. Animal models in congenital diaphragmatic hernia. Clin Perinatol. 23:813-822.

23. Glick PL, Stannard VA, Leach CL, Rossman J, Hosada Y, Morin FC, Cooney DR, Allen JE, Holm B, 1992. Pathophysiology of congenital diaphragmatic hernia II: the fetal lamb CDH model is surfactant deficient. J Pediatr Surg. 27:382-387.

24. Suen HC, Catlin EA, Ryan DP, Wain JC, Donahoe PK, 1993. Biochemical immaturity of lungs in congenital diaphragmatic hernia. J Pediatr Surg. 28:471-475.

25. Brandsma AE, Tibboel D, Vulto IM, Egberts J, Ten Have-Opbroek AA, 1993. Ultrastructural features of alveolar epithelial cells in the late fetal pulmonary acinus: a comparison between normal and hypoplastic lungs using a rat model of pulmonary hypoplasia and congenital diaphragmatic hernia. Microsc Res Tech. 26:389-399.

26. Wilcox DT, Glick PL, Karamanoukian HL, Azizkhan RG, Holm BA, 1995. Pathophysiology of congenital diaphragmatic hernia. XII: Amniotic fluid lecithin/sphingomyelin ratio and phosphatidylglycerol concentrations do not predict surfactant status in congenital diaphragmatic hernia. J Pediatr Surg. 30:410-412.

27. Alfanso LF, Arnaiz A, Alvarez FJ, Qi B, Diez-Pardo JA, Vallis-i-Soler A, Tovar JA, 1996. Lung hypoplasia and surfactant system immaturity induced in the fetal rat by prenatal exposure to nitrofen. Biol Neonate. 69:94-100.

28. Wilcox DT, Glick PL, Karamanoukian HL, Holm BA, 1997. Contributions by individual lungs to the surfactant status in congenital diaphragmatic hernia. Pediatr Res. 41:686-691.

29. Mysore MR, Margraf LR, Jaramillo MA, Breed DR, Chau VL, Arevalo M, Moya FR, 1998. Surfactant protein A is decreased in a rat model of congenital diaphragmatic hernia. Am J Respir Crit Care Med. 157:654-657.

30. Coleman C, Zhao J, Gupta M, Buckley S, Tefft JD, Wuenschell CW, Minoo P, Anderson KD, Warburton D, 1998. Inhibition of vascular and epithelial differentiation in murine nitrofen-induced diaphragmatic hernia. Am

J Physiol. 274:L636-646.

31. Losada A, Tovar JA, Xia HM, Diez-Pardo JA, Santisteban P, 2000. Down-regulation of thyroid transcription factor-1 gene expression in fetal lung hypoplasia is restored by glucocorticoids. Endocrinology. 141:2166-2173.

32. Benachi A, Chailley-Heu B, Barlier-Mur AM, Dumez Y, Bourbon J, 2002. Expression of surfactant proteins and thyroid transcription factor 1 in an ovine model of congenital diaphragmatic hernia. J Pediatr Surg. 37:1393-1398.

33. Guarino N, Oue T, Shima H, Puri P, 2000. Antenatal dexamethasone enhances surfactant protein synthesis in the hypoplastic lung of nitrofen-induced diaphragmatic hernia in rats. J Pediatr Surg. 35:1468-1473.

34. Shima H, Guarino N, Puri P, 2000. Effect of hyperoxia on surfactant protein gene expression in hypoplastic lung in nitrofen-induced diaphragmatic hernia in rats. Pediatr Surg Int. 16:473-477.

35. Guilbert TW, Gebb SA, Shannon JM, 2000. Lung hypoplasia in the nitrofen model of congenital diaphragmatic hernia occurs early in development. Am J Physiol Lung Cell Mol Physiol. 279:L1159-1171.

36. Bratu I, Flageole H, Laberge JM, Possmayer F, Harbottle R, Kay S, Khalife S, Piedboeuf B, 2001. Surfactant levels after reversible tracheal occlusion and prenatal steroids in experimental diaphragmatic hernia. J Pediatr Surg. 36:122-127.

37. Utsuki T, Hashizume K, Iwamori M, 2001. Impaired spreading of surfactant phospholipids in the lungs of newborn rats with pulmonary hypoplasia as a model of congenital diaphragmatic hernia induced by nitrofen. Biochim Biophys Acta. 1531:90-98.

38. Thébaud B, Barlier-Mur AM, Chailley-Heu B, Henrion-Caude A, Tibboel D, Dinh-Xuan AT, Bourbon JR, 2001. Restoring effects of vitamin a on surfactant synthesis in nitrofen- induced congenital diaphragmatic hernia in rats. Am J Respir Crit Care Med. 164:1083-1089.

39. Valls-i-Soler A, Alfonso LF, Arnaiz A, Alvarez FJ, Tovar JA, 1996. Pulmonary surfactant dysfunction in congenital diaphragmatic hernia: experimental and clinical findings. Biol Neonate. 69:318-326.

40. Jonker A, de Boer PA, van den Hoff MJ, Lamers WH, Moorman AF, 1997. Towards quantitative in situ hybridization. J Histochem Cytochem. 45:413-423.

41. Tenbrinck R, Tibboel D, Gaillard JL, Kluth D, Bos AP, Lachmann B, Molenaar JC, 1990. Experimentally induced congenital diaphragmatic hernia in rats. J Pediatr Surg. 25:426-429.

42. Keijzer R, Liu J, Deimling J, Tibboel D, Post M, 2000. Dual-hit hypothesis explains pulmonary hypoplasia in the nitrofen model of congenital diaphragmatic hernia. Am J Pathol. 156:1299-1306.

43. Korfhagen TR, Bruno MD, Glasser SW, Ciraolo PJ, Whitsett JA, Lattier DL, Wikenheiser KA, Clark JC, 1992. Murine pulmonary surfactant SP-A gene: cloning, sequence, and transcriptional activity. Am J Physiol. 263: L546-554.

44. D'Amore-Bruno MA, Wikenheiser KA, Carter JE, Clark JC, Whitsett JA, 1992. Sequence, ontogeny, and cellular localization of murine surfactant protein B mRNA. Am J Physiol. 262:L40-47.

45. Glasser SW, Korfhagen TR, Bruno MD, Dey C, Whitsett JA, 1990. Structure and expression of the pulmonary surfactant protein SP-C gene in the mouse. J Biol Chem. 265:21986-21991.

46. Moorman AF, De Boer PA, Ruijter JM, Hagoort J, Franco D, Lamers WH, 2000. Radio-isotopic in situ hybridization on tissue sections. Practical aspects and quantification. Methods Mol Biol. 137:97-115.

47. Han RN, Buch S, Freeman BA, Post M, Tanswell AK, 1992. Platelet-derived growth factor and growth-related genes in rat lung. II. Effect of exposure to 85% O2. Am J Physiol. 262:L140-146.

48. Zhou L, Lim L, Costa RH, Whitsett JA, 1996. Thyroid transcription factor-1, hepatocyte nuclear factor-3beta, surfactant protein B, C, and Clara cell secretory protein in developing mouse lung. J Histochem Cytochem. 44:1183-1193.

49. Pringle KC, Turner JW, Schofield JC, Soper RT, 1984. Creation and repair of diaphragmatic hernia in the fetal lamb: lung development and morphology. J Pediatr Surg. 19:131-140.

50. Brandsma AE, ten Have-Opbroek AA, Vulto IM, Molenaar JC, Tibboel D, 1994. Alveolar epithelial composition and architecture of the late fetal pulmonary acinus: an immunocytochemical and morphometric study in a rat model of pulmonary hypoplasia and congenital diaphragmatic hernia. Exp Lung Res. 20:491-515.

51. Janssen DJ, Tibboel D, Carnielli VP, van Emmen E, Luijendijk IH, Darcos Wattimena JL, Zimmermann LJ, 2003. Surfactant phosphatidylcholine pool size in human neonates with congenital diaphragmatic hernia requiring ECMO. J Pediatr. 142:247-252.

52. Cogo PE, Zimmermann LJ, Rosso F, Tormena F, Gamba P, Verlato G, Baritussio A, Carnielli VP, 2002. Surfactant synthesis and kinetics in infants with congenital diaphragmatic hernia. Am J Respir Crit Care Med. 166:154-158.

53. Bohn D, 2002. Congenital diaphragmatic hernia. Am J Respir Crit Care Med. 166:911-915.

54. Ruijter JM, Hagoort J, De Boer PA, Moorman AFM, 2001. Calibration of densitometry in radio-isotopic in situ hybridization. Image Anal Stereol. 20:219-224.

55. Moorman AF, Schumacher CA, de Boer PA, Hagoort J, Bezstarosti K, van den Hoff MJ, Wagenaar GT, Lamers JM, Wuytack F, Christoffels VM, Fiolet JW, 2000. Presence of functional sarcoplasmic reticulum in the developing heart and its confinement to chamber myocardium. Dev Biol. 223:279-290.

56. Schellhase DE, Emrie PA, Fisher JH, Shannon JM, 1989. Ontogeny of surfactant apoproteins in the rat. Pediatr Res. 26:167-174.

57. Losty PD, Pacheco BA, Manganaro TF, Donahoe PK, Jones RC, Schnitzer JJ, 1996. Prenatal hormonal therapy improves pulmonary morphology in rats with congenital diaphragmatic hernia. J Surg Res. 65:42-52.

58. Kitterman JA, Chapin CJ, Vanderbilt JN, Porta NF, Scavo LM, Dobbs LG, Ertsey R, Goerke J, 2002. Effects of oligohydramnios on lung growth and maturation in the fetal rat. Am J Physiol Lung Cell Mol Physiol. 282: L431-439.

59. Suen HC, Bloch KD, Donahoe PK, 1994. Antenatal glucocorticoid corrects pulmonary immaturity in experimentally induced congenital diaphragmatic hernia in rats. Pediatr Res. 35:523-529.

60. Hedrick HL, Kaban JM, Pacheco BA, Losty PD, Doody DP, Ryan DP, Manganaro TF, Donahoe PK, Schnitzer JJ, 1997. Prenatal glucocorticoids improve pulmonary morphometrics in fetal sheep with congenital diaphragmatic hernia. J Pediatr Surg. 32:217-221.

61. IJsselstijn H, Pacheco BA, Albert A, Sluiter W, Donahoe PK, De Jongste JC, Schnitzer JJ, Tibboel D, 1997. Prenatal hormones alter antioxidant enzymes and lung histology in rats with congenital diaphragmatic hernia. Am J Physiol. 272:L1059-1065.

62. Kapur P, Holm BA, Irish MS, Sokolowski J, Patel A, Glick PL, 1999. Lung physiological and metabolic changes in lambs with congenital diaphragmatic hernia after administration of prenatal maternal corticosteroids. J Pediatr Surg. 34:354-356.

63. Bos AP, Tibboel D, Hazebroek FW, Molenaar JC, Lachmann B, Gommers D, 1991. Surfactant replacement therapy in high-risk congenital diaphragmatic hernia. Lancet. 338:1279.

64. Glick PL, Leach CL, Besner GE, Egan EA, Morin FC, Malanowska-Kantoch A, Robinson LK, Brody A, Lele AS, McDonnell M, Holm B, Rodgers BT, Msall ME, Courney NG, Karp MP, Allen JE, Jewett Jr TC, Cooney DR, 1992. Pathophysiology of congenital diaphragmatic hernia. III: Exogenous surfactant therapy for the high-risk neonate with CDH. J Pediatr Surg. 27:866-869.

65. Lotze A, Knight GR, Anderson KD, Hull WM, Whitsett JA, O'Donnell RM, Martin G, Bulas DI, Short BL, 1994. Surfactant (beractant) therapy for infants with congenital diaphragmatic hernia on ECMO: evidence of persistent surfactant deficiency. J Pediatr Surg. 29:407-412.

Chapter 8

Prenatal exposure to thyroid hormone is necessary for normal postnatal development of murine heart and lungs

Minke van Tuyl[*1,2], Pietjan E. Blommaart[*1,2], Piet A.J. de Boer[2], Susan E. Wert[3], Jan M. Ruijter[2], Saleem Islam[4], Jay Schnitzer[4], Aaron R. Ellison[5], Dick Tibboel[1], Antoon F.M. Moorman[2], and Wouter H. Lamers[2]

[1]Department of Pediatric Surgery, Sophia Children's Hospital, Erasmus University Medical Center Rotterdam, Rotterdam, The Netherlands
[2]Department of Anatomy and Embryology, Academic Medical Center, University of Amsterdam, Amsterdam, The Netherlands
[3]Divisions of Pulmonary Biology and Neonatology, Children's Hospital Medical Center, Cincinnati, OH 45229, U.S.A.
[4]Pediatric Surgical Research Laboratories, Massachusetts General Hospital, Harvard Medical School, Boston, MA 02114, U.S.A.
[5]BitTech, Inc., Westlake Village, CA 91361, U.S.A.
[*]These authors contributed equally to this work

Developmental Biology 2004; 272:104-117

Abstract

Maternal hypothyroxinemia during early pregnancy poses an increased risk for poor neuropsychological development of the fetus. We tested the hypothesis that maternal hypothyroidism before the onset of fetal thyroid function also affects postnatal development of heart and lungs. This question was addressed in transgenic mice that express herpes simplex thymidine kinase in their thyroidal follicle cells. Treatment with ganciclovir rendered these mice severely hypothyroid, because viral thymidine kinase converts ganciclovir into a cytotoxic nucleoside analog. Because ganciclovir crosses the placenta, it also destroyed the thyroid of transgenic embryos while leaving the thyroids of nontransgenic littermates unaffected. Hypothyroidism of both mother and fetus did not affect prenatal heart and lung development. However, the postnatal switch from β- to α-myosin heavy chain (β- and α-MHC, respectively) gene expression and the increase of SERCA-2a mRNA expression did not occur in the ventricular myocardium of either the transgenic (thyroid destroyed) or nontransgenic (intact thyroid) offspring of hypothyroid mothers. Similarly, postnatal animals of the latter two groups retained elevated surfactant protein (SP)-A, -B, and -C mRNA levels in their alveolar epithelium. In hypothyroid pups from hypothyroid mothers, these changes were accompanied by decreased alveolar septation. Our study shows that these effects of maternal hypothyroidism become manifest after birth and are aggravated by the concomitant existence of neonatal hypothyroidism.

Introduction

In mammals, the concentration of fetal circulating thyroid hormone rises only late in gestation (1), most likely because the placenta partly inactivates maternal thyroid hormone (2) and the fetal hypothalamic-pituitary-thyroid system matures relatively late in gestation (1, 3). The association of iodine deficiency, causing hypothyroidism in both mother and fetus, with cretinism is well established (4). The importance of thyroid hormone for the developing fetus has nevertheless been questioned because postnatal substitution of thyroid hormone almost completely prevents the detrimental effects of congenital hypothyroidism (5). Recently, however, the significance of a normal maternal thyroid hormone status for proper organ development in the offspring, in particular that of the brain, has again attracted attention (6-9). It was shown that the fetal brain was most sensitive to maternal hypothyroxinemia between the 3rd and 5th month (10), that is, when the fetal thyroid is not yet functional.

In addition to the brain, the heart and lungs are known targets of thyroid hormone. In the heart, thyroid hormone stimulates the transcription of α-myosin heavy chain (α-MHC) and inhibits that of β-myosin heavy chain (β-MHC) (11-13). Before birth, the ventricles express high levels of β-MHC and only low levels of α-MHC; whereas after birth, the α-MHC level increases and virtually replaces β-MHC by postnatal day 7 (13). The postnatal increase in α-MHC and decrease in β-MHC expression have been attributed to the postnatal increase in circulating thyroid hormone (14). Similarly, the sarcoplasmatic reticulum ATPase isoform 2a (SERCA-2a) and its regulatory subunit phospholamban (PLB) are reciprocally regulated by thyroid hormone (15-17). SERCA-2a and PLB expression are low in fetal hearts and increase after birth (18, 19). Neonatal hypothyroidism decreased SERCA-2a levels and increased cardiac PLB levels, whereas neonatal hyperthyroidism left SERCA-2a levels unchanged, but decreased cardiac PLB expression (17, 19, 20).

In perinatal lungs, the postnatal increase in thyroid hormone availability coincides with the acceleration of alveolar septation, suggesting that thyroid hormone enhances the structural development of the lungs (21). In agreement, the lungs of homozygous "hyt" mice, which suffer from congenital hypothyroidism due to a mutation in the thyroid-stimulating hormone (TSH) receptor (22), become affected only after birth (23). Lungs of homozygous "hyt" mice contain less saturated phosphatidylcholine and have thicker alveolar septa and smaller airspaces than euthyroid littermates (23). A role for thyroid hormone in functional development of the perinatal lung is however disputed (24). Thus, it was both reported that prenatal thyrotropin-releasing hormone or triiodothyronine (T_3) treatment of fetal rat lungs *in vitro* or *in vivo* did not enhance surfactant protein (SP)-A, -B, and -C expression (25-28), and that thyroid hormone stimulated the functional maturation of the surfactant-producing type II cells of the lung (29). However, it was also reported that during early embryonic lung development, thyroid hormone accelerated epithelial

and mesenchymal cell differentiation at the expense of branching morphogenesis and lung growth (30), suggesting that an untimely exposure to an effective level of thyroid hormone can prematurely halt organogenesis and precipitate functional maturation. Because human fetal lungs express a relatively high level of thyroid hormone receptors as early as 13 weeks of gestation (31, 32), maternal hypothyroidism in man may also affect fetal lung development.

Given the effect of maternal hypothyroidism on prenatal brain development, we hypothesized that maternal hypothyroidism before the onset of fetal thyroid function could similarly affect heart and/or lung morphogenesis and maturation. In the present study, we have used "TG-TKT2" transgenic mice to experimentally address this question. TG-TKT2 transgenic mice harbor a construct, consisting of the bovine thyroglobulin (TG) promoter coupled to the herpes simplex thymidine kinase type 2 (TKT2) structural gene (33). The thyroglobulin promoter confers specific expression of the TKT2 gene in the follicle cells of the thyroid. Because viral thymidine kinase renders the nucleoside analog ganciclovir cytotoxic by phosphorylation, treatment of transgenic mice with ganciclovir causes the specific destruction of these follicle cells. Because ganciclovir crosses the placenta, it can also be used to destroy the follicle cells of transgenic embryos (34, 35).

We demonstrate that hypothyroidism of both the mother and the fetus did not affect the parameters investigated during prenatal myocardial or pulmonary development. However, the postnatal switch in the heart from β- to α-MHC gene expression and the increase of SERCA-2a mRNA expression did not occur in either the transgenic (thyroid destroyed) or nontransgenic (intact thyroid) offspring of hypothyroid dams. Similarly, such pups retained elevated SP-A, -B, and -C mRNA levels in their alveolar epithelium, whereas the postnatal hypothyroid pups from hypothyroid mothers also suffered from impaired morphological development of the lungs. These results indicate that an adequate function of the maternal thyroid is important for normal postnatal development of both heart and lungs.

MATERIALS AND METHODS

Animals

Adult transgenic mice of the TG-TKT2 strain (C57Bl/6 background) were obtained from the AFCR Center for Genomic Research, University of Edinburgh (United Kingdom), whereas wild-type C57Bl/6J mice were obtained from the Broekman Institute BV, Someren (The Netherlands). The mice were kept in a controlled light-dark cycle. Food and water were supplied *ad libitum*. Heterozygous TG-TKT2 females were mated with wild-type males. The day a plug was detected was destined day 1 of gestation (ED1). Transgenic mice were identified by polymerase chain reaction (PCR) analysis. The forward primer was 5'-GCG TTC

GGT CAG GCT GCT CGT GC-3' and the reversed primer 5'-GCC AGT AAG TCA TCG GCT CGG G-3', resulting in a PCR product with a length of 234 bp. For control embryos and neonates, non-transgenic C57Bl/6J male and female mice were used. All animal experiments were carried out in accordance with the guidelines of the local Animal Research Committee of the Academic Medical Center of the University of Amsterdam.

At embryonic day 14 (ED14), ED16, and ED18 pregnant females were sacrificed and the embryos were dissected from the uterus. Embryos were fixed after death by cooling on ice. Neonatal day 1 (ND1) and ND7 animals were fixed after decapitation, removal of the skin, and opening of the thorax for optimal penetration of the fixative. Heart and lungs of ND14 and ND28 animals were removed en bloc from the body before fixation. All tissues were fixed at 4°C in 4% phosphate-buffered formaldehyde (w/v) for 16-18 hours, dehydrated in a graded series of ethanol, cleared with 1-butanol, and embedded in Paraplast Plus (Monoject, Kildare, Ireland). Serial 7 µm frontal sections were cut and mounted onto RNAse-free 3-aminopropyltriethoxysilane (Sigma Chemical Co., St. Louis, MO, U.S.A.) - coated slides.

To ablate the maternal thyroid, nonpregnant female transgenic TG-TKT2 mice were treated twice daily for 3 days with an intraperitoneal injection of ganciclovir (9-[(1,3-dihydroxy-2-propoxy)methyl]guanine; Cymevene®, Syntex BV, Rijswijk, The Netherlands; 150 µg Na-ganciclovir/g body weight/injection), starting at least 2 weeks before mating (Fig. 1 and Wallace *et al*. (36)). These mice were designated as pretreated mice. Before treatment, blood samples were taken under light ether anesthesia via an orbital puncture. A blood sample from the caval vein was taken at sacrifice. The levels of thyroxine (T_4) were determined with a radioimmunoassay (courtesy Department of Endocrinology, Academic Medical Center, University of Amsterdam, The Netherlands). Pregnant pretreated transgenic mice were treated twice daily with intraperitoneal injections of ganciclovir (150 µg ganciclovir/g body weight/injection) on ED13, ED14, and ED15 to ablate the developing thyroids of transgenic embryos (TT group), while leaving the thyroids of nontransgenic fetuses unaffected (TNT group) (Fig. 1). Control, nontransgenic mice, were similarly treated before and during pregnancy.

Immunohistochemistry

All antibodies except that against thyroglobulin were obtained from Dr. J.A. Whitsett (Division of Pulmonary Biology, Children's Hospital Medical Center, Cincinnati, OH, U.S.A.). A guinea pig polyclonal antibody against rat SP-A, a rabbit polyclonal antibody against mature bovine SP-B (R28031), and a rabbit polyclonal antibody against human proSP-C (R68514) were applied at a dilution of 1:300, 1:2000, and 1:2000, respectively, to 7 µm deparaffinized sections. For SP-A, a Vectastain ABC Peroxidase kit and for SP-B and proSP-C a Vector Elite ABC-DAB kit (Vector Laboratories, Burlingame, CA, U.S.A.) were used to detect antigen-antibody complexes (37). The enzymatic reaction product was enhanced

with nickel/cobalt to produce a black precipitate. Sections were counterstained with nuclear fast red. Thyroglobulin antibody was provided by Dr. J.J.M. de Vijlder (Department of Pediatric Endocrinology, Emma Children's Hospital, Academic Medical Center, University of Amsterdam, The Netherlands) and used at a dilution of 1:5000.

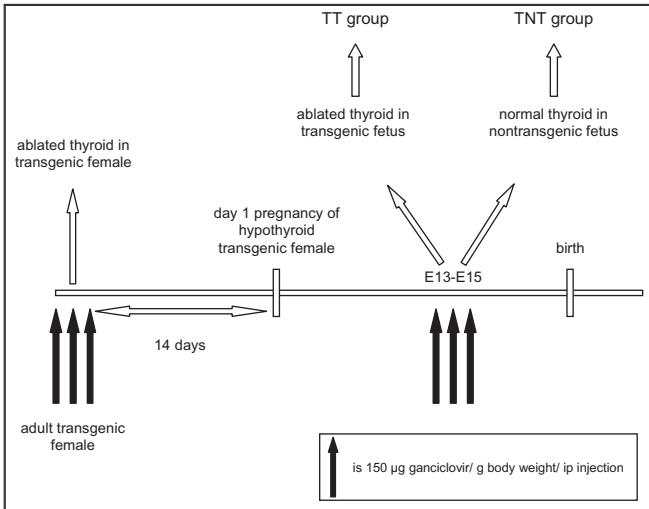

Figure 1. Schematic representation of ganciclovir treatment of transgenic (TG-TKT2) mice. Adult TG-TKT2 females were twice daily injected intraperitoneally (ip) with 150 µg ganciclovir/g body weight for 3 days (indicated by black arrows). After 14 days, when the follicle cells in the thyroids were destroyed, the hypothyroid transgenic females were mated. At days 13, 14, and 15 of gestation, the hypothyroid pregnant mice were again treated with ganciclovir (indicated by black arrows) to ablate the thyroidal follicle cells of the transgenic fetuses (TT group), while leaving the thyroids of nontransgenic littermates (TNT group) unaffected.

In situ hybridization

[α-^{35}S]dCTP-labeled antisense probes for α-MHC, β-MHC, SERCA-2a, and PLB were generated as described before (38). Plasmids containing mouse SP-A and SP-C (both in pGEM3Z) and SP-B (in pBS-SKII) cDNA were obtained from Dr. J.A. Whitsett (Division of Pulmonary Biology, Children's Hospital Medical Center, Cincinnati, OH, U.S.A.) (39-41). [α-^{35}S]dCTP-labeled antisense probes for SP-A, -B, and -C were generated with T7 polymerase, after linearization of the plasmids with *Apa*LI, *Eco*RI, and *Hin*dIII, respectively. The hybridization conditions were as detailed elsewhere (42). Exposure time to nuclear autoradiographic emulsion (Ilford Nuclear Research Emulsion G-5) was 14 days for SP-A and 7 days for SP-B and -C. The development time was 4 min. After development, the sections were dehydrated in a graded series of ethanol and xylol, and mounted in Malinol (Chroma-Gesellshaft, Schmidt Gmbh+Co, Köngen, Germany).

Image acquisition and analysis

For image acquisition, a Photometrics cooled-CCD camera (Tucson, AZ, USA; 12-bit dynamic range; 1317x1035 pixels), attached to an Axioplan microscope (Carl Zeiss, Oberkochen, Germany) equipped with a 5x objective (N.A.: 0.15), a stabilized power supply, and an infrared-blocking filter was used. The low-power objective was used to assure the sampling of several respiratory acini in an image, representing 2.5 mm^2 of the lung section. Digital

images from the *in situ* hybridization procedure were recorded using white light (43). The digital transmission images were converted to optical density (OD) images by calculating the negative logarithm of the transmission image divided by an image of the light source ($OD = -^{10}\log(I/I_0)$ for each pixel). This conversion implicitly corrects background shading.

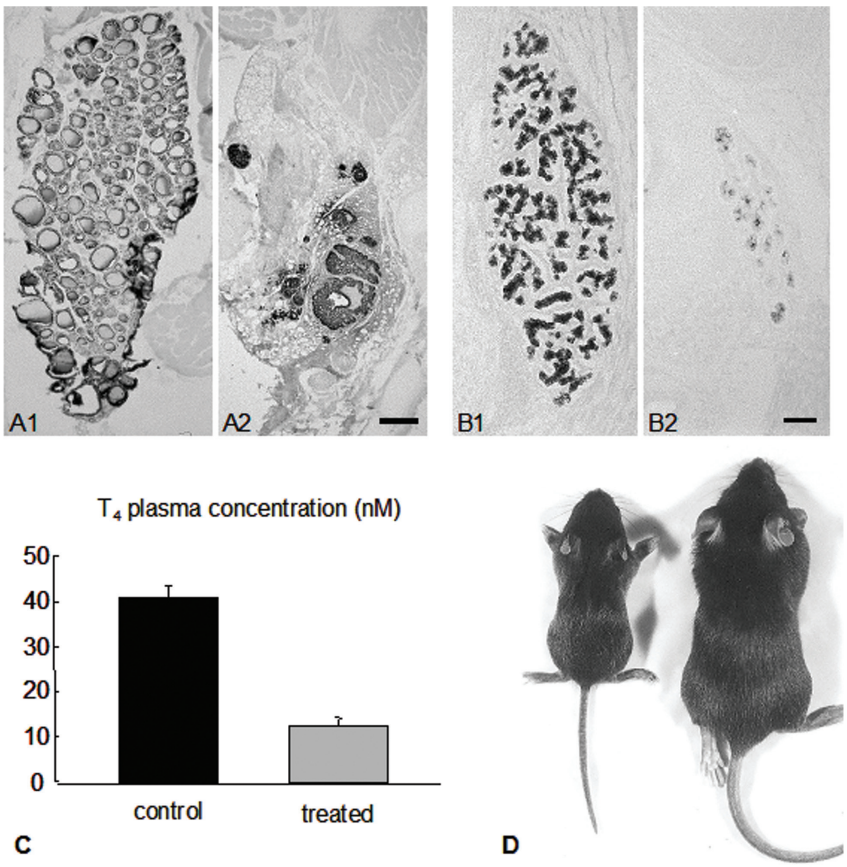

Figure 2. Effectiveness of ganciclovir treatment. Thyroid glands were stained for the presence of thyroglobulin in control and ganciclovir-treated transgenic (TT) mice. In control adult (panel A1) and ED16 mice (panel B1), numerous follicles were present. In ganciclovir-treated transgenic (TT) adult (panel A2) and ED16 mice (panel B2), most follicles had disappeared, leaving a disorganized thyroid with few, usually large follicles behind in the adult. The two consecutive ganciclovir treatments decreased plasma thyroxine (T_4) levels more than threefold in female transgenic mice (panel C). Ganciclovir-treated transgenic neonates (TT group, panel D, left animal, 4 weeks old) were hypothyroid and failed to thrive when compared to ganciclovir-treated nontransgenic littermates (TNT group) that also lacked maternal thyroid hormone but had normal fetal and neonatal thyroid function (panel D, right animal, 4 weeks old).

The OD images were analyzed using the public domain image analysis program from the National Institutes of Health-*Image* (available at rsb.info.nih.gov/nih-image; version 1.61). The areas to be measured were marked by an interactive density slice, which identifies structures based on a selected lower and upper density value. Tissue background was

defined as nonstaining tissue such as esophagus or cartilage tissue. Signal was defined as specific positive staining due to hybridization (signal in the alveolar epithelium or myocardium) (42, 43). The definitive signal value, expressed as mean OD, is obtained by subtracting the mean tissue background density from the mean signal density (42, 43). The positive signal is plotted as mean OD (± SEM) per group and age. The volume fraction of SP mRNA-expressing cells (% Area) was calculated from the area of positive staining cells in the section and the total lung area (excluding airspaces). All lung measurements were carried out three times with a randomized series of images. No differences were observed between the three measurements and, therefore, a mean value per lung was calculated. For the heart, the resulting specific OD values are displayed using a look-up table that indicates the intensity of the positive signal as fold tissue background.

Lung morphometry

Sections stained with haematoxylin and azophloxine were analyzed as described (44). Digital images were recorded with a high resolution CCD-color camera (DXC-151, Sony Inc., Park Ridge, NJ, U.S.A.) attached to a Microphot-FXA microscope (Nikon Inc., Melville, NY, U.S.A.) equipped with a 40x objective. The video image was overlain with a 42-point equidistant counting grid, calibrated with an individual probe length line Z, where Z = 20 µm. Lungs from control and TT mice were evaluated and analyzed in a blinded manner.

Volume fractions were established by counting test points falling on airspaces (volume fraction of airspaces: V_{Valv}) and alveolar septa (volume fraction of airspace walls: V_{Vsept}). Airspace number per unit volume (N_V) was calculated from the formula $N_V = K (N_A)^{3/2} / \beta (V_{Valv})^{1/2}$, where K is the size distribution coefficient (taken to be 1), $\beta = 1.55$, from the Weibel and Gomez shape constant and N_A is the number of airspaces (N_{alv}) per unit area of the counting grid ($A_T = 15{,}129\ \mu m^2$). Average airspace volume (AAV) was estimated from the following formula: $AAV = (V_{Valv}) / (N_V)$. Alveoli were defined as closed airspaces divided by septa in the periphery of the lung.

Statistics

In situ hybridization

Variation in staining intensity due to the different *in situ* hybridization sessions were removed by subtracting the session effects calculated from the log-transformed data with the general linear model ANOVA without interaction (SPSS version 10.0.7; SPSS Inc., Chicago, IL, U.S.A.). Differences between treatment and age groups (two animals per group per age) were tested with a two-way ANOVA. Because of significant age*treatment interactions, a one-way ANOVA per age group was carried out to determine which groups differed at that age.

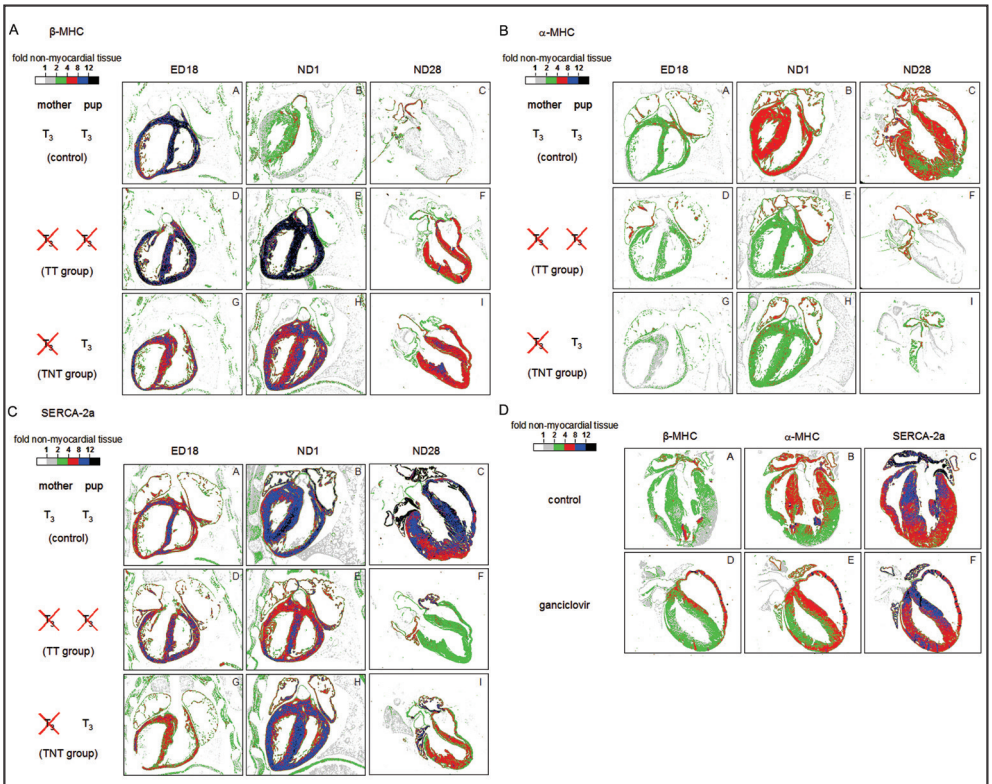

Figure 3. Effect of prenatal hypothyroidism on myosin heavy chain (MHC) and sarcoplasmatic-reticulum ATPase (SERCA-2a) gene expression in the heart. The control ventricle switched from expressing β-MHC (panel A, subpanels A-C) before birth to expressing α-MHC (panel B, subpanels A-C) shortly after birth. Meanwhile SERCA-2a expression was upregulated (panel C, subpanels A-C). In ganciclovir-treated transgenic (hypothyroid) offspring of hypothyroid transgenic mothers (TT group), β-MHC expression was maintained postnatally (panel A, subpanels D-F), whereas α-MHC expression (panel B, subpanels D-F) and SERCA-2a expression (panel C, subpanels D-F) were not upregulated. Note that β- and α-MHC expression, as well as SERCA-2a expression in the hearts of ganciclovir-treated non-transgenic (euthyroid) offspring of hypothyroid transgenic mothers (TNT group) behaved similarly to that in their hypothyroid transgenic littermates (TT group) (panels A-C, subpanels G-I). Ganciclovir treatment of wild-type mice did not affect β-, α-MHC, or SERCA-2a mRNA levels in the heart (panel D, ND28 hearts). Tissue mRNA staining was recorded and digital transmission images were converted to OD images.

Lung morphometry

Results are expressed as mean ± SEM (two animals per group per age). Statistical analysis of the morphometric data was performed using the unpaired *t* test, with $p < 0.05$ considered significant.

Results

Transgenic dams were treated with ganciclovir before pregnancy to ablate their thyroids as well as during pregnancy to ablate the thyroids of their transgenic fetuses (Fig. 1). In this study, three groups of fetuses and neonates were studied. The treated transgenic (TT) group included transgenic offspring from transgenic mothers. The mothers were made hypothyroid before pregnancy and the fetal thyroids were ablated *in utero*. As a result, the TT group lacked exposure to maternal and their own thyroid hormone. The treated nontransgenic (TNT) group included the nontransgenic littermates of the TT animals. The thyroids of TNT mice were not destroyed upon ganciclovir treatment, and as a result TNT mice lacked exposure to maternal thyroid hormone only (34). The control animals were offspring from nontransgenic dams and were hence exposed to both maternal and their own thyroid hormone, as well as to ganciclovir.

The efficacy of the ganciclovir treatment protocol, which was developed by Wallace *et al*. (36), was assessed by staining the thyroid remnants for the presence of thyroglobulin (Fig. 2). In control adult animals (panel A1) and fetuses (panel B1), strong staining for thyroglobulin was seen in the follicle cells of the thyroid. In the TT animals, the structure of the thyroid was disrupted and thyroglobulin staining was dramatically decreased and only seen in some remaining large follicles (panels A2 and B2). In accordance with these findings, blood T_4 levels in adult transgenic animals decreased from 41 nmol/l before ganciclovir treatment to 12 nmol/l 2 weeks after treatment (Fig. 2C). Finally, the ganciclovir-treated hypothyroid neonates (TT group) clearly lagged behind in growth compared to their nontransgenic littermates (TNT group) (Fig. 2D).

Heart

We studied heart development in control and transgenic mice at ED18, ND1, ND7, ND14, and ND28.

Myosin heavy chain mRNA

In ED18 hearts, β-MHC was strongly and similarly expressed in the ventricles of control, TT, and TNT fetuses (Fig. 3A, panels A, D, G). By ND1, β-MHC expression had decreased dramatically in the control group (panel B) and had become all but detectable at ND28 (panel C). In neonatal TT ventricles however, β-MHC expression remained unchanged (panel E). Moreover, β-MHC gene expression did not decrease in TNT neonates (panel H). At ND28, both TT and TNT animals still showed strong β-MHC expression in their ventricles (panels F and I). Ganciclovir treatment of wild-type embryos did not affect postnatal β-MHC expression in the heart (Fig. 3D, panels A and D).

In ED18 hearts, α-MHC expression in the ventricles was relatively low in all groups (Fig. 3B, panels A, D, G). At ND1, α-MHC expression was upregulated in the ventricular myocardium of controls (panel B) and remained high thereafter (panel C). In TT and TNT neonates however, α-MHC expression did not increase (panels E and H) but instead had even decreased by ND28 (panels F and I). Ganciclovir treatment of wild-type embryos did not prevent postnatal α-MHC expression in the heart (Fig. 3D, panels B and E).

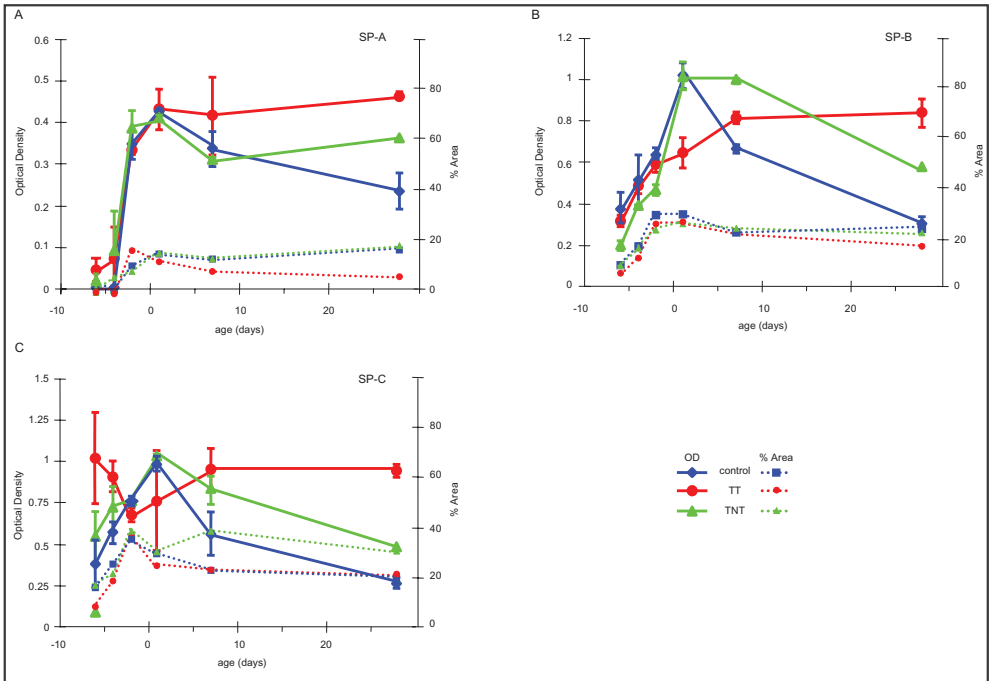

Figure 4. Quantification of SP-A, -B, and -C mRNA levels in perinatal lungs. Cellular concentrations (mean OD) of SP-A, -B, and -C are shown in panels A, B, and C, respectively. Mean ODs were determined by quantification of the in situ hybridization signal in the alveolar and bronchiolar epithelium, whereas the volume fraction of cells (% Area) expressing SP mRNA was calculated as a percentage of total lung tissue (staining and nonstaining tissue, excluding airspaces). The light absorption by the resulting silver grains and the volume fraction SP mRNA-positive cells are expressed on the y-axis as mean OD (full lines) and % Area (interrupted lines), respectively. TT mice are ganciclovir-treated transgenic (hypothyroid) offspring of hypothyroid transgenic mothers, whereas TNT mice are the nontransgenic littermates that also lacked maternal thyroid hormone, but had their own fetal and neonatal thyroid function. For mean OD: SP-A: one-way ANOVA at ND28: $p = 0.059$. SP-B: one-way ANOVA at ND7 and ND28: both $p < 0.05$. SP-C: $p = 0.01$ at ND28. The volume fraction of SP mRNA-positive cells (% Area) did not differ between the three groups except at ND 7 in the TNT group.

Sarcoplasmatic Reticulum ATPase-2a and phospholamban mRNA

In control mice, ventricular SERCA-2a mRNA levels were lower before than 1 day after birth (Fig. 3C, panels A and B). By ND28, SERCA-2a levels had increased only marginally compared to ND1 (panel C). In hypothyroid TT mice, ventricular SERCA-2a did not increase after birth (panel E) and had even decreased by ND28 (panel F). In the TNT neonates, SERCA-2a mRNA

levels had increased slightly at ND1 (panel H), but as in the TT mice, subsequently declined (panel I). PLB mRNA levels slightly increased perinatally in all groups (not shown), but in contrast to the controls, PLB mRNA levels did not decline in the next 4 weeks in the TT and TNT groups (not shown). Ganciclovir treatment of wild-type embryos did not affect fetal or postnatal SERCA-2a (Fig. 3D, panels C and F) or PLB (not shown) expression in the heart.

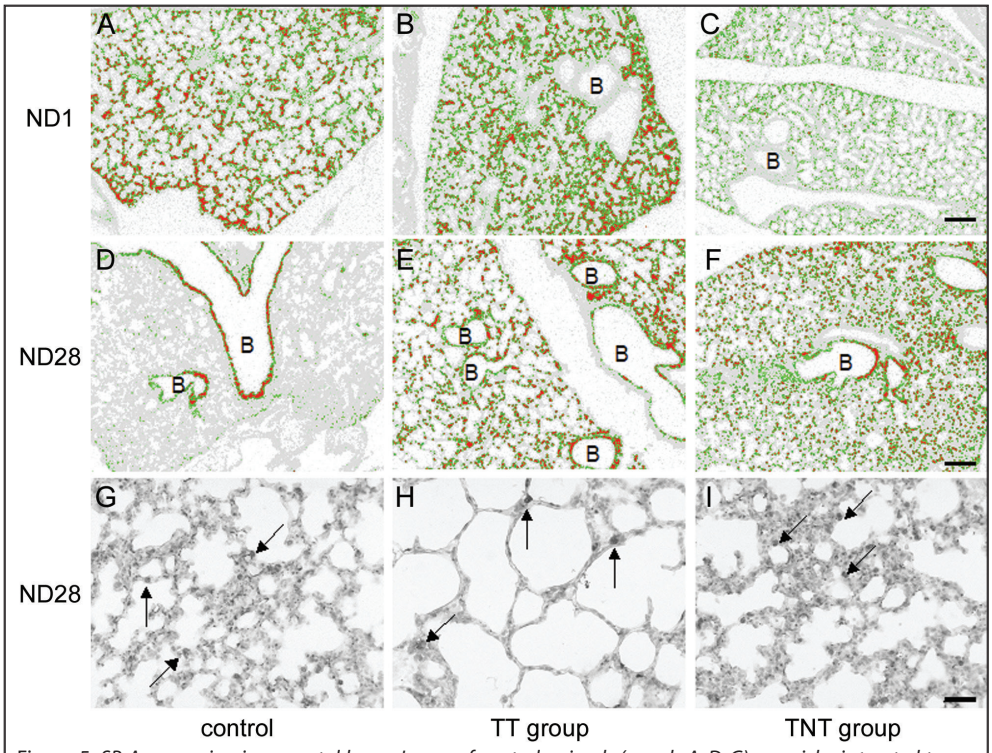

Figure 5. *SP-A expression in neonatal lungs. Lungs of control animals (panels A, D, G), ganciclovir-treated transgenic (hypothyroid) offspring of hypothyroid transgenic mothers (TT group; panels B, E, H), and their nontransgenic littermates that lacked maternal thyroid hormone but had their own fetal and neonatal thyroid function (TNT group; panels C, F, I) at ND1 (panels A-C) and ND28 (panels D-I). Panels A-F were stained for the presence of SP-A mRNA, whereas panels G-I were stained for the presence of SP-A protein. Note the increased SP-A mRNA expression in alveolar epithelium of TT and TNT lungs (panels E, F, respectively) compared to control lungs (panel D) at ND28 and comparable SP-A protein staining intensity between the three groups (panels G-I). "B" represents bronchiole. Arrows (panels G-I) indicate SP-A-positive cells. Bar (A-F): 200 µm and (G-I): 50 µm.*

LUNG

We studied lung development in control and transgenic mice at ED14, ED16, ED18, ND1, ND7, ND14, and ND28. Before birth the experimental groups showed only marginal differences. ND7 and ND14 mice have intermediate staining patterns for the different surfactant proteins between ND1 and ND28 (not shown).

Surfactant protein mRNA

SP-A mRNA was undetectable at ED14, but its cellular concentration (mean OD) rapidly increased in the epithelial cells of the lung in all three groups between ED16 and ND1 (Fig. 4A, full lines). After ND1, the cellular concentration of SP-A mRNA declined in the control and TNT groups, whereas it remained high in the TT group (Fig. 4A, full lines; one-way ANOVA for difference between groups at ND28: $p = 0.059$). The volume fraction of cells (% Area) expressing SP-A mRNA was similar between all three groups (Fig. 4A, interrupted lines). Prenatally (not shown) and during the first postnatal week (Fig. 5, panels A-C), SP-A mRNA expression was confined to alveolar epithelial cells. In control animals, SP-A mRNA expression subsequently became concentrated in bronchiolar epithelial cells (Fig. 5, panel D). However, in TT (Fig. 5, panel E) and TNT lungs (Fig. 5, panel F), SP-A mRNA remained abundantly expressed throughout the alveolar epithelium, whereas expression in bronchiolar epithelial cells remained less pronounced than in the control animals. The SP-A protein staining intensity was comparable among control, TT, and TNT lungs at ND28 (Fig. 5, panels G-I). Note, however, that the alveolar spaces in TT animals were much larger than in control or TNT animals, indicating abnormal structural development of TT lungs.

Before birth, the cellular concentration (mean OD) of SP-B mRNA increased similarly in all groups (Fig. 4B, full lines). However, in ND1 neonates, the cellular concentration for SP-B mRNA was significantly lower in the TT group than in the control or TNT groups (Fig. 4B, full lines). Due to a steep decline in SP-B mRNA content in control lungs, the SP-B mRNA content in TT and TNT lungs became significantly higher than in controls at ND7 and ND28 (one-way ANOVA: both $p < 0.05$). Pre- and postnatally (Fig. 6, panels A-C), SP-B mRNA was present in both alveolar and bronchiolar epithelium of all groups. Bronchiolar SP-B mRNA levels were similar between the three groups, whereas alveolar SP-B mRNA expression remained high in TT and TNT lungs (Fig. 6, panels E and F) when compared to controls (Fig. 6, panel D). The volume fraction of SP-B-positive cells (% Area) was similar in all groups (Fig. 4B, interrupted lines). Also, the staining intensity for SP-B protein was similar in all groups at all the gestational ages investigated (Fig. 6, panel G-I).

SP-C mRNA was already detectable in ED14 lungs (Fig. 4C, full lines). At that age, SP-C mRNA was only expressed in alveolar epithelial cells and this expression pattern remained unchanged throughout lung development in all three groups (Fig. 7, panels A-F). A pronounced decline in the cellular concentration (mean OD) of SP-C mRNA was observed in neonatal controls, whereas the mean OD for SP-C mRNA in the TT group remained high, with the TNT group occupying an intermediate position (Fig. 4C, full lines) (one-way ANOVA at ND28: $p = 0.01$). The volume fraction of cells (% Area) expressing SP-C mRNA was similar in all groups except at ND7 in the TNT group (Fig. 4C, interrupted lines). After birth, the staining intensity for proSP-C protein was always lower in TT lungs (Fig. 7, panel H) than in control or TNT lungs (Fig. 7, panels G and I, respectively).

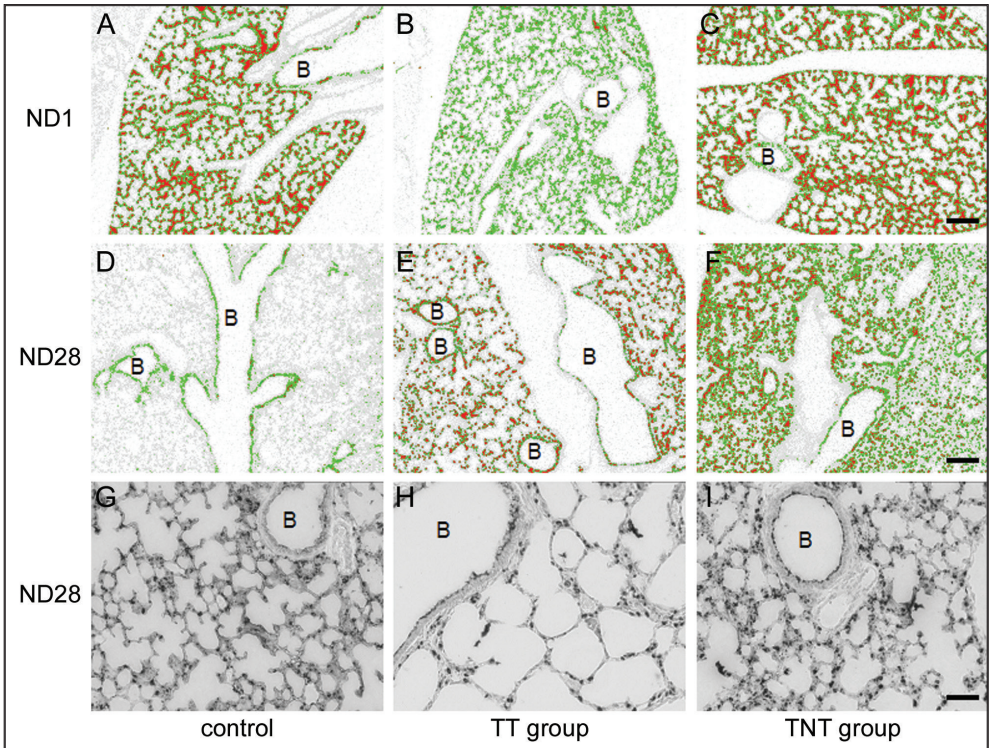

Figure 6. SP-B expression in neonatal lungs. Lungs of control animals (panels A, D, G), ganciclovir-treated transgenic (hypothyroid) offspring of hypothyroid transgenic mothers (TT group; panels B, E, H), and their nontransgenic littermates that lacked maternal thyroid hormone but had their own fetal and neonatal thyroid function (TNT group; panels C, F, I) at ND1 (panels A-C) and ND28 (panels D-I). Panels A-F were stained for the presence of SP-B mRNA, whereas panels G-I were stained for the presence of SP-B protein. Note the increased SP-B mRNA expression in the alveolar epithelium of TT and TNT lungs (panels E, F, respectively) when compared to control lungs (panel D) at ND28 and decreased SP-B mRNA expression in TT lungs at ND1 (panel B). SP-B protein staining intensity was comparable between the three groups (panels G-I). "B" represents bronchiole. Bar (A-F): 200 µm and (G-I): 50 µm.

Structural development

The morphometric analysis was carried out for the TT (hypothyroid) and the control groups only. Morphologically, there were no gross differences between control and hypothyroid lungs before birth. However, after birth, when the alveolar phase of lung development takes place, the hypothyroid lungs showed progressively larger airspaces, with less alveolar septa compared to control and TNT lungs (Figs. 5-7; compare panels H (TT group) with panels G (control group) and I (TNT group). No evidence of hemorrhage or inflammation was observed in either group. Three morphometric parameters were used to quantify the morphologic differences between control and hypothyroid lungs: the number of airspaces per unit volume (N_V), the volume fraction of septa (V_{Vsept}), and average airspace volume per μm^3 (AAV). N_V was significantly reduced in postnatal hypothyroid lungs (Fig. 8A). At the same time, the AAV of an individual hypothyroid airspace was three- to fourfold larger

than in comparable control lungs (Fig. 8B). Together with the two- to threefold decrease in the contribution of V_{Vsept} in hypothyroid lungs (Fig. 8C), these data show that the postnatal hypothyroid animals have decreased alveolar septation resulting in large saclike alveoli that resemble emphysema. The apparent inhibition of alveolar septation suggests an important role for thyroid hormone in the postnatal structural maturation of the lungs.

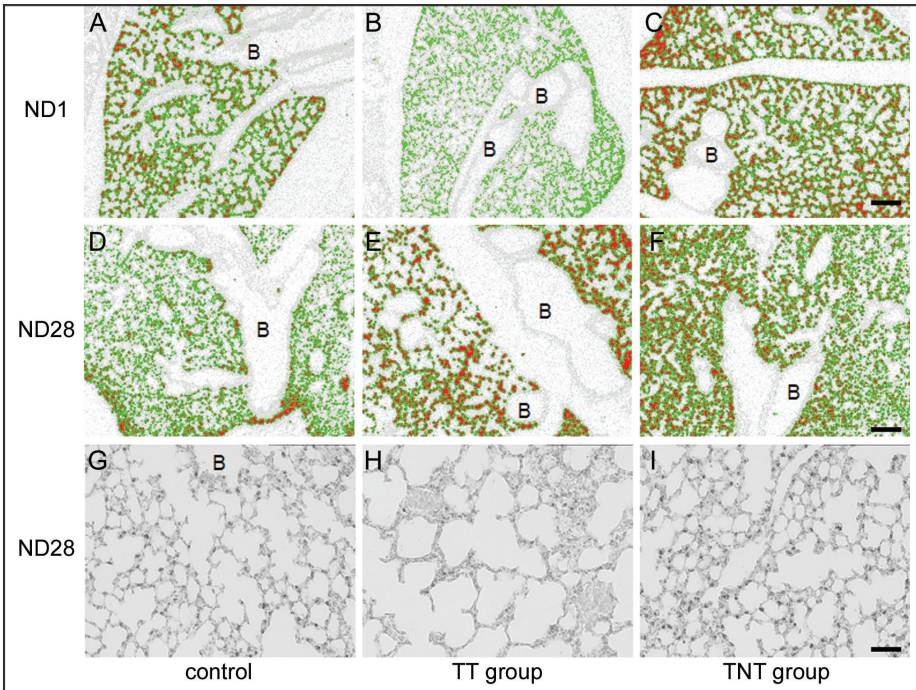

Figure 7. SP-C expression in neonatal lungs. Lungs of control animals (panels A, D, G), ganciclovir-treated transgenic (hypothyroid) offspring of hypothyroid transgenic mothers (TT group; panels B, E, H), and their nontransgenic littermates that lacked maternal thyroid hormone but had their own fetal and neonatal thyroid function (TNT group; panels C, F, I) at ND1 (panels A-C) and ND28 (panels D-I). Panels A-F were stained for the presence of SP-C mRNA, whereas panels G-I were stained for the presence of proSP-C protein. Note the increased SP-C mRNA expression in the alveolar epithelium of TT and TNT lungs (panels E, F, respectively) compared to control lungs (panel D) at ND28 and decreased SP-C mRNA expression at ND1 in TT lungs (panel B). proSP-C protein staining intensity was less in TT lungs (panel H) compared to control and TNT lungs at ND28 (panels G, I, respectively). "B" represents bronchiole. Bar (A-F): 200 µm and (G-I): 50 µm.

DISCUSSION

The importance of a functioning thyroid gland for normal postnatal development is clear from the severe mental retardation that develops in newborns with congenital hypothyroidism (45). If T_4 supplementation is started within two weeks after birth, the athyroid newborn is completely rescued from neurological damage (5, 46). Such data have suggested that the availability of thyroid hormone to the fetus was of minimal importance for normal prenatal development. The high deiodinase type III activity of the placenta

(47-49), together with the very low circulating T_3 level in the fetus (50), supported this line of thought. Nevertheless, the neurological cretinism that results from severe iodine deficiency during early pregnancy (4, 51), clearly demonstrates that thyroid hormone does play an important role in the normal development of most vertebrate tissues, in particular the brain (52). Because T_4 was shown to be present in the fetus before the fetal thyroid is capable of producing it, it was concluded that thyroid hormone of maternal origin could pass the placenta despite the high deiodinase activity in this organ (53). More recently, it was further demonstrated that (subclinical) maternal hypothyroidism during early pregnancy can cause neurological deficits in the offspring, even when the mother and offspring are euthyroid at birth (6, 8, 9).

Based on the outcome of these studies, we wondered whether maternal hypothyroidism during early pregnancy might also affect the postnatal development of organs other than the brain, that is, heart and lungs. We chose the TG-TKT2 transgenic mouse model as described by Ellison and co-workers (33) to investigate this question. We demonstrated that also in our hands the administration of ganciclovir to these transgenic mice resulted in an almost complete destruction of the thyroidal follicle cells and a dramatic decrease in circulating T_4 levels. The earlier conclusion that T_4 levels became undetectable after ganciclovir treatment of these mice (36) was due to the lower sensitivity of the assay used at the time. With the same assay, circulating T_4 was below the limit of detection in TT pups, whereas that in TNT littermates was normal (34).

Our study showed that in the heart, the neonatal switch from β-MHC to α-MHC expression in the cardiac ventricles did not occur in either the TT (thyroid destroyed) or TNT (intact thyroid) group, even though thyroid hormone production in the latter group was intact (34). Similarly, SERCA-2a expression declined postnatally in the TT and TNT groups compared to controls, although the effect was less pronounced in the TNT than in the TT group. Tissue architecture of perinatal hearts was not affected by the experimental conditions. Similarly, lung development up to the saccular phase (ED18-ND5) was not affected by maternal or fetal hypothyroidism. Our histological data (Figs. 5-7, panels G-I and Fig. 8), in conjunction with those in the hypothyroid "hyt" mouse model (54), do indicate however that alveolar formation, that is, postnatal lung development, was affected by postnatal thyroid hormone deficiency. In agreement with the largely normal structural development of the lungs in control, TT, and TNT fetuses, we did not observe differences in prenatal SP expression between these groups. After birth, the cellular concentration of SP-A, -B, and -C mRNA remained high in the alveolar epithelium of TT and, to a lesser extent, of TNT lungs compared to control lungs. Had we related the levels of gene expression to a global tissue base, such as organ weight or protein content, the altered expression pattern of SP-A and -B in the distal epithelium of the hypothyroid animals would have escaped our attention. This finding underlines the suitability of the quantitative *in situ* hybridization technique to measure differences in cellular mRNA concentration in the context of both the changing

tissue architecture and the changing topographic pattern of a gene expression (42, 43, 55). Despite high cellular SP mRNA levels, the staining intensity for the corresponding proteins was not increased. In perinatal liver, like the lungs, a derivate of the embryonic foregut, such comparatively high mRNA-protein ratios reflect immaturity (56). Together, these data indicate that alveolar morphogenesis is sensitive to postnatal thyroid hormone deficiency, but that tissue maturation as reflected by cellular SP mRNA concentrations is, in addition, also affected by embryonic thyroid hormone deficiency.

These observations confirm earlier claims that thyroid hormone is an important determinant for perinatal lung development (57, 58) but at the same time demonstrate that the effects of hypothyroidism on lung development are virtually undetectable before birth and only become overt after birth. Also, our results demonstrate that hypothyroidism (maternal and/or fetal) does result in the maintenance of relatively high mRNA concentrations and high SP mRNA-protein ratios for all three SPs and no evidence for an SP-A and -B deficiency after birth. These findings may therefore explain the lack of effect of prenatal thyroid hormone treatment to prevent postnatal respiratory distress syndrome (59, 60). The limited role of thyroid hormone in prenatal heart and lung development is also underscored by the relatively normal prenatal development of mice that are devoid of all known thyroid hormone receptors (61).

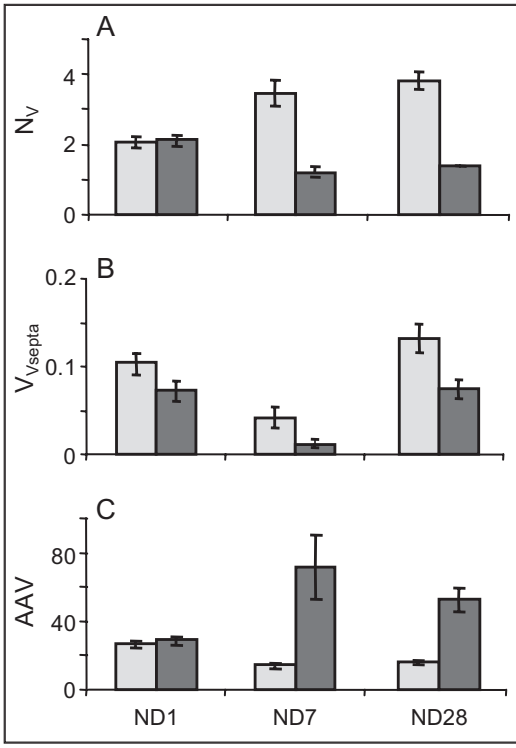

Figure 8. *Morphometry of neonatal lungs. The number of airspaces per unit volume (N_V, panel A), the volume fraction of septa (V_{Vsept}*10^2, panel B), and the average airspace volume per μm^3 (AAV*10^4, panel C) in control mice (light bars) and in ganciclovir-treated transgenic (hypothyroid) offspring of hypothyroid transgenic mothers (TT group, dark bars) were determined at ND1, ND7, and ND28. At ND7 and ND28, hypothyroid mice showed a statistically significant increase in AAV and a statistically significant decrease in V_{Vsept} and N_V compared to control mice, indicating the presence of poorly septated lungs with large alveoli in postnatal hypothyroid mice. At ND7 and ND28, N_V, V_{Vsept}, and AAV of TT mice differ from those in wild-type mice ($p < 0.05$).*

Our key finding that nontransgenic neonates (with intact thyroids) from hypothyroid mothers have a similar early postnatal phenotype as their transgenic littermates (with destroyed thyroids) is remarkable. Our observations do not distinguish in the nontransgenic neonates (intact thyroid) between a hypothyroid state and a euthyroid state with "peripheral" resistance to thyroid hormone as a result of maternal hypothyroidism. However, several observations argue in favor of the second mechanism. At 3 weeks after birth, transgenic pups (destroyed thyroid) from ganciclovir-treated dams had undetectable levels of $T_{4,}$ whereas their nontransgenic littermates (intact thyroid) had normal T_4 levels (34). Also, growth during the first 10 days after birth was dominated by the T_4 status of the dam during gestation (35). Likewise, the brains of wild-type pups that were born to hypothyroid TG-TKT2 dams were just as deficient in oligodendrocytes as the brains of their hypothyroid transgenic littermates (62), suggesting that maternal thyroid hormone acts early in pregnancy to influence oligodendrocyte development and that the consequences of deprivation of thyroid hormone early in pregnancy on postnatal oligodendrocyte development are not reversed by thyroid hormone production in the fetal thyroid. Similarly, administration of inhibitors of thyroid-hormone synthesis to dams before and during early pregnancy suppressed neuroendocrine-specific protein (NSP-A) expression in the fetal brain cortex before the onset of thyroid function in the rat fetus on gestational day 17 (63).

A conceptual context for the development of a euthyroid state with peripheral resistance to thyroid hormone as a result of maternal hypothyroidism became available when it was shown that expression of α-internexin persisted in euthyroid fetuses born to hypothyroid (thyroidectomized) dams, but not in those born to euthyroid dams (64). α-Internexin is the first neuronal intermediate filament to be expressed in newly differentiating neurons and constitutes the major neural intermediate filament prior to the onset of fetal thyroid hormone secretion. Failure of α-internexin to decline in late fetal life may have serious consequences if not corrected soon after birth, because overexpression of α-internexin in transgenic mice is associated with deficits in motor coordination (64). Together, these findings show that the fetal thyroid is not able to rescue the deleterious effects of early maternal hypothyroidism and argue in favor of a euthyroid state with peripheral thyroid hormone resistance rather than a deficiency of thyroid hormone itself in postnatal offspring with an intact thyroid that are born to hypothyroid dams.

A rescue experiment with thyroid hormone supplementation to the pregnant dam would have added elegance to our arguments. However, such a rescue experiment is not straightforward because it appears almost impossible to predict T_4 levels in a fetus upon T_4 administration to the dam. Infusion of T_4 into methimazole-treated hypothyroid dams resulted in maternal euthyroidism, but fetal plasma T_4 did not exceed 40% of normal and plasma TSH remained high (65). Titration of T_4 over time was also difficult in such rats because serum T_4 levels initially stayed rather low during T_4 substitution but then increased

rapidly but transiently, with TSH remaining high despite T_4 substitution (66). Moreover, when T_4 levels normalized, T_3 levels remained low and TSH levels elevated, whereas the transport of T_4 from plasma to organs was decreased in pregnant thyroidectomized rats compared to euthyroid pregnant dams, even after thyroid hormone treatment (67). In our view, a rescue experiment with T_4 is therefore complex and may not produce clear answers.

It is obvious that thyroid hormone deficiency is more detrimental to a developing organism than a deficiency of nuclear thyroid hormone receptors (51, 61, 68). This conclusion suggests that the detrimental effect of maternal thyroid hormone deficiency on the fetus is caused by a biological effect of thyroid hormone nuclear receptors that are not occupied by their ligand (69) or alternatively does not require thyroid hormone signaling via thyroid hormone nuclear receptors. Additional possibilities are that the effect is mediated by a different isoform of the steroid hormone nuclear receptor family, or that maternally derived thyroid hormone determines the set point for the number and/or the isoform of thyroid hormone receptors expressed in a developing organ. Based on our key finding that prenatal deficiency of maternally derived thyroid hormone affects postnatal responses in cardiac and pulmonary gene expression, we favor the first and last alternatives over the other two possibilities.

Our finding that hypothyroidism during early development does not impair organ morphogenesis but does affect adaptive responses in gene expression in these organs postnatally is especially important in the light of recent studies that describe a negative effect of (undetected) maternal hypothyroidism on brain development (6, 8, 9). A free T_4 concentration below the 10^{th} percentile at 12 weeks gestation was a significant risk factor for impaired psychomotor development of the children at 10 months of age (9). Furthermore, children born to women with an undiagnosed (mild) hypothyroidism performed less well on IQ tests at 7-9 years of age (8). Accordingly, we hypothesize that maternal hypothyroidism also causes changes in gene expression in the fetal heart and lungs that cannot be reversed by fetal and/or neonatal thyroid hormone.

Acknowledgements

We are indebted to Dr. J.J.M. de Vijlder (Department of Pediatric Endocrinology, Emma Children's Hospital, Academic Medical Center, University of Amsterdam, Amsterdam, The Netherlands) and Dr. J.A. Whitsett (The Children's Hospital Research Foundation, Division of Neonatology and Pulmonary Biology, Cincinnati, OH, U.S.A.) for providing valuable antibodies and cDNAs, to E. Endert (Department of Endocrinology, Academic Medical Center, University of Amsterdam, Amsterdam, The Netherlands) for kindly assaying T_4 levels, and to Ms. Paula Blair for technical assistance with immunohistochemistry for SP-B and proSP-C. M. van Tuyl was supported by a student's grant, P.J.E. Blommaart was supported by the Sophia Foundation and the Ludgardina Bouman Foundation, and S.E. Wert was supported, in part, by National Institutes of Health grant HL56387.

References

1. Thorpe-Beeston JG, Nicolaides KH, Felton CV, Butler J, McGregor AM, 1991. Maturation of the secretion of thyroid hormone and thyroid-stimulating hormone in the fetus. N Engl J Med. 324:532-536.

2. Calvo R, Obregon MJ, Escobar del Rey F, Morreale de Escobar G, 1992. The rat placenta and the transfer of thyroid hormones from the mother to the fetus. Effects of maternal thyroid status. Endocrinology. 131:357-365.

3. Fisher DA, Klein AH, 1981. Thyroid development and disorders of thyroid function in the newborn. N Engl J Med. 304:702-712.

4. Delange F, 2001. Iodine deficiency as a cause of brain damage. Postgrad Med J. 77:217-220.

5. Bongers-Schokking JJ, Koot HM, Wiersma D, Verkerk PH, de Muinck Keizer-Schrama SM, 2000. Influence of timing and dose of thyroid hormone replacement on development in infants with congenital hypothyroidism. J Pediatr. 136:292-297.

6. Morreale de Escobar G, Obregon MJ, Escobar del Rey F, 2000. Is neuropsychological development related to maternal hypothyroidism or to maternal hypothyroxinemia? J Clin Endocrinol Metab. 85:3975-3987.

7. Glinoer D, Delange F, 2000. The potential repercussions of maternal, fetal, and neonatal hypothyroxinemia on the progeny. Thyroid. 10:871-887.

8. Haddow JE, Palomaki GE, Allan WC, Williams JR, Knight GJ, Gagnon J, O'Heir CE, Mitchell ML, Hermos RJ, Waisbren SE, Faix JD, Klein RZ, 1999. Maternal thyroid deficiency during pregnancy and subsequent neuropsychological development of the child. N Engl J Med. 341:549-555.

9. Pop VJ, Kuijpens JL, van Baar AL, Verkerk G, van Son MM, de Vijlder JJ, Vulsma T, Wiersinga WM, Drexhage HA, Vader HL, 1999. Low maternal free thyroxine concentrations during early pregnancy are associated with impaired psychomotor development in infancy. Clin Endocrinol. 50:149-155.

10. Fisher DA, Nelson JC, Carlton EI, Wilcox RB, 2000. Maturation of human hypothalamic-pituitary-thyroid function and control. Thyroid. 10:229-234.

11. Mahdavi V, Izumo S, Nadal-Ginard B, 1987. Developmental and hormonal regulation of sarcomeric myosin

heavy chain gene family. Circ Res. 60:804-814.

12. Gustafson TA, Markham BE, Morkin E, 1986. Effects of thyroid hormone on alpha-actin and myosin heavy chain gene expression in cardiac and skeletal muscles of the rat: measurement of mRNA content using synthetic oligonucleotide probes. Circ Res. 59:194-201.

13. Lompré AM, Nadal-Ginard B, Mahdavi V, 1984. Expression of the cardiac ventricular alpha- and beta-myosin heavy chain genes is developmentally and hormonally regulated. J Biol Chem. 259:6437-6446.

14. Chizzonite RA, Zak R, 1984. Regulation of myosin isoenzyme composition in fetal and neonatal rat ventricle by endogenous thyroid hormones. J Biol Chem. 259:12628-12632.

15. Arai M, Otsu K, MacLennan DH, Alpert NR, Periasamy M, 1991. Effect of thyroid hormone on the expression of mRNA encoding sarcoplasmic reticulum proteins. Circ Res. 69:266-276.

16. Rohrer D, Dillmann WH, 1988. Thyroid hormone markedly increases the mRNA coding for sarcoplasmic reticulum Ca2+-ATPase in the rat heart. J Biol Chem. 263:6941-6944.

17. Kiss E, Jakab G, Kranias EG, Edes I, 1994. Thyroid hormone-induced alterations in phospholamban protein expression. Regulatory effects on sarcoplasmic reticulum Ca2+ transport and myocardial relaxation. Circ Res. 75:245-251.

18. Moorman AF, Schumacher CA, de Boer PA, Hagoort J, Bezstarosti K, van den Hoff MJ, Wagenaar GT, Lamers JM, Wuytack F, Christoffels VM, Fiolet JW, 2000. Presence of functional sarcoplasmic reticulum in the developing heart and its confinement to chamber myocardium. Dev Biol. 223:279-290.

19. Reed TD, Babu GJ, Ji Y, Zilberman A, Ver Heyen M, Wuytack F, Periasamy M, 2000. The expression of SR calcium transport ATPase and the Na(+)/Ca(2+)Exchanger are antithetically regulated during mouse cardiac development and in Hypo/hyperthyroidism. J Mol Cell Cardiol. 32:453-464.

20. Cernohorsky J, Kolar F, Pelouch V, Korecky B, Vetter R, 1998. Thyroid control of sarcolemmal Na+/Ca2+ exchanger and SR Ca2+-ATPase in developing rat heart. Am J Physiol. 275:H264-273.

21. Massaro D, Massaro GD, 2002. Invited Review: pulmonary alveoli: formation, the "call for oxygen," and other regulators. Am J Physiol Lung Cell Mol Physiol. 282:L345-358.

22. Stein SA, Oates EL, Hall CR, Grumbles RM, Fernandez LM, Taylor NA, Puett D, Jin S, 1994. Identification of a point mutation in the thyrotropin receptor of the hyt/hyt hypothyroid mouse. Mol Endocrinol. 8:129-138.

23. deMello DE, Heyman S, Govindarajan R, Sosenko IR, Devaskar UP, 1994. Delayed ultrastructural lung maturation in the fetal and newborn hypothyroid (Hyt/Hyt) mouse. Pediatr Res. 36:380-386.

24. Moya FR, Sanchez I, Baudy D, 1992. Effects of betamethasone and thyroid hormone on fetal rat lung maturation in vivo. Dev Pharmacol Ther. 18:14-19.

25. Nichols KV, Floros J, Dynia DW, Veletza SV, Wilson CM, Gross I, 1990. Regulation of surfactant protein A mRNA by hormones and butyrate in cultured fetal rat lung. Am J Physiol. 259:L488-495.

26. Yokoyama N, Takada S, Uetani Y, Nakamura H, 1995. Effects of maternal administration of dexamethasone and thyrotropin- releasing hormone on fetal rat pulmonary surfactant synthesis. Biol Neonate. 68:39-46.

27. Veletza SV, Nichols KV, Gross I, Lu H, Dynia DW, Floros J, 1992. Surfactant protein C: hormonal control of SP-C mRNA levels in vitro. Am J Physiol. 262:L684-687.

28. Floros J, Gross I, Nichols KV, Veletza SV, Dynia D, Lu HW, Wilson CM, Peterec SM, 1991. Hormonal effects on the surfactant protein B (SP-B) mRNA in cultured fetal rat lung. Am J Respir Cell Mol Biol. 4:449-454.

29. Ansari MA, de Mello DE, Devaskar UP, 2000. Effect of prenatal glucocorticoid on fetal lung ultrastructural maturation in hyt/hyt mice with primary hypothyroidism. Biol Neonate. 77:29-36.

30. Archavachotikul K, Ciccone TJ, Chinoy MR, Nielsen HC, Volpe MV, 2002. Thyroid hormone affects embryonic mouse lung branching morphogenesis and cellular differentiation. Am J Physiol Lung Cell Mol Physiol. 282:L359-369.

31. Bernal J, Pekonen F, 1984. Ontogenesis of the nuclear 3,5,3'-triiodothyronine receptor in the human fetal brain. Endocrinology. 114:677-679.

32. Gonzales LW, Ballard PL, 1981. Identification and characterization of nuclear 3,5,3'-triiodothyronine-binding sites in fetal human lung. J Clin Endocrinol Metab. 53:21-28.

33. Ellison AR, Wallace H, al-Shawi R, Bishop JO, 1995. Different transmission rates of herpesvirus thymidine kinase reporter transgenes from founder male parents and male parents of subsequent generations. Mol Reprod Dev. 41:425-434.

34. Wallace H, McLaren K, al-Shawi R, Bishop JO, 1994. Consequences of thyroid hormone deficiency induced by the specific ablation of thyroid follicle cells in adult transgenic mice. J Endocrinol. 143:107-120.

35. Wallace H, Pate A, Bishop JO, 1995. Effects of perinatal thyroid hormone deprivation on the growth and behaviour of newborn mice. J Endocrinol. 145:251-262.

36. Wallace H, Ledent C, Vassart G, Bishop JO, al-Shawi R, 1991. Specific ablation of thyroid follicle cells in adult transgenic mice. Endocrinology. 129:3217-3226.

37. Zhou L, Lim L, Costa RH, Whitsett JA, 1996. Thyroid transcription factor-1, hepatocyte nuclear factor-3beta, surfactant protein B, C, and Clara cell secretory protein in developing mouse lung. J Histochem Cytochem. 44:1183-1193.

38. Moorman AF, Vermeulen JL, Koban MU, Schwartz K, Lamers WH, Boheler KR, 1995. Patterns of expression of sarcoplasmic reticulum Ca(2+)-ATPase and phospholamban mRNAs during rat heart development. Circ Res. 76:616-625.

39. Korfhagen TR, Bruno MD, Glasser SW, Ciraolo PJ, Whitsett JA, Lattier DL, Wikenheiser KA, Clark JC, 1992. Murine pulmonary surfactant SP-A gene: cloning, sequence, and transcriptional activity. Am J Physiol. 263: L546-554.

40. D'Amore-Bruno MA, Wikenheiser KA, Carter JE, Clark JC, Whitsett JA, 1992. Sequence, ontogeny, and cellular localization of murine surfactant protein B mRNA. Am J Physiol. 262:L40-47.

41. Glasser SW, Korfhagen TR, Bruno MD, Dey C, Whitsett JA, 1990. Structure and expression of the pulmonary surfactant protein SP-C gene in the mouse. J Biol Chem. 265:21986-21991.

42. Moorman AF, De Boer PA, Ruijter JM, Hagoort J, Franco D, Lamers WH, 2000. Radio-isotopic in situ hybridization on tissue sections. Practical aspects and quantification. Methods Mol Biol. 137:97-115.

43. Jonker A, de Boer PA, van den Hoff MJ, Lamers WH, Moorman AF, 1997. Towards quantitative in situ hybridization. J Histochem Cytochem. 45:413-423.

44. Hedrick HL, Kaban JM, Pacheco BA, Losty PD, Doody DP, Ryan DP, Manganaro TF, Donahoe PK, Schnitzer JJ, 1997. Prenatal glucocorticoids improve pulmonary morphometrics in fetal sheep with congenital diaphragmatic hernia. J Pediatr Surg. 32:217-221.

45. Foley JP, Jr: Congenital hypothyroidism. In Braverman LE,Utiger RD (eds): Werner & Ingbar's the thyroid: a fundamental and clinical text, 8th 8th, p 977-983. Philadelphia, Lippincott-Williams & Wilkins, 2000.

46. van Vliet G, 2001. Treatment of congenital hypothyroidism. Lancet. 358:86-87.

47. Burrow GN, Fisher DA, Larsen PR, 1994. Maternal and fetal thyroid function. N Engl J Med. 331:1072-1078.

48. Koopdonk-Kool JM, de Vijlder JJ, Veenboer GJ, Ris-Stalpers C, Kok JH, Vulsma T, Boer K, Visser TJ, 1996. Type II and type III deiodinase activity in human placenta as a function of gestational age. J Clin Endocrinol Metab. 81:2154-2158.

49. Santini F, Chiovato L, Ghirri P, Lapi P, Mammoli C, Montanelli L, Scartabelli G, Ceccarini G, Coccoli L, Chopra IJ, Boldrini A, Pinchera A, 1999. Serum iodothyronines in the human fetus and the newborn: evidence for an important role of placenta in fetal thyroid hormone homeostasis. J Clin Endocrinol Metab. 84:493-498.

50. Polk DH, 1995. Thyroid hormone metabolism during development. Reprod Fertil Dev. 7:469-477.

51. Cao XY, Jiang XM, Dou ZH, Rakeman MA, Zhang ML, O'Donnell K, Ma T, Amette K, DeLong N, DeLong GR, 1994. Timing of vulnerability of the brain to iodine deficiency in endemic cretinism. N Engl J Med. 331:1739-1744.

52. Porterfield SP, Hendrich CE, 1993. The role of thyroid hormones in prenatal and neonatal neurological development--current perspectives. Endocr Rev. 14:94-106.

53. Vulsma T, Gons MH, de Vijlder JJ, 1989. Maternal-fetal transfer of thyroxine in congenital hypothyroidism due to a total organification defect or thyroid agenesis. N Engl J Med. 321:13-16.

54. Beamer WJ, Eicher EM, Maltais LJ, Southard JL, 1981. Inherited primary hypothyroidism in mice. Science. 212:61-63.

55. Ruijter JM, Hagoort J, De Boer PA, Moorman AFM, 2001. Calibration of densitometry in radio-isotopic in situ hybridization. Image Anal Stereol. 20:219-224.

56. Lamers WH, Boon L, Van Hemert FJ, Labruyere WT, De Jong P, Ruijter JM, Moorman AF, 1999. Glutamine synthetase expression in perinatal spiny mouse liver. Eur J Biochem. 262:803-809.

57. Massaro D, Teich N, Massaro GD, 1986. Postnatal development of pulmonary alveoli: modulation in rats by thyroid hormones. Am J Physiol. 250:R51-R55.

58. Holt J, Canavan JP, Goldspink DF, 1993. The influence of thyroid hormones on the growth of the lungs in perinatal rats. Int J Dev Biol. 37:467-472.

59. Ballard RA, Ballard PL, Cnaan A, Pinto-Martin J, Davis DJ, Padbury JF, Phibbs RH, Parer JT, Hart MC, Mannino FL, Sawai SK, 1998. Antenatal thyrotropin-releasing hormone to prevent lung disease in preterm infants. North American Thyrotropin-Releasing Hormone Study Group. N Engl J Med. 338:493-498.

60. ACTOBAT, 1995. Australian collaborative trial of antenatal thyrotropin-releasing hormone (ACTOBAT) for prevention of neonatal respiratory disease. Lancet. 345:877-882.

61. Göthe S, Wang Z, Ng L, Kindblom JM, Barros AC, Ohlsson C, Vennström B, Forrest D, 1999. Mice devoid of all known thyroid hormone receptors are viable but exhibit disorders of the pituitary-thyroid axis, growth, and bone maturation. Genes Dev. 13:1329-1341.

62. Ahlgren SC, Wallace H, Bishop J, Neophytou C, Raff MC, 1997. Effects of thyroid hormone on embryonic oligodendrocyte precursor cell development in vivo and in vitro. Mol Cell Neurosci. 9:420-432.

63. Dowling AL, Iannacone EA, Zoeller RT, 2001. Maternal hypothyroidism selectively affects the expression of neuroendocrine-specific protein A messenger ribonucleic acid in the proliferative zone of the fetal rat brain cortex. Endocrinology. 142:390-399.

64. Sampson D, Pickard MR, Sinha AK, Evans IM, Leonard AJ, Ekins RP, 2000. Maternal thyroid status regulates the expression of neuronal and astrocytic cytoskeletal proteins in the fetal brain. J Endocrinol. 167:439-445.

65. Calvo R, Obregon MJ, Ruiz de Ona C, Escobar del Rey F, Morreale de Escobar G, 1990. Congenital hypothyroidism, as studied in rats. Crucial role of maternal thyroxine but not of 3,5,3'-triiodothyronine in the protection of the fetal brain. J Clin Invest. 86:889-899.

66. Dowling AL, Martz GU, Leonard JL, Zoeller RT, 2000. Acute changes in maternal thyroid hormone induce rapid and transient changes in gene expression in fetal rat brain. J Neurosci. 20:2255-2265.

67. Versloot PM, van der Heide D, Schroder-van der Elst JP, Boogerd L, 1998. Maternal thyroxine and 3,5,3'-tri-iodothyronine kinetics in near-term pregnant rats at two different levels of hypothyroidism. Eur J Endocrinol. 138:113-119.

68. Gauthier K, Chassande O, Plateroti M, Roux JP, Legrand C, Pain B, Rousset B, Weiss R, Trouillas J, Samarut J, 1999. Different functions for the thyroid hormone receptors TRalpha and TRbeta in the control of thyroid hormone production and post-natal development. EMBO J. 18:623-631.

69. Hashimoto K, Curty FH, Borges PP, Lee CE, Abel ED, Elmquist JK, Cohen RN, Wondisford FE, 2001. An unliganded thyroid hormone receptor causes severe neurological dysfunction. Proc Natl Acad Sci U S A. 98:3998-4003.

Chapter 9

General discussion

Based on:

Minke van Tuyl, Veronica Del Riccio and Martin Post*. Lung branching morphogenesis: potential for regeneration of small conducting airways. In: Lung Development and Regeneration (Lung Biology in Health and Disease). Eds: D. Massaro, G. Massaro, P. Chambon. Marcel Dekker, New York, 2004, 355-393

Minke van Tuyl and Martin Post*. Molecular Mechanisms of Lung Development and Lung Branching Morphogenesis. In: Fetal and Neonatal Physiology 3rd edition. Eds: R.A. Polin, W.W. Fox, S.H. Abman. Saunders, Philadelphia, Harcourt Health Sciences 2004, 812-821

**The CIHR Group in Lung Development, Hospital for Sick Children Research Institute, Departments of Pediatrics and Physiology, University of Toronto, Toronto, ON, Canada*

Introduction

The concept that signaling cascades that pattern the embryo into a functioning human being are, or can be, possibly be reactivated in neonatal and/or adult life is one of the reasons to study the molecular basis of normal development. Knowing the exact function and regulatory cascades of embryonic building pathways could provide us with therapeutic tools to either reactivate the appropriate cascade to stimulate growth and differentiation or to interrupt abnormal processes in end stage lung diseases such as chronic obstructive pulmonary disease (emphysema and chronic bronchitis), pulmonary fibrosis, cystic fibrosis, lung cancer, and bronchopulmonary dysplasia (BPD) in the newborn. Regeneration of small airways in order to restore normal gas exchange function could be a valuable therapeutic option for these lung diseases. Besides lung transplantation, at present there is no method to regenerate functional gas exchange units in humans. Restoration of damaged lung units requires the regeneration of the epithelial, mesenchymal, and vascular components, organized into a proper alveolar architecture. Epithelial airways are rendered useless without adjacent capillaries, whereas supportive fibroblasts and mesenchyme are crucial to keep lung structure together. Ideally, all appropriate types of cells should proliferate and differentiate to restructure the lung. Therefore, it is important to identify the angiogenesis and branching morphogenetic factors guiding small airway formation during normal development.

Pneumonectomy and airway regeneration

Probably one of the best established models for airway regeneration is the adult dog pneumonectomy model, in which either the left or the right lung is removed, which causes compensatory lung growth, including alveolar development in the remaining lung (1, 2). The exact mechanism responsible for the compensatory lung growth, however, remains largely unknown, especially at the molecular level. Mechanical lung strain is thought to be a major player in compensatory lung growth. Implanting an inflatable prosthesis in the empty thorax after pneumonectomy prevented a mediastinal shift, but only partially prevented compensatory lung growth, indicating that other signals than mechanical strain are implicated in compensatory lung growth as well (3). The observation that left pneumonectomy performed at different gestational stages in pregnant rats enhanced fetal lung growth without affecting maturation, led to the suggestion that a lung specific growth factor is released into the circulation after pneumonectomy, which is responsible for compensatory lung growth (4).

Recent studies have identified several potential factors to be responsible for postnatal compensatory lung growth. In 3 weeks old rats, with pneumonectomy of the left lung, compensatory lung growth was blocked by decoy inhibition of the receptor for native platelet derived growth factor-B (PdgfB); Pdgf receptor-β (Pdgfrβ), using truncated soluble Pdgfrβs, indicating a role for PdgfB signaling via Pdgfrβ in compensatory lung growth (5).

In contrast, *in vivo* overexpression of PdgfA in distal airway epithelium doubled lung size and increased distal branching morphogenesis (6). Tropoelastin and type I pro-collagen mRNA increased dramatically in the alveolar walls of postpneumonectomy rat lungs compared to sham-treated controls (7). This is an intriguing finding considering the key role of tropoelastin in normal alveolar formation and maintenance (8).

At late gestation and early postnatal life, rodent pulmonary fibroblasts contain a considerable amount of vitamin A (9-11). Before birth, pulmonary fibroblasts contain retinyl esters, which around birth are converted into retinol and all-*trans*-retinoic acid (RA), the active components of vitamin A (10). Both endogenous (12) and exogenous RA (13) increased levels of tropoelastin mRNA almost threefold in neonatal rat lung fibroblasts, whereas inhibition of the production of RA decreased tropoelastin gene expression in postnatal rat lung fibroblast (12). Further evidence that RA plays a role in lung elastin maintenance and alveolarization was provided by genetic manipulation of the retinoic acid receptors RAR and RXR in mice. Compound mice homozygous for a RARγ and heterozygous for a RXRα deletion had a reduced number of alveoli and less elastic fiber in their alveolar walls (14). Conversely, RARβ appears to be an endogenous inhibitor of septation because RARβ null mutant mice showed early onset septation resulting in twice as many alveoli in null mutant lungs compared to wild-type lungs (15). Most significantly, RA administration has been shown to increase the number of alveoli in postnatal rats and even to abrogate decreased alveolarization that was seen after the experimental use of dexamethasone or elastase, which both decrease alveolar formation. Taken together, these data provide evidence that RA might be a powerful factor in "alveolar neogenesis" after lung injury (16-20). Moreover, these results show the importance of RA and tropoelastin as key regulators of alveolar development and maintenance and therefore their use in alveolar regeneration should be investigated.

Fibroblast growth factor-7 (Fgf7) was recently shown to significantly enhance compensatory lung growth after left pneumonectomy in adult rats (21). Compared to untreated-pneumonectomized rats, weekly systemic injections of Fgf7 increased lung weight and lung volume, as well as the total volume of the alveolar region and the alveolar surface area per unit lung volume (21). Moreover, Fgf7 treatment greatly enhanced postpneumonectomy-alveolar BrdU incorporation, indicating a role in alveolar proliferation during compensatory lung growth (21).

Hepatocyte growth factor/Scatter factor (Hgf) expression is also upregulated in the remaining lung after left pneumonectomy in mice (22). Interestingly, Hgf mRNA levels were transiently upregulated in the liver and kidney as well, findings that suggest the existence of a systemic factor or response after pneumonectomy. The increase in Hgf expression was accompanied by a short but dramatic increase in the expression of the Hgf receptor, c-met/Hgfr (22). A neutralizing antibody against Hgf significantly attenuated DNA synthesis

as measured by BrdU labeling in the remaining lungs, whereas systemic treatment with Hgf increased pulmonary BrdU labeling (22). However, Hgf mRNA was also rapidly induced in adult rat lungs following hepatic or renal injury (23). These results favor a "universal" role for Hgf in organ regeneration (24). In human patients, it was shown that Hgf serum levels were upregulated after lung resection compared to patients undergoing mastectomy (25) and in patients with various lung diseases (26), findings that indicate a role for Hgf in lung regeneration or compensatory lung growth in humans. This is further supported by the unique characteristics of Hgf, being a mitogen (27), morphogen (28), and inducer of pulmonary blood vessel formation *in vivo* (29, 30). During embryonic lung development, Hgf mRNA is expressed in pulmonary mesenchyme, whereas the receptor c-met/Hgfr is expressed in adjacent epithelium, an expression pattern indicative of mesenchymal-epithelial tissue interactions (31). The prenatal influence of Hgf on lung development is somewhat unclear. Hgf null mice die around E14.5 *in utero* with no reported abnormalities of the lungs (32, 33). Exogenous Hgf had no effect on branching morphogenesis of E14.5 rat lung explants in one study (34), but stimulated growth and branching morphogenesis in another (31). Also, both the addition of antisense oligonucleotides (ODNs) targeted against Hgf or the addition of anti-Hgf antibodies inhibited branching morphogenesis of embryonic rat lungs *in vitro* (31). Similar to Fgf7, Hgf stimulated DNA synthesis and proliferation of adult rat alveolar type II cells in primary culture (35). Interestingly, postnatal dexamethasone therapy to reduce inflammation and subsequent development of BPD in premature infants reduced Hgf levels in tracheal aspirates (36). Taking into account its positive effect on lung growth, reduced levels of Hgf may explain the suppressive effect of dexamethasone on lung development (36).

Endothelial nitric oxide synthetase (eNOS) is another protein, which is upregulated 3 days after left pneumonectomy, together with an increase in right lung weight and volume, indicating a role for eNOS in compensatory lung growth (37). Indeed, eNOS-null mice failed to upregulate lung weight and volume and showed no signs of alveolar cell proliferation after left pneumonectomy, findings suggesting an impairment of compensatory alveolar growth in these mice (37). Similar results were obtained when mice were treated with a NOS inhibitor (L-NAME) after pneumonectomy (37). Because Vegf is known to upregulate eNOS, an intriguing explanation for these results is that impaired vascular development prevents compensatory alveolar growth (37). Therefore, it is important to study whether coordinated stimulation of vascularization can be used as a tool for proper airway regeneration.

Growth and transcription factors in airway regeneration

Because of their profound influence on embryonic lung development and branching morphogenesis, Fgfs are excellent candidates to guide regeneration of airways following injury. The high postnatal expression of both the Fgf receptors (Fgfr) and ligands further indicates a role in postnatal alveolarization and lung homeostasis (38-41). For example;

the inhibition of postnatal Fgfr signaling rendered male mice susceptible to oxygen-induced injury what resulted in increased alveolar-capillary leak, inflammation, surfactant protein-B (SP-B) deficiency, and mortality (42). Also, the combined inhibition of Fgfr3 and Fgfr4 caused a complete block in the formation of secondary septae what resulted in the absence of alveoli (41). These results suggest a role for Fgf signaling in postnatal lung alveolarization and in homeostasis following injury. Important data will be coming from the conditional overexpression of Fgfs during pre- and postnatal lung development (43). Conditional overexpression of Fgf7 in the proximal airways of the mouse using the rat CCSP promoter induced cystadenomatoid malformations when overexpressed in the fetal lung, but epithelial cell hyperplasia and type II cell differentiation when overexpressed postnatally (44). Similar results were obtained with the overexpression of Fgf10 (45). In embryonic lungs, the overexpression of Fgf10 resulted in adenomatoid hyperplasia and marked hyperplasia of epithelial cells in small conducting airways, whereas overexpression of Fgf10 in the postnatal lung caused the formation of multifocal tumors with type II cell differentiation (45). Other studies showed that the intratracheal installation of exogenous Fgf7 in the adult rat lung caused diffuse alveolar cell hyperplasia and a transient increase in surfactant protein mRNA expression (46, 47). Also, rats receiving intratracheal exogenous Fgf7 exhibited a dramatic reduction in mortality after exposure to hyperoxia (48). Both intra-alveolar hemorrhage and exudation were greatly reduced as a result of exogenous Fgf7 administration (48). Regulated overexpression of Fgf3 in distal epithelial cells of the adult lung using the human SP-C promoter, resulted in an inflammation reaction consisting of an influx of alveolar macrophages and an upregulation of interleukin-7 (IL-7) and granulocyte macrophage-colony stimulating factor (GM-CSF), together with an intense increase in alveolar type II cell proliferation, including increased expression levels of thyroid transcription factor-1 (Ttf-1) and surfactant protein mRNA (49). Both inflammation and subsequent proliferation recapitulate regeneration after lung injury, suggesting a role for Fgf3 in this process.

In addition to its role in prenatal lung development, Ttf-1 also regulates postnatal lung development and homeostasis. Although Ttf-1 expression decreases dramatically after birth, it remains detectable in adult alveolar type II cells (50-52). Overexpression of Ttf-1 in distal lung epithelial cells, using the SP-C promoter, did not affect prenatal lung development, but perturbed postnatal alveolarization, causing emphysema, severe inflammation, and fibrosis (53). In human cases of pulmonary hypoplasia, Ttf-1 was found to be upregulated in proximal airways such as bronchi and bronchioles (54). It has been suggested that a sustained high expression of Ttf-1 may result in pulmonary hypoplasia (54). On the other hand, another study reported decreased Ttf-1 and hepatocyte nuclear factor-3β (Hnf3β or Foxa2) expression in inflamed and atelectic areas of human infant BPD lungs. Ttf-1, Foxa2 and surfactant proteins, however, reappeared in regions of regeneration, supporting the possibility that Ttf-1 may be a critical factor in restoration of alveolar structures after neonatal lung injury (51, 55).

Tgf-α is a member of the epidermal growth factor (Egf) family that signals via the Egf receptor (Egfr) and both were shown to be expressed and involved in pre- and postnatal lung development (56). The Egfr null mutant dies soon after birth with immature lung morphology, impaired alveologenesis, and surfactant protein deficiency, which is a phenotype that resembles human respiratory distress syndrome (RDS) (57, 58). Conversely, the Tgf-α null mutant survived into adulthood without reported lung abnormalities, indicating that other factors than Tgf-α that signal via the Egfr are important in lung development (59). However, overexpression of Tgf-α in distal pulmonary epithelial cells using the human SP-C promoter resulted in disruption of postnatal alveolarization causing lung emphysema and fibrosis (60). This approach increased proliferation of alveolar epithelial cells including SP-C-expressing type II cells, without causing inflammation (61). Elastin fibers were abnormal in the bronchiolar regions and deficient in alveolar septae, most likely contributing to the emphysematic lesion of SPC-Tgf-α lungs (60). Interestingly, Tgf-α is upregulated in a number of lung disorders like RDS, BPD (56), and idiopathic pulmonary fibrosis (62). Tgf-α-deficient mice are protected from lung fibrosis after bleomycin instillation, implying that Tgf-α contributes to the pathogenesis of lung fibrosis after acute lung injury (63). Similarly, Tgf-β1 was increased in bronchiolar alveolar lavage (BAL) fluid form from infants with RDS that went on to develop chronic lung disease (CLD) compared to children with RDS that did not develop CLD, indicating that Tgf-β1 may contribute to the fibrotic response that is observed in the lungs of infants with CLD (64, 65).

Taken together, these results demonstrate the powerful capacity of growth factors and in particular, of Fgfs, to induce type II cell proliferation, which places them high up in the list of potential tools in pulmonary regeneration. It is important to realize that the conditional overexpression-systems allow re-expression of embryonic growth- and transcription factors in the adult lung. The challenge will now be to use these systems in disease models like BPD and emphysema to investigate the rescue-potential of embryonic developmental factors in airway repair and regeneration. Therefore, it is equally important to realize that the data also indicate that increased proliferation of alveolar type II cells does not always results in a better lung. It is clear that both lung development and small airway regeneration are a fine balance between the right amount of stimulatory and inhibitory regulating factors.

Vascular development and airway regeneration

The finding that abnormal vascular development occurs in diseases like BPD and hyperoxia-induced lung injury supports our hypothesis that vascular development takes a leading role in pulmonary development. BPD is characterized by remarkably decreased numbers of distal respiratory units and abnormal microvessels (66, 67). Infants dying of BPD have decreased levels of pulmonary Vegf and Pecam expression compared to infants that do not develop BPD (68). Similarly, it was shown that preterm infants that go on to develop

BPD had lower Vegf levels in their tracheal aspirates during the first 10 postnatal days than those preterms that did not develop BPD (69). Also, hyperoxia induced two weeks after birth reduced alveolarization in the neonatal rat lung (70) and these abnormalities continued even after recovery in room air (71). In the neonatal and adult rabbit lung, hyperoxic injury decreased Vegf expression, which however did increase again with recovery in room-air (72). The initial decrease in Vegf expression as seen in both studies might well be responsible for the vascular abnormalities in hyperoxic injury.

The above-mentioned findings suggest that stimulating vascular development could be a potential tool for alveolar regeneration. Exogenous Vegf has been shown to stimulate airway epithelial cell proliferation and differentiation in human fetal lungs *in vitro* (73). Further evidence for a potential use of Vegf to stimulate alveolar development was provided by a recent study on hypoxia-inducible transcription factors (74). The hypoxia-inducible transcription factors (Hif), Hif-1α and Hif-2α, are upregulated in response to hypoxia and in turn upregulate the expression of oxygen-sensitive target genes such as Vegf (75, 76). Hif-1α null mutants die early in gestation, whereas Hif-2α-deficient mice die after birth with RDS-like symptoms (74, 77). Compared to control mice, lungs of Hif-2α-deficient mice have decreased Vegf protein levels. Histological analysis of the Hif-2α-deficient lungs revealed normal numbers of alveoli, but alveolar septae were abnormally thick with scattered and abnormal alveolar capillaries. Type II cells were immature and produced less surfactant phospholipids and proteins (74). When exogenous Vegf was injected either intra-amniotic or intratracheally one day before preterm delivery, it significantly improved lung maturation and decreased mortality due to RDS in premature mice (74). Based on these intriguing observations, it is evident that therapeutic Vegf in a clinical setting needs immediate attention, if only for the possibility to reduce corticosteroid usage or oxygen levels in the treatment of RDS (74).

Stem cells and airway regeneration

Lung regeneration *in situ* likely requires a combined stimulation of angiogenesis and alveologenesis via induction of branching from existing small airways. This might be achieved by gene delivery of angiogenesis and/or branching morphogenesis factors via tissue-specific or multipotent stem cells (78).

Type II, Clara, and neuroendocrine (PNEC) cells have all been pursued as potential "tissue-born stem cells". The alveolar type II cells have been found to have an unlimited potential to proliferate (79). They serve as the putative stem cells for type I cells and having an excess of type II cells during development will ensure that enough type I cells are formed during alveolarization (79). Type I cells are critical in the maturation of the air-blood barrier during alveolarization and are solely responsible for gas exchange in human lungs (80, 81). The pulmonary type II cell is geared for self-maintenance, terminal differentiation, including surfactant production, and source for type I cells, all characteristics of a tissue-derived stem

cell (79). In other words, the type II cell acts as the "caretaker" of the alveolar compartment. When vulnerable type I cells are injured, type II cells react by extensive proliferation, acting as a progenitor cell for both type I and type II cells (79). During the resolution phase of the repair process, type II cells undergo extensive apoptosis (82) to re-establish a functional air-blood barrier (83). The administration of rhFgf7, a potent mitogen of alveolar epithelial type II cells, resulted in type II hyperplasia (46,84). Restoration of normal alveolar epithelium after instillation of Fgf7, is accomplished by terminal differentiation into type I cells and apoptosis of hyperplastic alveolar type II cells *in vivo*. Taken together, these results indicate that pulmonary type II cells may serve as the putative stem cells for the alveolar region during regeneration.

Due to their overlapping localization during lung development and regeneration Clara cells and PNEC have been thought to be potential airway stem cell (85). Naphthalene-induced lung injury denudes the proximal and terminal bronchioles selectively of their nonciliated CCSP-positive epithelium, that is, Clara cells (86,87). Naphthalene is cytotoxic to Clara cells, because Clara cells contain the cytochrome P-450 2F2 isozyme that metabolizes Naphthalene to a toxic substance (88). Regeneration after Naphthalene-induced injury involves re-occurrence of CCSP-positive cells predominantly at bronchiolar bifurcations (87). On the other hand, PNECs were unaffected by Naphthalene and showed extensive proliferation in the repair phase of Naphthalene-induced injury, resulting in PNEC hyperplasia (89). Some "variant" Clara cells that appeared to lack detectable cytochrome P450 2F2 isozyme protein survived and proliferated after Naphthalene-induced lung injury in close apposition to hyperplastic PNECs in neuroendocrine bodies (NEBs) located at bronchiolar branch points (90,91). These results support a role for NEBs in the maintenance of multiple progenitor cell population in the mature airway. However, other studies do not support this concept. Transgenic CCtk mice allow the timed and selective ablation of CCSP-positive cells (92). In these mice, treatment with ganciclovir, which renders the thymidine kinase (tk) cytotoxic by phosphorylation, resulted in a complete ablation of CCSP-positive cells, whereas proliferation and hyperplasia of calcitonin gene-related peptide (cGRP)-positive PNECs was unaffected (92). Regeneration of CCSP-positive cells that normally occurs in the regeneration phase after Naphthalene-induced lung injury was absent in these CCtk mice, indicating that PNECs are unable to differentiate into CCSP-positive cells (91). Also, ciliated bronchiolar epithelial cells similarly disappeared and did not regenerate in these transgenic mice (92). Moreover, Mash-1 null mutant lungs have no PNECs however, type II and Clara cell markers were expressed normally (93). Summarizing, these results indicate a role for CCSP-positive cells for their own regeneration and the maintenance of ciliated bronchiolar epithelial cells, but CCSP-positive cells are not important for the proliferation of PNECs (92). Furthermore, it suggests that PNECs merely function as a self-renewing population (91).

Kotton *et al*. (94) have provided some interesting information with respect to the

use of multipotent bone marrow stem cells in lung repair. Cultured fibroblast-like GTRosa26 bone marrow-derived stem cells were tail vein-injected into either normal or intratracheally bleomycin-injured mice. LacZ-positive cells were found 30 days after injection in subpleural regions of control lungs. In the injured lung, considerably more LacZ-positive cells were found, predominantly as clusters in the alveolar regions of the lung. These cells appeared to be type I cells as demonstrated by their morphological features and positive immunohistochemical staining for type I cell markers. These results suggest that cultured bone marrow cells can serve as type I cell precursors and that their engraftment is enhanced when the lung is injured (94). Recently, it has been reported that type II alveolar epithelial cells can be derived form murine embryonic stem cells *in vitro* (95). Yet, another study strongly argues against the transdifferentiation of hematopoietic stem cells into non-hematopoietic tissue specific cells making up the lung. In contrast to the previous study, injected hematopoietic green fluorescent protein (GFP)-positive cells mainly localized to the hematopoietic system except for a few cells in the liver and a single cell in the brain. Tissue injury did not push transdifferentiation, because irradiation of the intestine did not result in the accumulation of GFP-positive intestinal specific cells (96). Also, long-term joining of the circulatory systems of a GFP-positive and a GFP-negative mouse (parabiotic system) did not result in GFP-positive cells in GFP-negative organs other than the hematopoietic system (96). However, another study showed the absence of significant bone marrow-derived progenitor cell contribution to pulmonary endothelium, fibroblasts, or smooth muscle cells in compensatory lung growth induced by unilateral pneumonectomy (97). Thus, whether multipotent bone marrow-derived stem cells can be used to deliver gene therapy to lung epithelium remains to be seen.

This thesis- interpretations and future perspectives

The aims of the studies described in this thesis were:

1. To examine the role of vascular development and hypoxia in fetal lung development.

2. To investigate the role of the homeobox transcription factors Irx in lung development.

3. To study the expression pattern of the genes involved in the Notch signaling pathway during embryonic lung development and especially the role of Lunatic fringe herein.

4. To investigate the expression of pulmonary surfactant proteins in experimental congenital diaphragmatic hernia

5. To examine the effect of maternal and/or fetal hypothyroidism on heart and lung development

Chapter 3

In chapter 3 of this thesis we demonstrate that a low oxygen environment (3% oxygen) stimulates pulmonary vascular and epithelial branching morphogenesis *in vitro*. In *Drosophila* tracheal development, hypoxia greatly enhanced branching of the terminal tubules (98). Although *Bnl*, the fly homologue for Fgf, was identified as the critical signal in this hypoxic response, no oxygen-dependent differences in the expression of Fgf10 or its receptor Fgfr2 were observed in the presented study. We also showed that the inhibition of vascularization *in vitro* resulted in a dramatic decrease in epithelial branching morphogenesis, suggesting that pulmonary vascular development is a rate-limiting step for epithelial branching morphogenesis. We did not find the mechanism responsible for hypoxia-induced branching morphogenesis in mouse lung explants. Although we show upregulation of potent angiogenic factors like Vegf in hypoxic lung cultures, more research is necessary to prove that Vegf induces vessel formation and that these vessels in turn are primary inducers of branching morphogenesis.

Should this hypothesis be true, this information is of great importance and could be of crucial benefit in the neonatal intensive care unit. In this clinical setting, the lungs of premature babies are suddenly exposed to high levels of oxygen at birth. However, the lungs should have developed for several more weeks in the relatively hypoxic environment of the uterus and compared to this situation is even room air hyperoxic. As suggested from experimental results in this study and from the clinical picture of BPD (99), high levels of oxygen could potentially halt pulmonary vascular development, subsequently leading to an arrest of (alveolar) lung development. Postnatal re-initiation of the same molecular cascade that is responsible for airway and vascular branching *in utero* might therefore be beneficial in the prevention of alveolar hypoplasia as seen in BPD (99).

In this study we did not further address the specific cell types involved in the hypoxic response of lung explants. Because the driving force behind pulmonary endothelial proliferation and guidance is clearly epithelial-derived Vegf, it is possible that a regulatory loop is established in which Vegf is produced by the epithelium, induces vascular development, and the endothelium signals back either directly to the epithelium or via the mesenchymal compartment. Such indirect reciprocal paracrine interactions involving other lung cell types are of crucial information in the understanding of hypoxia-induced branching morphogenesis.

Clearly, just adding Vegf to the lung is not going to solve the problem because overexpression of Vegf164 in distal airway epithelium of the developing lung resulted in gross abnormalities in lung branching morphogenesis and in an increase in peritubular vascularity (100). Overexpression of Vegf164 using the CCSP promoter in neonatal mice (day 1-14), caused pulmonary hemorrhage, hemosiderosis and air space enlargement

together with a 50% increase in neonatal mortality (101). Altogether this illustrates that vascular development is a highly orchestrated process during lung development, which is not only regulated by Vegf and that disturbing the fine balance of growth and angiogenic factors profoundly disturbs lung development.

Chapter 4

In chapter 4 we report that in addition to lung hypoplasia (102, 103), mice deficient for the morphogen Sonic hedgehog (Shh) have abnormalities in pulmonary vascular development. A loss of Shh did not affect early pulmonary vasculogenesis and angiogenesis, but reduced the expression of the vascular stabilizing factor Angiopoietin-1 (Ang-1), thereby perhaps leading to diminished stabilization of the primitive vascular network at later gestation. Intriguingly, restoration of the pulmonary vascular defect in Shh-deficient lungs with the angiogenic factor Fgf2, also partially recovered the airway branching abnormalities as seen in Shh null mice. These results may again suggest that proper vascularization is important for normal branching morphogenesis. The next step in this study is to confirm functionality of the vessels induced by Fgf2 alone or in combination with Ang-1 by electron microscopy. The angiopoietins are known for their effect on vascular stabilization via remodeling of the vasculature into a hierarchical network of mature vessels composed of endothelial and adventitial cells (104-111). The mesenchymal compartment is a direct cellular target of Shh (102, 103) in which Shh is required for the formation of smooth muscle cells (112). Whether Shh mediates its effect on these cells via Ang-1 remains to be investigated but Ang-1 has been shown to play a role in the interaction of endothelial cells and surrounding support cells such as pericytes and smooth muscle cells (113).

Ang-1 did not (but Fgf2 did) restore vascular and epithelial branching brings into question the decrease in Ang-1 as a causative factor in the Shh-deficient lung phenotype. However, Ang-1 was shown to be a chemotactic, but not a proliferation factor for endothelial cells (114). One can think of a model in which Fgf2 induces proliferation of endothelial cells and Ang-1 establishes proper aligning of the epithelial and endothelial layers by means of chemotaxis. Detailed examination of this model is needed for proof of our hypothesis. In favor of this hypothesis is however the finding that eNOS-deficient mice die at birth with respiratory distress and cyanosis. Postnatal lung histology revealed reduced alveolar formation and inflation, with thick alveolar septae and surfactant deficiency (115). Fetal eNOS-deficient lungs showed evidence of lung hemorrhaging and had decreased levels of Ang-1 and Tie2, as well as misalignment of pulmonary vessels, which resembles the characteristics of alveolar capillary dysplasia (115). Also, the areas of abnormal enlargement and atelectic parts as found in eNOS lungs are reminiscent of lung histology seen in BPD, suggesting that abnormal vascular development might partly be responsible for this neonatal disease (115).

COUP-TFII is a member of the steroid/thyroid hormone receptor superfamily, which consists of a large group of ligand-activated transcription factors (116). Ang-1 is downregulated in COUP-TFII mutants and angiogenesis and vascular remodeling are defective in these mice (117). In COUP-TFII mutants, the combination of normal-elevated levels of Tie2 and Vegf, but a decreased level of Ang-1 expression is very similar to the present findings in Shh-deficient lungs. It is therefore warranted to examine the role of COUP-TFII in Shh-deficient lungs before and after the addition of Fgf2 alone or with Ang-1.

The spatial expression of Fgf2 should be examined together with proliferation and apoptosis parameters in Shh-deficient lungs with or without Fgf2 because we speculate that exogenous Fgf2 increased the amount of mesenchymal mass surrounding the growing lung buds of $Shh^{-/-}$ mice. Also, changes in cell types and growth- and transcription factors in Fgf2-treated explants should be investigated.

In support of our hypothesis that pulmonary blood vessels are required for epithelial branching are recent data on liver organogenesis presented by Matsumoto *et al*. (118, 119). These authors used Vegfr2 (Flk-1)-deficient mice that die early in embryogenesis as a result of a lack of blood vessel formation (120). Because Vegfr2-deficient mice die before proper liver formation can occur, the liver bud regions of Vegfr2-deficient mice were taken into culture. It occurred that the initial liver epithelial layers formed, but that subsequent migration of liver epithelial cells into the surrounding septum transversum failed (119). They also showed that cultured wild-type liver bud regions form a considerably amount of hepatic cells, but treatment with an angiogenesis inhibitor resulted in similar growth characteristics as cultured Vegfr2-deficient liver buds (119). Pancreatic development was similarly shown to be regulated by vascular development when instructive signals from blood vessel endothelium induced endocrine pancreatic differentiation (118, 121, 122). Together these studies strongly suggest that endothelial cells support the developing endothelium.

Chapter 5

In chapter 5 we demonstrate that Iroquois (Irx) homeobox genes play an important role in lung branching morphogenesis and proximal-distal epithelial differentiation. Evidence is provided that the Irx genes are not components of well-known signaling pathways critical for lung development such as the Shh, Bmp4, and Fgf signaling pathways. We speculate that Irx genes are additional transcriptional components of the complex genetic network directing lung morphogenesis. Based on the early gestational and epithelial specific expression patterns of the Irx genes, we hypothesized that the Irx genes are involved in early lung branching morphogenesis. *In vitro* inhibition of Irx signaling by means of antisense Irx ODN-treated explants caused a disproportional development of the

pulmonary airways in which proximal airways developed relatively normal, whereas the distal structures were almost completely abrogated. The results indicate that Irx genes are specifically important for the development of the distal airways, which include future alveolar structures.

Further investigation of the proximal airways should provide information on whether this epithelium is normal or aberrant, by examining Foxj1 and -tubulin expression, which are both markers of pulmonary ciliated cells that are normally restricted to the conducting airways. Also, vascular development in antisense Irx ODN-treated explants should be examined. The next step in this study will be the *in vivo* knockdown of Irx genes. From the Irx2 and Irx4-deficient mice no obvious lung phenotype has been reported so far (123, 124), suggesting that there is high redundancy among the different Irx genes. Knockout mice for two or more Irx genes should provide further information on the role of Irx genes from the very start of lung development. Also, it is useful to examine the role of these transcription factors in lung hypoplasia as seen in congenital diaphragmatic hernia.

In this study we were unable to find a down- or up-stream pathway of Irx genes responsible for the apparent halt of distal airway development. However, a phenotype resembling the antisense Irx-deficient lungs was seen in retinoic acid (RA)-treated mouse lung explants (125). In Xenopus, RA increases Xiro expression in the neural plate, but it decreases Xiro expression outside this plate (126). If we extrapolate these findings to the present study, it would mean that RA downregulates the Irx genes, which in turn leads to outgrowth of proximal and inhibition of distal lung structures. Preliminary results to test this hypothesis did not reveal a downregulation of Irx genes in RA-treated lung explants (unpublished results). Nonetheless we did not rule out the possibility that Irx genes function upstream from RA. Further investigations will be required to explore the putative interactions between Irx and other key signaling cascades during lung development.

Chapter 6

If the mature lung alone consists of at least 40 different cell types (127), one can imagine the enormous amount of different cell types it takes to built the entire human body with all its organs. It needs no explanation that (in)vertebrates use complex signaling pathways that are specifically designed to create these differences. The Notch signaling pathway is an important evolutionary conserved pathway involved in creating differences between neighboring cells or groups of cells (128) and regulates cell fate in many (branched) organs (129, 130) including the developing lung (131, 132).

Pulmonary neuroendocrine cells (PNEC) are the first epithelial cells to differentiate in the primitive lung and it was recently shown that Mash-1, a downstream player in the Notch

signaling cascade, was necessary for PNEC development (93, 131). Mash-1-deficient mice specifically lacked PNECs, whereas neuroendocrine cells in other organs were unaffected (93, 131). It therefore is reasonable that the Notch signaling pathway is involved in the very early differentiation events of the developing lung.

Fringe proteins modulate the Notch signaling pathway (133) and were shown to play a crucial role in defining borders in (in)vertebrates. We demonstrate however that fringe proteins do likely not define epithelial morphogenic boundaries along the anterior-posterior axis of the developing airways. Overexpression of Lfng in distal lung epithelial cells did not influence the expression of downstream bHLH factors, such as Hes1 and Mash-1. Lfng makes a complex with the Notch receptor before being secreted to the cell-surface thereby potentiating Dll-induced Notch signaling, while inhibiting Jagged-induced Notch signaling (134, 135). Thus, Lfng needs to be present in the same cell as the Notch receptor to have an effect on Notch signaling. In the present study, the SP-C promoter directed Lfng expression towards distal lung endoderm, which is same tissue layer where Notch1 is expressed (136). Nonetheless it is possible that the used method of overexpression, using the SP-C promoter, is not the appropriate way of overexpressing Lfng in distal pulmonary epithelial cells. Further research to unravel the mechanism involved in the correct transcription, translation and secretion of Lfng in the lung is needed.

Even so, other members of the Notch signaling pathway like the Notch receptors themselves or the Hes transcription factors have to be studied to unravel the role of the Notch signaling pathway in lung development. It is necessary to further study the role of Notch signaling in the developing lung because in addition to its role in development, Notch signaling was recently linked to human lung (adeno)carcinoma (137-139).

Chapter 7

CDH is characterized by a diaphragmatic defect, pulmonary hypoplasia and pulmonary hypertension. In the CDH neonate, pulmonary hypoplasia is often complicated by respiratory failure, low lung compliance, increased inspiratory resistance, and hyaline membrane formation (140). Based on inconsistent results from human and experimental animal studies with regards to the use of surfactant (prophylactic or rescue therapy) in CDH, we tested the hypothesis that CDH lungs are surfactant-deficient, which could explain in part the respiratory failure and difficulties in treating CDH infants. This study demonstrates that there is no primary deficiency of surfactant proteins in the nitrofen-induced CDH rat model. This study however does not provide information on the amount of disaturated phosphatidylcholine (DSPC) in CDH lungs. DSPC is nonetheless an important component of secreted surfactant, which is composed of 90% lipids, 9% proteins, and 1% carbohydrate. Other (human) studies have however failed to proof a DSPC deficiency in CDH lungs,

let alone an effect of surfactant therapy in CDH infants (141). Obviously, treatment of CDH infants is neither easy nor always successful despite technical improvements and enormous efforts of pediatric intensivists. Therefore, CDH should be tackled from the basic side, investigating molecular, genetic and environmental factors (142). Also, vascular development should be investigated, especially in the light of pulmonary hypertension, which is largely responsible for the treatment difficulties in newborns with CDH. A start has been made with mapping vascular development in CDH (143-148). The recent finding that both familial and non-familial primary pulmonary hypertension is associated with mutations in the Bmpr-II gene, combined with the important role of Bmp4 in embryonic lung development, makes it tempting to investigate the role of this receptor pathway in CDH (149).

Chapter 8

The importance of a functioning thyroid gland for normal postnatal development is clear from the severe mental retardation that develops in newborns with congenital hypothyroidism (150). If T_4 supplementation is started within two weeks after birth, the athyroid newborn is completely rescued from neurological damage (151,152). Nevertheless, the neurological cretinism that results from severe iodine deficiency during early pregnancy (153, 154), clearly demonstrates that thyroid hormone does play an important role in the normal development of most vertebrate tissues, in particular the brain (155). We decided to study the involvement of thyroid hormone in lung development because earlier studies showed an effect of thyroid hormone on lung development, thyroid hormone has been used in clinical trials in an attempt to lower the amount of prenatal corticosteroids in order to stimulate preterm lung maturation, and because we wanted to know whether maternal hypothyroidism affects postnatal heart and lung development as was recently shown for the developing brain (156-158). The study presented in this thesis showed that in the heart, the physiological neonatal switch from β-MHC to α-MHC expression in the cardiac ventricles did not occur in hypothyroid pups that had lacked maternal thyroid hormone. However, neither did the switch occur in pups that had similarly lacked maternal thyroid hormone but did produce their own thyroid hormone. Lung development up to the saccular phase was not affected by maternal or fetal hypothyroidism. After birth, surfactant protein mRNA, but not protein expression remained high in the alveolar epithelium of pups that had lacked maternal thyroid hormone, irrespective of the ability to produce their own thyroid hormone. In perinatal liver, like the lungs a derivate of the embryonic foregut, such comparatively high mRNA:protein ratios reflect immaturity (159). The next step in this study will be to investigate the way maternal thyroid hormone affects postnatal thyroid hormone homeostasis in the neonate. It would be interesting to look at the expression level of thyroid hormone receptors to investigate whether maternal thyroid

hormone acts early in development to influence the set point for the number and/or the isoform of thyroid hormone receptors expressed in a developing organ. Furthermore, our key finding that hypothyroidism during early development does not impair organ morphogenesis, but does affect adaptive responses in gene expression in these organs postnatally, is reminiscent of the hypothesis that several of the major diseases of later life, including coronary artery disease, hypertension, and diabetes, may originate in impaired intrauterine growth and development (160). The challenge will be to unravel the mechanism underlying this prenatal "programming" of postnatal development.

References

1. Hsia CC, Herazo LF, Fryder-Doffey F, Weibel ER, 1994. Compensatory lung growth occurs in adult dogs after right pneumonectomy. J Clin Invest. 94:405-412.

2. Hsia CC, Zhou XS, Bellotto DJ, Hagler HK, 2000. Regenerative growth of respiratory bronchioles in dogs. Am J Physiol Lung Cell Mol Physiol. 279:L136-L142.

3. Hsia CC, Wu EY, Wagner E, Weibel ER, 2001. Preventing mediastinal shift after pneumonectomy impairs regenerative alveolar tissue growth. Am J Physiol Lung Cell Mol Physiol. 281:L1279-L1287.

4. Faridy EE, Sanii MR, Thliveris JA, 1988. Influence of maternal pneumonectomy on fetal lung growth. Respir Physiol. 72:195-209.

5. Yuan S, Hannam V, Belcastro R, Cartel N, Cabacungan J, Wang J, Diambomba Y, Johnstone L, Post M, Tanswell AK, 2002. A role for platelet-derived growth factor-BB in rat postpneumonectomy compensatory lung growth. Pediatr Res. 52:25-33.

6. Li J, Hoyle GW, 2001. Overexpression of PDGF-A in the lung epithelium of transgenic mice produces a lethal phenotype associated with hyperplasia of mesenchymal cells. Dev Biol. 239:338-349.

7. Koh DW, Roby JD, Starcher B, Senior RM, Pierce RA, 1996. Postpneumonectomy lung growth: a model of reinitiation of tropoelastin and type I collagen production in a normal pattern in adult rat lung. Am J Respir Cell Mol Biol. 15:611-623.

8. Wendel DP, Taylor DG, Albertine KH, Keating MT, Li DY, 2000. Impaired distal airway development in mice lacking elastin. Am J Respir Cell Mol Biol. 23:320-326.

9. Okabe T, Yorifuji H, Yamada E, Takaku F, 1984. Isolation and characterization of vitamin-A-storing lung cells. Exp Cell Res. 154:125-135.

10. Shenai JP, Chytil F, 1990. Vitamin A storage in lungs during perinatal development in the rat. Biol Neonate. 57:126-132.

11. Chytil F, 1996. Retinoids in lung development. Faseb J. 10:986-992.

12. McGowan SE, Doro MM, Jackson SK, 1997. Endogenous retinoids increase perinatal elastin gene expression in rat lung fibroblasts and fetal explants. Am J Physiol. 273:L410-L416.

13. Liu B, Harvey CS, McGowan SE, 1993. Retinoic acid increases elastin in neonatal rat lung fibroblast cultures. Am J Physiol. 265:L430-437.

14. McGowan S, Jackson SK, Jenkins-Moore M, Dai HH, Chambon P, Snyder JM, 2000. Mice bearing deletions of retinoic acid receptors demonstrate reduced lung elastin and alveolar numbers. Am J Respir Cell Mol Biol. 23:162-167.

15. Massaro GD, Massaro D, Chan WY, Clerch LB, Ghyselinck N, Chambon P, Chandraratna RA, 2000. Retinoic acid receptor-beta: an endogenous inhibitor of the perinatal formation of pulmonary alveoli. Physiol Genomics. 4:51-57.

16. Massaro D, Teich N, Massaro GD, 1986. Postnatal development of pulmonary alveoli: modulation in rats by thyroid hormones. Am J Physiol. 250:R51-R55.

17. Massaro GD, Massaro D, 1996. Postnatal treatment with retinoic acid increases the number of pulmonary alveoli in rats. Am J Physiol. 270:L305-L310.

18. Massaro GD, Massaro D, 1997. Retinoic acid treatment abrogates elastase-induced pulmonary emphysema in rats. Nat Med. 3:675-677.

19. Massaro GD, Massaro D, 2000. Retinoic acid treatment partially rescues failed septation in rats and in mice. Am J Physiol Lung Cell Mol Physiol. 278:L955-L960.

20. Belloni PN, Garvin L, Mao CP, Bailey-Healy I, Leaffer D, 2000. Effects of all-trans-retinoic acid in promoting alveolar repair. Chest. 117:235S-241S.

21. Kaza AK, Kron IL, Leuwerke SM, Tribble CG, Laubach VE, 2002. Keratinocyte growth factor enhances post-pneumonectomy lung growth by alveolar proliferation. Circulation. 106:I120-124.

22. Sakamaki Y, Matsumoto K, Mizuno S, Miyoshi S, Matsuda H, Nakamura T, 2002. Hepatocyte growth factor stimulates proliferation of respiratory epithelial cells during postpneumonectomy compensatory lung growth in mice. Am J Respir Cell Mol Biol. 26:525-533.

23. Yanagita K, Nagaike M, Ishibashi H, Niho Y, Matsumoto K, Nakamura T, 1992. Lung may have an endocrine function producing hepatocyte growth factor in response to injury of distal organs. Biochem Biophys Res Commun. 182:802-809.

24. Matsumoto K, Nakamura T, 1997. Hepatocyte growth factor (HGF) as a tissue organizer for organogenesis and regeneration. Biochem Biophys Res Commun. 239:639-644.

25. Sugahara K, Matsumoto M, Baba T, Nakamura T, Kawamoto T, 1998. Elevation of serum human hepatocyte growth factor (HGF) level in patients with pneumonectomy during a perioperative period. Intensive Care Med. 24:434-437.

26. Yanagita K, Matsumoto K, Sekiguchi K, Ishibashi H, Niho Y, Nakamura T, 1993. Hepatocyte growth factor may act as a pulmotrophic factor on lung regeneration after acute lung injury. J Biol Chem. 268:21212-21217.

27. Rubin JS, Chan AM, Bottaro DP, Burgess WH, Taylor WG, Cech AC, Hirschfield DW, Wong J, Miki T, Finch PW, et al., 1991. A broad-spectrum human lung fibroblast-derived mitogen is a variant of hepatocyte growth factor. Proc Natl Acad Sci U S A. 88:415-419.

28. Montesano R, Matsumoto K, Nakamura T, Orci L, 1991. Identification of a fibroblast-derived epithelial morphogen as hepatocyte growth factor. Cell. 67:901-908.

29. Grant DS, Kleinman HK, Goldberg ID, Bhargava MM, Nickoloff BJ, Kinsella JL, Polverini P, Rosen EM, 1993. Scatter factor induces blood vessel formation in vivo. Proc Natl Acad Sci U S A. 90:1937-1941.

30. Ono M, Sawa Y, Matsumoto K, Nakamura T, Kaneda Y, Matsuda H, 2002. In vivo gene transfection with hepatocyte growth factor via the pulmonary artery induces angiogenesis in the rat lung. Circulation. 106: I264-I269.

31. Ohmichi H, Koshimizu U, Matsumoto K, Nakamura T, 1998. Hepatocyte growth factor (HGF) acts as a mesenchyme-derived morphogenic factor during fetal lung development. Development. 125:1315-1324.

32. Schmidt C, Bladt F, Goedecke S, Brinkmann V, Zschiesche W, Sharpe M, Gherardi E, Birchmeier C, 1995. Scatter factor/hepatocyte growth factor is essential for liver development. Nature. 373:699-702.

33. Uehara Y, Minowa O, Mori C, Shiota K, Kuno J, Noda T, Kitamura N, 1995. Placental defect and embryonic lethality in mice lacking hepatocyte growth factor/scatter factor. Nature. 373:702-705.

34. Shiratori M, Oshika E, Ung LP, Singh G, Shinozuka H, Warburton D, Michalopoulos G, Katyal SL, 1996. Keratinocyte growth factor and embryonic rat lung morphogenesis. Am J Respir Cell Mol Biol. 15:328-

338.

35. Panos RJ, Rubin JS, Csaky KG, Aaronson SA, Mason RJ, 1993. Keratinocyte growth factor and hepatocyte growth factor/scatter factor are heparin-binding growth factors for alveolar type II cells in fibroblast-conditioned medium. J Clin Invest. 92:969-977.

36. Lassus P, Nupponen I, Kari A, Pohjavuori M, Andersson S, 2002. Early postnatal dexamethasone decreases hepatocyte growth factor in tracheal aspirate fluid from premature infants. Pediatrics. 110:768-771.

37. Leuwerke SM, Kaza AK, Tribble CG, Kron IL, Laubach VE, 2002. Inhibition of compensatory lung growth in endothelial nitric oxide synthase-deficient mice. Am J Physiol Lung Cell Mol Physiol. 282:L1272-L1278.

38. Partanen J, Makela TP, Eerola E, Korhonen J, Hirvonen H, Claesson-Welsh L, Alitalo K, 1991. FGFR-4, a novel acidic fibroblast growth factor receptor with a distinct expression pattern. Embo J. 10:1347-1354.

39. Hughes SE, Hall PA, 1993. Immunolocalization of fibroblast growth factor receptor 1 and its ligands in human tissues. Lab Invest. 69:173-182.

40. Powell PP, Wang CC, Horinouchi H, Shepherd K, Jacobson M, Lipson M, Jones R, 1998. Differential expression of fibroblast growth factor receptors 1 to 4 and ligand genes in late fetal and early postnatal rat lung. Am J Respir Cell Mol Biol. 19:563-572.

41. Weinstein M, Xu X, Ohyama K, Deng CX, 1998. FGFR-3 and FGFR-4 function cooperatively to direct alveogenesis in the murine lung. Development. 125:3615-3623.

42. Hokuto I, Perl AK, Whitsett JA, 2004. FGF signaling is required for pulmonary homeostasis following hyperoxia. Am J Physiol Lung Cell Mol Physiol. 286:L580-587.

43. Perl AK, Tichelaar JW, Whitsett JA, 2002. Conditional gene expression in the respiratory epithelium of the mouse. Transgenic Res. 11:21-29.

44. Tichelaar JW, Lu W, Whitsett JA, 2000. Conditional expression of fibroblast growth factor-7 in the developing and mature lung. J Biol Chem. 275:11858-11864.

45. Clark JC, Tichelaar JW, Wert SE, Itoh N, Perl AK, Stahlman MT, Whitsett JA, 2001. FGF-10 disrupts lung morphogenesis and causes pulmonary adenomas in vivo. Am J Physiol Lung Cell Mol Physiol. 280:L705-715.

46. Ulich TR, Yi ES, Longmuir K, Yin S, Biltz R, Morris CF, Housley RM, Pierce GF, 1994. Keratinocyte growth factor is a growth factor for type II pneumocytes in vivo. J Clin Invest. 93:1298-1306.

47. Yano T, Mason RJ, Pan T, Deterding RR, Nielsen LD, Shannon JM, 2000. KGF regulates pulmonary epithelial proliferation and surfactant protein gene expression in adult rat lung. Am J Physiol Lung Cell Mol Physiol. 279:L1146-L1158.

48. Panos RJ, Bak PM, Simonet WS, Rubin JS, Smith LJ, 1995. Intratracheal instillation of keratinocyte growth factor decreases hyperoxia-induced mortality in rats. J Clin Invest. 96:2026-2033.

49. Zhao B, Chua SS, Burcin MM, Reynolds SD, Stripp BR, Edwards RA, Finegold MJ, Tsai SY, DeMayo FJ, 2001. Phenotypic consequences of lung-specific inducible expression of FGF-3. Proc Natl Acad Sci U S A. 98:5898-5903.

50. Zhou L, Lim L, Costa RH, Whitsett JA, 1996. Thyroid transcription factor-1, hepatocyte nuclear factor-3beta, surfactant protein B, C, and Clara cell secretory protein in developing mouse lung. J Histochem Cytochem. 44:1183-1193.

51. Stahlman MT, Gray ME, Whitsett JA, 1996. Expression of thyroid transcription factor-1(TTF-1) in fetal and neonatal human lung. J Histochem Cytochem. 44:673-678.

52. Ikeda K, Clark JC, Shaw-White JR, Stahlman MT, Boutell CJ, Whitsett JA, 1995. Gene structure and expression of human thyroid transcription factor-1 in respiratory epithelial cells. J Biol Chem. 270:8108-8114.

53. Wert SE, Dey CR, Blair PA, Kimura S, Whitsett JA, 2002. Increased expression of thyroid transcription factor-1 (TTF-1) in respiratory epithelial cells inhibits alveolarization and causes pulmonary inflammation. Dev Biol. 242:75-87.

54. Zhou H, Morotti RA, Profitt SA, Langston C, Wert SE, Whitsett JA, Greco MA, 2001. Expression of thyroid transcription factor-1, surfactant proteins, type I cell-associated antigen, and Clara cell secretory protein in pulmonary hypoplasia. Pediatr Dev Pathol. 4:364-371.

55. Stahlman MT, Gray ME, Whitsett JA, 1998. Temporal-spatial distribution of hepatocyte nuclear factor-3beta in developing human lung and other foregut derivatives. J Histochem Cytochem. 46:955-962.

56. Strandjord TP, Clark JG, Guralnick DE, Madtes DK, 1995. Immunolocalization of transforming growth factor-alpha, epidermal growth factor (EGF), and EGF-receptor in normal and injured developing human lung. Pediatr Res. 38:851-856.

57. Miettinen PJ, Berger JE, Meneses J, Phung Y, Pedersen RA, Werb Z, Derynck R, 1995. Epithelial immaturity and multiorgan failure in mice lacking epidermal growth factor receptor. Nature. 376:337-341.

58. Miettinen PJ, Warburton D, Bu D, Zhao JS, Berger JE, Minoo P, Koivisto T, Allen L, Dobbs L, Werb Z, Derynck R, 1997. Impaired lung branching morphogenesis in the absence of functional EGF receptor. Dev Biol. 186:224-236.

59. Mann GB, Fowler KJ, Gabriel A, Nice EC, Williams RL, Dunn AR, 1993. Mice with a null mutation of the TGF alpha gene have abnormal skin architecture, wavy hair, and curly whiskers and often develop corneal inflammation. Cell. 73:249-261.

60. Korfhagen TR, Swantz RJ, Wert SE, McCarty JM, Kerlakian CB, Glasser SW, Whitsett JA, 1994. Respiratory epithelial cell expression of human transforming growth factor-alpha induces lung fibrosis in transgenic mice. J Clin Invest. 93:1691-1699.

61. Hardie WD, Piljan-Gentle A, Dunlavy MR, Ikegami M, Korfhagen TR, 2001. Dose-dependent lung remodeling in transgenic mice expressing transforming growth factor-alpha. Am J Physiol Lung Cell Mol Physiol. 281: L1088-L1094.

62. Baughman RP, Lower EE, Miller MA, Bejarano PA, Heffelfinger SC, 1999. Overexpression of transforming growth factor-alpha and epidermal growth factor-receptor in idiopathic pulmonary fibrosis. Sarcoidosis Vasc Diffuse Lung Dis. 16:57-61.

63. Madtes DK, Elston AL, Hackman RC, Dunn AR, Clark JG, 1999. Transforming growth factor-alpha deficiency reduces pulmonary fibrosis in transgenic mice. Am J Respir Cell Mol Biol. 20:924-934.

64. Kotecha S, Wangoo A, Silverman M, Shaw RJ, 1996. Increase in the concentration of transforming growth factor beta-1 in bronchoalveolar lavage fluid before development of chronic lung disease of prematurity. J Pediatr. 128:464-469.

65. Lecart C, Cayabyab R, Buckley S, Morrison J, Kwong KY, Warburton D, Ramanathan R, Jones CA, Minoo P, 2000. Bioactive transforming growth factor-beta in the lungs of extremely low birthweight neonates predicts the need for home oxygen supplementation. Biol Neonate. 77:217-223.

66. Jobe AJ, 1999. The new BPD: an arrest of lung development. Pediatr Res. 46:641-643.

67. Hazinski TA: Bronchopulmonary Dysplasia. In Chernick V,Boat TF (eds): Kendig's disorders of the respiratory tract in children, 6th 6th, p 364-385. Philadelphia, W. B. Saunders Company, 1998.

68. Bhatt AJ, Pryhuber GS, Huyck H, Watkins RH, Metlay LA, Maniscalco WM, 2001. Disrupted pulmonary vasculature and decreased vascular endothelial growth factor, Flt-1, and TIE-2 in human infants dying with bronchopulmonary dysplasia. Am J Respir Crit Care Med. 164:1971-1980.

69. Lassus P, Turanlahti M, Heikkila P, Andersson LC, Nupponen I, Sarnesto A, Andersson S, 2001. Pulmonary vascular endothelial growth factor and Flt-1 in fetuses, in acute and chronic lung disease, and in persistent pulmonary hypertension of the newborn. Am J Respir Crit Care Med. 164:1981-1987.

70. Blanco LN, Frank L, 1993. The formation of alveoli in rat lung during the third and fourth postnatal weeks: effect of hyperoxia, dexamethasone, and deferoxamine. Pediatr Res. 34:334-340.

71. Randell SH, Mercer RR, Young SL, 1990. Neonatal hyperoxia alters the pulmonary alveolar and capillary structure of 40-day-old rats. Am J Pathol. 136:1259-1266.

72. Maniscalco WM, Watkins RH, D'Angio CT, Ryan RM, 1997. Hyperoxic injury decreases alveolar epithelial cell expression of vascular endothelial growth factor (VEGF) in neonatal rabbit lung. Am J Respir Cell Mol Biol. 16:557-567.

73. Brown KR, England KM, Goss KL, Snyder JM, Acarregui MJ, 2001. VEGF induces airway epithelial cell proliferation in human fetal lung in vitro. Am J Physiol Lung Cell Mol Physiol. 281:L1001-L1010.

74. Compernolle V, Brusselmans K, Acker T, Hoet P, Tjwa M, Beck H, Plaisance S, Dor Y, Keshet E, Lupu F, Nemery B, Dewerchin M, Van Veldhoven P, Plate K, Moons L, Collen D, Carmeliet P, 2002. Loss of HIF-2alpha and inhibition of VEGF impair fetal lung maturation, whereas treatment with VEGF prevents fatal respiratory distress in premature mice. Nat Med. 8:702-710.

75. Maxwell PH, Ratcliffe PJ, 2002. Oxygen sensors and angiogenesis. Semin Cell Dev Biol. 13:29-37.

76. Semenza GL, 2000. Expression of hypoxia-inducible factor 1: mechanisms and consequences. Biochem Pharmacol. 59:47-53.

77. Kotch LE, Iyer NV, Laughner E, Semenza GL, 1999. Defective vascularization of HIF-1alpha-null embryos is not associated with VEGF deficiency but with mesenchymal cell death. Dev Biol. 209:254-267.

78. Otto WR, 2002. Lung epithelial stem cells. J Pathol. 197:527-535.

79. Sutherland LM, Edwards YS, Murray AW, 2001. Alveolar type II cell apoptosis. Comp Biochem Physiol A Mol Integr Physiol. 129:267-285.

80. Burri PH: Lung development and pulmonary angiogenesis. In Gaultier C, Bourbon JR,Post M (eds): Lung Development, p 122-151. New York, Oxford University Press Inc, 1999.

81. Uhal BD, Flowers KM, Rannels DE, 1991. Type II pneumocyte proliferation in vitro: problems and future directions. Am J Physiol. 261:110-117.

82. Bardales RH, Xie SS, Schaefer RF, Hsu SM, 1996. Apoptosis is a major pathway responsible for the resolution of type II pneumocytes in acute lung injury. Am J Pathol. 149:845-852.

83. Bitterman PB, Polunovsky VA, Ingbar DH, 1994. Repair after acute lung injury. Chest. 105:118S-121S.

84. Fehrenbach H, Kasper M, Tschernig T, Pan T, Schuh D, Shannon JM, Muller M, Mason RJ, 1999. Keratinocyte growth factor-induced hyperplasia of rat alveolar type II cells in vivo is resolved by differentiation into

type I cells and by apoptosis. Eur Respir J. 14:534-544.

85. Khoor A, Gray ME, Singh G, Stahlman MT, 1996. Ontogeny of Clara cell-specific protein and its mRNA: their association with neuroepithelial bodies in human fetal lung and in bronchopulmonary dysplasia. J Histochem Cytochem. 44:1429-1438.

86. Plopper CG, Suverkropp C, Morin D, Nishio S, Buckpitt A, 1992. Relationship of cytochrome P-450 activity to Clara cell cytotoxicity. I. Histopathologic comparison of the respiratory tract of mice, rats and hamsters after parenteral administration of naphthalene. J Pharmacol Exp Ther. 261:353-363.

87. Stripp BR, Maxson K, Mera R, Singh G, 1995. Plasticity of airway cell proliferation and gene expression after acute naphthalene injury. Am J Physiol. 269:L791-L799.

88. Buckpitt A, Buonarati M, Avey LB, Chang AM, Morin D, Plopper CG, 1992. Relationship of cytochrome P450 activity to Clara cell cytotoxicity. II. Comparison of stereoselectivity of naphthalene epoxidation in lung and nasal mucosa of mouse, hamster, rat and rhesus monkey. J Pharmacol Exp Ther. 261:364-372.

89. Stevens TP, McBride JT, Peake JL, Pinkerton KE, Stripp BR, 1997. Cell proliferation contributes to PNEC hyperplasia after acute airway injury. Am J Physiol. 272:L486-L493.

90. Reynolds SD, Giangreco A, Power JH, Stripp BR, 2000. Neuroepithelial bodies of pulmonary airways serve as a reservoir of progenitor cells capable of epithelial regeneration. Am J Pathol. 156:269-278.

91. Hong KU, Reynolds SD, Giangreco A, Hurley CM, Stripp BR, 2001. Clara cell secretory protein-expressing cells of the airway neuroepithelial body microenvironment include a label-retaining subset and are critical for epithelial renewal after progenitor cell depletion. Am J Respir Cell Mol Biol. 24:671-681.

92. Reynolds SD, Hong KU, Giangreco A, Mango GW, Guron C, Morimoto Y, Stripp BR, 2000. Conditional clara cell ablation reveals a self-renewing progenitor function of pulmonary neuroendocrine cells. Am J Physiol Lung Cell Mol Physiol. 278:L1256-L1263.

93. Borges M, Linnoila RI, van de Velde HJ, Chen H, Nelkin BD, Mabry M, Baylin SB, Ball DW, 1997. An achaete-scute homologue essential for neuroendocrine differentiation in the lung. Nature. 386:852-855.

94. Kotton DN, Ma BY, Cardoso WV, Sanderson EA, Summer RS, Williams MC, Fine A, 2001. Bone marrow-derived cells as progenitors of lung alveolar epithelium. Development. 128:5181-5188.

95. Ali NN, Edgar AJ, Samadikuchaksaraei A, Timson CM, Romanska HM, Polak JM, Bishop AE, 2002. Derivation of type II alveolar epithelial cells from murine embryonic stem cells. Tissue Eng. 8:541-550.

96. Wagers AJ, Sherwood RI, Christensen JL, Weissman IL, 2002. Little evidence for developmental plasticity of adult hematopoietic stem cells. Science. 297:2256-2259.

97. Voswinckel R, Ziegelhoeffer T, Heil M, Kostin S, Breier G, Mehling T, Haberberger R, Clauss M, Gaumann A, Schaper W, Seeger W, 2003. Circulating vascular progenitor cells do not contribute to compensatory lung growth. Circ Res. 93:372-379.

98. Jarecki J, Johnson E, Krasnow MA, 1999. Oxygen regulation of airway branching in Drosophila is mediated by branchless FGF. Cell. 99:211-220.

99. Coalson JJ, 2003. Pathology of new bronchopulmonary dysplasia. Semin Neonatol. 8:73-81.

100. Zeng X, Wert SE, Federici R, Peters KG, Whitsett JA, 1998. VEGF enhances pulmonary vasculogenesis and disrupts lung morphogenesis in vivo. Dev Dyn. 211:215-227.

101. Le Cras TD, Spitzmiller RE, Albertine KH, Greenberg JM, Whitsett JA, Akeson AL, 2004. VEGF causes

pulmonary hemorrhage, hemosiderosis, and air space enlargement in neonatal mice. Am J Physiol Lung Cell Mol Physiol. 287:L134-142.

102. Pepicelli CV, Lewis PM, McMahon AP, 1998. Sonic hedgehog regulates branching morphogenesis in the mammalian lung. Curr Biol. 8:1083-1086.

103. Litingtung Y, Lei L, Westphal H, Chiang C, 1998. Sonic hedgehog is essential to foregut development. Nat Genet. 20:58-61.

104. Yancopoulos GD, Klagsbrun M, Folkman J, 1998. Vasculogenesis, angiogenesis, and growth factors: ephrins enter the fray at the border. Cell. 93:661-664.

105. Thurston G, Suri C, Smith K, McClain J, Sato TN, Yancopoulos GD, McDonald DM, 1999. Leakage-resistant blood vessels in mice transgenically overexpressing angiopoietin-1. Science. 286:2511-2514.

106. Hanahan D, 1997. Signaling vascular morphogenesis and maintenance. Science. 277:48-50.

107. Ferrara N, Davis-Smyth T, 1997. The biology of vascular endothelial growth factor. Endocr Rev. 18:4-25.

108. Gale NW, Yancopoulos GD, 1999. Growth factors acting via endothelial cell-specific receptor tyrosine kinases: VEGFs, angiopoietins, and ephrins in vascular development. Genes Dev. 13:1055-1066.

109. Suri C, Jones PF, Patan S, Bartunkova S, Maisonpierre PC, Davis S, Sato TN, Yancopoulos GD, 1996. Requisite role of angiopoietin-1, a ligand for the TIE2 receptor, during embryonic angiogenesis. Cell. 87:1171-1180.

110. Folkman J, D'Amore PA, 1996. Blood vessel formation: what is its molecular basis? Cell. 87:1153-1155.

111. Maisonpierre PC, Suri C, Jones PF, Bartunkova S, Wiegand SJ, Radziejewski C, Compton D, McClain J, Aldrich TH, Papadopoulos N, Daly TJ, Davis S, Sato TN, Yancopoulos GD, 1997. Angiopoietin-2, a natural antagonist for Tie2 that disrupts in vivo angiogenesis. Science. 277:55-60.

112. Apelqvist A, Ahlgren U, Edlund H, 1997. Sonic hedgehog directs specialised mesoderm differentiation in the intestine and pancreas. Curr Biol. 7:801-804.

113. Holash J, Wiegand SJ, Yancopoulos GD, 1999. New model of tumor angiogenesis: dynamic balance between vessel regression and growth mediated by angiopoietins and VEGF. Oncogene. 18:5356-5362.

114. Witzenbichler B, Maisonpierre PC, Jones P, Yancopoulos GD, Isner JM, 1998. Chemotactic properties of angiopoietin-1 and -2, ligands for the endothelial-specific receptor tyrosine kinase Tie2. J Biol Chem. 273:18514-18521.

115. Han RN, Babaei S, Robb M, Lee T, Ridsdale R, Ackerley C, Post M, Stewart DJ, 2004. Defective lung vascular development and fatal respiratory distress in endothelial NO synthase-deficient mice: a model of alveolar capillary dysplasia? Circ Res. 94:1115-1123.

116. Tsai SY, Tsai MJ, 1997. Chick ovalbumin upstream promoter-transcription factors (COUP-TFs): coming of age. Endocr Rev. 18:229-240.

117. Pereira FA, Qiu Y, Zhou G, Tsai MJ, Tsai SY, 1999. The orphan nuclear receptor COUP-TFII is required for angiogenesis and heart development. Genes Dev. 13:1037-1049.

118. Nikolova G, Lammert E, 2003. Interdependent development of blood vessels and organs. Cell Tissue Res. 314:33-42.

119. Matsumoto K, Yoshitomi H, Rossant J, Zaret KS, 2001. Liver organogenesis promoted by endothelial cells prior to vascular function. Science. 294:559-563.

120. Shalaby F, Rossant J, Yamaguchi TP, Gertsenstein M, Wu XF, Breitman ML, Schuh AC, 1995. Failure of blood-island formation and vasculogenesis in Flk-1-deficient mice. Nature. 376:62-66.

121. Lammert E, Cleaver O, Melton D, 2001. Induction of pancreatic differentiation by signals from blood vessels. Science. 294:564-567.

122. Lammert E, Cleaver O, Melton D, 2003. Role of endothelial cells in early pancreas and liver development. Mech Dev. 120:59-64.

123. Bruneau BG, Bao ZZ, Fatkin D, Xavier-Neto J, Georgakopoulos D, Maguire CT, Berul CI, Kass DA, Kuroski-de Bold ML, de Bold AJ, Conner DA, Rosenthal N, Cepko CL, Seidman CE, Seidman JG, 2001. Cardiomyopathy in Irx4-deficient mice is preceded by abnormal ventricular gene expression. Mol Cell Biol. 21:1730-1736.

124. Lebel M, Agarwal P, Cheng CW, Kabir MG, Chan TY, Thanabalasingham V, Zhang X, Cohen DR, Husain M, Cheng SH, Bruneau BG, Hui CC, 2003. The Iroquois homeobox gene Irx2 is not essential for normal development of the heart and midbrain-hindbrain boundary in mice. Mol Cell Biol. 23:8216-8225.

125. Cardoso WV, Williams MC, Mitsialis SA, Joyce-Brady M, Rishi AK, Brody JS, 1995. Retinoic acid induces changes in the pattern of airway branching and alters epithelial cell differentiation in the developing lung in vitro. Am J Respir Cell Mol Biol. 12:464-476.

126. Gómez-Skarmeta JL, Glavic A, de la Calle-Mustienes E, Modolell J, Mayor R, 1998. Xiro, a Xenopus homolog of the Drosophila Iroquois complex genes, controls development at the neural plate. Embo J. 17:181-190.

127. Warburton D, Schwarz M, Tefft D, Flores-Delgado G, Anderson KD, Cardoso WV, 2000. The molecular basis of lung morphogenesis. Mech Dev. 92:55-81.

128. Artavanis-Tsakonas S, Rand MD, Lake RJ, 1999. Notch signaling: cell fate control and signal integration in development. Science. 284:770-776.

129. McLaughlin KA, Rones MS, Mercola M, 2000. Notch regulates cell fate in the developing pronephros. Dev Biol. 227:567-580.

130. Apelqvist A, Li H, Sommer L, Beatus P, Anderson DJ, Honjo T, Hrabe de Angelis M, Lendahl U, Edlund H, 1999. Notch signalling controls pancreatic cell differentiation. Nature. 400:877-881.

131. Ito T, Udaka N, Yazawa T, Okudela K, Hayashi H, Sudo T, Guillemot F, Kageyama R, Kitamura H, 2000. Basic helix-loop-helix transcription factors regulate the neuroendocrine differentiation of fetal mouse pulmonary epithelium. Development. 127:3913-3921.

132. Kong Y, Glickman J, Subramaniam M, Shahsafaei A, Allamneni KP, Aster JC, Sklar J, Sunday ME, 2004. Functional diversity of notch family genes in fetal lung development. Am J Physiol Lung Cell Mol Physiol. 286:L1075-1083.

133. Wu JY, Rao Y, 1999. Fringe: defining borders by regulating the notch pathway. Curr Opin Neurobiol. 9:537-543.

134. Ju BG, Jeong S, Bae E, Hyun S, Carroll SB, Yim J, Kim J, 2000. Fringe forms a complex with Notch. Nature. 405:191-195.

135. Hicks C, Johnston SH, diSibio G, Collazo A, Vogt TF, Weinmaster G, 2000. Fringe differentially modulates Jagged1 and Delta1 signalling through Notch1 and Notch2. Nat Cell Biol. 2:515-520.

136. Post LC, Ternet M, Hogan BL, 2000. Notch/Delta expression in the developing mouse lung. Mech Dev. 98:95-98.

137. Dang TP, Gazdar AF, Virmani AK, Sepetavec T, Hande KR, Minna JD, Roberts JR, Carbone DP, 2000. Chromosome 19 translocation, overexpression of Notch3, and human lung cancer. J Natl Cancer Inst. 92:1355-1357.

138. Chen H, Thiagalingam A, Chopra H, Borges MW, Feder JN, Nelkin BD, Baylin SB, Ball DW, 1997. Conservation of the Drosophila lateral inhibition pathway in human lung cancer: a hairy-related protein (HES-1) directly represses achaete- scute homolog-1 expression. Proc Natl Acad Sci U S A. 94:5355-5360.

139. Sriuranpong V, Borges MW, Ravi RK, Arnold DR, Nelkin BD, Baylin SB, Ball DW, 2001. Notch signaling induces cell cycle arrest in small cell lung cancer cells. Cancer Res. 61:3200-3205.

140. Thébaud B, Mercier JC, Dinh-Xuan AT, 1998. Congenital diaphragmatic hernia. A cause of persistent pulmonary hypertension of the newborn which lacks an effective therapy. Biol Neonate. 74:323-336.

141. Lally KP, Lally PA, Langham MR, Hirschl R, Moya FR, Tibboel D, Van Meurs K, 2004. Surfactant does not improve survival rate in preterm infants with congenital diaphragmatic hernia. J Pediatr Surg. 39:829-833.

142. van Dooren MF, 2004. PhD thesis: Congenital diaphragmatic hernia. The importance of genetic and environmental factors, Erasmus MC Rotterdam, The Netherlands

143. Chang R, Andreoli S, Ng YS, Truong T, Smith SR, Wilson J, D'Amore PA, 2004. VEGF expression is downregulated in nitrofen-induced congenital diaphragmatic hernia. J Pediatr Surg. 39:825-828; discussion 825-828.

144. Oue T, Yoneda A, Shima H, Taira Y, Puri P, 2002. Increased vascular endothelial growth factor peptide and gene expression in hypoplastic lung in nitrofen induced congenital diaphragmatic hernia in rats. Pediatr Surg Int. 18:221-226.

145. Guilbert TW, Gebb SA, Shannon JM, 2000. Lung hypoplasia in the nitrofen model of congenital diaphragmatic hernia occurs early in development. Am J Physiol Lung Cell Mol Physiol. 279:L1159-1171.

146. Okazaki T, Sharma HS, Aikawa M, Yamataka A, Nagai R, Miyano T, Tibboel D, 1997. Pulmonary expression of vascular endothelial growth factor and myosin isoforms in rats with congenital diaphragmatic hernia. J Pediatr Surg. 32:391-394.

147. Shehata SM, Mooi WJ, Okazaki T, El-Banna I, Sharma HS, Tibboel D, 1999. Enhanced expression of vascular endothelial growth factor in lungs of newborn infants with congenital diaphragmatic hernia and pulmonary hypertension. Thorax. 54:427-431.

148. Shehata SM, Tibboel D, Sharma HS, Mooi WJ, 1999. Impaired structural remodelling of pulmonary arteries in newborns with congenital diaphragmatic hernia: a histological study of 29 cases. J Pathol. 189:112-118.

149. De Caestecker M, Meyrick, B., 2001. Bone morphogenetic proteins, genetics and the pathophysiology of primary pulmonary hypertension. Respiratory research. 2.

150. Foley JP, Jr: Congenital hypothyroidism. In Braverman LE, Utiger RD (eds): Werner & Ingbar's the thyroid: a fundamental and clinical text, 8th 8th, p 977-983. Philadelphia, Lippincott-Williams & Wilkins, 2000.

151. Bongers-Schokking JJ, Koot HM, Wiersma D, Verkerk PH, de Muinck Keizer-Schrama SM, 2000. Influence of timing and dose of thyroid hormone replacement on development in infants with congenital hypothyroidism. J Pediatr. 136:292-297.

152. van Vliet G, 2001. Treatment of congenital hypothyroidism. Lancet. 358:86-87.

153. Cao XY, Jiang XM, Dou ZH, Rakeman MA, Zhang ML, O'Donnell K, Ma T, Amette K, DeLong N, DeLong GR, 1994. Timing of vulnerability of the brain to iodine deficiency in endemic cretinism. N Engl J Med.

331:1739-1744.

154. Delange F, 2001. Iodine deficiency as a cause of brain damage. Postgrad Med J. 77:217-220.

155. Porterfield SP, Hendrich CE, 1993. The role of thyroid hormones in prenatal and neonatal neurological development--current perspectives. Endocr Rev. 14:94-106.

156. Haddow JE, Palomaki GE, Allan WC, Williams JR, Knight GJ, Gagnon J, O'Heir CE, Mitchell ML, Hermos RJ, Waisbren SE, Faix JD, Klein RZ, 1999. Maternal thyroid deficiency during pregnancy and subsequent neuropsychological development of the child. N Engl J Med. 341:549-555.

157. Morreale de Escobar G, Obregon MJ, Escobar del Rey F, 2000. Is neuropsychological development related to maternal hypothyroidism or to maternal hypothyroxinemia? J Clin Endocrinol Metab. 85:3975-3987.

158. Pop VJ, Kuijpens JL, van Baar AL, Verkerk G, van Son MM, de Vijlder JJ, Vulsma T, Wiersinga WM, Drexhage HA, Vader HL, 1999. Low maternal free thyroxine concentrations during early pregnancy are associated with impaired psychomotor development in infancy. Clin Endocrinol. 50:149-155.

159. Lamers WH, Boon L, Van Hemert FJ, Labruyere WT, De Jong P, Ruijter JM, Moorman AF, 1999. Glutamine synthetase expression in perinatal spiny mouse liver. Eur J Biochem. 262:803-809.

160. Barker DJ, 1998. In utero programming of chronic disease. Clin Sci. 95:115-128.

Chapter 10

Summaries / samenvattingen

Summaries

Chapter 1 reviews the current literature on molecular lung development. The different phases of lung development are described, highlighting the most important transcription and growth factors for that specific stage.

Chapter 2 gives an outline of the thesis. Studying normal lung development is central to our understanding of "pulmonary health" and embryonic signaling pathways could potentially be re-initiated during postnatal pulmonary injury and disease.

In **chapter 3** we demonstrate that a low oxygen environment (hypoxia; 3% oxygen) stimulates pulmonary vascular and epithelial branching morphogenesis *in vitro*. Culturing in 3% oxygen significantly increased vascular endothelial growth factor (Vegf) and Pecam-1 mRNA levels. In vertebrates, Vegf is one of the most important growth factors involved in the development of the vasculature. The increase in branching morphogenesis was not the result of differences in the mRNA expression of fibroblast growth factor-10 (Fgf-10) or its receptor Fgfr2, which were shown to regulate the hypoxic-induced increase in tracheal branching in *Drosophila*. Furthermore, we show that the inhibition of vascularization *in vitro*, using antisense oligonucleotides (ODNs) targeted against hypoxia inducible factor-1α or Vegf, dramatically decreased epithelial branching morphogenesis. We conclude that a low oxygen environment is important for the branching of both distal lung epithelium and vascular tissue and that pulmonary vascular development appears to be a rate-limiting step for epithelial branching morphogenesis.

In **chapter 4** we investigate pulmonary vascular development in mice deficient for Sonic hedgehog (Shh). Shh-deficient mice have severely hypoplastic lungs with extended branching defects. Early embryonic vascular development *in vivo* was appropriate for the degree of epithelial branching in Shh-deficient lungs. mRNA levels for Pecam-1, Vegf, and its receptor Flk-1 were unchanged as assessed by real-time RT-PCR. However, the mRNA expression of Angiopoietin-1 (Ang-1), but not Ang-2, or the angiopoietin receptor Tie2 was reduced. Ang-1 has been shown to play a role in the interaction of endothelial cells and surrounding support cells in order to stabilize the vascular network. At later gestation, a rapid decline and disorganization of the vascular structures was seen in cultured Shh-deficient lungs. Intriguingly, partial restoration of the pulmonary vascular paucity in Shh-deficient lungs with the angiogenic factor Fgf2 also partially recovered airway branching morphogenesis. We conclude that early vascular development, mediated by Vegf/Vegfr2 signaling, proceeds normally in Shh-deficient mice, whereas vascular development at later stages, mediated by Ang/Tie2 signaling, is defective, what in turn might be responsible for the reduction in epithelial branching morphogenesis.

In **chapter 5** we demonstrate that Iroquois (Irx) homeobox genes play an important role in lung branching morphogenesis and proximal-distal epithelial differentiation. We found that Irx1, -2, -3, and -5 mRNA were expressed in the epithelial cell layer of early gestational lungs. *In vitro* inhibition of Irx signaling with antisense ODNs targeted against Irx1-3 and Irx 5 caused an almost complete absence of distal epithelial structures, whereas proximal airways developed relatively normal. In these explants, the smooth muscle cell layer was abnormal and the mass of mesenchyme was severely reduced. Although *Ci*, which is the *Drosophila* homologue of vertebrate Gli1-3, was shown to positively control the *Drosophila* counterparts of the vertebrate Irx genes, we did not observe any difference in Irx gene expression in Shh or Gli mutant lungs. We conclude that the Irx genes are involved in the regulation of proximal-distal branching morphogenesis but are not downstream of the Shh/Gli signaling pathway.

In **chapter 6** we demonstrate that Lunatic fringe (Lfng) mRNA is expressed in the early epithelial cell layer of the lung and rapidly declines with advancing gestational age. Fringe proteins modulate Notch signaling, which is a signaling pathway that regulates cell fate decisions and patterning in various tissues during development. Hes1 and Mash-1 are bHLH factors that are both regulated by Notch. We detected Hes1 mRNA in the early pulmonary epithelial cell layer and at later stages in epithelial cells of terminal bronchioles. Mash-1 mRNA expression was specifically detected in the neuroendocrine cells of the lung. Overexpression of full-length mouse Lfng cDNA in distal pulmonary epithelial cells did not affect lung development nor did it influence the temporal, spatial, or quantitative expression of Hes1 or Mash-1 mRNA. We conclude that Lfng does likely not define epithelial morphogenic boundaries along the anterior-posterior axis of the developing airways.

In **chapter 7** we tested the hypothesis that lungs in congenital diaphragmatic hernia (CDH) are surfactant-deficient, which could explain in part the respiratory failure and difficulties in treating CDH infants. We used the nitrofen-induced CDH rat model and found that the spatial and temporal expression patterns of SP-A, -B, and -C mRNA, the cellular concentration and the volume fraction of SP-expressing cells were unchanged. Also, at the protein level, no differences in SP expression were observed. To specifically assess the cellular concentrations of SP mRNA within the architecture of the tissue, we used a quantitative *in situ* hybridization technique. This study demonstrates that there is no primary deficiency of surfactant proteins in the nitrofen-induced CDH rat model.

In **chapter 8** we demonstrate that before birth, hypothyroidism of mother and fetus had no effect on the structural development of the heart and lungs or on the temporal, spatial, or level of mRNA expression of β- and α-myosin heavy chain (MHC) in the heart and surfactant proteins in the lungs. The neonatal switch from β- to α-MHC expression in the cardiac ventricles did not occur in hypothyroid pups that had lacked maternal thyroid hormone (TH). However, neither did the switch occur in pups that also had lacked maternal

TH but did produce their own TH. Postnatal structural lung development was severely affected in hypothyroid pups from hypothyroid mothers, but not in euthyroid pups from hypothyroid mothers. Surfactant protein mRNA expression remained high in the alveolar epithelium of pups that had lacked maternal TH, irrespective of the ability to produce their own TH. This study shows that hypothyroidism during early development does not impair organ morphogenesis, but does affect adaptive responses in gene expression in these organs postnatally.

Taken together, the data presented in this thesis provide the following new viewpoints in fetal lung development:

1. Pulmonary vascular and epithelial branching are regulated by oxygen and vascular development is a rate-limiting step in epithelial branching morphogenesis.
2. The vasculature-stabilizing factor Ang-1 is significantly decreased in Shh-deficient lungs.
3. Fgf2 partially restores vascular and epithelial branching in Shh-deficient lungs.
4. The Irx homeobox genes are involved in the regulation of proximal-distal lung branching morphogenesis.
5. Lunatic fringe does not play a significant role in the determination of pulmonary cell fate.
6. Lungs from rats with nitrofen-induced CDH are not deficient for pulmonary surfactant proteins.
7. Maternal thyroid hormone plays an important role in postnatal adaptive gene expression in neonatal heart and lungs.

Samenvattingen

Hoofdstuk 1 reviews de bestaande literatuur op het gebied van moleculaire longontwikkeling. De verschillende fases van longontwikkeling worden besproken en de meest belangrijke transcriptie- en groeifactoren voor de betreffende fases worden nader toegelicht.

Hoofdstuk 2 geeft een kort overzicht van dit proefschrift. In dit hoofdstuk wordt toegelicht dat het bestuderen van normale longontwikkeling essentieel is voor onze kennis van de gezondheid van de longen na de geboorte. Embryonale signaal cascades kunnen van potentieel belang zijn en misschien zelfs "herstart" worden bij postnatale longschade en -ziekte.

In **hoofdstuk 3** laten we zien dat een laag zuurstofgehalte (hypoxie) van de omgeving (3% zuurstof) het aantal vertakkingen van longvaten en luchtwegen in gekweekte longen doet toenemen. Kweken in 3% zuurstof verhoogde de mRNA expressie van vascular endothelial growth factor (Vegf) en Pecam-1 significant. Vegf is in vertebraten één van de meest belangrijke groeifactoren die verantwoordelijk zijn voor de ontwikkeling van de bloedvaten. De toename in epitheelvertakkingen was niet het resultaat van een verandering in de expressie van fibroblast growth factor-10 (Fgf-10) of de receptor Fgfr2, hoewel van beide bekend is dat zij in *Drosophila* het aantal trachea vertakkingen doen toenemen als reactie op hypoxie. We laten vervolgens zien dat wanneer bloedvatvorming wordt geremd door middel van antisense oligonucleotiden (ODNs) gericht tegen hypoxia inducible factor-1α of tegen Vegf dit een dramatische reductie van de epitheelvertakkingen geeft. We concluderen dat een laag zuurstofgehalte van de omgeving de vertakkingen van zowel pulmonale bloedvaten als distale luchtwegen stimuleert en dat de groei van het pulmonale vaatbed limiterend is voor de ontwikkeling van de luchtwegvertakkingen.

In **hoofdstuk 4** hebben we de pulmonale bloedvatontwikkeling in Sonic hedgehog (Shh) deficiënte muizen bestudeerd. Deze Shh deficiënte muizen hebben zeer onderontwikkelde longen met een drastisch verminderd aantal luchtwegvertakkingen. We laten zien dat de vroege embryonale vaatontwikkeling in Shh deficiënte longen relatief normaal verloopt. Met real-time RT-PCR laten we tevens zien dat de mRNA expressie voor Pecam-1, Vegf en de Vegf receptor Flk-1 onveranderd is. De mRNA expressie voor Angiopoietin-1 (Ang-1), maar niet die van Ang-2 of van de angiopoietin receptor Tie2 bleek echter drastisch verlaagd te zijn. Ang-1 speelt normaal gesproken een rol in de interactie tussen de endotheel cellen en de omliggende steuncellen om zo het bloedvaten netwerk te stabiliseren. Gekweekte Shh deficiënte longen vertoonden een snelle achteruitgang van de pulmonale bloedvaten in zowel complexiteit als structuur. Deze achteruitgang kon gedeeltelijk worden hersteld met het bloedvatgroei bevorderende Fgf2. Naast een herstel van het pulmonale vaatbed werd tevens een gedeeltelijk herstel van het luchtwegvertakkingspatroon waargenomen.

We concluderen dat vroege vaatontwikkeling via het Vegf/Vegfr2 signaal systeem relatief normaal verloopt in Shh deficiënte longen, maar dat verdere bloedvatontwikkeling en stabilisatie van het vaatnetwerk inefficiënt is door een tekort aan Ang-1/Tie2 signaal wat op zich een oorzaak zou kunnen zijn van de verminderde ontwikkeling van de epitheelvertakkingen.

In **hoofdstuk 5** beschrijven we de rol van de Iroquois (Irx) homeobox genen in de ontwikkeling van epitheelvertakkingen met proximaal-distale epitheel differentiatie. We tonen aan dat in de vroeg embryonale long, Irx1, -2, -3 and -5 mRNA specifiek tot expressie komt in het epitheel van de luchtwegvertakkingen. Antisense ODNs gericht tegen de translatie-initiatie plaats van Irx1-3 en Irx 5 veroorzaakten een enorme reductie in distale epitheelvertakkingen in gekweekte embryonale longen, terwijl de proximale luchtwegstructuren relatief onveranderd bleven. Met immunohistochemie tonen we vervolgens aan dat de gladde spiercellaag onderbroken en het totale mesenchyme oppervlak verminderd is. Hoewel *Ci* de *Drosophila* homoloog van Gli1-3 is en positief gereguleerd wordt door de *Drosophila* homologen van de vertebrate Irx genen, werden er geen verschillen in mRNA expressie patronen gezien voor de verschillende Irx genen in Shh en Gli mutante longen. We concluderen dat de Irx genen een rol spelen in de regulatie van proximaal-distale longontwikkeling, maar niet gereguleerd worden door de Shh/Gli signaal cascade.

In **hoofdstuk 6** tonen we aan dat Lunatic (Lfng) mRNA tot expressie komt in de epitheelcellen van de zich ontwikkelende long en verdwijnt tegen de geboorte. Fringe eiwitten moduleren de Notch cascade, wat een cascade is die essentieel is voor het afbakenen van morphogene grenzen in een aantal organen. Lfng en Hes1 mRNA expressie werden beide gezien in de vroeg embryonale epitheliale cellaag. Hes1 and Mash-1 zijn bHLH factoren die beide gereguleerd worden door Notch. We laten zien dat Hes1 mRNA tot expressie komt in de epitheelcellen van de zich ontwikkelende long en tegen de geboorte geconcentreerd wordt in de terminale bronchioli. Mash-1 mRNA expressie was specifiek in de neuroendocriene cellen van de long. Overexpressie van Lfng in de distale epitheelcellen had geen effect op de temporele, spatiale of kwantitatieve mRNA expressie van Hes1 of Mash-1. We concluderen dat Lfng waarschijnlijk geen rol speelt in de regulatie van proximaal-distale ontwikkeling en differentiatie van de epitheelvertakkingen.

In **hoofdstuk 7** beschrijven we een onderzoek naar de expressie van surfactant eiwitten in longen van ratten met congenitale hernia diaphragmatica (CHD). Een surfactant deficiëntie zou mogelijk een reden kunnen we zijn voor de problemen bij de behandeling van respiratoire insufficiëntie bij CHD. We hebben gebruik gemaakt van het nitrofen-geïnduceerde hernia model in de rat. De spatiale and temporele expressie van SP-A, -B en -C mRNA, de cellulaire concentratie en de volume fractie van cellen die SP tot expressie brengen waren ongewijzigd in de CHD longen. Deze resultaten werden bevestigd op eiwit

niveau. Om specifiek de concentratie van SP mRNA op cellulair niveau te bepalen hebben we gebruik gemaakt van een kwantitatieve *in situ* hybridisatie techniek. Deze studie toont aan dat longen in nitrofen-geïnduceerde CHD niet primair surfactant deficiënt zijn.

In **hoofdstuk 8** tonen we aan dat hypothyreoïdie van de moeder en het embryo voor de geboorte geen effect heeft op de embryonale structurele ontwikkeling van hart en longen. Er was tevens geen effect op de cardiale mRNA expressie van β-myosine heavy chain (MHC) of α-MHC of op de mRNA expressie van surfactant eiwitten (SP) in de longen. Na de geboorte vindt normaal gesproken een switch plaats β-MHC naar α-MHC in de ventrikels van het hart. Deze switch bleef echter uit in de hypothyreote pups van moeders die zelf ook hypothyreoot waren, maar evengoed trad deze switch niet op in pups die wel in staat waren hun eigen schildklierhormoon te maken, maar ook niet aan maternaal schildklierhormoon blootgesteld waren. De structurele longontwikkeling was ernstig aangedaan in hypothyreote pups van hypothyreote moeders, terwijl de longstructuur in pups die wel hun eigen schildklierhormoon maakten vergelijkbaar was met die van controle longen. SP mRNA expressie bleef hoog in het alveolaire epitheel van pups die maternaal schildklierhormoon gemist hadden, ongeacht of ze zelf in staat waren om schildklierhormoon te produceren. Deze studie toont aan dat hypothyreoïdie tijdens vroege ontwikkeling geen gevolgen heeft voor de prenatale organogenese, maar wel voor de postnatale adaptieve veranderingen in gen expressie in hart en longen.

Samengevat geven de data zoals gepresenteerd in dit proefschrift de volgende nieuwe gezichtspunten in embryonale longontwikkeling:

1. De ontwikkeling van bloedvaten en epitheelvertakkingen in de longen wordt gereguleerd door zuurstof en de bloedvatontwikkeling speelt een belangrijke limiterende rol in de ontwikkeling van luchtwegvertakkingen.
2. Angiopoietin-1, wat een bloedvat stabiliserende factor is, komt significant lager tot expressie in Shh deficiënte longen.
3. Fgf2 gedeeltelijk herstelt zowel bloedvat als epitheelvertakkingen in Shh deficiënte longen.
4. De Irx homeobox genen zijn van belang voor de regulatie van de proximaal-distale ontwikkeling van epitheelvertakkingen.
5. Lunatic fringe speelt geen belangrijke rol in de determinatie van pulmonale cel differentiatie.
6. Longhypoplasie in embryonale ratten met nitrofen-geïnduceerde CHD gaat niet gepaard met een primaire deficiëntie van surfactant eiwitten.
7. Maternaal schildklierhormoon speelt een belangrijke rol in de postnatale adaptieve veranderingen in gen expressie in neonatale hart en longen.

Appendices

Acknowledgements

Acknowledgements

During the lab work and the writing of this thesis many people have supported me and without them it would never have been finished. I thank all of you that have helped me so much. I would like to mention some people in particular.

Allereerst mijn promotoren, **Prof. dr. D. Tibboel** en **Prof. dr. M. Post**.

Beste **Dick**, bedankt voor het scheppen van mogelijkheden, voor de vrijheid waarmee ik dit onderzoek uit heb kunnen voeren en het blijvende vertrouwen. Met zeer veel plezier denk ik terug aan de congressen, Keystone en the Lion King; naast hard werken maak jij tijd voor the good things in life; dat moet ik onthouden!

Beste **Martin**, jij zit zo boordevol ideeën dat het geweldig is om met je te werken. Dankzij jouw vertrouwen en enthousiasme heb ik veel geleerd in korte tijd en ben ik gevallen voor de research! Ik zal het onderzoek missen en hoop er na mijn klinische opleiding weer mee verder te kunnen gaan. Veel dank ook voor je steun op persoonlijk vlak; jij vergat nooit hoe belangrijk Dennis voor me was en hoe het is om lang weg te zijn van huis.

Prof. dr. W. H. Lamers, mijn 3e baas! Beste Wout, de allereerste *in situ* heb ik in jouw lab gedaan. Als long tussen het hart en de lever zat ik eigenlijk prima op mijn plaats. We hebben heel wat discussie gevoerd per e-mail, met resultaat! Dank je wel voor al je hulp.

Dear **Prof. dr. E. A. Dzierzak**, thank you for taking part in the small committee and your valuable comments on the thesis.

Beste **Prof. dr. J. B. van Goudoever**, bedankt voor uw waardevolle beoordeling van het manuscript en uw bereidheid deel te nemen aan de kleine commissie.

Beste **Prof. dr. L. J. Zimmermann**, bedankt voor uw bereidheid plaats te nemen in de grote commissie. We kunnen altijd nog over T.O. en de Alan Brown Building van gedachten wisselen!

Beste **Prof. dr. J. C. de Jongste**, dank u wel voor uw bereidheid plaats te nemen in de grote commissie.

Beste **Prof. dr. H. S. A. Heymans**, zeer veel dank voor uw tijd en bereidheid om deel te nemen aan de grote commissie. Ik ben vereerd dat u nu het stokje overneemt van Prof. D. Tibboel en Prof. M. Post in het begeleiden van mijn opleiding tot kinderarts.

Beste **Dr. R. J. Rottier**, beste Robbert, dank je wel voor het deelnemen aan de grote commissie. Ik begrijp (weer) waarom je Memphis nog steeds mist! Heel veel succes met je lab!

Beste **Dr. R. R. de Krijger**, dank u wel voor het plaatsnemen in de grote commissie. Zeer veel dank ook voor uw belangstelling voor mijn onderzoek de afgelopen jaren!

Het **Sophia** kinderziekenhuis/**EMC** in **Rotterdam** is de afgelopen jaren het coördinatiepunt van dit promotieonderzoek geweest. Een aantal mensen wil ik daar in het bijzonder bedanken. **Annemarie Illsley**, beste Annemarie, mijn aanspreekpunt in Rotterdam. Bedankt voor je gezellige mail, onmisbare hulp tijdens SSWO report time en vooral voor de soepele communicatie met Prof. Tibboel! Beste **Richard Keijzer**, bedankt dat je me (alweer jaren geleden) voorgesteld hebt aan Dick; ik had het onderzoek niet willen missen. Een korte tussenstop op Lab 785 van de afdeling Celbiologie en Genetica van de Erasmus Universiteit in Rotterdam, **Prof. dr. F. Grosveld** en **Dr. Robbert Rottier**, dank jullie wel voor de gastvrijheid en belangstelling. Beste **Marieke van Dooren**, dank je wel voor je support en gezelligheid!

Op de afdeling **Anatomie en Embryologie** van de **UvA** heb ik de eerste stappen in de research gezet en heb ik het bijzonder naar mijn zin gehad met name door de gezellige sfeer en goede begeleiding door **Prof. dr. Wout Lamers**, **Prof. dr. Antoon Moorman** en **Dr. Pietjan Blommaart**. Lieve Pietjan, zelden ben ik iemand tegengekomen die zoveel tijd vrijmaakt om anderen te helpen. Ik heb van jou de meest belangrijke basis van het "lableven" geleerd. Als witjas had ik het soms zwaar te verduren van je, en ja het heeft even geduurd, maar hier dan toch dat boekje! Lieve **Marry**, naast alle coupes en eindeloze gesprekken in de trein ben ik blij dat we nog steeds doorkletsen over non-lab zaken. Lieve **Jacqueline**, veel van je geleerd op ISH gebied; dank voor al je hulp; see you around in the AMC! Bedankt **Marian van Roon** (kamergenoot, ook in Toronto geweest!), **John Spijkers** (kamergenoot, altijd in voor een praatje), **Piet de Boer** (ISH-koning!), **Wil Labruyère** (organizing RA-lab), **Vincent Christoffels** en **Danielle Clout** (dank jullie wel voor Irx), **Wouter de Jonge** (we mailen!), **Robbert Storm van Leeuwen** (bakkie koffie en ISH ontwikkelen), **Ying Ya** (how many coupes can you make?), **Cees Hersbach** (voor gezelligheid en high quality last minute dia's), **Jan Ruijter** (redder in statistiek nood), **Jaco Hagoort** (computerman), **Cars Gravemeijer** (foto expert), de ladies van de coupes en immuno's: **Corrie de Gier-de Vries** en **Sabina Tesink-Taekema**. Dank aan **Maurice van den Hoff**, **Ronald Lekanne dit Deprez** en **Theo Hakvoort** voor advies en comments tijdens werkbesprekingen. O, en Maurice, sinds de invoering van de Euro is dit valse kwartje niet meer teruggeweest!

Met het einde van dit proefschrift is ook een einde gekomen aan mijn tijd in "***Toronno***".

The **Post lab** has not only taught me the science of lung biology, but they made me feel at home in Toronto and introduced me to their homes and families. Dear **Irene**, running the lab smoothly, placing emergency orders and taking me out with your family to see your nephew play professional ice hockey. Thank you for your friendship. Dear **Jinxia**, I learned a lot from you about molecular biology, RT-PCR and about making constructs and probes. Thank you for your understanding. Dear **Maciek**, thanks for oligo's and RNA

isolation and above all for your optimistic view on (lab)-life; you cheered up my day many times! Dear **Jason**, thanks for your help and teaching me doing explants; they're my favorite experiment! Dear **Anna**, excellent secretary and wonderful mother; the twins have a special place in my hart. Don't forget to visit Holland when you show them Italy! Dear **Marjorie**, woman of the world, always time for a chat; thanks for your help. Dear **Ian**, thank you for introducing me to Thanksgiving, your family and the farm. Good luck with your thesis! **Ross**, thanks for your help with electron microscopy and other jabberwocky; good luck with your thesis! Dear **Dave Koehler**, bench neighbor during my first year in the lab; learnt a lot from you! Dear **Martin Rutter**, your reservation to sit on my couch when you come to Holland is still open! Dear **Freek** (also known as Freak), thanks voor Toronto-updates; jij weet hoeveel ik het mis en ik hoop dat ik nog een keer mag komen logeren in m'n oude kamer! Succes met het afronden van je onderzoek. Dear **Matthias**, good luck with finishing your research; see you in Switzerland? Dear **Angie**, thank you for taking good care of our mice and your help in the lab. Good luck with your studies. Dear **Robin**, thanks for your help with Pecam immuno's! The **Sweezey lab**, thanks **Stephane**, **Lami**, and **Bahar**. Dear Lami and Bahar, we had the best conversations at night in the fellows room; I'm still convinced that Masters/PhD life is not easy!! The **O'Brodovich lab**, thanks **Gail**, **Bijan**, **Kathy**, and **Mike** (how is your Europe experience?). The **Rotin lab**, thanks **Pauline**, **Dave Hanwell**, **Youngshil**, **Nam**, **Roberta**, **Marylisa**, and **Chrissie** for support and beers on Friday afternoon! The **Tanswell lab**, thanks for sharing space and material, helping out and a lot of fun; thanks **Rose**, **Leslie**, **Robert**, and **Judy**. **Prof. dr. Keith Tanswell**, thank you very much for your support and advice during the years and for taking me to the NICU, which reminded me again why we study lung development. Your English humor was excellent in times of homesickness. Dear **Veronica**, thanks for your friendship at work, for inviting me into your home (for best gnocchi in the world), meeting your wonderful parents and your good advice on how to handle Canadians. I'll never forget our (nerd) nights out, evacuating a dying -80 freezer in the middle of Friday (!) night, the feeling of being an old cow and doing Toronto with bag pack by foot!! Good luck in medical school! Dear **Francesca** and **Sergio**, thanks for the fun nights out and excellent Italian dinners! See you in Siena. And last but not least: **Brent** (superb cook!) and **Jan Evert** (the winters do get worse!), **Chris** (haunted house), **Jane** and **Pam** (smart moms, always time to listen; to both of you I look up to! Any chance I can join the Batt/Plant lab in the future?), **Scott** (firecracker on a bike, it still makes me smile!!), **Sharon** (fast woman), and **Rob** (always on call); friends from the lab, but special friends forever; about Sinterklaas, haunted house, film festival, street parties, video night and sleepovers, and most importantly: you made me feel at home!

Weer thuis in Nederland ben ik begonnen aan een nieuw avontuur in **Amsterdam**.

Heel veel dank aan mijn nieuwe collega's en bazen van de kindergeneeskunde in het **Emma/AMC**. Het kostte even wat moeite om weer te settelen in Nederland, maar ik voel

me helemaal "adopted" door jullie en ben daar elke dag weer blij mee. Jullie gezelligheid, collegialiteit, supervisie en begrip hebben me het laatste zetje gegeven dit proefschrift af te schrijven. Speciale dank aan **Aline**, **Hanneke**, **Frea** en **Harriet** voor jullie support. Veel dank aan **Prof. dr. H. S. A. Heymans, Dr. F. A. Wijburg** en **Dr. A. P. Bos** voor begrip en schrijfvrij! En dan de **Neonatologie** (**Prof. dr. J. H. Kok**), met als onderwerp long ontwikkeling zit ik daar als een vis in het water. Jullie hebben de eindspurt van dit boekje mee- maar vooral mogelijk gemaakt; Dank!! Ondanks de hoeveelheid stress die het afmaken van dit boekje met zich mee heeft gebracht heb ik elke dag met plezier gewerkt en gelachen!

A big thank you to **Jarrod Leeds** for the beautiful cover and layout of this thesis and your excellent own input! You took away a lot of stress!

En dan het **thuisfront**, onmisbaar voor geluk en sanity in life!

Lieve vriendinnen van **jaarclub Steyl**, dank jullie wel voor al jullie begrip en interesse; ik vond het geweldig dat jullie naar Toronto zijn gekomen. Mede door jullie steun is dit proefschrift tot een eind gekomen!

Lieve **Liesbeth**, al vanaf de eerste jaren Geneeskunde samen, lief en leed en zo nu en dan een beetje drama, een heerlijke week in Toronto, moeder en bijna Internist; ik ben supertrots op je!

Lieve **Marion** en **Gideon**, we kwamen er in Toronto achter dat we in Rotterdam bij elkaar om de hoek woonden. Some things are meant to be. YMCA, Cinnabons, Starbucks, Algonquin, babysitten, GAP, Chapters, Mr. Spock, the Islands, film, uithuilen, en weer opnieuw beginnen; zonder jullie was het nooit zo goed gegaan.

Lieve **Jos** en **Miny**, dank je wel voor jullie interesse al die jaren; heel leuk dat jullie in Toronto zijn geweest; volgende keer Frankrijk! Lieve **Felice** en **Jeroen**, zet de spelletjes maar vast klaar!

Mijn lieve broers **Martijn** en **Emile**, dank voor jullie support en jullie relativerende kijk op mijn geploeter; wat dat betreft heb ik nog veel van jullie te leren. Ik heb geluk met jullie en mijn twee lieve (bijna!?) schoonzussen **Sigrid** en **Jean-Marie**.

Lieve **papa** en **mama**, jullie zullen je vaak afgevraagd hebben waarom het allemaal zo moeilijk moet. Gelukkig hebben jullie er nooit aan getwijfeld dat het goed ging komen (toch?!). Dank je wel dat jullie er altijd voor me zijn; een beter thuis kan ik me niet wensen. Ik hou van jullie!

Lieve Dennis, het leven samen is zoveel beter! Luv you!

Appendices

Curriculum Vitae

Curriculum Vitae

Minke van Tuyl was born on June 15, 1974 in Heinenoord, the Netherlands. In June 1992 she passed her VWO high school exam at the Lingecollege in Tiel. In the same year she started medical school at the Erasmus University in Rotterdam, where she obtained her medical degree (cum laude) in 1999. From 1993 to 1997 she worked as nurse assistant in the Thoracic Surgery medium care department at the Thorax Center, Erasmus Medical Center in Rotterdam. In 1996 she started her research training in Lung Development under the guidance of Prof. dr. D. Tibboel. During 1 year (1996 to 1997) she worked as research student in the department of Anatomy and Embryology at the Academic Medical Center in Amsterdam (Prof. dr. W. H. Lamers). From August 1999 to September 2003 she worked on her PhD project in the department of Lung Biology Research at the Hospital for Sick Children Research Institute in Toronto, Canada (Prof. dr. M. Post). For 5 months (May to September 2001) she worked in the laboratory of Experimental Pediatric Surgery in the department of Cell Biology and Genetics at the Erasmus Medical Center in Rotterdam (Prof. dr. F. Grosveld). In January 2004 she started working as resident in Pediatrics in the Emma children's Hospital at the Academic Medical Center in Amsterdam, where her official training started on July 1st, 2004 (Prof. dr. H. S. A. Heymans).